The role of FASN in the development and severity of Prostate cancer

De Piano, Mario Matthew

Awarding institution:
King's College London

The role of FASN in the development and severity of Prostate cancer

A thesis submitted to fulfil the requirements for the degree of Doctor of Philosophy

Mario De Piano

April 2017

Division of Cancer studies

King's College London

London

UK

Declaration of authorship

I declare that the work presented in this thesis is the work of the author. Any contributions from others is properly acknowledged and cited where appropriate. This copy of the thesis has been supplied on the condition that anyone who consults it is understood to recognise that its copyright rests with the author and no quotation from it or extract derived from it may be published without full attribution.

Acknowledgements

The first two people I would like to express my sincerest gratitude to are my supervisors Dr Claire Wells and Dr Mieke Van Hemelrijck. To Dr Claire Wells, my first supervisor, thank you for your guidance and constant support. Through you I believe I have become a far more astute scientist who has learnt how to think more openly and creatively. To Mieke Van Hemelrijck, my second supervisor, thank you for teaching me something completely new. Prior to my Ph.D I had never done any epidemiology work and initially I found it tough, but you helped me through it (with a lot of patience) and it ended up becoming a really enjoyable part of my project. Thank you both for accommodating me over the last three years; I am extremely grateful for the opportunity.

I also want to thank Prostate Cancer UK for funding my Ph.D project and for inviting me to attend their yearly early researcher's conferences where I got the opportunity to network with several prostate cancer scientists from around the UK. In addition, I want to thank our collaborators in Boston, Dr Giorgia Zadra and Professor Massimo Loda, for their contributions and support to this project.

I owe a big thank you to all the members in the Wells Lab. I am indebted to the past members of the group for their support and assistance. Thank you Dr Nouf Babteen, Dr Anna Dart, Dr Nicole Nicholas, Dr Helen King and Dr Fahim Ismail. I also want to thank our current postdoc Dr Michaela Lesjak for her support in my last year. I especially want to thank the Wells members Katerina Pipili (partner in crime over the last three years), Dr Nouf Babteen (lab mentor), Hoyin Lam (lab Bro), Dr Kiruthikah Thillai (resident lab doctor) and Maddie 'Penguin' Gale (undisputed cake baker of the lab). You guys have made King's a great place to work over the last three years; I'll always value your friendship and wish you all the best with your future endeavours.

I also need to thank members in the Van Hemelrijck Lab, both past and present, for their support including Dr Wulaningsih Wahyu, Dr Rhonda Arthur, Dr Jennie Melvin, Dr Danielle Crawley, Aida Santa Olalla Revenga and Cecilia Bosco. I also want to thank other members of the Cancer Epidemiology group including Rosemary Drescher,

Philomena Bredin, Fee Cahill and Dr Hans Garmo. I am also indebted to Professor Lars Holmberg for all his time, help and contributions to this project.

I also want to acknowledge several other members who worked on Floor 2 of New hunt's house including Dr Fabian Flores, Dr James Monypenny, Dr Ritu Garg, Dr Jeremy 'Jez' Carlton, Dr Jonathon Morris and Dr James Arnold. I am extremely grateful for all your suggestions, support and genuine interest towards my project over the last three years.

Lastly, I would like to thank my family for the overwhelming support they have provided me over the last three years. To my parents Angelo and Michelina De Piano, my sister Anna Thomas and her husband Barnaby Thomas, my brother Salvatore De Piano and his wife Vicki De Piano, thank you for listening to me when I needed an ear, and lifting my spirits when I was feeling under pressure. I know I would not have been able to get this far without you guys, especially 'Ma' and 'Pa', you two have always been super parents encouraging me to do better, thank you for everything.

Abstract

Fatty acid synthase (FASN), a lipogenic enzyme, is responsible for the *de novo* synthesis of endogenously derived fatty acids in the human body including palmitate; the building block of protein palmitoylation. Recent work has suggested that alongside an established role in promoting cell proliferation FASN may also specifically promote an invasive phenotype; although this is less-well documented. Understanding the influence of FASN on cell invasion is critical given that FASN is commonly overexpressed in prostate cancer and is associated with poor survival and tumour progression. In this study it was found that the depletion of FASN altered the cellular metabolome of prostate cancer cells and decreased their rate of proliferation. Moreover, changes in prostate cancer cell morphology were found to be synonymous with FASN expression levels. In addition, FASN knockdown increased cell adhesiveness, impaired HGF-mediated cell migration and reduced 3D invasion of prostate cancer cells. These changes in migratory ability suggest that FASN can mediate actin cytoskeletal remodelling, a process known to be downstream of Rho family GTPase signalling. Here, the modulation of FASN expression was observed to impact specifically on the palmitoylation of the atypical GTPase RhoU. RhoU has previously been shown to be required to deliver paxillin serine phosphorylation to drive adhesion turnover. In this study it was found that the loss of RhoU palmitoylation led to reduced adhesion turnover downstream of paxillin serine phosphorylation. The addition of exogenous palmitate was able to rescue adhesive and morphological defects seen in FASN deleted prostate cancer cells. Interestingly, it was also observed that the expression of the Rho GTPase Cdc42 decreased concomitantly with loss of FASN expression, but this is not dependent on palmitoylation; rather the findings from this study suggest that stable Cdc42 expression is dependent on the palmitoylation status of RhoU. Thus by modulating FASN activity and reducing the availability of *in cellulo* palmitate a novel relationship between RhoU and Cdc42 has been exposed which directly influences cell migration potential and provides compelling evidence that FASN activity directly supports cell migration. Additionally, a pilot patho-epidemiological study using radical prostatectomy specimens revealed an association between increased expression of FASN, RhoU and Cdc42 with prostate cancer severity.

Table of Contents

List of Figures

List of Tables

Abbreviations

2BP	2-Bromopalmitate
ACC	Acetyl-CoA carboxylase
ACP	Acyl carrier protein
ADT	Androgen deprivation therapy
ALA	Alpha-linolenic acid
AMPK	Adenosine monophosphate-activated protein kinase
APS	Ammonium persulfate
APT	Acyl protein thioesterases
AR	Androgen receptor
AP1	Activator protein 1
Arp2/3	Actin-related proteins 2/3
ATP	Adenosine triphosphate
BCL2	B-cell lymphoma 2
Biotin-BMCC	1-Biotinamido-4-[4'-(meleimidomethyl) cyclohexanecarboxamido]butane
BM	Basement membrane
BPE	Bovine pituitary extract
BPH	Benign prostatic hyperplasia
BSA	Bovine serum albumin
CAFs	Carcinoma-associated fibroblasts
CDK	Cyclin-dependent kinase
CE	Cholesterol ester
CO_2	Carbon dioxide
Co-IP	Co-immunoprecipitation
CPT1	Carnitine palmitoyltransferase
CRPC	Castrate-resistant prostate cancer
CUL3	Cullin 3
DAG	Diacylglyceride
DAPI	4,6-diamidino-2-phenylindole
DG	Dominant Gleason
DH	Dehydrase
dH_2O	Distilled water
DHT	Dihydrotestosterone
DMSO	Dimethyl sulfoxide
DNA	Deoxyribonucleic acid
dNTP	Deoxyribonucleotide triphosphate
DTT	Dithiothreitol
ECM	Extracellular matrix
ECL	Enhance chemiluminescence
E.coli	*Escherichia coli*
EGR	Epidermal growth factor
EGFR	Epidermal growth factor receptor
EMT	Epithelial-mesenchymal transition
ER	Enoyl reductase
ER	Endoplasmic reticulum
FA	Fatty acid

F-actin	Filamentous actin
FACs	Flow cytometric analysis of cell cycle
FAK	Focal adhesion kinase
FASN	Fatty acid synthase
FBS	Fetal bovine serum
FILIP1	Filamin A binding protein
Gab1	GRB2-assocaited-binding protein 1
G-actin	Globular actin
GAPs	GTPase-activating proteins
GDIs	Guanine nucleotide-dissociation inhibitors
GDP	Guanosine diphosphate
GEFs	Guanine nucleotide-exchange factor
GFP	Green fluorescent protein
Grb2	Growth factor receptor-bound protein 2
GTP	Guanosine triphosphate
H&E	Haematoxylin and eosin stain
H_2O	Water
HEPES	4-(2-hydroxyethyl)-1-piperazineethanesulfonic acid
HER2	Human epidermal growth factor receptor 2
HCL	Hydrochloric acid
HG	Highest Gleason
HGF	Hepatocyte growth factor
Hpr	Heptoglobin-related protein
HRP	Horseradish peroxidase
HSP90	Heat shock protein 90
Icmt	Isoprenylcysteine--*O*-carboxyl methyltransferase
iGluR	Ionotropic glutamine receptor
mGluR	Metabotropic glutamine receptor
JNK	Jun N-terminal kinase
kDa	Kilodaltons
KR	Ketoacyl reductase
KS	β-Ketoacyl synthase
KSFM	Keratinocyte serum free media
LB-agar	Luria-Bertani agar
LB-Broth	Luria-Bertani broth
LIMK	LIM kinase
LPA	Lysophosphatidic acid
MAPK	Mitogen-activated protein kinase
MAT	Malonyl/acetyltransferase
MAS-NMR	Magic angle spinning nuclear magnetic resonance
MET	Mesenchymal-epithelial transition
$MgCl_2$	Magnesium chloride
MLC	Myosin light chain
MMP	Matrix metalloproteinase
mRNA	Messenger RNA
mTOR	Mammalian target of rapamycin
MTT	3-(4,5-Dimethylthiazol-2-yl)-2,5-Diphenyltetrazolium Bromide
NADPH	Nicotinamide adenine dinucleotide phosphate

Na_3VO_4	Sodium orthovandate
NaCl	Sodium chloride
NAF	Sodium fluoride
NEM	*N*-Ethylmaleimide
Nck1	Noncatalytic region of tyrosine kinase adaptor protein 2
NF-κB	Nuclear transcription factor B
NH_2OH	Hydroxylamine
NOTCH1	Neurogenic locus notch homolog protein 1
OA-519	Oncogenic antigen-519
OR	Odds ratio
PA	Phosphatidic acid
PAKs	p21 activated kinases
PAR6	Partitioning defective 6
PAT	Palmitoyltransferases
PBS	Phosphate buffered saline
PCR	Polymerase chain reaction
PFA	Paraformaldehyde
PI3K	Phosphatidylinositol-3 kinase
PIA	Proliferative inflammatory atrophy
PIN	Prostatic intraepithelial neoplasia
PKC	Protein kinase C
PMSF	Phenylmethylsulfonylfluoride
RPMI-1640	Roswell Park Memorial Institute-1640
PSA	Prostate specific antigen
PUFAs	Polyunsaturated fatty acids
Rce1	Ras-converting enzyme 1
RNA	Ribonucleic acid
ROCK	Rho-associated, coiled-coil containing protein kinase 1
RTK	Receptor tyrosine kinase
SCAR/WAVE	Suppressor of cAMP receptor/WASP verprolin-homologous
SD	Standard deviation
SDS-PAGE	Sodium dodecyl sulphate polyacrylamide gel electrophoresis
SEM	Standard error of the mean
shRNA	Shot hairpin ribonucleic acid
siRNA	Short interfering ribonucleic acid
SKP2	S phase kinase-associated protein 2
SREBP-1c	Sterol regulatory element binding protein-1c
TAG	Triacylglyceride
TBST	Tris-buffered saline with Tween20
TCA	Tricarboxylic cycle
TE	Thioesterase
TEMED	Tetramethylethylenediamine
TGFβ1	Transforming growth factor beta 1
TIMP2	Tissue inhibitor of metalloproteinase 2
TNM	Tumour, Node, Metastasis
u-PA	urokinase-type plasminogen activator
UPS2α	Ubiquitin-specific protease-2α
VEGF	Vascular endothelial growth factor

WASP	Wiskott-Aldrich Syndrome Protein
WCL	Whole cell lysate
WHAMM	WASP homologue associated with golgi membranes and microtubules

Chapter 1

Introduction

Chapter 1 – Introduction

1.1 The Prostate and Prostate Cancer

1.1.1. Prostate anatomy and function

The prostate is a tubuloalveolar exocrine gland of the male reproductive system which by adulthood is roughly the size of a walnut and weighs approximately 20 grams (Hammerich et al., 2009). It is located in the subperitoneal compartment between the pelvic diaphragm and the peritoneal cavity (Bhavsar and Verma, 2014). The prostate is divided into four distinct regions including the peripheral zone, central zone, transition zone and the anterior fibromuscular zone (**Figure 1.1**). The peripheral zone comprises most of the prostatic glandular tissue which covers the posterior and lateral aspects of the prostate and surrounds the distal urethra. The central zone is defined by its cone-like shape with the apex of this structure surrounding the ejaculatory ducts. The transition zone consists of two equal portions of the glandular tissue which surround the proximal urethra. The glandular component of the prostate is composed of large peripheral ducts which contain acini at the terminal end (McNeal et al., 1991). The lumen of the ducts and acini are lined by two layers of epithelial cells, basal and luminal, as well as a minor population of neuroendocrine cells which are mainly distributed within the basal layer (Tomlins et al., 2006). The luminal secretory cells express the androgen receptor (AR) and secrete several products including prostate-specific antigen (PSA) and acid muscin (Oyasu et al., 2008). The basal epithelial cells form a flattened layer over the surrounding basement membrane which keeps the underlying stroma separate from the luminal cells (Bonkhoff et al., 1994; Oyasu et al., 2008). The basal cell layer is also thought to contain a small stem cell population that gives rise to all epithelial cell lineages (Bonkhoff et al., 1994; Oyasu et al., 2008). Neuroendocrine cells also differentiate from basal cells and are strictly AR negative (Oyasu et al., 2008). The main function of these cells is unknown, however they are thought have an endocrine-paracrine regulatory role in growth and development in addition to maintaining homeostatic control of the secretory processes of the prostate (Oyasu et al., 2008). The anterior fibromuscular zone of the prostate is devoid of glandular components and is formed from striated muscle and fibrous tissue which is important in regulating sphincter functions (Hammerich et al., 2009).

In addition to zonal classification, the prostate can also been divided by a lobe classification system. This consists of the anterior lobe (roughly correlates to the transitional zone), posterior lobe (roughly correlates to the peripheral zone), lateral lobes (consists of all zones) and median lobe (roughly correlates to the central zone) (Kumar and Majumder, 1995).

The prostate gland has several functions including controlling urine output from the bladder as well as the seminal fluid during ejaculation, providing essential proteins for the function of sperm including acid phosphatase, citrate and zinc (also acts as an antibacterial agent), and producing polyamine which regulates the alkaline pH nature of the sperm within the acidic female cervix (Kumar and Majumder, 1995).

1.1.2 Prostate carcinogenesis

Prostate cancer is the most commonly diagnosed noncutaneous malignancy in the world and has now become the leading cause of cancer related deaths in males of the western population (Tomlins et al., 2006). Current figures show that one in eight men will get prostate cancer accounting for a total of 40,000 incident cases and approximately 10,000 prostate cancer related deaths each year in the United Kingdom (Wilt and Ahmed, 2013). The five-year survival rate of patients with localized prostate cancer is approximately 98% which drops drastically to 28% if the prostate cancer has spread to other parts of the body (ACS, 2016). Despite modern efforts of early detection, 10-20% of cases present with widespread metastasis at the time of diagnosis (Dasgupta et al., 2012). This has led to an increased need for the development of more stringent detection tools and novel therapeutics in the treatment of this disease (Wilt and Ahmed, 2013).

Prostate cancer is a multifocal disease with 75% of the cases occurring in the peripheral zone; 20-25% of cases occurring in the transition zone; and 1-5% of cases occurring in the central zone (**Figure 1.1**) (Akin et al., 2006). The transition zone is also the most common location for the development of another well-known condition that afflicts the prostate in older men, benign prostatic hyperplasia (BPH). BPH develops due to hormonal imbalances which alter the expression of growth factor receptors in

glandular epithelial cells causing an increase in cellular proliferation. This rapid growth leads to the subsequent enlargement of discrete nodules within the transition zone which increases the overall size of the prostate (Dasgupta et al., 2012). Interestingly, there is a high incidence of prostate cancer arising in prostates that already have BPH. Despite this, BPH is not a precursor to prostate cancer and is usually easily distinguishable by the existence of a well-defined basal cell layer and underlying stroma (Chang et al., 2012). Although prostate cancer can in some cases mimic the obstructive symptoms of BPH, due to it primarily developing in the peripheral zone of the prostate it is rarely associated with any urinary-related symptoms. This means in most individuals prostate cancer in the early stages is asymptomatic or clinically silent and it is only when the disease progresses to the advanced stages that symptoms start manifesting (Hammerich et al., 2009).

Pathologically, biopsies have indicated that several morphological lesions are potential precursors to the development of prostate cancer which are identified by the cellular, histological and architectural nature of the glandular epithelium (Chrisofos et al., 2007). Currently, the earlier stages of prostate cancer carcinogenesis are still being debated. The most recent evidence suggests that inflammation plays a role in the development of prostate cancer (Felgueiras et al., 2014). In an ageing prostate, inflammation associated focal atrophy lesions are common and are characterised by a fraction of epithelial cells with an increased proliferation index and reduced apoptotic rate compared to normal epithelium (De Marzo et al., 2007). These lesions have been defined as proliferative inflammatory atrophy (PIA) and are located in the peripheral zone of the prostate. Morphological studies have shown that PIA is a precursor lesion to prostate cancer in addition to the most frequently associated precursor lesion to prostate cancer, prostatic intraepithelial neoplasia (PIN) (Putzi and De Marzo, 2000). PIN is the dysplasia of the epithelium lining the prostate glands which results in tissue disorganisation and is usually defined as either low-grade or high-grade (Ayala and Ro, 2007). Low-grade PIN is characterized by crowded and irregularly spaced epithelial cells with variable degrees of nuclear enlargement. In High-grade PIN, most cells exhibit anisonucleosis in addition to hyperchromasia (elevated chromatin) and pleomorphism (variation in cell size and shape) (Ayala and Ro, 2007).

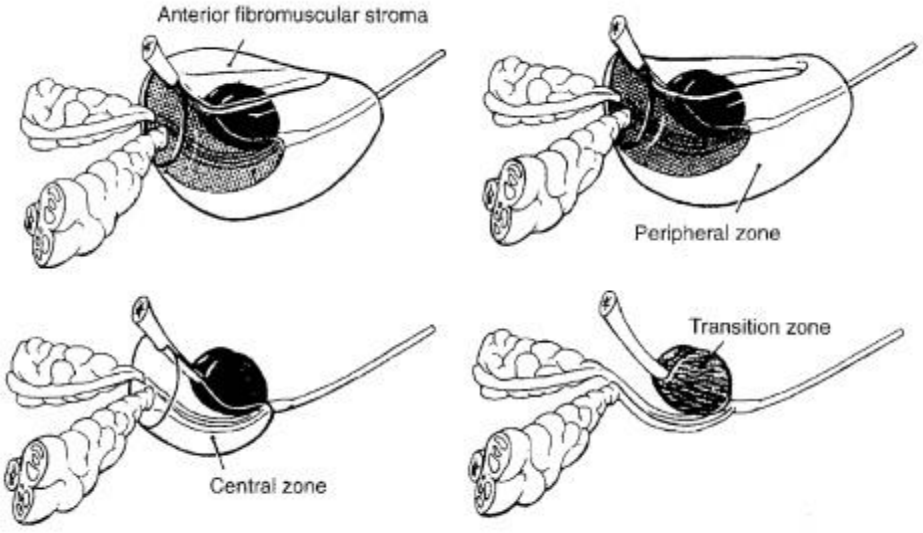

	Peripheral zone	Transition zone	Central zone
Benign prostatic hyperplasia (BPH)			
High grade PIN			
Prostate carcinoma			

Figure 1.1 Anatomical sections of the human prostate: The prostate can be divided into four main parts, starting with the inner-most section, the transition zone, which lies upon the central zone that is within the peripheral zone and has the anterior fibromuscular stroma sitting on-top. The table below shows where within the prostate abnormalities are most likely to occur. Red indicates a high prevalence, orange indicates a low prevalence, yellow indicates rare prevalence, and white indicates none. This figure was adapted from (Hammrich *et al*, 2009).

High-grade PIN shares several similarities with prostate cancer, including zonal distribution frequency, cellular crowding and stratification, hyperchromatism, proliferative and apoptotic indices, and increased microvessel density (Chrisofos et al., 2007). In addition, urologic pathologists have discovered that in the peripheral zone of the prostate, areas of transition exist between High-grade PIN and cancer (**Figure 1.1**). Prostatic ducts with High-grade PIN appear in continuity with smaller, separate malignant acini within the microcarcinoma foci (McNeal et al., 1991). The major difference between High-grade PIN and prostate cancer is that in High-grade PIN the basal cell layer is disrupted but cells do not invade into the basement membrane unlike in prostate cancer (Chrisofos et al., 2007). Unlike PIA, males who develop high-grade PIN are increasingly monitored due to the increased likelihood of developing prostate cancer which could take up to 10 years from diagnosis (Kryvenko et al., 2012).

1.1.3 Tumour grading and staging

Histologically, the majority of prostate cancers are diagnosed as acinar adenocarcinomas. This tumour type is characterised by the formation of an acini within neoplastic tissue that is composed of malignant cells with a cuboidal-to-columnar shape. Comparatively, non-acinar carcinomas or other types of prostatic carcinomas account for 5-10% of carcinomas that originate in the prostate. These histological variants include ductal adenocarcinoma, neuroendocrine carcinoma, sarcomatoid carcinoma, urothelial carcinoma, squamous and adenosquamous carcinoma and basal cell carcinoma (Humphrey, 2012).

The Gleason grading system is the most widely used grading scheme in the world. The technique was developed by Dr Donald F. Gleason in the 1960s-1970s and was designed to be a prognosis indicator that measured the aggressiveness of prostate cancer (Humphrey, 2004). This method uses H&E-stained tissue specimens that have been taken from biopsies and prepared onto microscope slides. The slides are then examined by a pathologist who will assess the histological pattern and give a score based on the degree of differentiation in glandular tissue and by the growth pattern of the tumour within the prostatic stroma (Chen and Zhou, 2016; Humphrey, 2004).

The classical Gleason system has five levels of histological grades (**Table 1.1**). Grade 1 is the lowest grade on the scale and is defined by glands that are well-differentiated and uniform. As the grades increase, glands become increasingly less recognisable and poorly-differentiated. Specimens with a Grade 5 pattern show practically no differentiation with sheets of tumour mass becoming indistinguishable from the surrounding stroma (Humphrey, 2004).

Due to most patients presenting with a heterogeneous population of malignant cells, two grades are given per specimen to the two most common tumour patterns. The primary grade is assigned to the dominant pattern of the tumour and has to correspond to more than 50% of the histological architecture. The secondary grade is assigned to the next-most frequent pattern and has to correspond to less than 50%, but more than 5% of the histological architecture otherwise it is ignored (Chen and Zhou, 2016; Humphrey, 2004). The primary and secondary grades are added together to get a 'Gleason score', i.e if primary tumour pattern of the biopsy is Grade 3 and the secondary tumour pattern is Grade 4, then the Gleason score is 3+4=7. Different individual scores can give the same overall Gleason score (i.e 4+3=7 and 3+4=7), however if the primary grade is higher than the secondary, then the carcinoma is more aggressive (Wright et al., 2009). Some pathologists also give a tertiary grade which generally corresponds to a small part of the tissue with the most aggressive pattern. The secondary grade is replaced by the tertiary grade if it constitutes more than 5% of the tumour (Gordetsky and Epstein, 2016)

Several studies have shown the validity of using the Gleason scoring system to predict overall prostate cancer survival in men (Koochekpour et al., 2012; Mian et al., 2002; Wright et al., 2009). An example of this can be seen in a study by Wright *et al* where they found that men with a Gleason score of 6 or less, 3+4, 4+3 and 8-10 had a 10-year survival rate of 98.4%, 92.1%, 76.5% and 69.9% respectively (Wright et al., 2009).

Table 1.1 Example tissue sections corresponding to their respective Gleason grade as defined by histological assessment: Figure was adapted from (Humphrey *et al*, 2004).

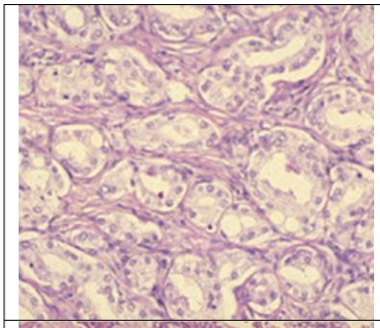	**Grade pattern 1:** The cancerous prostate closely resembles normal prostate tissue. A well-circumscribed nodular lesion composed of uniform, closely packed, well-differentiated glands of moderate size. Stroma is intact.
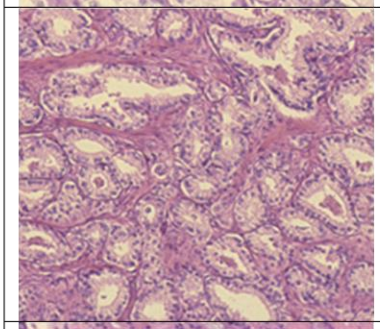	**Grade pattern 2:** Variation between well-differentiated and moderately-differentiated glands moderate in size. Tumour mass is less well-circumscribed and stoma can be seen filtering between the glands.
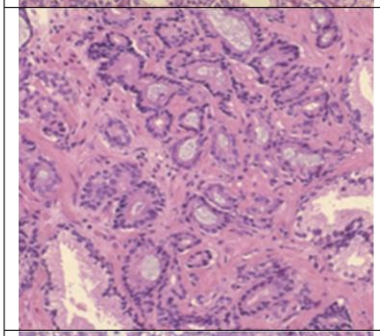	**Grade pattern 3:** Comprised of individual, discrete and distinct neoplastic glands (moderately differentiated) which are variable in shape and size (small to moderate). Cancerous cells have begun invading into the surrounding tissue, or have an infiltrative pattern.
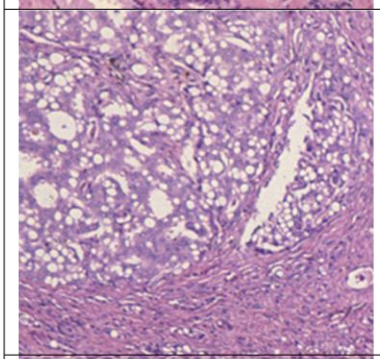	**Grade pattern 4:** Features fused glands which are no longer individual or distinct. This results in a poorly-differentiated tumour with broad, irregular fused glandular or cribriform patterns. Gland sizes can range from anywhere from small and large in size. A significant proportion of cells have invaded into the surrounding stroma.
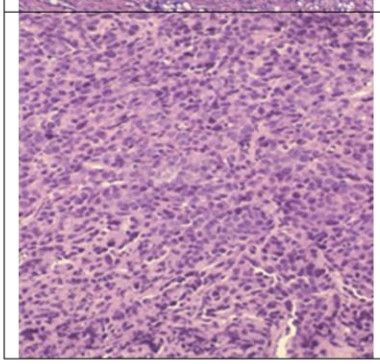	**Grade pattern 5:** This tissue has no recognizable glands. Most poorly-differentiated pattern. Necrosis can sometimes be seen in the centre of the tissue surrounded by papillary, cribriform, or solid masses of carcinoma.

In addition to Gleason scoring, staging of the cancer is also carried out to determine if the tumour has spread beyond the prostate. TNM (Tumour, Node, and Metastasis) staging was developed by the Union for International Cancer Control (UICC). The classification system works by assessing the size and extent of the tumour (T), degree of spread to the regional lymph nodes (N) and identifying sites of metastasis (M). Each classification group has a number and letter assigned to it to give more in-depth information about tumour localisation, nodes examined and where the cancer has spread to (Wallace et al., 1975).

1.1.4 Progression to castrate resistance in prostate cancer

A substantial minority of the 40,000 incidence prostate cancer cases will present with locoregional or metastatic spread at the time of diagnosis. Those whose disease is at an earlier stage and found to be localised at presentation may later progress to a more advanced stage of prostate cancer after initial treatment. At this juncture, the next option is to treat the cancer through hormone manipulation using primary androgen deprivation therapy (ADT) (Afshar et al., 2015; Lonergan and Tindall, 2011). Androgens and the AR receptor play an essential role in the normal growth and development of the prostate gland. Prostate cancer cells are also initially dependent on androgen stimulation. Activation of the AR via circulating androgens leads to a conformational change in the AR which allows it to dissociate from heat-shock proteins (HSPs). The AR then localizes to the nucleus where it binds androgen-response elements in the promotor regions of target genes involved in survival and growth. Activation or repression of these target genes increases the ratio of proliferating cells relative to cells undergoing apoptosis which leads to increased tumour growth (Feldman and Feldman, 2001). ADT has been shown to provide effective prostate cancer remission, however after a mean time of 2-3 years the disease usually progresses despite continuous deprivation treatment (Karantanos et al., 2013). This type of cancer is no longer dependent on androgens and is known as castrate-resistant prostate cancer (CRPC). The androgen-independent phenotype encompassed by CRPC has been shown to be more malignant and metastatic than androgen-dependent prostate cancer (Karantanos et al., 2013; Thalmann et al., 1994).

There are currently five proposed models for the mechanisms of developing androgen independence in prostate cancer (**Figure 1.2**) (Feldman and Feldman, 2001; Pienta and Bradley, 2006). The first is the hypersensitive pathway which increases AR expression (usually by gene amplification), enhances AR sensitivity, and increases DHT locally through 5α-reductase. This pathway is not strictly speaking androgen independent; however the cells are far less dependent on the concentration of circulating androgens as the threshold for AR pathway activation is much lower. The second model is the promiscuous pathway which broadens the binding specificity of the androgen receptor through mutations in its ligand-binding domain. This allows AR to bind hormones and non-androgenic steroid molecules normally present in the circulation and resume normal activity (Veldscholte et al., 1992). The third model is called the outlaw pathway and it relies on non-steroid molecules such as hormones or receptor tyrosine kinases (RTKs). AKT (protein kinase B) and mitogen-activated protein kinase (MAPK) are two RTK pathways which have been shown to cross-talk and phosphorylate AR. This pathway leads to a ligand-independent AR which is able to function normally. The fourth mechanism is the bypass pathway which activates parallel survival pathways obviating the need for AR or its ligand altogether. Examples of these pathways include the AKT and MAPK, or pathways which upregulate the expression of the anti-apoptotic protein BCL2 (B-cell lymphoma 2). The fifth model involves prostate cancer stem cells which are not natively dependent on the androgen receptor for growth and survival. The cells continually resupply the tumour cell population regardless of ADT (Feldman and Feldman, 2001; Pienta and Bradley, 2006).

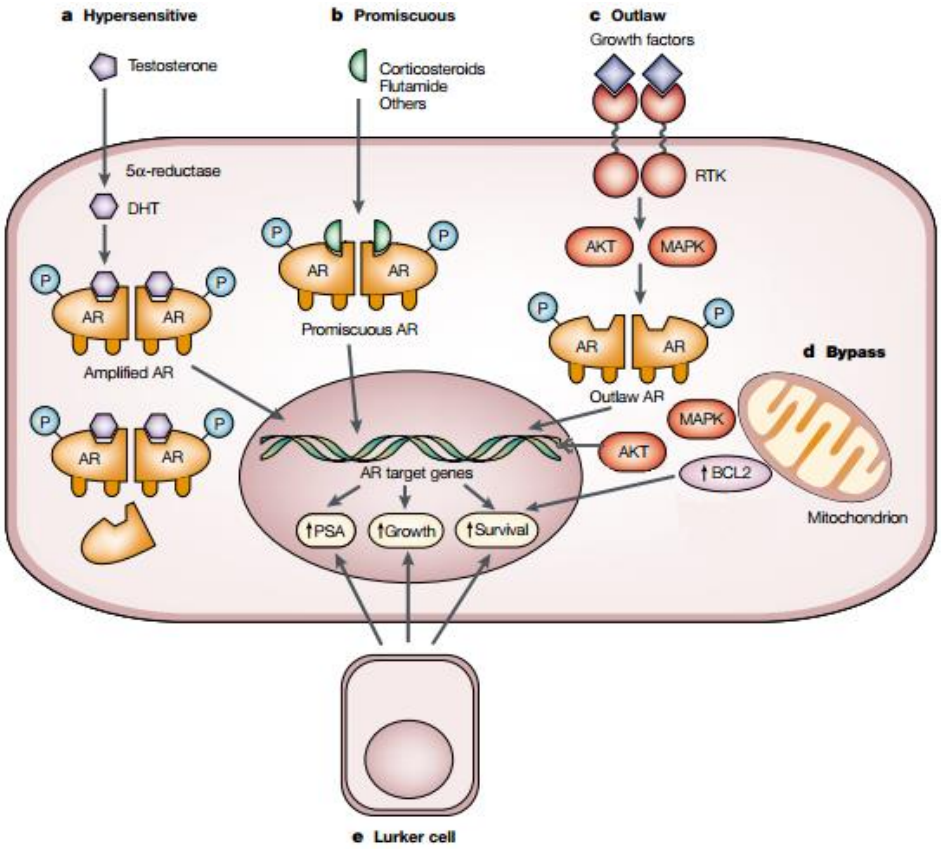

Model	Ligand dependence	Mechanism
Hypersensitive AR	Androgen dependent	Amplified AR. Sensitive AR. Increased DHT.
Promiscuous AR	Pseudo-androgens	Mutated androgen receptor broadens binding specificity. Non-androgens and hormone activation.
Outlaw AR	Androgen independent	Activated PI3K Activated MAPK Mutant *PTEN*
Bypass AR	Androgen independent	Activation of alternative signalling pathways (AKT and MAPK). Overexpression of BCL2. Activation of other oncogenes.
Prostate cancer stem cell (lurker cell)	Androgen independent	Malignant epithelial stem cells.

Figure 1.2 Pathways to androgen independence: There are currently five pathways that lead to androgen-independence in prostate cancer including the hypersensitive pathway, promiscuous pathway, outlaw pathway, bypass pathway, and the prostate cancer stem cell/lurker cell pathway. Details of the underlying mechanism for each of these pathways are presented in the figure above. Figure was adapted from (Feldman and Feldman, 2001).

1.2 Metastasis

1.2.1 Metastatic cascade

It is cancer metastasis and not cancer at the primary site which is mainly responsible for cancer mortality; overall accounting for 90% of cancer related deaths. Metastasis is a process which involves the dissemination of cancer cells from the primary tumour site to a distant site or organ in the body (Yamaguchi et al., 2005). Approximately 90% of prostate cancer patients with CRPC will develop metastasis, which is mainly to the bone. Those with metastasised CRPC have a poor prognosis and a mean survival time of only 16-18 months (Karantanos et al., 2013). At this point drug treatments such as abiraterone, enzulutamide, docetaxel, samarium-152 and zoledronic acid are offered as well as sipuleucel-T immunotherapy, bone targeting radium-233 and second-line cabazitaxel (Afshar et al., 2015). These treatments have been shown to increase overall survival time by up to 5 months (Karantanos et al., 2013). However, due to the systemic nature of disseminated cancer cells and resistance to existing therapeutic agent's metastatic disease is virtually incurable. (Guan, 2015).

Metastasis is a multi-step process which is often referred to as the metastatic cascade (**Figure 1.3**) (van Zijl et al., 2011a). It is initiated by the detachment of cancer cells from the primary tumour. Under normal circumstances, epithelial and endothelial cells trying to disseminate from the rest of the cell population would undergo anoikis, a form of programmed cell death caused by the detachment of cells from the extracellular matrix (ECM) (Sakamoto and Kyprianou, 2010). Metastatic cells are thought to break away from the primary tumour and resist anoikis by undergoing the process of epithelial-mesenchymal transition (EMT) (Alizadeh et al., 2014). EMT involves non-motile, polarized epithelial cells, which are collectively embedded via cell-to-cell and cell-matrix adhesions, becoming individual, non-polarized, motile and invasive mesenchymal cells (Yilmaz and Christofori, 2009). There is considerable data which suggests that EMT contributes to prostate cancer progression and metastasis, however it has been shown to be dispensable for the metastasis of other cancers such as lung and pancreatic (Fischer et al., 2015; Khan et al., 2015; Zheng et al., 2015).

During EMT, cells lose several cell-cell adhesion proteins that are classical markers of an epithelial phenotype including E-cadherin, occludin, ZO-1, claudin, cytokeratin,

catenin and desmoplakin. These are substituted with markers typical of a mesenchymal phenotype such as N-cadherin and vimentin, both of which have been linked with cell invasiveness and resistance to anoikis in prostate cancer. (Heerboth et al., 2015; Khan et al., 2015; Wei et al., 2008). The levels of these proteins are regulated by the pleiotropic action of EMT-inducing proteins such as Snail, Zeb1, Zeb2, Slug and Twist (Khan et al., 2015). It should also be noted that during metastasis, prostate cancer cells can undergo partial EMT (Chao et al., 2012). This phenotype is associated with a higher aggressiveness when compared to complete epithelial or mesenchymal states and does not involve the complete loss of epithelial markers (Armstrong et al., 2011; Li and Kang, 2016).

Once detached from the primary tumour, cancer cells invade into the surrounding tumour-associated stroma and then into the adjacent normal tissue parenchyma (**Figure 1.3**). To infiltrate into the stroma cancer cells must first breach the basement membrane (BM), a specialized ECM that separates the epithelium from the underlying connective tissue (Valastyan and Weinberg, 2011). Cancer cells accomplish this by active proteolysis, a process coordinated by matrix metalloproteinases (MMPs). MMPs are zinc-dependent endopeptidase which are involved in the degradation of the ECM and play an important role in tissue remodelling. Analysis of MMP mRNA and protein levels in prostate cancer patient tissue and serum has revealed that the expression of MMP2, MMP7, MMP9, MMP13, MMP14 (MT1-MMP), MMP15 (MT2-MMP) and MMP26 is correlated with advanced or metastatic disease (Gong et al., 2014). Most MMPs are secreted as inactive pro-enzymes which become activated when cleaved by extracellular proteinases. MT1-MMP and MT2-MMP are the exception as they contain transmembrane domains indicating they are expressed at the cell surface rather than secreted (Ellerbroek and Stack, 1999).

Once the invading cells have dissolved the BM they are confronted with what is known as a “reactive” stroma. Reactive stromas develop as a result of primary tumour progression. They share many attributes with stroma tissue that is chronically inflamed or in the midst of wound repair. The ECM of the stroma is composed of many proteins including collagens, elastin, laminins, tenascin, fibulin, versican and fibronectin (Krušlin et al., 2015; Tuxhorn et al., 2002). Two fibroblast cell types, carcinoma-associated

fibroblasts (CAFs) and myofibroblasts, are also a main component of the reactive stroma in prostate cancer (**Figure 1.3**). These stromal cells play a role in further enhancing the aggressive nature of cancer cells through there secretion of chemokines and growth factors (Barron and Rowley, 2012). An example of this is the abundant secretion of hepatocyte growth factor (HGF) in the prostate tumour microenvironment. HGF has been identified as a prominent growth factor for driving prostate cancer progression and metastasis through its binding to the cell surface receptor c-Met (Varkaris et al., 2011).

Once the carcinoma cells have navigated through the ECM of the stroma the next stage is to migrate into the lymph nodes or haematogenous vessels in a process known as Intravasation (**Figure 1.3**). Cancer cells can enter these vessels either by transmigrating between the endothelial cells (paracellular) or through the endothelial cells (transcellular) (Reymond et al., 2013). When the cancer cells have successfully entered into the lumina of blood vessels they can disseminate widely throughout the body.

Whilst in the blood vessels cancer cells have to survive a variety of stresses including becoming trapped by various capillary beds, prolonged matrix detachment, hemodynamic shear forces and predation by cells of the innate immune system. In addition, once at a distal site, colonization may not occur due to an incompatibility for the cancer cell to adapt within foreign tissue architecture. It is thus speculated that less than 0.1% of disseminated cancer cells successfully develop secondary tumours (van Zijl et al., 2011b). Successful carcinoma cells penetrate the endothelial and pericyte layers and extravasate into the stromal microenvironment of the distant organ. Here cancer cells can revert to a more epithelial cell type in a process known as mesenchymal-epithelial transition (MET) and form a microcolony which is initially programmed for excelled growth at this new site (**Figure 1.3**) (Valastyan and Weinberg, 2011). In the case of prostate cancer, the main sites of metastasis are to the bone, lung and liver (Ye et al., 2007).

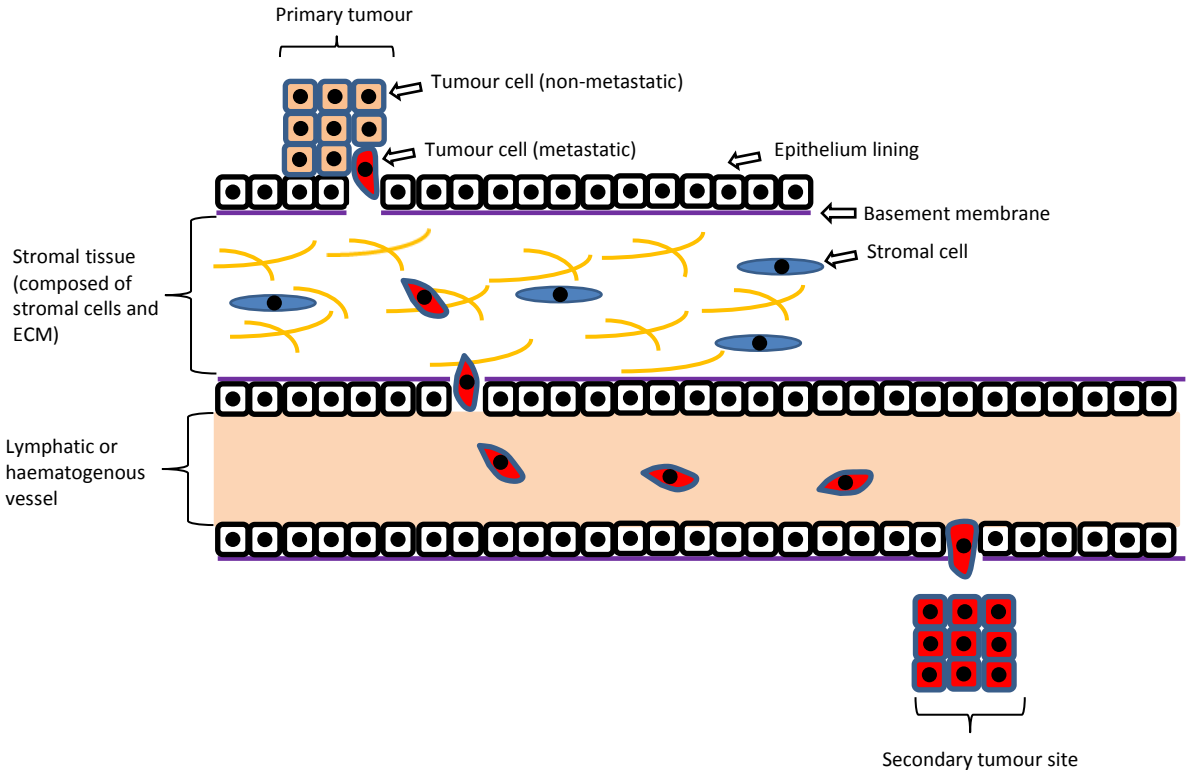

Figure 1.3 Diagram of the metastatic cascade: A selective few cancer cells will acquire a metastatic phenotype and disseminate from the primary tumour into the surrounding stroma. Eventually some metastatic cells will intravasate into blood or lymphatic vessels where they will be carried to distant sites in the body. Cells that survive can then extravasate out of the blood or lymphatic vessels and form a secondary tumour site.

1.2.2 Cell migration and invasion

A prerequisite of metastasis is the adoption of a migratory phenotype by cancer cells (Friedl and Wolf, 2003). It is through migration and invasion that cancer cells are able to navigate the stoma, enter lymphatic or blood vessels and spread to distant organs or tissues (Friedl and Wolf, 2003). During metastasis cancer cells are exposed to different environmental conditions which may require them to alter their "mode" of migration in order to progress (Friedl and Alexander, 2011; Friedl and Wolf, 2003). To date, tumour cells have been observed to migrate as individual single cells or as a collective body of well-organised adherent cells (**Figure 1.4**) (Clark and Vignjevic, 2015).

All forms of migration rely on the ability of cancer cells to reorganise their actin cytoskeleton which in turn leads to an alteration in the shape of the cell making them more adaptable to their surrounding environment (Machesky, 2008). Single-cell migration is characterized by a lack of cell-cell interactions during migration with cells either displaying a mesenchymal-like phenotype or an amoeboid-like phenotype (Clark and Vignjevic, 2015). Both of these phenotypes have previously been observed in PC3 and DU145 prostate cancer cell populations (Morley et al., 2014; Taddei et al., 2011).

Cancer cells that adopt a mesenchymal phenotype typically have fibroblast-like spindle shaped morphology and move via a five-step migration cycle. During the first step of this cycle cells become polarised producing protrusions which are either large, broad and fan-like, termed lamellipodia, or microspike projections that emanate from the frontier of this structure, termed filopodia (Ridley et al., 2003). The leading edge protrusion then stabilizes itself by anchoring to the underlying ECM through the formation of focal contacts. The physical ECM barrier situated rearward of the leading edge is then broken down via focalised proteolysis. Actomyosin-mediated contraction then allows the cell body to effectively translocate in the direction of migration leaving a tail-like projection at the rear-end which retracts following focal contact disassembly (Friedl and Wolf, 2009). In addition to forming leading edge protrusions, cancer cells can also form ventral surface protrusions called invadopodia. Invadopodia are especially important in extravasation and allow the cell to move into, or through the basement membrane and surrounding tissue (Murphy and Courtneidge, 2011).

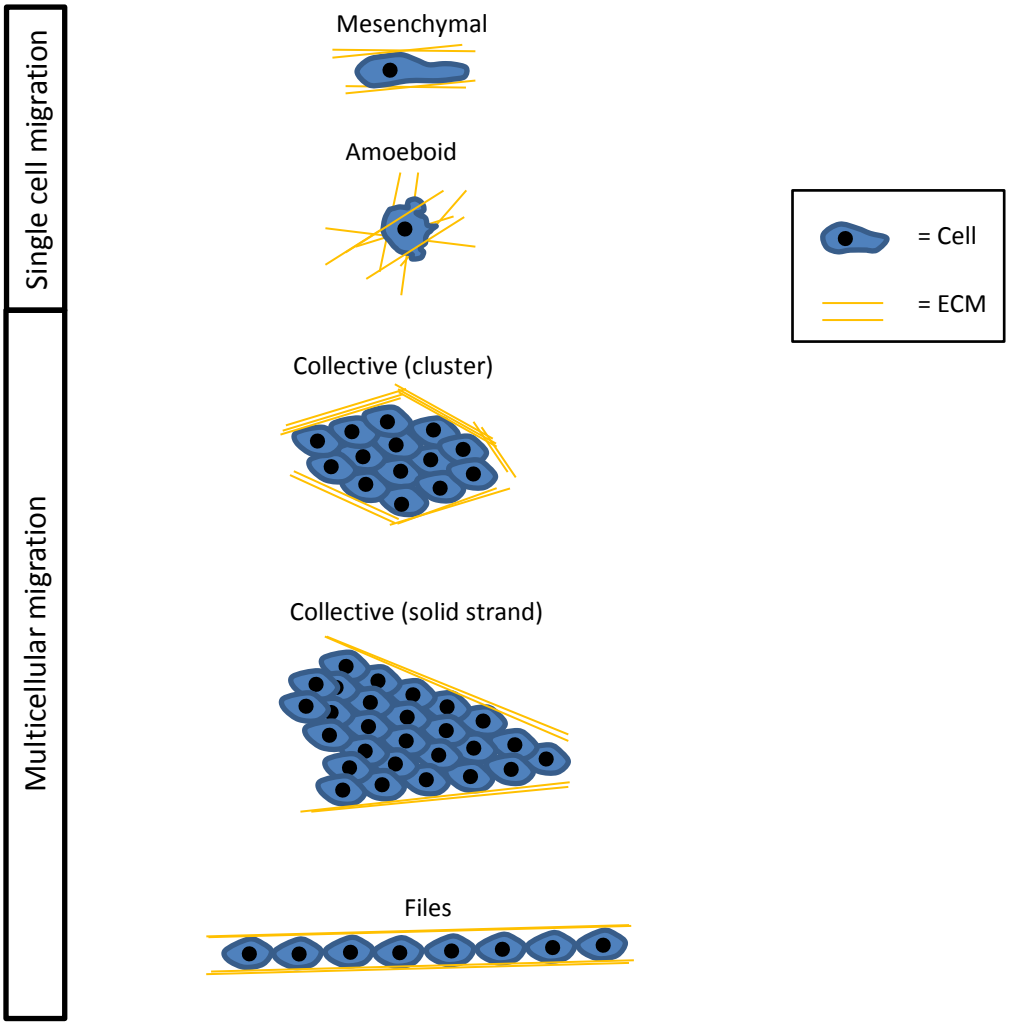

Figure 1.4 Mechanisms of single cell and collective cell migration: There are currently two modes of cell migration, single cell and multicellular migration. Single cells either migrate with a mesenchymal phenotype which is characterised by an elongated cell shape that uses protease degradation, or an amoeboid phenotype which is characterised by high contractility, a rounded cell shape and protease degradation. In multicellular migration cancer cells can invade collectively in a small cluster, as sheets, a solid strand or in files (line of cells migrating on a single path in contact with the leading and following cell).

Cells that adopt an amoeboid-like morphology have spherical shapes, low adhesion force and high actomyosin-mediated contractility (Friedl and Alexander, 2011). Amoeboid-like cells are characterized by rapid deformability, adapting their shape according to the surrounding ECM which allows them to penetrate though narrow spaces. Propulsion of the cell through the interstitial matrix is achieved by dynamic cycles of expansion and contraction of the cells body. During movement amoeboid-like cancer cells produce protrusive structures known as “blebs” which act as sensors testing if the cell can bypass the obstructing ECM. Similar to mesenchymal motility, amoeboid movement also relies on proteolysis to break down ECM fibres (Krakhmal et al., 2015; Orgaz et al., 2014).

Collective migration has also been reported in prostate cancer, both *in vivo* and *in vitro,* and involves the movement of a group of cells that all travel in the same relative direction (Brandt et al., 1996; Cui and Yamada, 2013; Friedl and Wolf, 2003). Cells that invade collectively may adopt different morphologies which is dependent on the cell type, the number of cells moving as a collective, and the structure of the tissue being invaded into (Friedl and Alexander, 2011). These include groups of cells forming small clusters, solid strands, or files (Clark and Vignjevic, 2015; Friedl and Alexander, 2011). In the majority of cases regarding collective cell migration, one or several leader cells with mesenchymal-like characteristics form a tip and generate forward migratory traction though pericellular proteolysis (Friedl and Alexander, 2011). It has been reported that when collective migration occurs in soft tissue the tip of the invading mass becomes blunt with several cells of strong polarity protruding into the surrounding matrix. Cells migrating collectively can also display a different phenotype, either mesenchymal or epithelial, to their neighbouring cells. Cell-to-cell and cell-matrix adhesions are an important feature of collective migration. Antagonists of integrins, obligate transmembrane receptors that link the cell to the ECM, have been shown to be effective in blocking collective cell migration (Friedl and Wolf, 2003).

1.2.3 The actin cytoskeleton in cell migration

The continuous movement of cancer cells during metastasis is powered by protrusive machinery that is built from the constant reorganisation and turnover of the actin cytoskeleton (Yamaguchi and Condeelis, 2007). The actin cytoskeleton of the cell is made from thin flexible helical fibres called filamentous actin (F-actin) (Jiang et al., 2009). F-actin itself is made from adenosine triphosphate (ATP) dependent polymerization of individual actin molecules, termed globular actin (G-actin) (Jiang et al., 2009). F- actin filaments grow with functional polarity and are defined by a slow-growing pointed end, referred to as the minus (-) end, and a fast-growing barded end which is commonly referred to as the plus (+) end (Mullins et al., 1998). Typically, extension of actin filaments at the plus (+) end coincides with a dissociation of actin subunits at the minus (-) end. This is due to the hydrolysis of ATP to ADP (adenosine diphosphate) which gives ADP-bound G-actin monomers a much reduced binding affinity to the filaments (Small et al., 1978). It is believed in accordance of Brownian motion that there is a relative fluctuation of the actin plus (+) end polymerising against the plasma membrane. In this model, whilst one actin plus (+) end associates with the membrane, another actin filament can bend providing space for actin monomer insertion to the plus (+) end (Peskin et al., 1993). Actin filament assembly is regulated by heterodimeric capping proteins such as gelsolin and CapZ which inhibit the addition or loss of actin subunits at the barbed ends ensuring a well-defined cell shape for motility is achieved (Cooper and Sept, 2008). Actin assembly is mainly controlled by the seven subunit protein complex, the actin-related proteins 2/3 (Arp2/3) complex. The Arp2/3 complex is responsible for creating new nucleation cores that allow for continuous actin filament polymerization at the migrating or invasive front of a cell (Welch et al., 1997). Depending on the geometry of the polymerising actin filaments cells can form several different types of protrusions including lamellipodia, filopodia, invadopodia and pseudopodia (Machesky, 2008; Murphy and Courtneidge, 2011).

The continuous reorganisation of the actin cytoskeleton is essential during cell migration and invasion. A variety of extracellular stimuli can trigger these changes through the Rho GTPase family of proteins which are considered to be the master regulators of the actin cytoskeleton (Sit and Manser, 2011).

1.3 Rho GTPases

1.3.1 The family of Rho GTPases and their activation

The Rho GTPases are a group of proteins that have been implicated in the initiation of many cellular process including cell division, cytoskeletal reorganisation, motility, cell adhesion, vesicular trafficking and transcriptional regulation (Vega and Ridley, 2008). The Rho GTPases form a subgroup of the Ras-like protein superfamily of GTPases, which includes other distinct families such as Ras, Rab, Arf and Ran (Vega and Ridley, 2008). Rho members are small molecules, approximately 21-28 kDa in size, that share significant structural homology and differ from the other Ras-like GTPases by the presence of a Rho-specific insert domain (Parri and Chiarugi, 2010; Vega and Ridley, 2008). The family of Rho proteins are highly conserved and comprise 20 members divided into 8 different subfamilies (**Table 1.2**). The family of Rho GTPases are also often divided into two distinct types of Rho GTPases, classical and atypical. In humans, the classical Rho GTPases Rac1, RhoA, and Cdc42 remain the best studied in actin cytoskeletal reorganisation and cellular locomotion (Sit and Manser, 2011). These proteins, in addition to all classical Rho GTPases, act as sensitive molecular switches cycling between an inactive GDP-bound state and an active GTP-bound state (**Figure 1.5**).

The activity of the classical Rho GTPases is regulated by guanine nucleotide-exchange factors (GEFs), GTPase-activating proteins (GAPs) and guanine nucleotide-dissociation inhibitors (GDIs) (Heasman and Ridley, 2008). Over 70 GEFs have been described in humans and there function is to catalyse the exchange of GDP to GTP which leads to an increase in the proteins activity. Conversely, GAPs, of which over 80 have been identified in mammals, stimulate the hydrolysis of GTP leading to an increase in inactive GDP-bound Rho proteins. GDIs function to sequester particular Rho proteins into the cytoplasm away from any regulators or targets and prevent their activation through inhibiting the release of GDP from its partner GTPase (DerMardirossian and Bokoch, 2005; Heasman and Ridley, 2008).

Table 1.2 Rho GTPase subclass, corresponding family members, and observed post-translation modification: Grey colouring indicates classical Rho GTPase and colourless indicates the atypical Rho GTPases. Figure was adapted from (Roberts *et al*, 2008).

Subclass	Rho family members	Lipid modification
Cdc42	Cdc42	Prenylation/Palmitoylation (variant specific)
	RhoQ/TC10	Prenylation/Palmitoylation
	RhoJ/TCL	Prenylation
Rac	Rac1	Prenylation/Palmitoylation
	Rac2	Prenylation
	Rac3	Prenylation
	RhoG	Prenylation
Rho	RhoA	Prenylation
	RhoB	Prenylation/Palmitoylation
	RhoC	Prenylation
RhoF	RhoD	Prenylation
	RhoF/Rif	Prenylation
RhoUV	RhoU/Wrch	Palmitoylation
	RhoV/Chp	Palmitoylation
RhoBTB	RhoBTB1	-
	RhoBTB2/DBC-2	-
	RhoBTB3	Prenylation
RhoH	RhoH/TTF	Prenylation
Rnd	Rnd1/Rho6	Prenylation
	Rnd2/RhoN	Prenylation
	Rnd3/RhoE	Prenylation

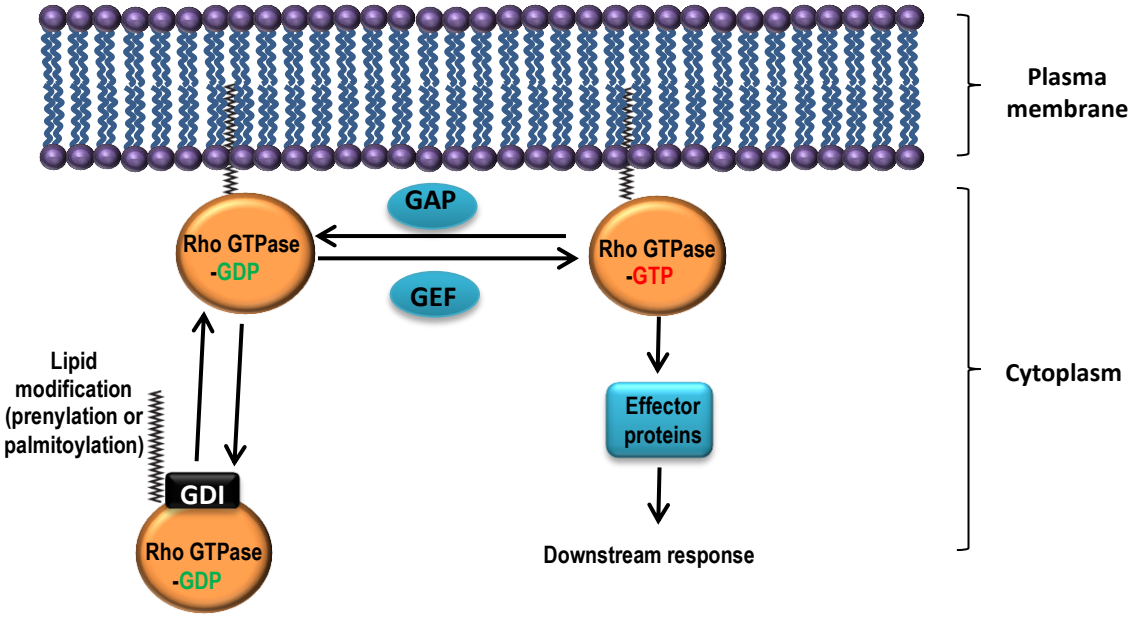

Figure 1.5 Regulation of Rho GTPase activity: At the membrane Rho GTPases cycle between an inactive GDP bound form and an active GTP bound form. Rho GTPases are activated by GEFs and inactivated by GAPs. The GTPase activation is also inhibited by the binding of GDIs which sequester the GTPase into the cytoplasm. The Rho GTPases are targeted to membrane by the post-translational addition of lipid moieties (prenylation or palmitoylation).

Unlike the classical Rho GTPases, the atypical GTPases are not generally regulated by GTP-GDP cycling and so do not require GEFs, GAPs or GDIs to modulate their activity. Instead, these proteins have been found to be in a constitutive GTP-bound state which may be the result of high intrinsic nucleotide exchange activity or due to mutations in their GTPase domain which permanently locks the protein in a GTP-bound state (Fransson et al., 2003; Hodge and Ridley, 2016). This means other mechanisms have been adopted to regulate their activity; which to date have not been fully elucidated. Currently, it is believed that protein-protein interactions or protein phosphorylation may be involved in regulating the atypical Rho GTPases. An example of this has been shown by the ability of plexin-B2, one of the three plexin-B proteins, to induce cell rounding through its interaction with Rnd3/RhoE (McColl et al., 2016).

1.3.2 Intracellular regulation of the Rho GTPases by lipids

The Rho GTPase proteins are also frequently post-translationally modified by lipids (**Figure 1.5**). This promotes specific subcellular localization of the proteins to membrane compartments that directly influence their interaction with other proteins and initiates downstream signalling (Roberts et al., 2008). The only exceptions are the two Rho GTPases RhoBTB1 and RhoBTB2 which are regarded as tumour suppressors and most likely localise to different cellular regions when coupled to cullin 3 (CUL3) ubiquitin ligase complexes (Berthold et al., 2008). There are two types of post-translational lipid modifications that can take place in Rho GTPases, prenylation and palmitoylation. These modifications are initiated by the recognition of a carboxyl-terminal *CAAX* tetrapeptide motif (C=cysteine, A= aliphatic amino acid, and X=any amino acid) (Roberts et al., 2008). Prenylation is the irreversible addition of either a farnesyl (15-carbon chain) or geranylgeranyl (20-carbon chain) isoprenoid lipid to the cysteine residue of the *CAAX* motif (Hodge and Ridley, 2016). Once bound, the terminal *AAX* peptide residues are cleaved by the Ras-converting enzyme 1 (Rce1) endoprotease. Then the prenylated cysteine residue is carboxymethalyted by isoprenylcysteine-*O*-carboxyl methyltransferase (Icmt).

Taken together these additional steps of processing increase the hydrophobicity of the protein and facilitate membrane association (Sebti and Der, 2003). Several Rho GTPase proteins have been found to be prenylated as shown in **Table 1.2**.

Palmitoylation is the covalent addition of the 16-carbon fatty acid palmitate predominately to the cysteine residues of a protein (Aicart-Ramos et al., 2011). Palmitoyl linkage can also occur on serine and threonine residues of a protein, however this has been less frequently documented (Anderson and Ragan, 2016). Unlike prenylation, palmitoylation is a reversible modification that enables Rho GTPase proteins to rapidly shuttle between intracellular membrane compartments. The atypical GTPases RhoU and RhoV are exclusively modified by palmitoylation (Hodge and Ridley, 2016). Other Rho GTPases such as Rac1 and the brain splice variant of Cdc42 have shown to be both palmitoylated and prenylated (Navarro-Lerida et al., 2012; Nishimura and Linder, 2013).

Both lipid modifications have been shown to be important in the normal signalling of Rho GTPases. Prevention of prenylation through pharmacological inhibition has been shown to mislocalize and decrease the activity of RhoA which in turn led to a decrease in the expression of several pro-invasive molecules including MMP7, tissue inhibitor of metalloproteinase 2 (TIMP2) and urokinase-type plasminogen activator (u-PA) (Caraglia et al., 2006; Konstantinopoulos et al., 2007). Similarly, the inhibition of palmitoylation in NIH 3T3 fibroblast cells led to the significant mislocalization of RhoU, decreased phosphorylation of PAK1, a member of the serine/threonine p21 activated kinases (PAKs), and led to pronounced morphology changes (Berzat et al., 2005).

1.3.3 Rho GTPases are master regulators of the actin cytoskeleton and cell migration

The Rho GTPases Cdc42, Rac1 and RhoA are well characterised in their ability to reorganise the actin cytoskeleton which is fundamental in inducing morphological changes and motility in cancer cells (Raftopoulou and Hall, 2004). Rac1 and Cdc42 are required at the front of migrating cells and drive motility through the formation actin based protrusive structures. Rac1 activity induces the formation of lamellipodia, whilst Cdc42 activity induces the formation of filopodia. Alternatively, RhoA activity is

associated with cell contractility and rear end retraction (Raftopoulou and Hall, 2004). All three of these Rho GTPases have been shown to induce cell migration in prostate cancer cells *in vitro* (Kato et al., 2014; Reymond et al., 2012; Zheng et al., 2006).

The cellular targets of Rac1, Cdc42 and RhoA that promote changes to the actin cytoskeleton have been extensively studied. Cdc42 primarily initiates the formation of filopodia through WASP (Wiskott-Aldrich Syndrome Protein). Rac1 on the other hand initiates the formation of lamellipodia through SCAR/WAVE (suppressor of cAMP receptor/WASP verprolin-homologous). Both WASP and SCAR/WAVE are actin-nucleation promoting factors that regulate the activity of the Arp2/3 complex which is responsible for the polymerization of new actin filaments (Sossey-Alaoui et al., 2005).

Rac1, Cdc42 and RhoA can also regulate cofilin, a small ubiquitous protein that is essential in regulating actin dynamics. Cofilin functions to depolymerize filaments to generate free actin that can be recycled for another round of polymerization (Yamaguchi et al., 2005). The Rho GTPases regulate cofilin by activating LIM kinase (LIMK) via PAK1. Cofilin is then phosphorylated and inactivated by LIMK which allows for F-actin stability and elongation (Raftopoulou and Hall, 2004; Sit and Manser, 2011).

Upon formation, the leading edge protrusion is anchored to the cell membrane and stabilised through focal adhesions. Focal adhesions are composed from a cluster of integrins and they connect to the cytoskeleton via linker proteins such as paxillin, zyxin, talin, vinculin and α-actinin (Huttenlocher and Horwitz, 2011; Smith et al., 2013). Rac1 and Cdc42 are responsible for the formation of focal adhesions at the leading edge of the cell which later mature into larger focal adhesions under the control of RhoA (Nobes and Hall, 1995). Adhesions are essential in cell migration as failure of this process results in the protruding membrane folding back onto the dorsal surface of the cell which creates membrane ruffles without distinct polarity (Parsons et al., 2010a).

Once the leading edge protrusion is stabilised contractility is required to move the cell body along the ECM. RhoA controls this function through ROCK (Rho-associated, coiled-coil containing protein kinase 1) which phosphorylates and activates myosin light chain (MLC) kinase (Narumiya et al., 2009). MLC kinase then phosphorylates the myosin light chain of myosin which allows it to tether to actin filaments and exert

contractile forces which leads to the cell body translocating (O'Connor and Chen, 2013). RhoA is also responsible for the formation of dorsal stress fibres which are assembled through the activation of its downstream effectors ROCK and mDia1. Focal adhesions are often connected to actin stress fibres during migration and their connection to myosin aids cell contractility (Huttenlocher and Horwitz, 2011). Continuous turnover of focal adhesions as the cell in migrating is also essential. Rac1, Cdc42, and RhoA have all been shown to regulate focal adhesion turnover (Huttenlocher and Horwitz, 2011; Parsons et al., 2010b). RhoA predominantly regulates the disassembly of focal adhesions at the rear-end of the cell which allows it to retract in the direction of migration (Parsons et al., 2010b).

During migration there is a significant amount of crosstalk between the Rho GTPases. For instance, Cdc42 controls the polarity and directional persistence of a cell during migration. One way it accomplishes this is by activing the Rac-GEF's βPIX and TIAM1 which recruits Rac1 to the front of the cell (Cau and Hall, 2005). In addition, Cdc42 has also been shown to exist in a complex with Rac1, the polarity protein complex known as partitioning defective 6 (PAR6), and protein kinase C (PKC) which has shown to be important for the ability of Rac1 to promote tumorigenesis (Sahai and Marshall, 2002; Wang et al., 2012). Crosstalk has also been observed between Rac1 and RhoA which exist in a double-negative feedback loop with each other. During the protrusion stage of cell migration Rac1 activity is high whilst RhoA activity is low, and during the contraction stage the opposite is occurring. This bistable relationship ensures that separate processes don't impede each other which results in efficient cell migration (Byrne et al., 2016). Rac1 inhibits RhoA through the activation of its GAP, p190RhoGAP (Mammoto et al., 2007). Conversely, RhoA can activate the Rac-GAP ARHGAP22 through ROCK which inhibits Rac1 activity. This suppression of Rac1 by RhoA is particularly notable in cells that migrate with an amoeboid phenotype (Parri and Chiarugi, 2010). Crosstalk between Cdc42 and RhoA has also been shown to be important in polarized cell migration. βPIX interacts with Cdc42 and regulates its localisation and activity at the cell front. At the same time the βPIX-Cdc42 complex binds srGAP1 which is needed to suppress RhoA activity. Depletion of βPIX in fibroblast cells leads to the hyperactivation of RhoA and impairs migration (Kutys and Yamada, 2014).

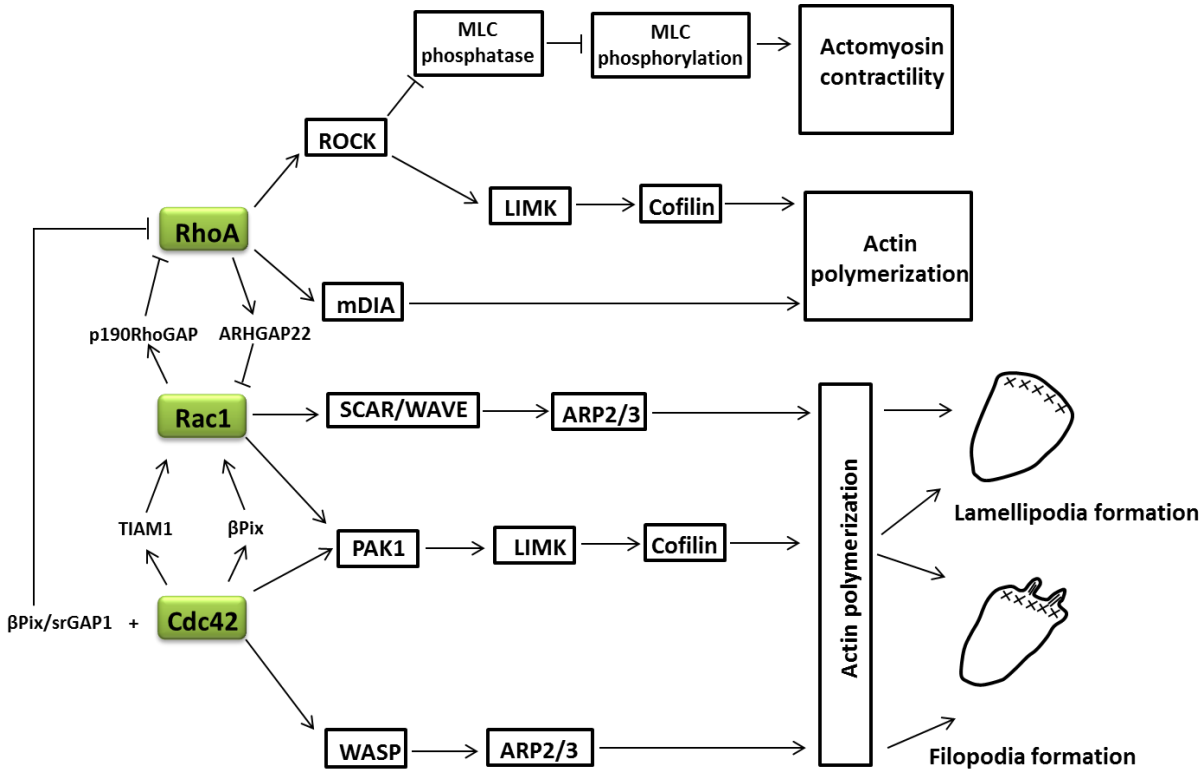

Figure 1.6 Rho GTPase regulated pathways that induce changes in the actin cytoskeleton: Rac1 and Cdc42 induce actin polymerization at the leading edge of the cell through SCAR/WAVE and WASP respectively. Both these nucleation factors complexes activate Arp2/3. Rac1 and Cdc42 can also mediate actin polymerization through PAK1 which acts on LIMK to regulate cofilin. During leading edge protrusion Rac1 and Cdc42 suppress RhoA activation through different mechanisms. RhoA activates ROCK which phosphorylates and inhibits MLC phosphatase leading to an increase in MLC phosphorylation and the generation of actomysoin contractility. RhoA also induces actin filament polymerization through mDIA and ROCK. LIMK is phosphorylated by ROCK which leads to cofilin phosphorylation. During contraction RhoA has been shown to supress Rac1 activity which prevents the further protrusions.

1.3.4 The atypical Rho GTPases in cancer cell migration

Relative to Rac1, Cdc42 and RhoA less is known about how some of the other Rho GTPases, particularly the atypical Rho GTPases, regulate actin cytoskeletal dynamics and cell migration. One atypical GTPase RhoF has been shown to utilise the actin nucleation effectors mDia1 and mDia2 to generate long actin- rich filopodia independent of the canonical Cdc42-WASP-Arp2/3 pathway (Pellegrin and Mellor, 2005). RhoD, which was more recently grouped as an atypical GTPase, was shown to be important in the directed migration of fibroblast cells and involved in the formation of actin stress fibres in fibroblast, cervical, osteosarcoma and glioblastoma cells (Blom et al., 2017). RhoD is believed to activate WHAMM (WASP homologue associated with golgi membranes and microtubules) and FILIP1 (filamin A binding protein). WHAMM binds and regulates the Arp2/3 complex whilst FILIP1 binds and regulates filamin A which is involved in actin filament cross linking (Gad et al., 2012). Interestingly, RhoH actually functions to antagonise Rac1 impairing cortical F-actin assembly and cell migration (Vega and Ridley, 2008).

RhoU is an atypical Rho GTPase that has accumulated quite a bit of attention more in the last decade or so. RhoU, alternatively known as wrch-1, was first identified in 2001 as a Wnt-inducible gene which was reported to be mediating Wnt-driven oncogenic transformation in mouse mammary epithelial cells (Berzat et al., 2005; Tao et al., 2001). RhoU shares significant sequence homology with Cdc42 but has an extended N-terminal proline rich domain which has only been found in one other atypical Rho GTPase, RhoV (Aspenstrom et al., 2007; Faure and Fort, 2011). This domain can bind several SH3 domain-containing proteins including growth factor receptor-bound protein 2 (Grb2), noncatalytic region of tyrosine kinase adaptor protein 2 (Nck1), Src and p120 (Risse et al., 2013). Interaction with Grb2 and Nck1 has been observed to increase the levels of active RhoU in fibroblast cells (Shutes et al., 2004). Conversely, Src, a non-receptor tyrosine kinase, can phosphorylate RhoU at residue Y254 within its c-terminal which leads to the translocation of RhoU from the plasma membrane to endosomes were its GTPase activity is reduced by unknown mechanisms (Alan et al., 2010).

RhoU has been shown to induce and regulate stress fibre formation, cell adhesion and cell migration in neural crest, prostate cancer, cervical cancer, breast cancer, pancreatic cancer, fibroblast and immune cells (Alinezhad et al., 2016; Dart et al., 2015; Fort et al., 2011; Ory et al., 2007; Zhang et al., 2011). RhoU interacts with the epidermal growth factor receptor (EGFR) receptor which leads to an increase in migration speed of pancreatic cancer cells through increased Jun N-terminal kinase (JNK)/ Activator protein 1 (AP1) signalling (Zhang et al., 2011). In a study by Aspenstrom *et al,* pyk2 was identified as a binding partner of RhoU. This interaction was dependent on the presence and activity of Src. The RhoU-pyk2 complex was found to be important for the formation of filopodia and unperturbed cell migration in T-cells (Aspenstrom et al., 2007; Vega and Ridley, 2008). Increased filopodia formation and stress fibre dissolution has also been observed in fibroblasts which are overexpressing RhoU (Saras et al., 2004). In addition to being involved in the formation of filopodia, active RhoU has been observed to localise at podosomes and influence their organisation in osteoclast cells (Brazier et al., 2009).

In a study by Alinezhad *et al* the authors reported that RhoU mRNA expression increased significantly in cancerous prostate tissue relative to benign prostate tissue (Alinezhad et al., 2016). In the same study RhoU was silenced in PC3 prostate cancer cells which led to impaired 2D migration and 3D invasion; however cytotoxicity and proliferative defects which were measured and confirmed in response to RhoU silencing were not controlled for in these assays (Alinezhad et al., 2016).

Cell adhesion turnover is also mediated by the activity of RhoU. In breast cancer cells knockdown of RhoU led to a decrease in the phosphorylation of paxillin which resulted in increased adhesiveness, larger focal adhesions and decreased cell migration (Dart et al., 2015). In a different study, RhoU silencing decreased MLC phosphorylation which resulted in increased adhesiveness and focal adhesion size in Hela S3 cells (Chuang et al., 2007). In the same study, a decrease in AKT and JNK phosphorylation was also observed and believed to be responsible for the migration defect seen in RhoU silenced Hela S3 cells (Chuang et al., 2007). In T-cell acute lymphoblastic leukaemia cells (T-ALL), the expression of RhoU was found to be regulated by neurogenic locus notch homolog protein 1 (NOTCH1), a member of the Notch family.

RhoU depletion induced a rounded morphology and decreased migration, however unlike the previous studies in breast and cervical cancer, decreased adhesion in T-ALL cells (Bhavsar et al., 2013). Similarly, RhoU silenced neural crest cells were observed to have a rounder morphology, reduced migratory and adherence capacity relative to control cells (Fort et al., 2011). These studies collectively show that RhoU is essential in cell adhesion to the ECM; however its specific function may be cell type specific.

RhoU is also known to have several other binding partners implicated in cell migration and adhesion including PAK4, PAK1, and the cytoplasmic tyrosine kinase FAK (focal adhesion kinase) (Dart et al., 2015; Risse et al., 2013; Ruusala and Aspenström, 2008; Tao et al., 2001). However, despite these findings, the complete mechanism of RhoU, along with several other Rho GTPases, is still unclear in cancer cell migration. What currently is relatively well established within the context of Rho GTPase activity is their dependency on lipid modifications such as palmitoylation (as briefly discussed in section 1.3.2). Cancer cells are more dynamically able to regulate intracellular proteins and pathways due to their acquisition of a lipogenic phenotype.

1.4 FASN and the lipogenic phenotype in prostate cancer

1.4.1 Altered metabolism in cancer

It has long been recognised now that cancer cells exhibit alterations in their metabolic activity. This metabolic reprogramming increases the production of metabolic intermediates that are required for the synthesis of proteins, nucleic acids and lipids, all of which are a prerequisite for cancer cells that rapidly proliferate (Baenke et al., 2013). There are currently two distinct and major changes in metabolism, attributing to a shift from catabolic to anabolic metabolism, which separate cancer cells from their normal cell counterparts. The first was identified by Otto Warburg in 1920 and describes an avid consumption of glucose by cancer cells which metabolise it via glycolysis leading to the production of lactic acid and pyruvate (the Warburg Effect) (Flavin et al., 2011). Each glucose molecule that is metabolized produces two pyruvate and four ATP molecules (two used in pathway, so a net of two are produced) (Alfarouk et al., 2014). It is believed cancer cells shifted to relying on glycolysis for several

reasons. Firstly, the reaction produces ATP 100 times faster than mitochondrial oxidative phosphorylation (the main method of metabolism in normal cells). Secondly, glycolysis allows for the production of ATP in the absence of oxygen (anaerobic) which is particularly advantageous for cancer cells trying to adapt to hypoxic conditions (Cairns et al., 2011). The glycolytic end product pyruvate is converted into acetyl-CoA in the mitochondria before entering the tricarboxylic acid cycle (TCA). In cancer the substantial increase in glycolysis leads to a large turnover of acetyl-CoA. Acetyl-CoA is utilised by the second metabolic pathway altered in cancer, *de novo* fatty acid (FA) synthesis (Suburu and Chen, 2012).

The synthesis of fatty acids in both eukaryotes and prokaryotes is crucial for fulfilling a variety of functions in cells, most of which are non-redundant (Maier et al., 2010). Fatty acids are aliphatic acids that serve as long term energy storage compounds yielding large quantities of ATP when metabolised. They also provide structural support in the form of glycerol esters for most cell membranes. Moreover, they have regulatory roles as secondary messengers performing many important roles in metabolic regulation (Maier et al., 2010; Rangan and Smith, 2002).

In normal human tissue *de novo* FA synthesis is suppressed and the expression of lipogenic enzymes is maintained at low levels. Normal cells preferentially rely on lipids that are from the diet to satisfy their metabolic needs. In comparison, increased lipogenesis is a major hallmark for tumour progression with cancer cells switching to dependence on *de novo* fatty acid synthesis in order to sustain rapid cell growth (Zaidi et al., 2013). The main metabolic enzyme responsible for the expression of fatty acids in the cell is fatty acid synthase (FASN) (Flavin et al., 2011).

1.4.2 The structural organisation of FASN

Currently, two classes of FASN have been identified, type I, which is utilised by mammals and fungi, and type II, which is found in archaebacteria and eubacteria. Type I FASN is a large single multifunctional polypeptide and differs from type II FASN which is characterised by discrete monofunctional enzymes (Chirala and Wakil, 2004).

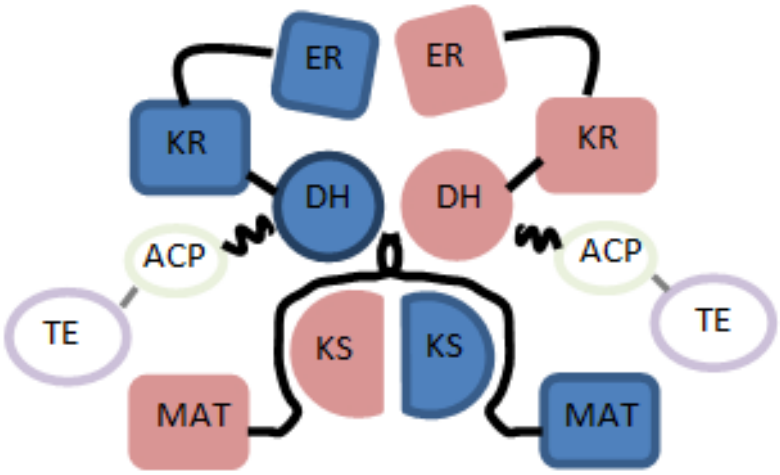

Figure 1.7 Schematic diagram of the structure of Fatty acid synthase: The head-to-head dimer model which is based on two monomers coming together and coiling to essentially form a symmetrical homodimer. Structural enzymes include β-Ketoacyl synthase (KS), malonyl/acetyltransferase (MAT), dehydrase (DH), enoyl reductase (ER), Ketoacyl reductase (KR), acyl carrier protein (ACP), and thioesterase (TE).

Human FASN is a homodimer that consists of two identical protein subunits approximately 250 kDa in size. The protein is characterised by three domains. Domain I contains three catalytic enzymes including β-Ketoacyl synthase (KS), malonyl/acetyltransferase (MAT), and dehydrase (DH). Domain II contains enoyl reductase (ER), Ketoacyl reductase (KR), and acyl carrier protein (ACP), and domain III contains thioesterase (TE) (**Figure 1.7**). These N-terminal domains (domain I) are separated from the C-terminal domains (domain II and III) by a ~640 amino acid long interdomain peptide (Chirala and Wakil, 2004). This interdomain region is believed to play an important role in the architecture of catalytically active FASN through its ability to bring the active centres of each domain together (Chirala et al., 2001).

FASN exists in a head-to-head coiled conformation comprising a body with two "arms", being composed of the dimmers ER and KS, and also the pseudodimeric DH pairs, and two "legs" being made up of the MAT domains (**Figure 1.7**). Due to the inherent mobility of the TE and ACP domains, they are currently unambiguously assigned in this structure (Smith, 2006). However, a reaction chamber exists where the KS and MAT enzymes lie closer to the centre of the dimer allowing for more proficient access to the ACP domain of either monomer (Smith, 2006). Whilst the head-to-head coiled conformation is currently the most accepted model for the structure of FASN, the definitive structure still remains to be elucidated. The identification of hinge regions suggests that the FASN complex may in-fact be able to adopt a wide range of conformations (Chirala and Wakil, 2004).

1.4.3 The function of FASN

The stoichiometry of fatty acyl chain assembly has been well defined in concert with the elucidation of FASN structure (**Figure 1.8**). Prior to the late 1950s it was assumed that fatty acid synthesis was a direct result of mitochondrial β-oxidation pathway reversal which is primarily involved in the degradation of fatty acids (Lynen and Ochoa, 1953). However, the *de novo* biosynthesis of fatty acids in animals actually occurs through a series of decarboxylative condensation reactions which involve sequential condensation of carbon atoms to a growing alkanoic chain (Chirala and Wakil, 2004).

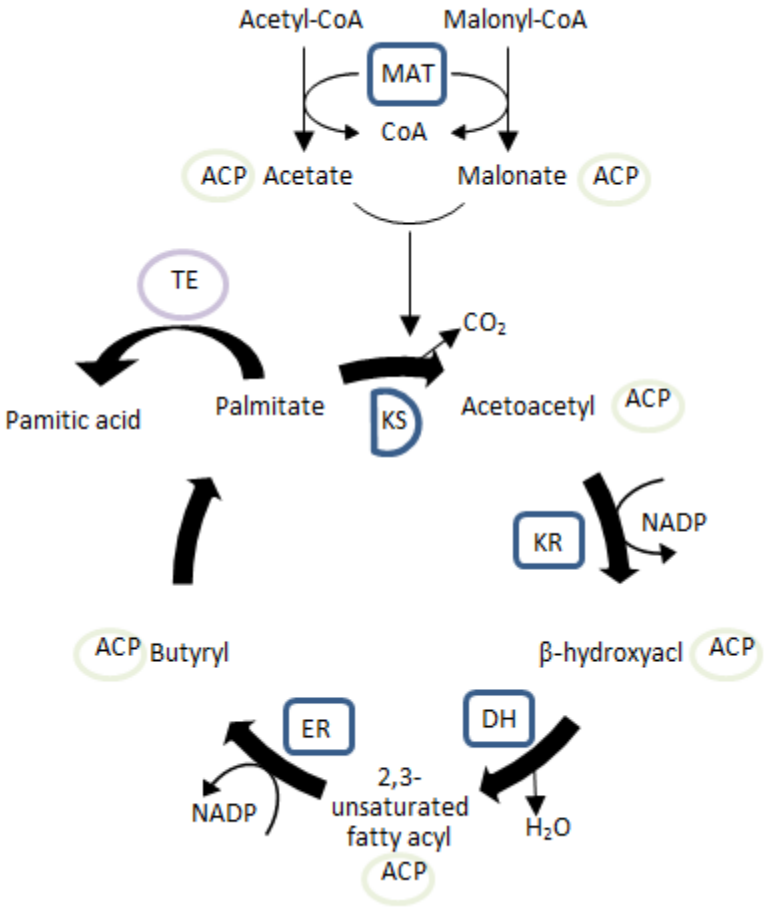

Figure 1.8 Reaction sequence for the biosynthesis of fatty acids by FASN: Decarboxylative condensation sees a stepwise elongation of the starter substrate acetyl-CoA by two carbons donated from malonyl-CoA. MAT initiates substrate loading. Decarboxylative condensation is catalysed by KS, with KR, DH, and ER responsible for modifying the acyl chain β-carbon position until full saturation of the fatty acid.

The process begins with the shuttling of citrate out of the mitochondria where it is converted into oxaloacetate and acetyl-CoA (coenzyme A) by ATP-citrate lyase (ACL). Acetyl-CoA is then transported to the cytoplasm where it is carboxylated by the rate limiting enzyme acetyl-CoA carboxylase (ACC) with the aid of ATP, CO_2, and biotin to form malonyl-CoA. The *de novo* synthesis of fatty acids is regulated by acetyl-CoA carboxylase which itself is regulated in a variety of ways including allosterically by citrate, hormonally by glucagon, epinephrine and insulin, or nutritionally (Naik, 2011). Sequential translocation of primer substrates acetate and malonate from their respective CoA thioester derivatives to the 4'-phosphopantetheine thiol of the ACP domain occurs. The phosphopantetheine contains a prosthetic group which is described as a long flexible arm that aids substrate bound thiol in binding different catalytic sites within FASN (Maier et al., 2010). Transfer of the substrates is catalysed by the monospecific acetyl and malonyl transacylases. Saturated acyl moieties from the acyl-ACP thioester are then transferred to the active cysteine residue of the KS domain. Here, decarboxylation of malonyl moieties yields a reactive carbanion which carries out a nucelophilic attack on the carbonyl carbon of the KS-bound acetyl moiety generating acetoacetyl-ACP and CO_2 from these substrates (Chirala and Wakil, 2004; Naik, 2011; Smith et al., 2003). The β-ketoacyl intermediate, acetoacetyl-ACP, undergoes reduction at the 3-keto group which is catalysed by NADPH dependent β-ketoacyl reductase (KR) to form β-hydroxacyl chain. The β-hydroxacyl product is dehydrated by β-hydroxyacyl dehydratase (DH) to yield a 2,3 unsaturated acyl enzyme. A second reduction by NADPH dependent enoyl reductase (ER) occurs to form a fully saturated four carbon acyl enzyme attached to ACP called butyryl-ACP. The saturated fatty acyl chain is then transferred from the pathetheine –SH group of ACP to the cysteine –SH group of KS by KS freeing ACP to accept a new malonyl residue (Chirala and Wakil, 2004; Naik, 2011; Smith et al., 2003). Thereafter, sequential addition of two carbons derived for malonyl- CoA to the growing acyl chain occurs until a saturated 16-carbon acyl radical called palmitate is synthesised. Overall the synthesis of palmitate requires 50 reactions, most of which are repeated, and a total of seven cycles. Palmitate is covalently attached to the serine side chain of the phosphopantetheine prosthetic group of ACP. It is hydrolysed and liberated from the complex by the enzyme thioesterase as palmitic acid (**Figure 1.8**) (Chirala and Wakil, 2004; Naik, 2011;

Smith et al., 2003). Whilst palmitate is the most abundant fatty acid synthesised by FASN, myristate and stearate have also been recorded to be products of FASN activity (Kuhajda et al., 1994).

1.4.4 FASN expression

In normal tissue, FASN is either expressed at very low levels or is practically undetectable (Thupari et al., 2004). The exception is in the cells of specialised tissue with high lipid metabolism such as liver, adipose, brain, lactating mammary glands, cycling endometrium and type II alveolar cells in the lung (Chirala and Wakil, 2004; Li et al., 2004).

Conversely, FASN has been found to be commonly overexpressed in almost every type of cancer and is associated with their development and progression (Kuhajda, 2006; Menendez and Lupu, 2007). The earliest studies found that the increased expression of Haptoglobin-related protein (Hpr) correlated with poor breast cancer prognosis, recurrence and patient survival (Kuhajda et al., 1989; Shurbaji et al., 1991). Shortly after this observation, Hpr was renamed as oncogenic antigen-519 (OA-519) and then identified as FASN (Epstein et al., 1995). Since then FASN has now been shown to be associated with a poor prognosis, progression and decreased overall survival in several types of cancer including prostate, melanoma, ovarian, gastric, non-small lung, pancreatic, colorectal, osteosarcoma, nasopharyngeal, retinoblastoma, soft tissue sarcoma, endometrium, diffuse large B-cell lymphoma and nephroblastoma (Alo et al., 2007; Camassei et al., 2003a; Camassei et al., 2003b; Cerne et al., 2010; Danilova et al., 2013; Epstein et al., 1995; Gansler et al., 1997; Hou et al., 2012; Innocenzi et al., 2003; Li et al., 2014b; Liu et al., 2012; Ogino et al., 2008; Sugino et al., 2011; Takahiro et al., 2003; Tsuji et al., 2004; Yang et al., 2011a). Additionally, there are other types of cancers which show increased FASN expression but have not as of yet been correlated with patient survival. These include thyroid, kidney, hepatocellular and mesothelium (Gabrielson et al., 2001; Hao et al., 2014; Siraj et al., 2014; Szolkiewicz et al., 2002).

With regards to prostate cancer, FASN has become an increasing attractive target. Several studies have collectively shown that FASN is consistently overexpressed in

prostatic tumour tissue compared with the adjacent normal tissue (Epstein et al., 1995; Swinnen et al., 2002; Tischler et al., 2010; Van de Sande et al., 2005). Moreover, FASN has been shown to be a useful biomarker in prostate cancer development and progression. Increased FASN expression is a common and early event in the development of prostate cancer being detectable in low grade PIN (Swinnen et al., 2002). Further Immunohistochemical staining has shown that different patterns of FASN expression are highly predictive in separating cases with organ-confined disease or capsular penetration versus cases with seminal vesicle invasion or lymph node metastasis (Epstein et al., 1995). FASN expression also correlates with Gleason grade and more importantly increases in castrate-resistant prostate cancer (Epstein et al., 1995; Rossi et al., 2003). In addition to being highly expressed at the protein level, studies have also found FASN to be over-expressed in surgical biopsies of prostate cancer at the mRNA level. More specifically, a DNA microarray carried out using primary prostate cancer tissue as well as established immortalised cell lines showed that out of 400 genes that were differentially regulated from normal tissue, FASN scored in the top 20 with a 5- fold overexpression (Welsh et al., 2001). Similar to protein levels, an increase in the expression of FASN at the mRNA level has also been shown to be associated with the aggressiveness of prostate cancer (Rossi et al., 2003). FASN expression has been noted to increase prior to any noticeable augmentations in phenotype such as active cell proliferation and accumulation of intracellular lipid droplets (Swinnen et al., 2002). This in accordance with all the published findings at this time suggests that FASN contributes strongly towards prostate cancer progression and may be a worthwhile target, even in the latter stages of the disease.

1.4.5 FASN regulation

In non-malignant tissues, FASN expression can be induced by several different mediators, although it is usually tightly regulated (**Figure 1.9**). The transcription of *FASN* can be stimulated by dietary carbohydrates, amino acids, glucagon and insulin. In addition, FASN expression can be stimulated in hormone-sensitive cells, such as the mammary breast glands, by various hormones such as prolactin, estrogen, cortisol, and progestins (Anderson et al., 2007; Fukuda et al., 1999; Katsurada et al., 1990; Sul and

Wang, 1998). Dietary fatty acids, particularly polyunsaturated fatty acids (PUFAs) such as alpha-linolenic (ALA), have been shown to down-regulate FASN expression in the liver and adipose tissue (Moon et al., 2002). However, regardless of their effect on FASN expression, the intake of PUFAs is still linked with an increased risk of developing cancer (Azrad et al., 2013). Sterols and the hormone leptin also repress FASN transcriptionally, and together with PUFAs, these mediators keep cellular lipogenesis in check (Menendez and Lupu, 2007).

Although it is not completely clear, nutritional and hormonal regulation of FASN is thought to transpire through the induction of Phosphatidylinositol-3 kinase (PI3K)/AKT and MAPK signalling (Huang et al., 2016). PI3K/AKT and MAPK transduction pathways affect FASN expression by modulation of its predominant transcription factor, sterol regulatory element-binding protein (SREBP)-1c. SREBP-1c interacts indirectly with proto-oncogene *FBI-1* (Pokemon), a transcription factor of the bric-à-brac tramtrack broad complex/pox viruses and zinc fingers (BTB/POZ) domain family. Together, these proteins synergistically activate the transcription of FASN by acting on the proximal GC-box and SRE/E-box (Choi et al., 2008).

In contrast to normal tissue, FASN expression is not tightly regulated in cancer cells and is typically overexpressed to levels beyond what would ever normally be seen (**Figure 1.9**). One of the main contributors to the overexpression of FASN in cancer is an increase in growth factors and growth factor signalling (Menendez and Lupu, 2007).

Receptor tyrosine kinases c-Met and HER2 (human epidermal growth factor receptor 2) have been shown to regulate FASN expression. An increase in c-Met expression has been correlated with a poor prognosis and progression to androgen independence in prostate cancer (Liu et al., 2013a; Varkaris et al., 2011). In a cohort of radical prostatectomy patients, Immunohistochemical staining revealed that c-Met was overexpressed in 83% of bone metastasis cases (Knudsen et al., 2002). HER2 is a well-recognised oncogene whose activation has been linked with FASN expression in cancer. HER2 is linked to prostate cancer aggressiveness and an increase in its expression is associated with Gleason grade, proliferation, and tumour recurrence (Minner et al., 2010).

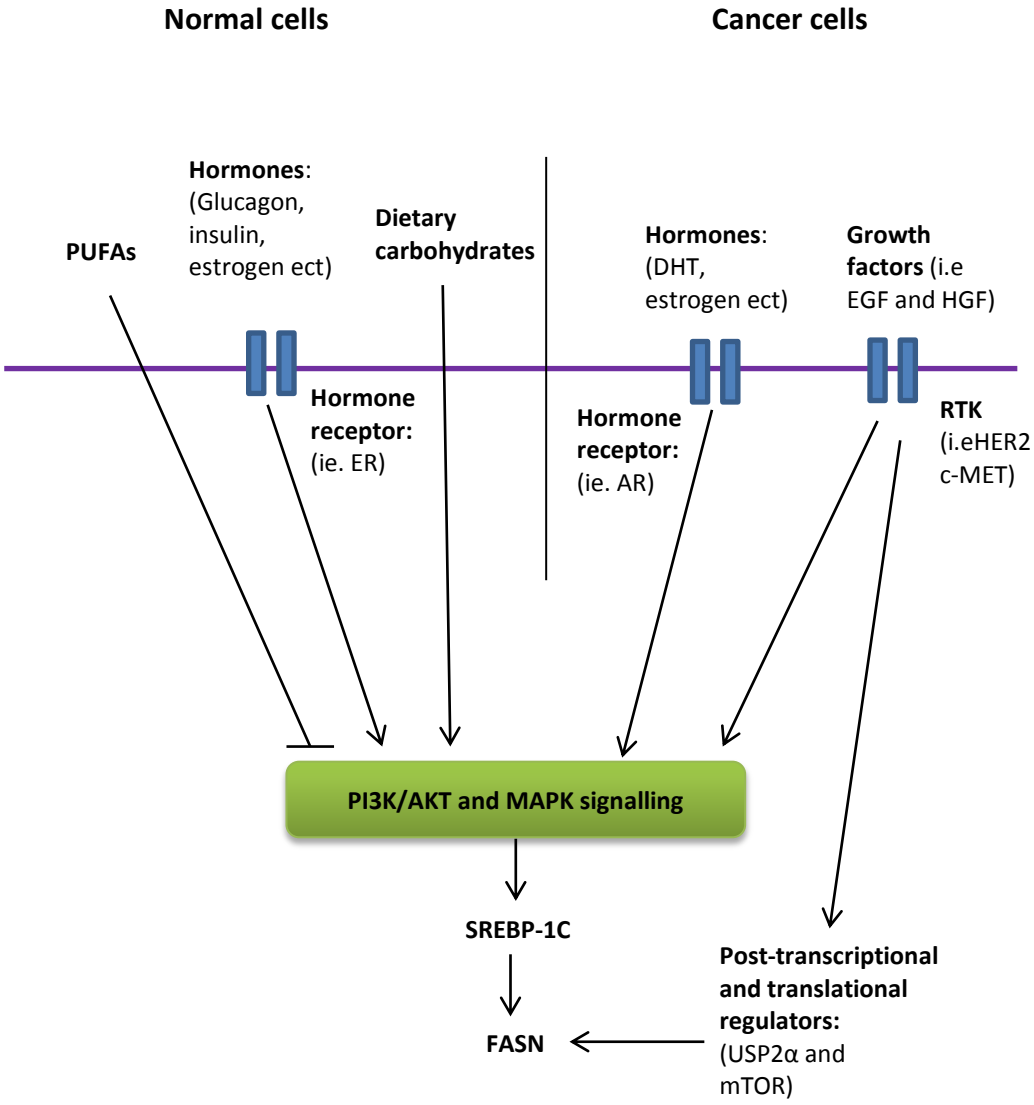

Figure 1.9 Regulation of FASN expression in normal and cancer cells: In normal cells FASN expression is regulated transcriptionally by multiple stimuli (dietary, hormonal, starvation). In cancer cells, FASN expression is regulated transcriptionally by growth factors and hormones. FASN expression can also be regulated via non-transcriptional mechanisms in cancer (mTOR and UPS2α). In both normal and cancer cells most mechanisms activate the PI3K/AKT and MAPK pathways which regulate the major transcription factor for FASN, SREBP1-c.

Stimulation of c-Met and HER2 via their cognate growth factors, HGF and EGF respectively, leads to the downstream activation of the PI3K/AKT and MAPK signalling pathways (Coleman et al., 2009; Saini et al., 2013). Just as in normal tissue, PI3K/AKT and MAPK signalling regulate FASN expression through SREBP-1c (Yang et al., 2002). Interestingly, HER2 signalling has also been shown to regulate FASN translationally through the activation of mammalian target or rapamycin (mTOR) (Yoon et al., 2007).

LNCaP prostate cancer cells are PTEN-null and express a high level of endogenous FASN protein. Treatment of these cells with the PI3K inhibitor LY294002 decreases FASN expression; however this effect is reversed with the introduction of a plasmid that expresses constitutively active AKT. PTEN naturally acts to control PI3K/AKT signalling and when re-introduced into LNCaP cells can decrease FASN expression through restricted PI3K/AKT activation (Van de Sande et al., 2002).

Unsurprisingly, hormones can also drive the expression of FASN in cancer. Stimulation of LNCaP cells with the androgen DHT significantly increases FASN expression through AR activation and SREBP-1c upregulation (Graner et al., 2004). Interestingly, in androgen-independent cell lines PC3 and DU145 FASN expression does not change in the presence of DHT but decreases when the AR is post-translationally degraded (Wen et al., 2016). Stimulation of HER2 has been shown to transactivate overexpressed AR in DU145 cells and induce MAPK-dependent induction of FASN in the absence of DHT (Yeh et al., 1999). These data supports the current notion that androgen receptor signalling still occurs in castrate-resistant prostate cancer (Shafi et al., 2013). FASN expression can also be induced by several other hormones (estrogen, progestins and progesterone) and their respective receptors (estrogen receptor-ER and Progesterone receptor-PR) (Lacasa et al., 2001; Lupu and Menendez, 2006).

FASN has also been shown to be regulated post-transcriptionally by ubiquitin-specific protease-2a (USP2a) in prostate cancer. FASN interacts and is stabilized by USP2a through the removal of ubiquitin which protects it from proteasome degradation. USP2a knockdown leads to a decrease in FASN expression which coincides with a decrease in cell proliferation and the induction of apoptosis in LNCaP cells (Graner et al., 2004).

1.4.6 The lipid network

Palmitate, the primary product of FASN activity, represents about 80% of the total fatty acids in the cell (Kuhajda et al., 1994). Palmitate can undergo further modifications to become secondary fatty acid intermediates that serve specific metabolic and cellular functions. This is accomplished in the mitochondria or at the cytoplasmic face of the endoplasmic reticulum (ER) membrane. Here, elongases and fatty acyl-CoA desaturases insert double bonds or increase the carbon chain length respectively (Vance and Vance, 2008). Esterification of palmitate leads to the generation of several secondary lipids including phospholipids, triacylglyceride (TAG), diacylglyceride, (DAG), lysophosphatidic acid (LPA), phosphatidic acid (PA) and cholesteryl ester (CE) (Zadra et al., 2013). Phospholipids make up the cell and organelle membrane (Schiller and Arnold, 2002). TAG and CE are storage lipids in the cell, although CE is specific to cholesterol storage. DAG, PA and LPA function as secondary messengers in signal transduction pathways and can act both intra- and extracellularly in a paracrine or autocrine manner (Zadra et al., 2013).

It should be noted that there is a degree of metabolic flexibility that alters in cancer. The current findings do suggest that most cancers if not all become more dependent on *de novo* lipogenesis (Rohrig and Schulze, 2016). However, the degree of this dependency can range from high to low in different cancer cells of the same origin or of a different origin. This has been observed in a study by Li *et al* where it was found that two different liver tumour types, hepatocellular carcinoma (HCC) and intrahepatic cholangiocarcinoma (ICC) responded differently to treatment. HCC express high levels of FASN and did not take up any exogenous lipids whilst ICC express low levels of FASN and were found to take up exogenous fatty acids (Li et al., 2016). In a different study it was shown that the breast cancer cell line SK-Br3, which expresses high levels of FASN, was not affected by the supraphysiological addition of linoleic acid or arachidonic acid. However when incubated with linolenic acid the SK-Br3 cells exhibited a strong suppression in their expression of FASN (Menendez et al., 2004b). These data suggest that the dependency and sensitivity of cancer cells to exogenous lipids and *de novo* lipogenesis is complex and could be unique to cancer type, lipid group, and FASN expression level.

1.4.7 The role of FASN in cancer

FASN has been identified to have numerous roles in cancer. One of its better known functions is supporting rapid cellular proliferation which relies heavily on *de novo* fatty acid synthesis (Flavin et al., 2010). Current evidence in the literature suggests that there are two lipogenic checkpoints in the cell cycle which occur at the G_2/M phase and the G_1/S phase (Scaglia et al., 2014). For these checkpoints to progress a sufficient supply of phospholipids must be available for the membrane expansion of rapidly proliferating cells. FASN overexpression typically means that cancer cells have a large pool of phospholipids available to carry out this function. Moreover, since FASN activity is not restricted in cancer cells there is very little reason that whilst under stable conditions, continuous cell growth cannot occur (Currie et al., 2013). The silencing or inhibition of FASN has been show to decrease the proliferation rate of almost every type of cancer including prostate, breast , lung, ovarian, colorectal, pancreatic , osteosarcoma, retinoblastoma, nasopharyngeal and liver (Daker et al., 2012; Deepa et al., 2013; Hu et al., 2016; Nishi et al., 2016; Singh et al., 2015; Veigel et al., 2015; Ventura et al., 2015; Yoshii et al., 2013; Zaytseva et al., 2012; Zecchin et al., 2011; Zhou et al., 2015).

In addition, a significant proportion of studies also found that targeting FASN is cytotoxic to cancer cells (De Schrijver et al., 2003). Interestingly, one study showed that unlike in cancer cells, FASN inhibition in the normal mouse embryonic fibroblast cell line NIH 3T3 and Müller glial cell line MIO-M1 did not affect cellular proliferation or induce toxicity (Deepa et al., 2012). This highlights a greater dependency on FASN in cancer cell growth and survival. Reduced viability in response to FASN inhibition could be due to numerous factors in addition to lipid starvation. FASN blockade has been shown to induce cell cycle arrest through SKP2 (S phase kinase-associated protein 2) downregulation. SKP2 is an F-box protein of SCF family of ubiquitin ligases and is known to be a negative regulator of cyclin-dependent kinase inhibitors of the Rb pathway including p21, p27, p57 and p130 (Deepa et al., 2013; Knowles et al., 2004). In addition, inhibition of FASN in breast cancer cells led to an increase in the nuclear ratio of BRCA1, a tumour suppressor protein, as well as induced the nuclear translocation of nuclear transcription factor- κB (NF- κB), a factor which has been shown to have both apoptotic and anti-apoptotic roles in cancer (Menendez et al., 2004a).

FASN inhibition can also lead to cell death through the toxic accumulation of malonyl-CoA. Since malonyl-CoA is no longer being utilised in the fatty acid synthesis pathway its levels increase which inhibits carnitine palmitoyltransferase (CPT1) (involved in β-oxidation) resulting in the up-regulation of ceramide and the induction of pro-apoptotic genes BNIP3, TRAIL, and DARK2 (Bandyopadhyay et al., 2006). The inhibition of FASN also leads to the inactivation of the PI3K/AKT/mTOR signalling pathway which is a well-known intracellular pro-survival system. AKT phosphorylates and inhibits the pro-apoptotic Bcl-2 family members Bad and Bax, caspase-3, caspase-9, GSK-3 and FOXO1. mTOR phosphorylation activates S6K1 and 4EBP1, two proteins which control cell division and protein biosynthesis (Dhanasekaran et al., 2008; Wagner et al., 2017). A decrease in DAG lipids as a result of FASN inhibition has also been shown to contribute to cancer cell death (Benjamin et al., 2015). DAG activates PKC which is involved in regulating the cell cycle through cycle regulatory molecules such as the cyclin-dependent kinases (CDK), CDK inhibitors and cdc25 phosphatases (Black and Black, 2012).

FASN is also known to induce changes in the plasma membrane fatty acid composition. Saturated fatty acids produced by FASN increase the size of the cell membrane and partition into detergent-resistant lipid raft domains at a higher rate than exogenously derived mono-and polyunsaturated fatty acids. These lipid rafts have been implicated in a variety of functions including stabilization of signalling receptors, intracellular trafficking, cell polarization and cell migration. A study by Swinnen *et al* showed that FASN inhibition significantly reduced lipid incorporation into the membrane which destabilised lipid raft-aggregates (Swinnen et al., 2003). The dynamics of the lateral and transversal membrane are also altered in cancer cells due to the more dense packing of saturated fatty acids compared to mono-and polyunsaturated fatty acids. Normally, the transversal mobility of membrane components, also referred to as “flip-flop”, occurs at a low rate unless facilitated by specific transporters. Commonly used chemotherapeutics such as doxorubicin use passive flip-flop as a mechanism of entry into cells, however there entry is restricted in cancers with “dense” membranes. A study by Rysman *et al* showed that the silencing of FASN significantly sensitized prostate cancer cells and breast cancer cells to doxorubicin-induced cytotoxity (Rysman et al., 2010). Breast cancer MCF7 cell clones generated to overexpress FASN

showed the opposite effect to FASN inhibition and the cells become more resistant to the chemotherapeutic drugs Adriamycin and mitoxantrone (Liu et al., 2008). Due to FASN playing a role in resistance, it has been suggested to treat cancer patients with FASN inhibitors in combination with the standard chemotherapy drugs (Blancafort et al., 2015; Flavin et al., 2010).

FASN is also thought to play an important role in cell survival through the initiation of angiogenesis (Seguin et al., 2012; Zaytseva et al., 2014). Neovascularisation is an important process during metastasis creating microvascular networks that supply oxygen and nutrients to the cells. FASN modulates tumour angiogenesis through differential expression of vascular endothelial growth factor-A (VEGF-A) isoforms. In melanoma and colorectal cancer cells, FASN inhibition led to the down-regulation of the pro-angiogenic isoform $VEGF^{189}$ and up-regulation of the anti-angiogenic isoform $VEGF^{165b}$ (Seguin et al., 2012; Zaytseva et al., 2014). When the FASN silenced colorectal cancer cells were implanted into the colonic submucosa of athymic mice a significant decrease in microvessel density and the diameter of blood vessels was observed when compared to control cells (Zaytseva et al., 2014).

1.4.8 Linking FASN to cancer cell migration and invasion

When FASN was originally discovered and studied it was thought that its only functions in cancer were to act as an energy source in conjunction to glycolysis, and synthesise the necessary metabolic products required for cellular proliferation. It was soon identified that FASN expression correlated with pathological stage and a poor prognosis (Epstein et al., 1995; Kuhajda et al., 1989). Despite these clinical findings, which were observed almost 30 years ago, it is only within the last decade that FASN has been considered as a marker of metastasis and its role in this process being researched. During this time it has been difficult to identify the exact underlying mechanisms through which FASN induces cell migration and invasion. This in part is due to the complex nature of the lipid network that sits downstream of FASN.

Currently, the majority of studies in the literature seem to suggest that FASN may be driving cell migration through activation of the PI3K/AKT pathway. AKT has been

reported to induce the migration and invasion of prostate cancer cells through activation of the Rho GTPase Rac1 (Henderson et al., 2015). The silencing of FASN has been shown to suppress PI3K/AKT signalling and impair cell migration in osteosarcoma and colorectal cancer cells (Coleman et al., 2009; Li et al., 2012a; Wang et al., 2013b). In addition, FASN inhibition with the flavonoid luteolin has been found to block AKT phosphorylation and impair HGF-induced scattering of DU145 cells (Coleman et al., 2009). In these studies the PI3K/AKT pathway is activated by the stimulation of either the HER2 or c-Met receptor. FASN and PI3K/AKT exist in a positive feedback loop and it is likely that FASN is regulating PI3K/AKT signalling through modulation of the upstream receptor tyrosine kinases. FASN is able to regulate c-Met and HER2 post-translationally though palmitoylation which regulates the receptors raft binding affinity and stabilises them at the membrane (Anderson and Ragan, 2016; Coleman et al., 2016; Levental et al., 2010). The implications of protein palmitoylation in cancer will be discussed in more detail in the next section of this chapter.

Alternatively, some studies have suggested an opposing paradigm whereby the PI3K/AKT pathway modulates FASN to induce cell migration and invasion (Long et al., 2014; Zhou et al., 2015). Osteocarcinoma cells treated with the PI3K/AKT inhibitor LY294002 show a decrease in FASN levels and have a reduced migratory and invasive capacity compared to control cells (Wang et al., 2014; Zhou et al., 2015). The consequence of this bi-directional relationship between FASN and the PI3K/AKT pathway has meant it has remained unclear as to exactly what proteins in this signalling axis are inducing a migratory phenotype.

In addition to activating the PI3K/AKT signalling pathway it was also shown in a study by Zhou *et al* that the regulation of HER2 by FASN increases glycolysis and migration in breast cancer cells (Zhou et al., 2016). In this study, the migration of MCF-7 cells treated with the FASN inhibitor cerulenin was tested in a wound healing assay and a transwell migration assay for 48 hours. Wound closure and trans-migration of cerulenin treated MCF-7 cells was found to decrease relative to control cells, although it should be noted that in these assays proliferation defects and inhibitor cytotoxity was not measured (Zhou et al., 2016). When investigating metabolic disparities, Zhou *et al* found that there was a decrease in glucose uptake and lactate production in

cerulenin treated MCF-7 cells indicating a change in glycolysis. Glycolysis results in the generation of citrate which is converted into acetyl-CoA, one of the primer substrates used by FASN. It is likely that the increase in glycolysis enhances FASN activity and increases the subsequent oncogenic signalling which leads to a more invasive and migratory phenotype (Zhou et al., 2016).

FASN has been found to be overexpressed in many primary tumours where it is believed to contribute to growth and survival. Less is known about its role in regulating the progression of cancer to a metastatic phenotype; however two studies have observed that FASN overexpression is associated with metastatic transformation. Gonzalez-Guerrico *et al* found that FASN overexpression in the normal breast cancer cell line MCF10A led to the upregulation of several mesenchymal markers including vimentin, N-cadherin and fibronectin. Conversely, the epithelial marker E-cadherin was downregulated in these cells. When comparing the FASN overexpressing MFC10A cell line to the wild-type they found the former produced tumourspheres which lacked a lumen indicating invasive behaviour (Gonzalez-Guerrico et al., 2016). Similarly, in another study it was found that the stable overexpression of FASN in the ovarian cancer cell line SW626, which normally expresses very low levels of FASN, induced the expression of several EMT markers including N-cadherin, vimentin, slug and snail. The expression of these markers correlated with a greater migratory and invasive capacity in the cells when compared to wild-type SW626 cells (Jiang et al., 2014). It is currently unclear how FASN is involved in regulating EMT in cancer. One study by Yang *et al* suggests that FASN and the EMT-inducing cytokine TGF-β1 (transforming growth factor beta 1) exist in a positive feedback loop which induces EMT in non-small cell lung cancer (Yang et al., 2016). However, this seems to be dependent on the cell type being cisplatin-resistant as TGF-β1 signalling suppressed FASN expression in non-small cell lung cancer cells that were not cisplatin-resistant (Yang et al., 2016).

Proteins involved in cell adhesion turnover, a key process of cell migration, have also been linked to FASN expression. The phosphorylation of FAK and paxillin were observed to decrease in FASN inhibited or silenced melanoma and colorectal cancer cells (Cao et al., 2015; Zaytseva et al., 2012). Additionally, in the study by Cao *et al*, phosphorylation of the adaptor protein Gab1 (GRB2-associated-binding protein 1),

PAK1 and PAK2 also decreased in response to FASN inhibition (Cao et al., 2015). Whilst in the study by Zaytseva *et al,* phosphorylation of Src and the total levels of the cell surface glycoprotein CD44 and the Rho GTPase RhoA were observed to decrease in response to FASN knockdown (Zaytseva et al., 2012). All these proteins have previously been shown to be involved in cell motility and there suppression in response to FASN inhibition also correlated with a defect in migration in their respective studies (Cao et al., 2015; Coleman et al., 2009; Zaytseva et al., 2012).

In a study by Yoshii *et al* , the migration of LNCaP prostate cancer cells decreased in response to the silencing of FASN with siRNA (Yoshii et al., 2013). In this study they performed a DNA microarray analysis and found one of the most significantly down-regulated genes was RAP2B. RAP2B is part of the RAP family of small GTP-binding proteins and is known to induce cytoskeletal reorganisation (Di et al., 2015b). RAP2B has been shown to induce proliferation, migration and invasion in breast cancer cells through ERK1/2 signalling (Di et al., 2015a). Further work has not currently been done to confirm whether RAP2B is indeed a key protein in FASN-induced cell migration.

More recently a study found that FASN induced colorectal cancer cell invasion through the Wnt signalling pathway. The silencing of FASN impaired the invasive capacity of the colorectal cancer cell lines HT-29 and SW40 through matrigel and led to the downregulation of the Wnt signalling proteins Wnt5a, Wnt5b and Fzd2 (Wang et al., 2016). These Wnt proteins are known to target β-catenin and together redistribute E-cadherin, increase the expression of MMP7, and increase the activity of Cdc42 and Rac1 (Iwai et al., 2010). The re-introduction of FASN into the FASN depleted colorectal cancer cell lines led to the re-expression of the Wnt proteins and rescued the invasive phenotype (Wang et al., 2016).

The findings from these studies indicate that FASN is linked to a plethora of proteins implicated in the migration and invasion of cancer. However, what is not known is exactly how FASN expression or activity regulates these proteins. Currently, the vast majority of studies, if not all, have silenced or inhibited FASN, and shown that a protein associated with motility downstream has become altered. What is not clear is how these proteins are being modulated by FASN, i.e through binding, pathway activation, transcriptionally or lipid-mediated. Moreover, there is currently vastly underwhelming

evidence which directly links FASN to the Rho GTPase proteins which are key regulators of the cytoskeleton and cell migration. RhoA expression has been shown to decrease in FASN silenced colorectal cancer cells; however why this occurs mechanistically remains to be elucidated (Zaytseva et al., 2012). In addition, no other Rho GTPases have been studied as potential targets of FASN in cancer which is somewhat surprising given that there activity at the membrane is partly dependent on lipid modification (see previous section on Rho GTPase regulation by lipids- 1.3.2). Furthermore, this thesis is focussing more specifically on the role of FASN in AR-independent prostate cancer. To date, it has not been shown if the direct involvement of FASN is essential in AR-independent prostate cancer migration.

1.4.9 The palmitoylated protein signalling network

FASN is responsible for the synthesis of palmitate, the most abundant fatty acid produced in cancer cells (Zadra et al., 2013). Most studies looking at the effects of *de novo* lipogenesis in cancer are usually more concerned with the secondary lipids that are formed from palmitate esterification. However, palmitate is also involved in the post-translational modification of proteins in a process known as palmitoylation (also see previous section on Rho GTPase regulation by lipids- 1.3.2 for more details) (Aicart-Ramos et al., 2011).

The palmitoylation of protein thiols can occur spontaneously and non-enzymatically if palmitoyl-CoA is enriched within specific membrane microdomains. However, protein palmitoylation is catalysed much more rapidly by the palmitoylating enzymes known as the DHHC palmitoyltransferases (PATs) (Guan and Fierke, 2011). PATs are characterised by a DHHC (Asp-His-His-Cys) motif and exist in a highly diverse family with 23 members currently identified in humans (Blaskovic et al., 2013; Guan and Fierke, 2011). It is currently unclear why cells express multiple DHHC PATs and what determines their specificity for particular substrates. The SNAP receptor (SNARE) protein SNAP25 has been observed to be modified by DHHC3, DHHC7 and DHHC17 (Greaves et al., 2009). In contrast the integrin receptor α6β4 is specifically modified by DHHC3 only (Sharma et al., 2012a). The N-terminal and C-terminal cytosolic domains of

DHHC proteins have been shown to greatly vary amongst family members and may contain sequences which mediate specific protein-protein interactions (Blaskovic et al., 2013).

Whilst the DHHC proteins are primarily involved in the S-palmitoylation of cysteine residues, a lesser studied group of proteins known as MBOAT (Membrane bound O-acyl transferase) have been identified to mediate O-palmitoylation of serine and threonine residues. Currently 16 MBOAT members have been identified with three being involved in protein acylation including Hedgehog acyltransferase (Hhat), Porcupine (Porcn) and Ghrelin O-acyltransferase (GOAT) (Resh, 2016).

Palmitoylated proteins can also undergo deacylation in the cytosol. This process is carried out enzymatically by acyl protein thioesterases (APTs) which act to remove the acyl moiety from the protein (Aicart-Ramos et al., 2011). Three APTs have so far been identified including APT1, APT2 and APT-1 like (Blaskovic et al., 2013). Similar to DHHC PATs, specific proteins are targeted by APTs for deacylation i.e APT1 depalmitoylates Gα proteins whilst APT2 depalmitoylates growth-associated protein-43 (GAP43) (Blaskovic et al., 2013).

Palmitoylation has been shown to be essential for protein function and stability. One example of this was seen in study by Anilkumar *et al* where they found the function and localisation of the metalloproteinase MMP14 to be dependent on palmitoylation. When palmitoylation was blocked MMP14 was unable to internalize and cell migration was significantly impaired in HT1080 fibroblast cells (Anilkumar et al., 2005). In another study the function and stability of the chemokine receptor CCR5 was found to be dependent on palmitoylation. Inhibition of S-acylation led to CCR5 accumulating intracellularly with kinetic experiments showing a profound decrease in its half-life which eventually lead to a reduction in the total expression of CCR5 (Percherancier et al., 2001).

To date 300 proteins have been identified to undergo palmitoylation and thus essentially exist in a palmitoylated protein signalling network downstream of FASN (Martin and Cravatt, 2009). Despite this, there are only a few studies which have looked into the repercussions of blocking FASN activity on downstream protein

palmitoylation events. One study by Bollu *et al* has shown that FASN inhibition decreases EGFR palmitoylation in PC3 prostate cancer cells. This prevented EFGR dimerization and kinase activation and even led to protein degradation after 24 hours. As expected the downstream signalling of EGFR was abolished and PC3 cell proliferation was significantly impaired (Bollu et al., 2015). Another study by Coleman *et al* found c-Met palmitoylation was dependent on FASN activity (Coleman et al., 2009; Coleman et al., 2016). Prevention of c-Met palmitoylation targeted the receptor for degradation and attenuated downstream AKT signalling which impeded the ability of DU145 cells to scatter in response to HGF (Coleman et al., 2009).

Conversely, the overexpression of FASN has also been shown to alter the palmitoylation status of proteins. Immortalised prostate epithelial cells (iPrEC) stably overexpressing FASN showed a significant increase in Wnt1 palmitoylation which caused β-catenin to become active and accumulate at the membrane and cytoplasm. Orthotopic transplantation of iPrEC cells overexpressing FASN in nude mice resulted in invasive tumours when compared to mice transplanted with wild-type iPrEC cells (Fiorentino et al., 2008).

The findings from these studies highlight the importance of FASN dependent palmitoylation in both a normal and tumour based setting. It is yet to be shown if targeting FASN affects the palmitoylation of cytoskeletal regulating proteins such as the Rho GTPases.

1.5 Aims of the project

In this thesis, the following aims will be investigated:

1. Characterise the effect of FASN knockdown on AR-independent prostate cancer proliferation, metabolism and cell morphology.
2. Assess if FASN knockdown alters any aspects of motility in AR-independent prostate cancer cells including adhesiveness, 2D migration and 3D invasion.
3. Identify an underlying mechanism through which FASN could be driving a more motile phenotype in AR-independent prostate cancer.
4. Perform a pilot patho-epidemiological study using radical prostatectomy samples to assess if the expression of FASN, along with any proteins identified in the mechanistic studies, is associated with prostate cancer severity.

Chapter 2

Materials and Methods

Chapter 2 – Materials and Methods

2.1 Materials

2.1.1 General Materials

1-Biotinamido-4-[4'-(meleimidomethyl)cyclohexanecarboxamido]butane (Biotin-BMCC) (**ThermoFisher Scientific, USA**)

2-bromopalmitate (2BP) (**Sigma-Aldrich, UK**)

3-(4,5-Dimethylthiazol-2-yl)-2,5-Diphenyltetrazolium Bromide (MTT) (**Sigma-Aldrich, UK**)

4-(2-hydroxyethyl)-1-piperazineethanesulfonic acid (HEPES) (**A&E Scientific**)

4-Methylene-2-octyl-5-oxotetrahydofuran-3-carboxylic acid (C75) (**BioVision**)

4', 6-diamidino-2-phenylindole (DAPI) (**Sigma-Aldrich, UK**)

Acrylamide (30%) (**Severn Biotech Ltd, UK**)

Agarose (**Invitrogen, UK**)

Ammonium persulfate (APS) (**Sigma-Aldrich, UK**)

Ampicillin (**Sigma-Aldrich, UK**)

Aprotinin (**Sigma-Aldrich, UK**)

BD Matrigel^{TM} Basement Membrane Matrix (**BD Biosciences, UK**)

Beta (β)- mercaptoethanol (**Sigma-Aldrich, UK**)

Bovine pituitary extract (BPE) (**ThermoFisher Scientific, USA**)

Bovine serum albumin (BSA) (**VWR International, UK**)

Bovine serum albumin (BSA)- Fatty acid free (**VWR International, UK**)

Bromophenol blue (**Bio-Rad, UK**)

Calcium phosphate transfection kit (**Invitrogen, UK**)

Cell dissociation buffer (**Sigma-Aldrich, UK**)

Deoxyribonucleotide triphosphate (dNTPs) (**New England Biolabs, UK**)

DH5α^{TM} competent *Escherichia coli (E. coli)* cells (**Invitrogen, UK**)

Dimethyl sulfoxide (DMSO) (**Sigma-Aldrich, UK**)

Dithiothreitol (DTT) (**Sigma-Aldrich, UK**)

Dulbecco's Modified Eagle's Medium (DMEM) (**Sigma-Aldrich, UK**)

DNA ladder (**New England Biolabs, UK**)

Epidermal growth factor (EGF) (**ThermoFisher Scientific, USA**)

Enhanced chemiluminescence (ECL) Prime western blotting detection reagent (**GE Healthcare Life Sciences, UK**)

Ethanol (**BDH Laboratory Supplies, UK**)

Ethidium bromide (**ThermoFisher Scientific, USA**)

Ethylenediaminetetraacetic acid (EDTA) (**Sigma-Aldrich, UK**)

Fibronectin (**Sigma-Aldrich, UK**)

FluorSave™ Reagent (**Calbiochem, UK**)

Foetal bovine serum (FBS) (**GIBCO®, Invitrogen, UK**)

FuGene 6 (**Promega, UK**)

Formaldehyde (**ThermoFisher Scientific, USA**)

X-ray film (**Scientific Laboratory Supplies, UK**)

Gentamycin (**Sigma-Aldrich, UK**)

G418 sulphate (**Cayman Chemical, USA**)

GFP-TRAP (**ChromoTek, Germany**)

Glycerol (**Sigma-Aldrich, UK**)

Glycine (**Sigma-Aldrich, UK**)

HCl (**VWR International, UK**)

Hepatocyte growth factor (HGF) (Recombinant Human) (**R&D systems, USA**)

Hydroxylamine solution (**Sigma-Aldrich, UK**)

Kanamycin solution (**Sigma-Aldrich, UK**)

Keratinocyte serum free media (KSFM) (**ThermoFisher Scientific, USA**)

Leupeptin (**Sigma-Aldrich, UK**)

Luria-Bertani agar (LB-agar) (**Sigma-Aldrich, UK**)

Luria-Bertani broth (LB-broth) tablets (**Sigma-Aldrich, UK**)

Magnesium Chloride ($MgCl_2$) (**Sigma-Aldrich, UK**)

Methanol (**VWR International, UK**)

Milk powder (**Marvel, UK**)

NEB®-10 beta competent *E.coli* cells (high efficiency) (**New England Biolabs, UK**)

N-Ethylmaleimide (**Sigma-Aldrich, UK**)

Nitrocellulose membrane (**PerkinElmer, UK**)

Nonidet™ P40 substitute (NP-40) (**Sigma-Aldrich, UK**)

Nuclease-free water (**ThermoFisher Scientific, USA**)

OptiMEM (**Invitrogen, UK**)

Orlistat (**Sigma-Aldrich, UK**)

Paraformaldehyde (PFA) (**Sigma-Aldrich, UK**)

Penicillin-Streptomycin (**Sigma-Aldrich, UK**)

Phenylmethylsulfonylfluoride (PMSF) (**Sigma-Aldrich, UK**)

Phosphate buffered saline (PBS) tablets (**Oxoid Limited, UK**)

Dulbecco's PBS with Calcium and Magnesium (**GIBCO®, Invitrogen, UK**)

Dulbecco's PBS without Calcium and Magnesium (**LONZA, UK**)

Pierce™ ECL western blotting substrate (**ThermoFisher Scientific, USA**)

Precision Plus Protein™ All Blue standards (**Bio-rad, UK**)

Precision Plus Protein™ dual colour standards (**Bio-rad, UK**)

Protein A Agarose beads (**Invitrogen, UK**)

Protein G Sepharose® beads, Fast Flow (**Sigma-Aldrich, UK**)

Purelink® HiPure Plasmid Filter Maxi-prep kit (**Invitrogen, UK**)

Puromycin (**Sigma-Aldrich, UK**)

REDTaq® ReadyMix™ PCR Reaction Mix (**Sigma-Aldrich, UK**)

Rhodamine Phalloidin (**ThermoFisher Scientific, USA**)

RNeasy® Mini Kit (**Qiagen, Germany)**

Roswell Park Memorial Institute (RPMI)-1640 medium (**Sigma-Aldrich, UK**)

Sodium Chloride (NaCl) (**Sigma-Aldrich, UK**)

Sodium dodecyl sulphate (SDS) (**Sigma-Aldrich, UK**)

Sodium deoxycholate (**Sigma-Aldrich, UK**)

Sodium fluoride (NaF) (**Alfa Aesar, UK**)

Sodium hydroxide (NaOH) (**Sigma-Aldrich, UK**)

Sodium orthovanadate (Na_3VO_4) (**New England Biolabs, UK**)

SuperScript® VILO™ cDNA Synthesis Kit (**ThermoFisher Scientific, USA**)

Tetramethylethylenediamine (TEMED) (**Sigma-Aldrich, UK**)

Tris-base (**Sigma-Aldrich, UK**)

Triton X-100 (**VWR International, UK**)

Tween® 20 (**VWR International, UK**)

Type I rat tail collagen (**Corning, USA**)

2.1.2 Buffers

Blocking solution: 5% w/v milk powder or 5% w/v BSA in Tris buffered saline (TBS)-Tween

GFP-Trap wash/dilution buffer: 10 mM Tris-HCl pH 7.5, 150 mM NaCl, 5 mM EDTA.

GFP-Trap Lysis buffer: 10 mM Tris-HCl pH 7.5, 150 mM NaCl, 5 mM EDTA, 0.5% NP-40

Gel Sample buffer (2x): 100 mM Tris-HCl pH 6.8, 4% w/v SDS, 20% v/v glycerol, 2% β-mercaptoethanol, 0.2% w/v bromophenol blue.

Gel Sample buffer (6x): 375 mM Tris-HCl pH 6.8, 10% w/v SDS, 30% v/v glycerol, 6% β-mercaptoethanol, 0.2% w/v bromophenol blue.

Mild stripping buffer: 25 mM Glycine pH 2, 1% w/v SDS

Palmitoylation buffer 1: 1 M hydroxylamine, 50 mM Tris, 150 mM NaCl, 5 mM EDTA, 0.2% Triton X-100, pH 7.4

Palmitoylation buffer 2: 4 μM BMCC-Biotin, 50 mM Tris, 150 mM NaCl, 5 mM EDTA, 0.2% Triton X-100, pH 6.2

Protease inhibitor cocktail: 1 mM DTT, 10 μg/ml leupeptin, 1 μg/ml aprotinin, 10 mM PMSF, 10 mM NaF, 1 mM Na_3VO_4

RIPA buffer: 20 mM Tris-HCl pH 7.4, 150 mM NaCl, 1 mM EDTA, 1% v/v Triton X-100, 0.5% w/v SDS, 1% w/v sodium deoxycholate

Sodium dodecyl sulphate-polyacrylamide gel electrophoresis (SDS-PAGE) running buffer (10x): 250 mM Tris-base, 1.92 M Glycine, 1% w/v SDS. Dilute to 1 x with distilled water for use

SDS-PAGE transfer buffer (10x): 250 mM Tris-base, 1.92 M Glycine. Dilute to 1 x with distilled water and methanol (20 % v/v) for use

(Tris acetate EDTA) TAE buffer: 40 mM Tris-HCl, 20mM acetate 10 mM EDTA in ddH_20

TBS-Tween (TBST): 25 mM Tris-HCl pH 7.6, 50 mM NaCl, 0.1% v/v Tween 20

2.1.3 Plasmids

Construct	Backbone	Source
GFP	pEGFP-N1	Kind gift from Professor Mark Evers, University of Kentucky
GFP-FASN	pEGFP-N1	Kind gift from Professor Mark Evers, University of Kentucky
GFP-RhoU	pEGFP-C1	Claire Wells group, King's College London
GFP-Rac1	pcDNA/4/TO	Kind gift from Stephen Terry, Eggert group, King's College London
GFP-Cdc42 (prenylated)	pEGFP-C1	Bought from Addgene (Alaa El-Husseini Lab - Addgene plasmid # 20142)
GFP-Cdc42 (palmitoylated)	pEGFP-C1	Bought from Addgene (Alaa El-Husseini Lab - Addgene plasmid # 20141)

Table 2.1 Constructs list

2.1.4 Primers

Gene	5'-3' sequence
Cdc42 Forward	taactcaccactgtccaaagactc
Cdc42 prenylated Reverse	tcatagcagcacacacctg
Cdc42 palmitoylated Reverse	gtttagaatatacagcacttccttttgg
β-actin Forward	catgtacgttgctatccaggc
β-actin Reverse	ctccttaatgtcacgcacgat

Table 2.2 List of Primers

2.1.5 Antibodies list

Antibody	Species	Company	Dilution for IF/IHC	Dilution for WB
AKT	Rabbit	Cell Signalling Technology	-	1:1000
Phospho AKT (ser473)	Rabbit	Cell Signalling Technology	-	1:1000
β-tubulin	Mouse	Sigma-Aldrich	-	1:1000
Cdc42	Rabbit	Cell Signalling Technology	-	1:1000
c-Met	Rabbit	Santa-Cruz	-	1:250
Phospho c-Met (Tyr1234/Tyr1235)	Rabbit	Cell Signalling Technology	-	1:1000
ERK (p42/44)	Rabbit	Cell signalling Technology	-	1:1000
Phospho ERK (p42/44) (Thr202/Thr204)	Rabbit	Cell signalling Technology	-	1:1000
FASN	Mouse	BD transduction laboratories	-	1:1000
GFP	Mouse	Roche	-	1:1000
HSP90	Rabbit	Santa-Cruz	-	1:2500
IgG mouse	Mouse	Santa-Cruz	-	1:330
IgG rabbit	Rabbit	Santa-Cruz	-	1:330
Paxillin	Mouse	BD transduction laboratories	1:100	1:2000

Phospho Paxillin (Ser272)	Rabbit	Invitrogen	-	1:1000
Rac1	Mouse	Millipore	-	1:1000
RhoU	Rabbit	Abcam	-	1:1000

Table 2.3 Primary antibodies

Antibody	Species	Company	Dilution for IF/IHC	Dilution for WB
Alexa Fluor®488 anti-mouse	Goat	Invitrogen	1:400	-
Alexa Fluor®488 anti-rabbit	Goat	Invitrogen	1:400	-
Alexa Fluor®647 anti-mouse	Goat	Invitrogen	1:200	-
Alexa Fluor® Rhodamine Phalloidin		Invitrogen	1:1000	-
HRP conjugated anti-mouse	Goat	DAKO	-	1:2000
HRP conjugated anti-rabbit	Goat	DAKO	-	1:2000
Streptavidin-HRP		CalbioChem	-	1:5000

Table 2.4 Secondary antibodies

2.2 Methods – In Vitro Laboratory studies

2.2.1 Cell lines and culture conditions

Human prostate cancer cell lines PC3 (derived from a bone metastasis) and DU145 (derived from a brain metastasis) were obtained from Claire Wells, King's College London. Both cell lines were cultured in Roswell Park Memorial Institute-1640 (RPMI-1640) media supplemented with 10% v/v fetal bovine serum (FBS) and 1 mM penicillin-streptomycin. The primary human prostate cancer cell line 1542 (obtained from Claire Wells, King's College London) was grown in keratinocyte serum-free media (KSFM) supplemented with 10% v/v FBS, 1 mM penicillin-streptomycin, 0.1 mg/ml bovine pituitary extract (BPE) and 5 ng/ml epidermal growth factor (EGF). The 1542 cell line was generated as part of a matched pairs set whereby cancerous and benign cells were excised from a radical prostatectomy, and then immortalised and cultured for *in vitro* use (Bright et al., 1997). More specially, the 1542 malignant cell line was excised from a grossly apparent tumour nodule and then characterised to be of epithelial origin through cytokeratin immunostaining and cancerous through loss of heterozygosity analysis (Bright et al., 1997). HEK293 cells (ATCC) were maintained in Dulbecco's modified Eagle's media (DMEM) supplemented with 10% v/v FBS and 1 mM penicillin-streptomycin. PC3, DU145 and 1542 cells were sent to the Dana-Farber Cancer Institute, Harvard (Massimo Loda group), where Giorgia Zadra generated stable FASN knockdown in each of our cell lines. This was done using pLKO.1 lentiviral constructs containing two different shRNA sequences generated by the RNAi Consortium (shFASN A3- CATGGAGCGTATCTGTGAGAA, shFASN A4- CGAGAGCACCTTTGATGACAT). In addition, a complimentary control shRNA was also generated for each cell line (shRNA Control- ACAACAGCCACAACGTCTATA). All stably supressed and control shRNA cell lines were grown in the same media as their respective wild-type non-infected cell line counterpart with the addition of 1 μg/ml puromycin added to the media. All cell lines were cultured at 37°C in a tissue culture incubator with humidified air and CO_2 levels at 5% typical atmospheric levels. The passaging of cells occurred once they reached above sub-confluent levels. During cell passaging the growth medium was removed from the flasks and the cells were washed once with 1x Phosphate Buffered Saline (PBS). Upon removal of PBS, trypsin/EDTA was added to the cells and then the flasks

were placed in the tissue culture incubator for 5-10 minutes. Once adherent cells were detached from the bottom of the flasks, the respective FBS supplemented media of each cell line was added to neutralise the trypsin. Cells were then pelleted by centrifugation at 1200 rpm for 5 minutes. Once complete, the supernatant was carefully removed and the pellets were resuspended in their respective media and split to a desired volume. Flasks were filled up with the appropriate volume of media and then placed back into the tissue culture incubator.

2.2.2 Acid treatment of coverslips

13 mm diameter round glass coverslips were placed in a beaker overnight containing a 4:6 solution mix of 1 M hydrochloric acid (HCl) and ethanol respectively. The following day the solution mix was dispensed gently avoiding any loss of coverslips and then the beaker was filled with 100 ml dH_2O. The dH_2O was brought to boil and then dispensed. After this the coverslips were washed six times with dH_2O and then coverslips were placed on whatman paper and left to dry. The coverslips were then placed into a 50 ml glass bottle and autoclaved for complete sterilisation.

2.2.3 Matrix coating of coverslips or wells

Matrix components Matrigel and type I rat tail Collagen were diluted to a final concentration of 10 μg/ml. Matrigel was diluted in 1x PBS, whilst type I Collagen was diluted in filter sterilised dH_2O with 0.02 M glacial acetic acid. Working concentrations of the matrices were then added to wells with, or without coverslips and then placed in the 4°C coldroom overnight. Before use, wells and coverslips would be washed twice with 1x PBS.

2.2.4 Transient transfections

Calcium phosphate transfection

The calcium phosphate transfection kit was used to transfect HEK293 cells. Cells were seeded at a density of $1x10^5$/ml and then placed in the tissue culture incubator for 24

hours. On the next day, media from the dishes was aspirated and replaced with fresh DMEM media. The transfection reaction was set up using the condition described in **Table 2.5**.

10 cm tissue culture dish	2 cm tissue culture dish
To tube A add:	**To tube A add:**
30 µl 2 M $CaCl_2$ 20 µg DNA Make volume up to 300 µl with sterile water	6 µl 2 M CaCl2 4 µg DNA Make volume up to 60 µl with sterile water
To tube B add:	**To tube B add:**
Add 300 µl HEPES buffered saline	Add 60 µl HEPES buffered saline

Table 2.5 Calcium phosphate transfection reaction mix

The contents of tube A were added to tube B and then the reaction mix was carefully aerated with gentle pipetting (**Table 2.5**). The transfection mix was then left at room temperature for 30 minutes. Once complexed, the mix was added to the cells in a dropwise fashion followed by a gentle gyration to evenly spread the mix. The dishes were incubated at 37°C overnight before replacing the medium with fresh medium. Then the dishes were left for a further 24 hours in the 37°C incubator before being harvested.

Fugene 6 and Viafect

Cells were seeded at a density of $2x10^4$/ml on coverslips, $5x10^4$/ml in the well of a 6 well plate, and $1x10^5$/ml in a 10 cm dish. Cells were left to adhere for 24 hours at 37°C and then the medium in the plates were replaced with either fresh medium or optiMEM. The transfection mix was then prepared according to **Table 2.6**.

Fugene 6 / Viafect	
$2x10^4$/ml – $5x10^4$/ml	**$1x10^5$/ml**
92-97 µl OptiMEM	470 µl OptiMEM
3-8 µl transfection reagent	30 µl transfection reagent
1-2 µg DNA	10 µg DNA

Table 2.6 Fugene 6 and viafect transfection reaction mix

The transfection mixes were left to complex for 25 minutes (Fugene6) and 17 minutes (Viafect) at room temperature. Once complexed the transfection mixes were added in a dropwise fashion to the plates/dishes, gyrated and placed in the 37°C incubator for 6-48 hours. If transfected in optiMEM for 6 hours media was replaced with fresh cell culture medium with 10% FBS and left to incubate for a further 24 hours. If transfecting in cell culture medium for 48 hours, media would be replaced with fresh growth medium after 24 hours.

2.2.5 Immunofluorescence

Cells were seeded onto either glass or matrix-coated coverslips at a seeding density of $2x10^4$/ml and left to settle for 2 days. Cells were then fixed in 4% Paraformaldehyde (PFA) for 20 minutes at room temperature before washing three times with 1x PBS. If staining was performed at a later date then PFA was removed from wells and replaced with 1x PBS before placing the plates at 4°C in the fridge. After PBS washing, cells were permeabilised in 0.2% Triton X-100:PBS for 5 minutes. Coverslips were washed three times in 1x PBS and then blocked with 5% Milk:PBS followed by 3% BSA:PBS, or 3% BSA:PBS alone for 30 minutes. Coverslips were then incubated with a primary antibody diluted in 3% BSA:PBS for 2 hours in a dark humidified environment (**Table 2.3**). Coverslips were then washed three times with 1x PBS before being incubated with secondary antibodies (**Table 2.4**). Secondary antibodies were diluted in 3% BSA:PBS along with Rhodamine-Phalloidin and DAPI for 1 hour and 5 minutes in a dark humidified environment. After final incubation coverslips were washed twice with 1x PBS and then twice with ddH_2O before mounting onto slides using FluorSave. Slides were left in the dark overnight either on the bench or in the fridge at 4°C before visualising on the Olympus IX71 inverted time-lapse microscope.

2.2.6 2D Random migration assay and time-lapse microscopy

Cells in full growth medium were seeded into matrix-coated wells of a 12 well plate at a cell density of $1x10^3$/ml and placed in the 37° incubator overnight. The next day each well was washed twice with 1x PBS followed by the addition of serum starvation

media. Plates were placed back in the 37° incubator for overnight serum starvation. Immediately prior to time-lapse acquisition, the media was supplemented with 20 ng/ml Hepatocyte growth factor (HGF) and 20 mM HEPES before the plates were sealed with parafilm and placed on the 37°C heated stage of the Olympus IX71 inverted time-lapse microscope. If the experiment involved using FASN inhibitors, then cells were incubated with 30 μM Orlistat and 25 μM C75 for 24 hours and 1 hour respectively before adding HGF and starting the image acquisition. Images were captured at 5 minute intervals for 16 hours using a Retiga SRV CCD camera and collated using the Image-Pro Plus software. After acquisition and extraction was complete, movie files were saved in AVI format and then imported into the open source software programme ImageJ. Once open in ImageJ, the Manual Tracking plugin was booted up and point and click style tracking was performed. Each click records the X and Y coordinates of a cell from one frame to the next. Typically, around 50-60 cells are tracked over at least three independent experiments per condition. These values are then saved and imported into Mathematica where post-tracking analysis is performed using the Chemotaxis 6.0 notebooks developed in-house by Graham Dunn and Gareth E. Jones.

2.2.7 Western blotting

Cell lysis

Cells were seeded into 6 or 12 well plates at a density of $1x10^5$/ml (Full growth medium experiment) or $5x10^4$/ml (stimulation experiment). For stimulation experiments, cells would be seeded in full growth medium and then serum starved for 24 hours before stimulating with HGF for 15 minutes and lysing. For looking at the expression of proteins in normal growth conditions, cells were left for 24 hours and then lysed. Wells of plates were washed twice with 1x PBS before adding the appropriate volume of gel sample buffer (2x). Immediately cells were scraped and transferred into labelled eppendorf tubes. Lysates were then boiled for 5 minutes and then stored at -20°C until use.

Tissue homogenization

Prostate tissue samples were kindly donated by Dr Jonathan Morris and were taken from patients who underwent a prostate biopsy. Three of the samples are from patients who tested positive for BPH (G36, G40 and H5) and four of the samples are from patients who tested positive for prostate cancer (F2, F4, D4 and F16). The samples required no ethical permission to use as they were obtained before the human tissue act (2004) came into action. Each prostate sample was placed into the well of a 4 well plate containing RIPA buffer (3 µl per mg) and then incubated on ice for 20 minutes. A scalpel was used to dice and shear the samples into smaller sections. Samples were then placed into eppendorf tubes and vortexed briefly before being subjected to high pulse centrifuging for 3 minutes at 4°C. Each tube then had an additional 200 µl of RIPA buffer added before attempting to homogenize with a syringe and needle. Complete homogenisation of tissue was not successful; however the liquid sample from each tube was drawn up and placed into fresh eppendorf tubes. The Bradford assay was used to confirm protein was extracted from each tissue sample. Following this the appropriate volume of 6 x gel sample buffer (to make 1 x) was added and then all the samples were boiled for 5 minutes at 95°C before placing them in the -80°C freezer.

Gel electrophoresis and immunoblotting

Lysates were thawed and then boiled (usually up to a minute) before running. Equal amounts of each sample were loaded (protein concentration was not measured) and proteins were separated by sodium dodecyl sulphate polyacrylamide gel electrophoresis (SDS-PAGE) on 6.5%-12.5% gels. Proteins were then electroblotted onto nitrocellulose membrane for 1-2 hours at 100 volts. Membranes were blocked in Tris-buffered saline with Tween20 (TBST) containing 5% w/v non-fat milk powder, or 5% w/v BSA for 1 hour at room temperature. Blots were then incubated on a roller overnight at 4°C in primary antibody diluted in either 5% Milk:TBST or 5% BSA:TBST (**Table 2.3**). Any unbound primary antibody was removed from the blots by washing them three times for 15 minutes in TBST. Membranes were incubated on a roller for 1 hour and 30 minutes in either 5% Milk:TBST or 5% BSA:TBST with the appropriate horseradish peroxidase conjugated secondary antibody (**Table 2.4**). Membranes were

washed a further three times in TBST to remove any unbound secondary antibody and then proteins were detected using ECL or ECL prime detection kits.

Stripping of nitrocellulose membrane

In some cases membranes were re-probed to visualise proteins that could not be probed for the first time round. In this case, membranes were incubated with constant agitation in stripping buffer twice for 15 minutes at room temperature. Stripping buffer was then removed and replaced with 1x PBS for a brief 5 minute wash before blocking and re-probing with a primary antibody as previously stated.

Densitometry

Scanned and digitized autoradiographs were opened into imageJ and converted into 8-bit images. Then densitometric analysis of protein bands was carried out by measuring the band densities. This was done by drawing a rectangular box of the same size around the desired bands and then using the measuring tool to measure the mean grey value within the box. Band densities of the proteins of interest were normalised to the band densities of a loading control. Once adjusted, these values were converted to a mean fold value relative to one condition.

2.2.8 Immunoprecipitation

General antibody Immunoprecipitation

Wells and dishes were washed twice with 1x PBS and then lysed in GFP-Trap lysis buffer supplemented with protease inhibitors (1 mM DTT, 10 μg/ml leupeptin, 1 μg/ml aprotinin, 10 mM PMSF, 10 mM NaF, 1 mM Na_3VO_4) for 10 minutes on ice. Cells were thoroughly scraped and transferred into eppendorf tubes prior to centrifugation of the lysates at 13,000 x g for 10 minutes at 4°C. During this time protein A/G beads were washed in GFP-Trap wash buffer three times. Supernatant from the eppendorf's was transferred into eppendorf tubes containing protein A/G beads and the sample was left to pre-clear for 1 hour at 4°C whilst spinning. A small amount of sample is kept back for the input and pipetted into a fresh eppendorf's. An equal volume of gel

sample buffer (2x) is added to the lysate and the sample is boiled for 3 minutes before placing in -20°C. After pre-clear is complete eppendorf tubes are centrifuged at 2,500 x g to separate the beads from the lysate. The lysate is then pipetted into a fresh eppendorf tube and incubated with a primary antibody (either 3 μl or 1 μg) for either 3 hours or overnight (**Table 2.3**). Fresh protein A/G beads are washed three times with GFP-Trap wash buffer and then mixed with the lysates for 1-2 hours at 4°C whilst spinning. The bead bound immune complexes were spun down at 2,500 x g and washed five times in GFP-Trap wash buffer before resuspending in 2x gel sample buffer and boiling for 5 minutes.

GFP Trap

Medium was removed from wells or dishes and replaced with ice cold 1x PBS before scrapping cells into eppendorf tubes. Eppendorf tubes were centrifuged at 300 xg for 3 minutes at 4°C. The resulting pellet was washed by resuspension in ice cold 1x PBS and centrifuged a further two times. Cell pellets were then resuspended in GFP-Trap lysis buffer (containing protease inhibitors) and kept on ice for 30 minutes with vigorous pipetting every 10 minutes. In the case of 1542 cells, lysis was carried out similar to that in the general immunoprecipitation procedure with the exception that once cell debris was scraped into eppendorf tubes they were left to lyse on ice for a further 20 minutes. Lysates were centrifuged at 20,000 x g for 10 minutes at 4°C. During this time GFP-Trap beads were equilibrated by washing then three times with GFP-Trap wash buffer. Lysates were then mixed with GFP-Trap beads and left to rotate for 1 hour at 4°C. As with above, a small sample of lysate was kept to be used as the input readout. Lysates were centrifuged at 2,500 x g and the protein complexed GFP-Trap beads were washed a further 3-5 times with GFP-Trap lysis buffer. Gel samples buffer (2x) was added to the beads and boiled for 5-10 minutes.

2.2.9 Palmitoylation assay

This assay was carried out to look at the palmitoylation of overexpressed and endogenous proteins. Cells seeded into plates or dishes were serum starved for 24 hours before carrying out the assay. An immunoprecipitation was performed as

described above to capture the protein of interest. The beads were then incubated with 20-50 mM *N*-Ethylmaleimide (NEM) for 2 hours or overnight at 4°C. Beads were then washed three time with GFP-Trap wash buffer to remove excess NEM and then incubated in Palmitoylation buffer 1 (1 M hydroxylamine, 50 mM Tris, 150 mM NaCl, 5 mM EDTA, 0.2% Triton X-100, pH 7.4) for 1-2 hours at room temperature on a shaker. Control samples were incubated in Palmitoylation buffer 1 without hydroxylamine leaving palmitoylated residues unmodified. Palmitoylation buffer 1 was then removed from beads by centrifugation at 2,500 x g and replaced with Palmitoylation buffer 2 (4 μM BMCC-Biotin, 50 mM Tris, 150 mM NaCl, 5 mM EDTA, 0.2% Triton X-100, pH 6.2) for 1-2 hours at room temperature on a shaker. Following incubation beads were washed three times with GFP-Trap wash buffer to remove excess biotin and then resuspended in gel sample buffer 2x and boiled for 3 minutes before storing them at -20°C.

2.2.10 MTT Proliferation and adhesion assay

Adhesion

Cells were seeded into plastic or matrix-coated 96 well plates at a cell density of $1x10^4$ in serum free media and placed in the 37°C incubator for 1 hour. Each well was washed twice with 1x PBS before adding Thiazolyl Blue Tetrazolium Bromide (MTT) diluted in serum free media (500 μg/ml) to each well and placing the plates in the 37°C incubator for 3 hours. MTT media was removed from the wells and the converted dye was then solubilized for 10 minutes using DMSO. The absorbance of the samples was measured at 540 nm using the alpha fusion plate reader.

Proliferation

Cells were seeded into plastic or matrix-coated 96 well plates at a cell density of $5x10^2$ in full growth medium and then placed in the 37°C incubator for 7 days. At day 1, 3, 5 and 7 plates were taken from the incubator and MTT was added to the wells in the same fashion described in the adhesion protocol with no deviations. It should be noted

that MTT is reduced metabolically by dehydrogenase enzymes and so proliferation is reflective of the metabolic activity of the cells being tested (Mosmann, 1983).

2.2.11 Inverted Invasion assay

Cells were passaged to a density of $4x10^5$/ml and then centrifuged in an eppendorf tube at 1200 rpm for 5 minutes. During this time the collagen mixture was prepared on ice (**Table 2.7**).

	1.5 mg/ml gel (1ml)
dH_2O	350 µl
5x DMEM	200 µl
1M NaOH	7.52 µl
Collagen (3.39 mg)	442.47 µl

Table 2.7 Collagen matrix mix for inverted invasion assay

The collagen mixture was mixed thoroughly, but gently. Supernatant from the eppendorf tubes was removed and then the collagen mixture was added to the tubes resuspending the cell pellets. A 96 well plate was placed on ice and to each well 100 µl collagen: cell mix was added. The 96 well plate was centrifuged at 600 xg for 6 minutes at 4°C forcing the suspended cells to move to the bottom of the plate. After checking on the microscope that the cells were on an even field, the plate was placed in the 37°C incubator. After 2 hours the plate was removed and 100 µl of medium + 10% FBS was pipetted into the top of each well and the plate was placed back in the 37°C incubator for a further 24 hours. After 24 hours 100 µl 8% formaldehyde containing 1 µl Hoechst stain was pipetted into each well and then the plate was left at 4°C overnight with continuous shaking.

The plates were imaged on the A1R confocal microscope where a series of z-stacked images were taken. From this analysis was done in the open access programme Fuji which involved comparing the invasion of cells at 50 microns relative to the bottom. Thresholding and particle analysis of cells was performed on both planes allowing for the relative % of Invasion to be calculated.

2.2.12 High Resolution-Magic Angle Spinning Nuclear Magnetic Resonance (MAS-NMR) sample preparation

Cells were seeded into 10 cm dishes at a cell density of $1x10^5$/ml and left to grow to 80% confluency. Nine plates were seeded per condition. Medium in the dishes was replaced with fresh medium +10% FBS one and a half days before harvesting. Media was removed from plates with 1 ml from each plate being centrifuged at 1200 rpm to remove any cellular debris and then pipetted into fresh eppendorf tubes. Plates were washed once with ice cold 1x PBS +Ca +Mg. For moderately adherent cell lines PC3 and DU145, 6 ml of 1x PBS +Ca +Mg was added to each plate and the cells were scraped and transferred into 15 ml Falcon tubes. For the highly adherent 1542 cell line 6 ml of cell dissociation buffer was added to each plate before placing them in the 37°C incubator for 20-30 minutes before scrapping and transferring into 15 ml Falcons tubes. 15 ml Falcon tubes were centrifuged at 1000 rpm for 4 minutes. Supernatant from the 15 ml Falcon tubes was discarded and cell pellets were re-suspended in 500 µl 1x PBS +Ca +Mg, transferred into eppendorf tubes and centrifuged at 200 x g for 5 minutes at 4°C. Supernatant from the eppendorf tubes was aspirated and then cell pellets and eppendorf tubes containing the 1 ml of media were snap frozen by immersion in liquid nitrogen for 3 minutes. Samples were then stored at -80°C or lyophilized overnight and stored at -20°C.

Samples were then sent for analysis to Tokuwa Kanno, a PhD student working in Dr Jason Mason's Lab group at King's College London. For the cell pellets high resolution-magic angle spinning nuclear magnetic resonance (HR-MAS NMR) spectra was recorded on the Bruker Avance 400 MHz spectrometer. For media (liquid state NMR), spectra were acquired on a Bruker Avance II 700 MHz NMR spectrometer.

2.2.13 Palmitate-BSA conjugate and cell treatment

Sodium palmitate (13.9 mg) was dissolved in 1 ml 50% v/v ethanol to make a 50 mM stock. Eppendorf tubes were placed in a heat pad and left for around 20-30 minutes at 70°C. Once the sodium palmitate had dissolved, the solution was diluted 1:10 to give a concentration of 5 mM sodium palmitate in 1 ml 50% v/v ethanol. Fatty acid free-BSA

(250 mg) was dissolved in 5 ml MilliQH_20 and then 4 volumes of 5% fatty acid free-BSA was mixed with 1 volume of 5 mM Palmitate. The mixture was placed in a 37°C water bath and left to conjugate for 1 hour forming a 1 mM palmitate-BSA complex. Aliquots were stored at - 20°C. Before using in cell culture, aliquots were defrosted on ice and then allowed to activate at 55°C for at least 15 minutes. Palmitate was used at a concentration of 50 μM in all experiments and incubated with cells for 1 hour. This time-point was chosen based on the observation of a time-lapse video which showed the cells morphology recovering at this point. Fatty acid free-BSA was used as a control and added to the cells of a different well at the same concentration for the same amount of time as cells incubated with palmitate.

2.2.14 Silencing of RhoU in prostate cancer cells

1542 cells were seeded to a density of $1x10^5$/ml in 6-well plates. Cells were reverse transfected with either control siRNA (sequence – AATTCTCCGAACGTGTCACGT) purchased from Qiagen or the RhoU SMARTpool siRNA (sequence 1- GTACTGCTGTTTCGTATGA, sequence 2- GAACGTCAGTGAGAAATGG, sequence 3- CAGAGAAGATGTCAAAGTC, sequence 4- AAGCAGGACTCCAGATAAA) purchased from Dharmacon. Control siRNA (50 nM) and RhoU SMARTpool siRNA (50 nM) were added to 500 μl Optim-Mem and 7.5 μl RNAiMAX before being gently mixed and pipetted in their respective wells for 30 minutes at room temperature. Plates were then placed in the 37°C incubator for 72 hours before the cells were lysed as normal.

2.2.15 Blocking palmitoylation with 2BP in prostate cancer cells

1542 cells were seeded to a density of $1x10^5$/ml in 6-well plates and left for 24 hours in the 37°C incubator. The following day 2 μl of either DMSO or 2 μl of 2-bromopalmitate (2BP) 100 μM dissolved in DMSO was added to the cells of individual wells. Plates were placed back in the 37°C incubator for 24 hours before the cells were lysed as normal.

2.2.16 Cell storage and recovery

Cell lines were frozen down at the earliest possible passage to preserve their phenotypic nature. Cells were grown to near full confluency and then passaged as normal. After centrifugation pellets were resuspended in 90% FBS and 10% DMSO, pipetted in cryogenic vials, and then left to steadily freeze in a Mr Frosty at -80°C overnight. Cyrogenic vials were then permanently placed in liquid nitrogen storage until needed for cell culture. For the recovery of cells, cryogenic vials were placed in a 30°C water bath until thawed and then mixed 1:1 with full growth medium before adding 4 ml of full growth medium, centrifuging, and adding the resuspended cells in growth medium into a flask. Medium was generally changed the next day.

2.2.17 Transformation of Escherichia coli cells

DH5α and NEB®-10 beta *E.coli* cells were thawed on ice for 10 minutes. 1 µl of plasmid DNA was then added to the bacteria, without mixing, and then left on ice for 30 minutes. Cells were then heat shocked by placing tubes in a 42°C water bath for 30 seconds and then back on ice immediately for 2 minutes. 500 µl LB-broth was added to the transformed bacteria and incubated in a shaking incubator at 37°C for 1 hour. The transformed bacteria were plated onto LB-agar plates containing the appropriate antibiotic and incubated at 37°C overnight.

2.2.18 DNA plasmid purification

Plasmid DNA was isolated and purified from overnight grown transformed *E.coli* bacteria using the Invitrogen Purelink® HiPure Plasmid Filter Maxi-prep kit. The procedure was carried out according to the manufacturers recommended protocol. The resulting purified DNA was resuspended in TE buffer and stored at -20°C.

2.2.19 RNA extraction and purification

Cells were seeded into 6 well plates at a cell density of $5x10^5$/ml and then placed in the 37°C incubator overnight. Media was removed and wells were washed once with 1x

PBS. RNA was then extracted and purified from the cells according to the manufacturer's instructions using the Qiagen RNeasy® Mini Kit. RNA was resuspended in nuclease-free water and stored long term at -80°C.

2.2.20 cDNA synthesis

RNA was converted into DNA using the Vilo cDNA synthesis kit purchased from Sigma. RNA concentration and purity was measured using the Nanodrop and then 1 μg of RNA was converted into 1 μg of DNA using the reaction mixture in **Table 2.8**. Once gently mixed, the reaction was initiated by incubating the PCR tubes at 25°C for 10 minutes, followed by 1 hour incubation at 42°C, and then finally the reaction was terminated following a 5 minute incubation at 85°C. The resulting DNA product was stored at -20°C.

Component	Volume/conc.
5x Vilo reaction mix	4 μl
10x SuperScript Enzyme mix	2 μl
RNA	1 μg
DEPC-treated water	Up to 20 μl

Table 2.8 RNA to cDNA reaction mix

2.2.21 Polymerase Chain Reaction (PCR)

PCR was carried out as a diagnostic tool using the REDTaq® ReadyMix™ PCR Reaction Mix. Sterile PCR tubes comprised the following reaction mix of 25 μl RedTaq ready mix (with Magnesium), 0.5 μM forward and reverse primers and 100 ng cDNA. The reaction volume was then made up to 50 μl with nuclease-free water. The PCR tubes were gently flicked, briefly centrifuged, and then placed in the PCR thermal cycler to undergo conditions described in **Table 2.9**. Samples were stored at -20°C

Number of cycles	Process	Temperature	Time
1	Pre-incubation	95°C	5 minutes
30-35	Denaturation	94°C	1 minute
	Annealing	55°C	1 minute
	Extension	72°C	1 minute
1	Final extension	72°C	10 minutes

Table 2.9 Conditions for PCR amplification

2.2.22 DNA Gel Electrophoresis

Electrophoresis gels consisted of Tris-acetate-EDTA (TAE) buffer containing 1-2% agarose and ethidium bromide (1:10,000). Once the gels had set they were covered with 1x TAE buffer and 20 µl of PCR amplification sample was loaded, alongside a DNA marker into the wells. The DNA fragments migrated through the gel at 100V for 1-2 hours before being visualised under ultraviolet (UV) light.

2.2.23 Statistical analysis

An unpaired Students t-test and a one-way ANOVA (analysis of variance) Tukey test was used to measure statistical significance. In addition, statistical significance, in terms of difference between cell line growth rates, was assessed using the 'compareGrowthCurves' function of the statmod software package of R (http://bioinf.wehi.edu.au/software/compareCurves). This software performs a mean t-statistic between two groups of growth curves which gives a P-value from a 1000 permutations. The initial P-values were then adjusted for multiple testing between groups using the Holm's method (Baldwin et al., 2007). A P-value of ≤0.05 (95% confidence interval) was used to consider statistical significance and would be indicted by a *. Increased significance was recorded at P-values ≤0.01 (99% confidence interval) **, and ≤0.001 (99.9% confidence interval) ***. Statistical packages used to calculate significance include IBM SPSS (statistical package for the social sciences), Statmod, Statistics 22 and GraphPad Prism. Error bars represent the standard error of the mean (SEM).

2.3 Methods – Pilot patho-epidemiological study

This pilot patho-epidemiological study was performed in collaboration with Professor Lars Holmberg, previous Director of the Regional Cancer Centre Uppsala Örebro and Professor at the department of Surgical Sciences, Uppsala University, Uppsala, Sweden. The staining and preparation was kindly funded by Professor Lars Holmberg using his Grant from the Swedish Cancer Society.

2.3.1 Cohort and tissue microarray (TMA) preparation

The cohort consists of 85 patients who underwent a radical prostatectomy. All samples were collected retrospectively at the UCAN biobank in Uppsala, Sweden and were histologically assessed by the pathologists Dr Anna Tolf and Dr Anca Dragomir (Uppsalsa University). Cores from the tissue samples were isolated to pertain to the dominant Gleason (DG), Highest Gleason (HG) and benign tissue. The dominant Gleason corresponds to the most widespread Gleason grade patterns of the core, whilst the highest Gleason corresponds to an area of the core with the most poorly differentiated tissue and thus the worst Gleason grades. The Gleason grading system for radical prostatectomy specimens was in accordance with the WHO classification of Tumours of the Urinary system, 2004. These cores were embedded on four separate tissue microarray's (TMA). Overall preparation of the TMA's was overlooked by Professor Fredrik Pontén and Professor Michael Häggman.

2.3.2 Staining and scoring of TMA's

TMA's were immunohistochemically stained by Dr Per-Henrik Edqvist (project coordinator, Uppsala University) for the proteins FASN, RhoU, Cdc42, c-Met, HER2 and Ki67 (**Table 2.10**). The overall staining intensity for the proteins FASN, RhoU and Cdc42 was assessed and scored by myself and confirmed by Dr Ashish Chandra, a lead pathologist for Uro-Oncology at Guy's and St Thomas' Hospital. Cdc42 staining was also confirmed by Dr Kiruthikah Thillai, a specialist registrar in Medical Oncology at Guy's and St Thomas' Hospital. Whilst the staining for c-Met and HER2 was assessed and scored by Dr Michelangelo Fiorentino and Dr Francesca Giunchi, two molecular

pathologists from the University of Bologna. FASN and RhoU were scored into categories of one to four, which correlated with a staining intensity that increased with each order of magnitude ranging from low to high. These categories were then dichotomised as negative/low staining intensity (categories one and two), and high staining (categories three and four). Cdc42 staining intensity was scored into three categories, which were then also dichotomised as categories one and two versus category three. c-Met and HER2 staining was dichotomised upfront into medium/low and high. For Ki67 a percentage score was given (scored by Dr Michelangelo Fiorentino and Dr Francesca Giunchi), which was defined by the percentage of positively stained cells among the entirety of the core. It was assessed as a dichotomous variable with a ≤5% cut-off point, consistent with past studies (Fisher et al., 2013).

Protein	Antibody No.
FASN	HPA006461
RhoU	HPA049592
Cdc42	Ab64533
c-Met	Ab51067
HER2	HPA062555
Ki67	CAB00005B

Table 2.10 TMA antibodies

2.3.3 Statistical analysis for Epi-study

First, a univariate logistic regression model was conducted to identify how tissue type (exposure variable defined as DG, HG, or benign tissue) was associated with increased levels of FASN , RhoU, Cdc42, c-Met and HER2 (outcome variables defined as dichotomous measurements). Next, a univariate and multivariable logistic regression model was conducted to assess how the expression of FASN, RhoU, Cdc42, c-Met and HER2 (exposure variables) was associated with increased levels of Ki67 expression (outcome variable defined as a dichotomous measurement).

All tissue staining analysis were conducted with Statistical Analysis Systems (SAS) release 9.4 (SAS Institute, Cary, NC).

Chapter 3

Metabolomic and morphological characterisation of FASN depleted Prostate cancer cell lines

Chapter 3 – Metabolomic and morphological characterisation of FASN depleted prostate cancer cell lines

3.1 Introduction

Prostate cancer is a highly prevalent disease that is difficult to accurately diagnose and treat as a result of its multifactorial development (Nwosu et al., 2001). There is currently a growing body of literature recognising altered lipid metabolism as a common feature in the pathogenesis of prostate cancer (Zadra et al., 2013). It is widely recognised that transcriptional upregulation of the metabolic oncogene FASN is responsible for the exacerbated lipogenesis in cancer (Swinnen et al., 2002). These lipids form a complex signalling network which has been described to have a pleiotropic role in cancer (Zadra et al., 2013).

In normal cells, FASN is tightly regulated and primarily only synthesises fatty acids for storage which are oxidised for energy when dietary nutrients are low (Kuhajda, 2006). In contrast to normal cells, the majority of cancers, including prostate, have a high growth rate which means a controlled and expendable energy source is required to sustain this action. Metabolically, cancer cells fulfil this requirement by high-jacking FASN to continuously synthesize fatty acids *de novo* (Kuhajda, 2006). Overexpression of FASN increases the synthesis of phospholipids which are one of the main building blocks of the cell membrane (Swinnen et al., 2003). Additionally, FASN overexpression affects the lipid composition of the membrane creating platforms for the assembly of signal transduction pathways involved in cell proliferation (Head et al., 2014). The importance of FASN in cell division has been well documented and several studies have shown that inhibiting its activity alone is enough to halt cell division (Horiguchi et al., 2008).

More recently there has been a shift in focussing on a potential role for FASN in the metastatic progression of cancer cells (Jiang et al., 2014). A characteristic phenotype of many metastatic cancer cells is the divergence in cell shape from their parental cells (Lyons et al., 2016). Changes in cell shape are largely dictated by the underlying cytoskeleton which provides the structural framework for the cell (Lyons et al., 2016). A few studies have observed changes in cell shape in response to altering FASN levels,

however for the majority of cancers it has not been documented (De Schrijver et al., 2003; Sadowski et al., 2014). Given that lipid enrichment of the plasma membrane and lipid raft formation are known to cause reorganisation of the actin cytoskeleton, it would be presumptive that FASN overexpression and activity is accompanied by changes in cellular morphology (Head et al., 2014).

The majority of studies carried out in prostate cancer looking at the role of FASN revolve around prostate cancer cells which are AR-dependent. This is not surprising as stimulating cells with androgens significantly increases FASN expression (Menendez and Lupu, 2004). More recently it has been found that after the transition from AR-dependent to AR-independent, FASN expression levels increase (Pizer et al., 2001). Little is known about the role of FASN in castration resistant prostate cancer cell lines such as PC3. However, since prostate cancer cells seem to be more dependent on FASN-catalysed fatty acid biosynthesis compared to exogenous lipids it would suggest that FASN is a viable target in the more aggressive forms of prostate cancer (Menendez and Lupu, 2004; Pizer et al., 2001).

This first chapter characterises the proliferative, metabolic and morphological properties of two AR-independent prostate cancer cell lines against their respective FASN knockdown clones.

3.2 Results

3.2.1 FASN is expressed in multiple cancers of differing origin

Initially detectable levels of FASN expression were monitored to confirm previous reports of its expression in cancer. Cell lines derived from human embryonic kidney (HEK293), prostate cancer (1542, PC3 and DU145), pancreatic cancer (PATU-T and PATU-8902), breast cancer (MDA-MB-231), normal breast (MCF10A) and melanoma cancer (A375) were used in the panel to probe for FASN expression. All the prostate cell lines are androgen depletion-independent (ADI) meaning they do not express the AR or respond to androgens (Litvinov et al., 2006). This makes them suitable lines for studying the role of FASN in what is considered an aggressive and incurable form of prostate cancer (Jeong et al., 2011). In addition, all the prostate cell lines have been shown to be highly migratory from studies in the literature or from work previously conducted in the Wells lab (Reymond et al., 2012; Wells et al., 2010). The pancreatic cancer cell lines used in this panel both express a mutant K-Ras isoform which has been speculated to increase the dependency of tumour cells on *de novo* lipogenesis (Hamidi et al., 2014; Ventura et al., 2015). MDA-MB-231 is a highly invasive triple negative breast cancer cell line, whilst MCF10A is a non-invasive normal human breast epithelial cell line (Nagaraja et al., 2006). The inclusion of these two lines in the panel is useful in determining if FASN is only expressed in cancer and if it correlates with invasiveness. In melanoma cancer there is evidence suggesting that FASN is useful prognostic marker and that its increased expression correlates with an aggressive form of this disease which is why the A375 cell line was included (Innocenzi et al., 2003). The HEK293 cell line was also used in this panel as it is a highly proliferative cell line and so it would be interesting to confirm if this phenotype correlates with high levels of FASN expression. Western blot analysis revealed that all the cell lines included in the panel express FASN and that there was no significant difference in FASN expression between cell lines of the same cancer origin, or of a different cancer origin (**Figure 3.1**). Moreover, the non-cancerous breast cell line MCF10A and the adenovirus transformed kidney cell line HEK293 expressed FASN to similar levels as the cancerous cell lines (**Figure 3.1**).

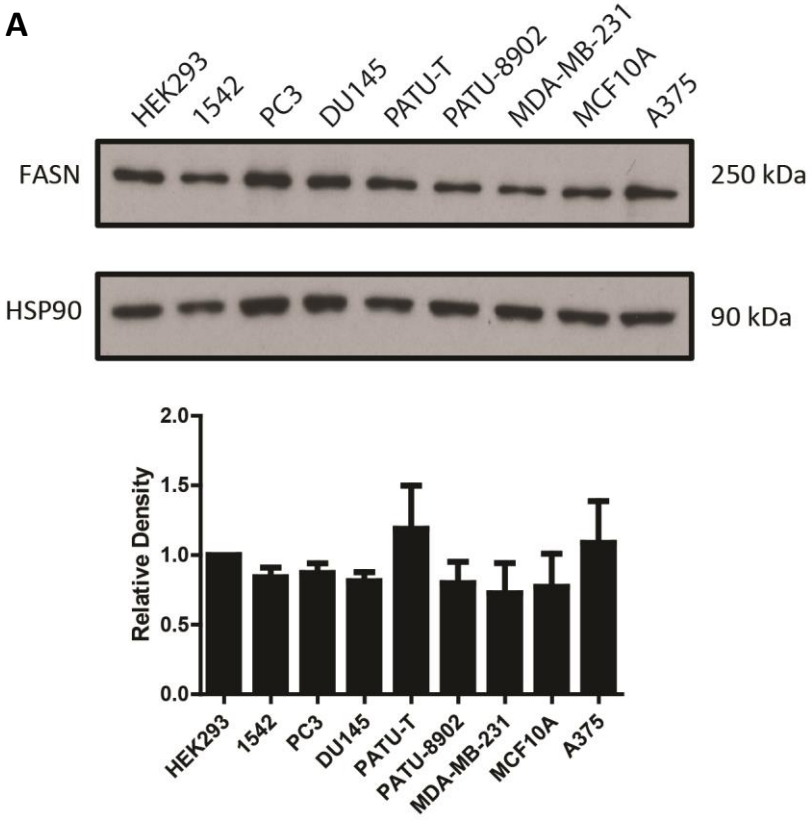

Figure 3.1 FASN is expressed in multiple cancer cell lines: The panel of different cancer cell lines were immunoblotted for FASN and the loading control HSP90 (**A**) which was then quantified via densitometry analysis. Data represents the mean values ± SEM accumulated from three independent experiments.

3.2.2 FASN expression increases in malignant prostate cancer

To compliment the expression profile of FASN in characterised cell lines a set of human primary prostate tissue samples taken from surgical biopsies were also evaluated for FASN expression (**Figure 3.2**). The panel consists of three samples that were classified as benign non-cancerous prostatic growths (G36, G40 and H5), and four that were classified as malignant tumours (F2, F4, D4 and F16). Details of the histopathological assessment of these specimens can be seen in **Figure 3.2A**. To be certain of a difference between malignant and benign prostate tissue, the expression level of FASN in all malignant samples was stratified against the benign tissue sample H5, which was found to have highest expression level of FASN (**Figure 3.2B**). The expression of FASN was significantly higher in all malignant tumour samples compared to the benign sample H5 (**Figure 3.2C**). Additionally, D4, which was histopathologically the most malignant sample, had the highest level of FASN expression compared to all other samples (**Figure 3.2C**).

A

Patient No.	Benign (%)	Malignant (%)
G36	100	0
G40	100	0
H5	100	0
F2	-	-
F4	80	20
D4	10	90
F16	90	10

B

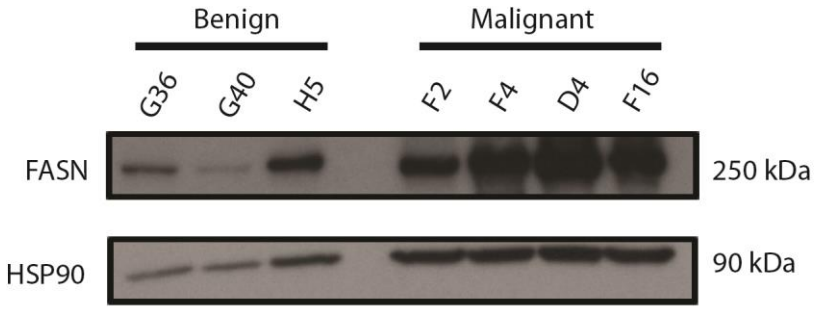

C

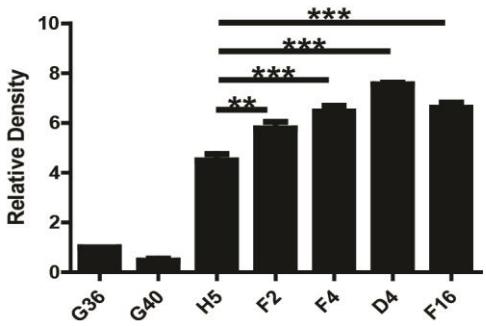

Figure 3.2 Expression of FASN in human primary prostate cancer tissue: Human primary prostate tissue was excised by surgical biopsy from seven different patients. Histopathological analysis on the samples was performed and documented (**A**). Exact histopathological data for sample F2 is missing, but was confirmed as a malignant sample. Whole cell lysates were prepared from the samples which were then tested for FASN expression levels via SDS-PAGE gel electrophoresis (**B**). Densitometry analysis was performed and relative quantification of FASN levels can be seen in (**C**). HSP90 was used as a loading control. Data represents the mean values ± SEM accumulated from three independent experiments. Statistical significance was determined by student's one-way ANOVA with Tukey's post-hoc test. ** $p<0.01$, ***$p<0.001$.

3.2.3 FASN knockdown in 1542, PC3 and DU145 prostate cancer cell lines

Having confirmed that FASN is expressed in the 1542, PC3 and DU145 prostate cancer cell lines, and that it is expressed at high levels in malignant tissue, it was decided to investigate if depleting FASN in these cells effects migratory capacity. All three prostate cancer cell lines are AR-independent and were excised from different sites in the body. The 1542 cell line, which is considered to be a slightly unusual cell type, was derived from a primary adenocarcinoma (Gleason score 8) that was resected from a 48-year old male patient (Bright et al., 1997; Topalian et al., 2006). PC3 cells were isolated from a lumbar metastasis of a 62-year old Caucasian male (Kaighn et al., 1979). They have been classically referred to as an adenocarcinoma of the prostate, however more recent evidence suggests they have features that are characteristic of prostatic small cell neuroendocrine carcinoma's (Tai et al., 2011). DU145 is a prostate adenocarcinoma cell line that was isolated from the dura mater of a 69-year old Caucasian male and unlike PC3 and 1542 cells is characteristically colony forming (Stone et al., 1978). All cell lines were sent to the Dana-Farber Cancer Institute, Harvard (Massimo Loda group), where they were lentivirally infected to produce three additional population of cells, one with a non-specific RNA target, and two with RNA sequences targeting FASN (refer to chapter 2 Methods for more details). It was confirmed by SDS-PAGE that in all prostate cell lines FASN expression significantly decreased in both shFASN knockdown clones when compared to their respective shControl cells (**Figure 3.3A and 3.3B**). In addition, in all cases the expression of FASN did not differ between shControl cells and wild-type cells (**Figure 3.3A and 3.3B**).

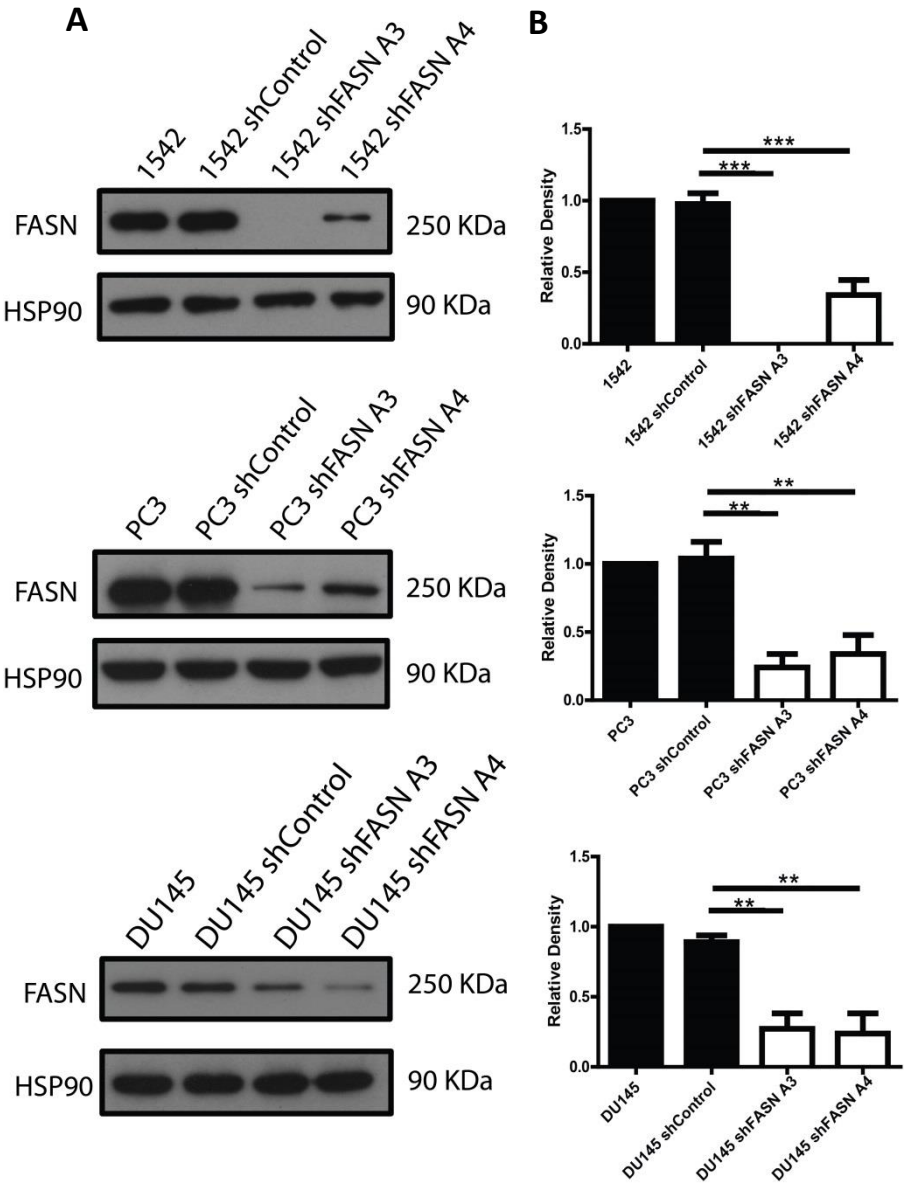

Figure 3.3 shRNA interference of FASN in prostate cancer cell lines: Whole cell lysates were prepared from 1542, PC3 and DU145 cell lines and their respective FASN knockdown/control generated clones. These were then subjected to SDS-PAGE and immunoblotted for FASN and the loading control HSP90 (**A**). Densitometry analysis was performed and relative quantification of FASN levels can be seen in (**B**) for all cell lines. Data represents the mean values ± SEM accumulated from three independent experiments. Statistical significance was determined by student's *t-test*. ** p<0.01, ***p<0.001.

3.2.4 FASN depletion has a significant impact on cell proliferation in prostate cancer cell lines

The role of FASN in cell proliferation has been well documented. Previous studies have shown that abolishing FASN activity causes embryonic lethality in mice and can retard the growth of cancer cells (Chirala et al., 2003; Wen et al., 2016). Prior to an investigation on migratory capacity, it was deemed prudent to assess if there was a proliferation defect in the FASN knockdown cell lines so that the appropriate proliferation independent motility-based assays would be used. To determine if there is a proliferation defect in any of the prostate cancer cell lines upon FASN depletion an MTT assay was carried out over the course of seven days. Wild-type, control and FASN knockdown cell lines were seeded onto plastic or a well coated with either matrigel or type I collagen. Different matrixes were used as it has been reported that cell-matrix interactions can influence the proliferative behaviour of cells (Ohtaka et al., 1996). Moreover, changes in lipids can affect the localisation and function of certain integrins (Pande, 2000).

The MTT assay confirmed that there was a significant decrease in the proliferation of FASN knockdown 1542 (**Figure 3.4**), PC3 (**Figure 3.5**), and DU145 cells (**Figure 3.6**) compared to their respective control cells. Additionally, in all three prostate cell lines the proliferation defect could be seen on plastic and matrix-coated surfaces (**Figure 3.4-3.6**). In PC3 and 1542 cells, differences in cell proliferation between control and FASN knockdown cells on matrix coated surfaces could be seen after Day one, whilst In DU145 cells proliferative differences could be seen after Day 3 (**Figure 3.4-3.6**). In addition to looking at differences in cell number at Day 7 using t-test analysis, control and FASN knockdown growth curves were also compared using a pairwise permutation test. The result of this analysis found that there were no statistical differences between the growth rates of shControl and FASN knockdown cells in all prostate cell lines (**Figure 3.4-3.6**).

Based on literature findings there is a concern that cell viability is affected when silencing or inhibiting FASN (Ventura et al., 2015). The MTT assay results for 1542, PC3 and DU145 shFASN cells showed an increase in the readout signal at day seven when compared to day one (**Figure 3.4-3.6**). This suggests that FASN knockdown is not

inducing cell cycle arrest in these cells. Moreover, no exacerbated cell death was seen when culturing shFASN cells and also no cell death was seen in the 2D migration assay movies in chapter 4. These findings indicate that the shFASN lines selected can be studied for cellular defects without the concern that they are undergoing apoptosis.

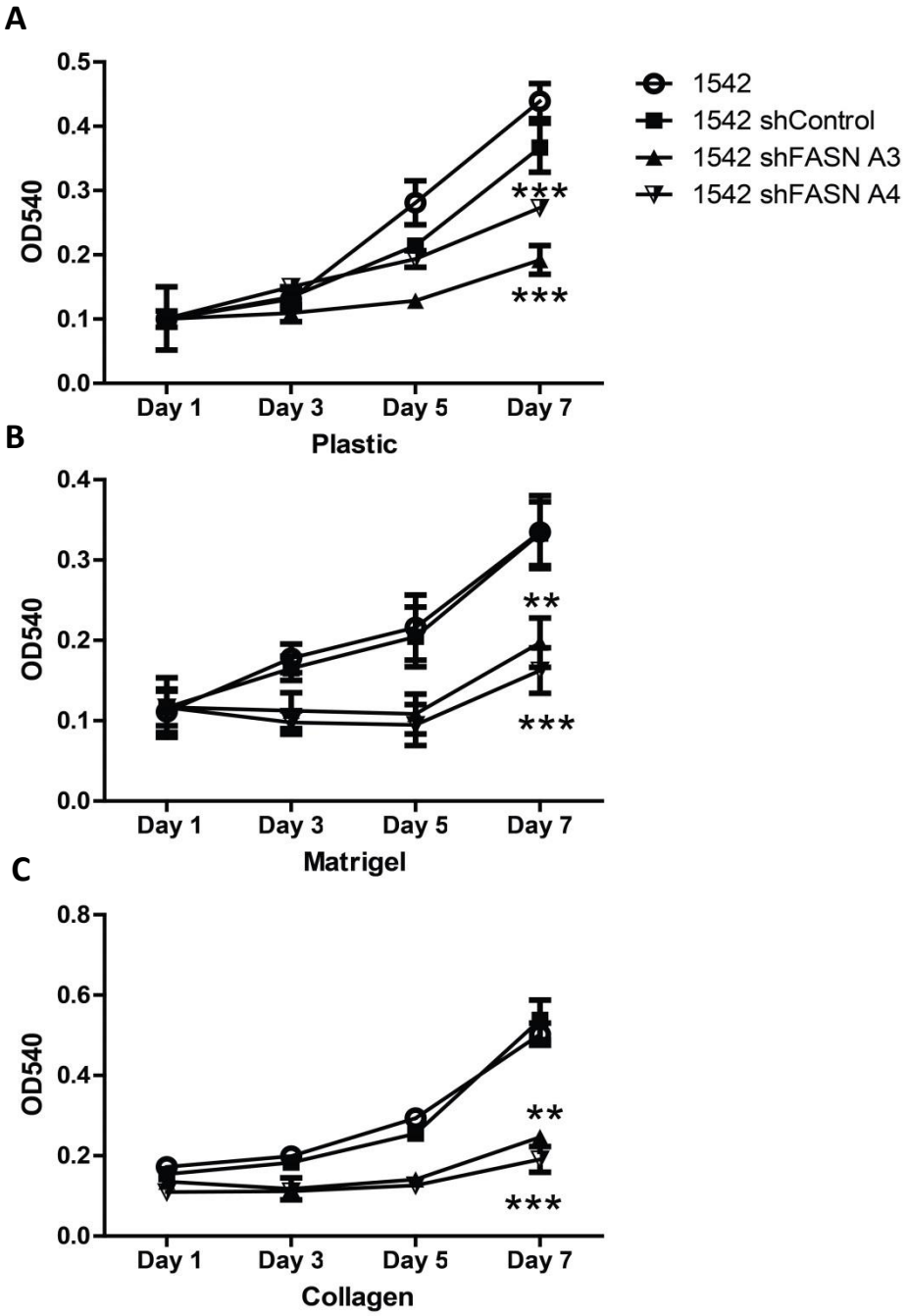

Figure 3.4 Depletion of FASN impairs 1542 cell proliferation: 1542, 1542 shControl, 1542 shFASN A3 and 1542 shFASN A4 cells were seeded in the well of a 96-well plate either non-coated (**A**) or coated with Matrigel (**B**) or type I collagen (**C**). Cells were left to grow over the course of seven days and subjected to an MTT assay at days 1,-3,-5 and 7. Data represents the mean values ± SEM accumulated from three independent experiments. Statistical significance was determined by student's *t-test*. ** p<0.01, ***p<0.001.

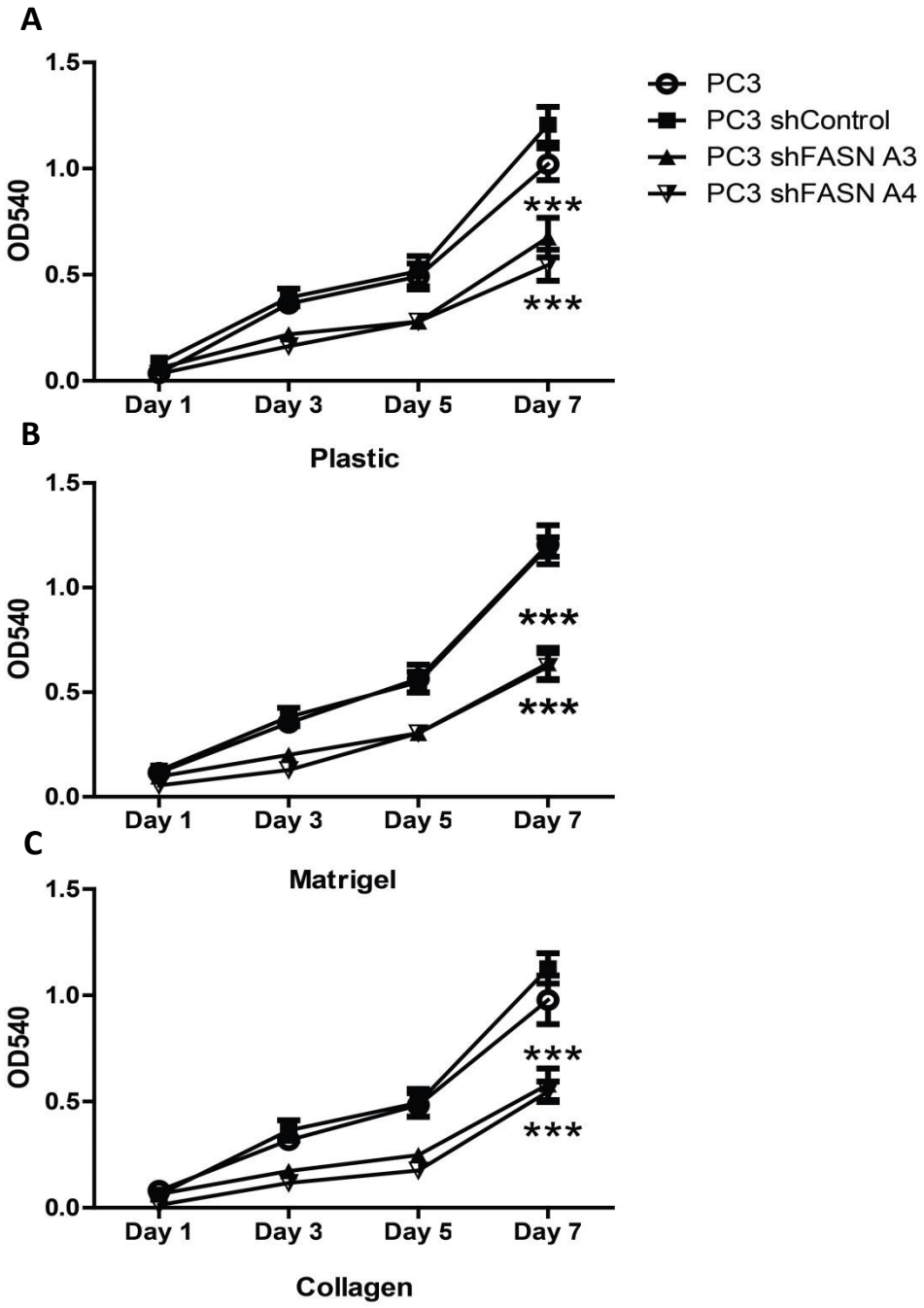

Figure 3.5 Depletion of FASN impairs PC3 cell proliferation: PC3, PC3 shControl, PC3 shFASN A3 and PC3 shFASN A4 cells were seeded in the well of a 96-well plate either non-coated (**A**) or coated with Matrigel (**B**) or type I collagen (**C**). Cells were left to grow over the course of seven days and subjected to an MTT assay at days 1,-3,-5 and 7. Data represents the mean values ± SEM accumulated from three independent experiments. Statistical significance was determined by student's *t-test*. ***p<0.001.

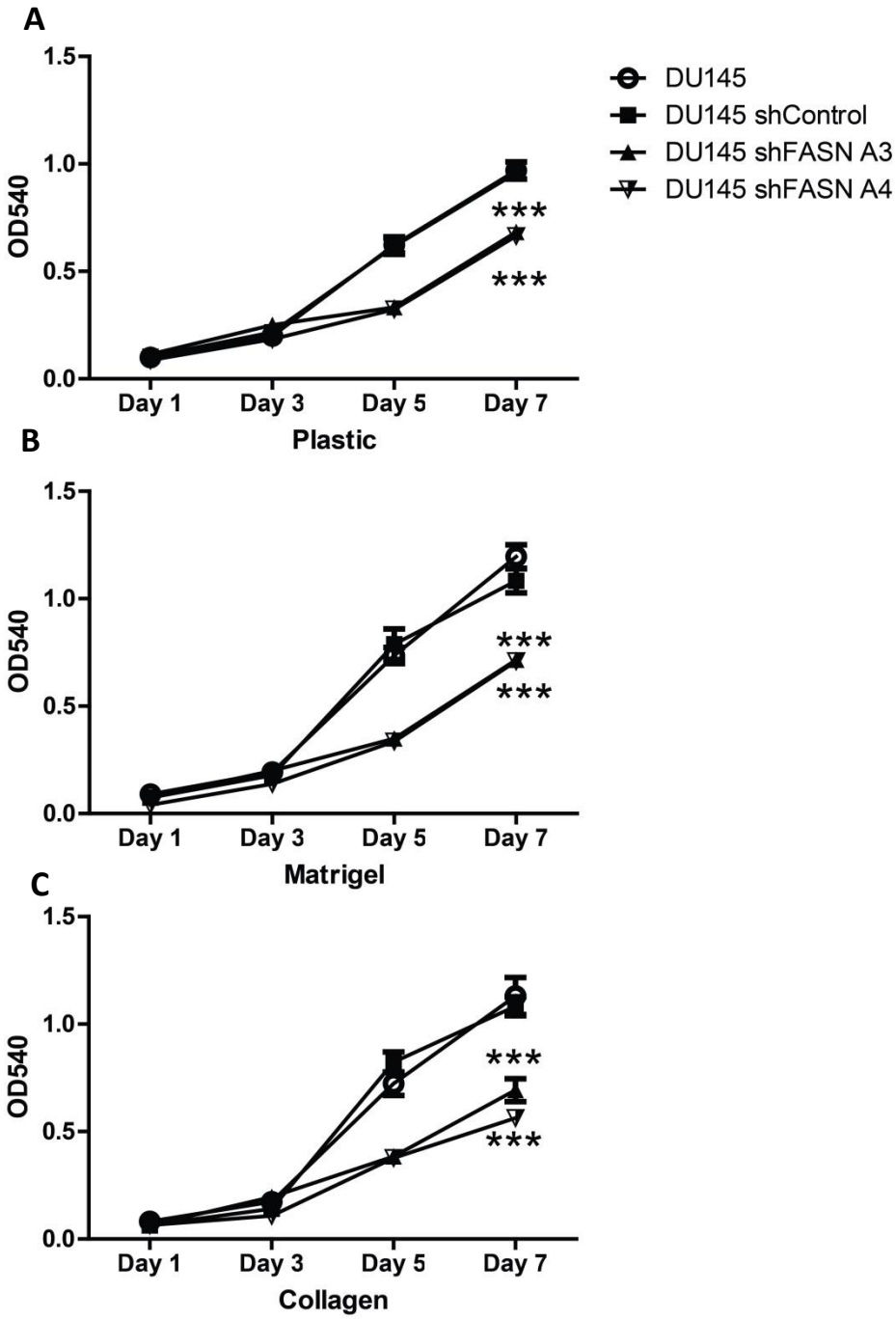

Figure 3.6 Depletion of FASN impairs DU145 cell proliferation: DU145, DU145 shControl, DU145 shFASN A3 and DU145 shFASN A4 cells were seeded in the well of a 96-well plate either non-coated (**A**) or coated with Matrigel (**B**) or type I collagen (**C**). Cells were left to grow over the course of seven days and subjected to an MTT assay at days 1,-3,-5 and 7. Data represents the mean values ± SEM accumulated from three independent experiments. Statistical significance was determined by student's *t-test*. ***p<0.001.

3.2.5 FASN knockdown leads to an altered cellular metabolome in prostate cancer cells

Upregulation of FASN, a metabolomic multi-enzyme, is one of the most frequent alterations in cancer cells (Kuhajda, 2000). The ability to control fatty acid biosynthesis and in turn modulate energy homeostasis gives cancer cells a survival advantage in environments where oxygen and nutrients are not abundantly available (Rohrig and Schulze, 2016). In addition to increasing fatty acid synthesis, FASN has also been functionally linked with glycolysis and associated with several respiratory metabolites such as glutamate (Zaytseva et al., 2015; Zhou et al., 2016). It might therefore be predicted that a shFASN cell should have an altered metabolic profile when compared to control cells.

To assess this NMR metabolic analysis was carried out on shControl and shFASN cells. Cells were cultured in 10 cm dishes (nine dishes per condition) until 80% confluent and then pelleted by scrapping and centrifugation. Cell pellets and 1 ml of media from each dish was snap frozen and then lyophilized. Samples were then rehydrated and subjected to high resolution-magic angle spinning nuclear magnetic resonance (HR-MAS NMR).

Scores plots and quality assessment (Q^2) histograms for cell pellets showed good separation between shControl and shFASN A3 clones in 1542 (Q^2 =0.973) and PC3 (Q^2 =0.783) cells (**Figure 3.7A** and **3.7B**). DU145 shControl and DU145 shFASN A3 cells also showed separation (Q^2 =0.178), however it was not as well defined in this cell line as the other two cell lines (**Figure 3.7C**). This suggests that FASN activity may not be as impaired in DU145 cells. Therefore subsequent metabolic disparities were analysed in the 1542 and PC3 cells but not in the DU145 cells.

Analysis of the cell pellets showed there was a significant decrease in the metabolite glycerophosphocholine in both FASN knockdown 1542 and PC3 cells compared to their respective control cells (**Figure 3.8A, -3.8B** and **Table 3.1**). In 1542 cells, phosphocholine and glutamate levels also significantly decreased in response to FASN depletion (**Figure 3.8A** and **Table 3.1**). These metabolites did not significantly alter in

PC3 cells, but did show a decreasing trend in response to FASN knockdown (**Figure 3.8B** and **Table 3.1**).

In addition to the cell pellets, good separation was observed between the media of shControl and shFASN A3 1542 (Q^2 =0.889) and PC3 cells (Q^2 =950) (**Figure 3.7D** and **3.7E**). NMR spectra analysis of the media showed there was significant decrease in glutamate levels in response to FASN knockdown which was consistent in both cell lines (**Figure 3.9A, -3.9B** and **Table 3.2**).

The NMR results presented here confirm that in the prostate cell lines 1542 and PC3, control and FASN knockdown cell populations are metabolically different. Due to there being minimal metabolic separation between DU145 shControl and shFASN A3 cells, it was decided to only pursue with the 1542 and PC3 cell lines in the subsequent functional assays.

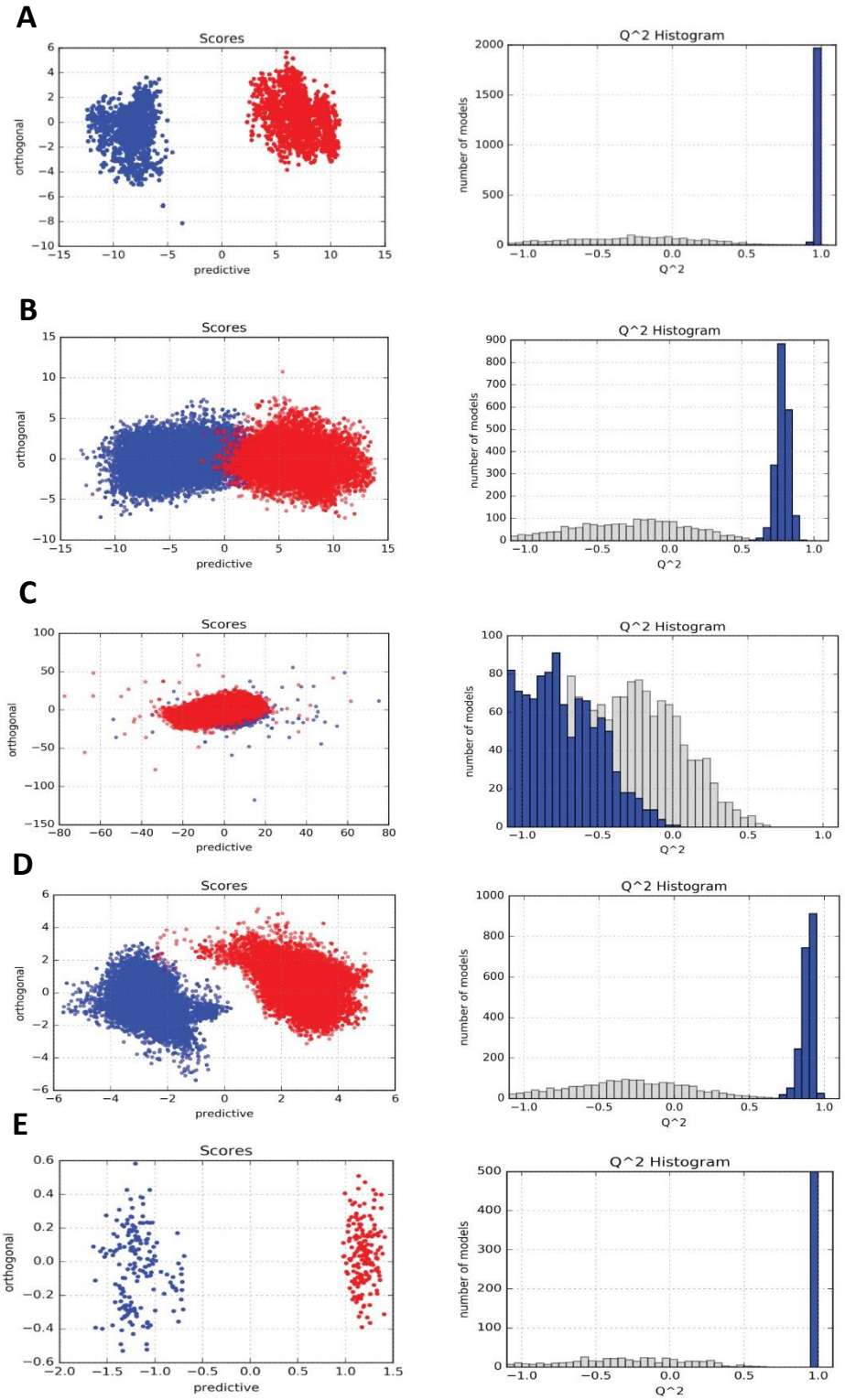

Figure 3.7 shControl and shFASN A3 separation analysis for the prostate cell lines 1542, PC3, and DU145 : Scores plot showing statistical separation between shControl (blue) and shFASN A3 (red) cell pellets and Q^2 histogram showing distribution of OPLS-DA models for the cell lines 1542 (**A**), PC3 (**B**), and DU145 (**C**). Similar plots but instead for media readings can be seen for 1542 cells in (**D**) and PC3 cells in (**E**).

A

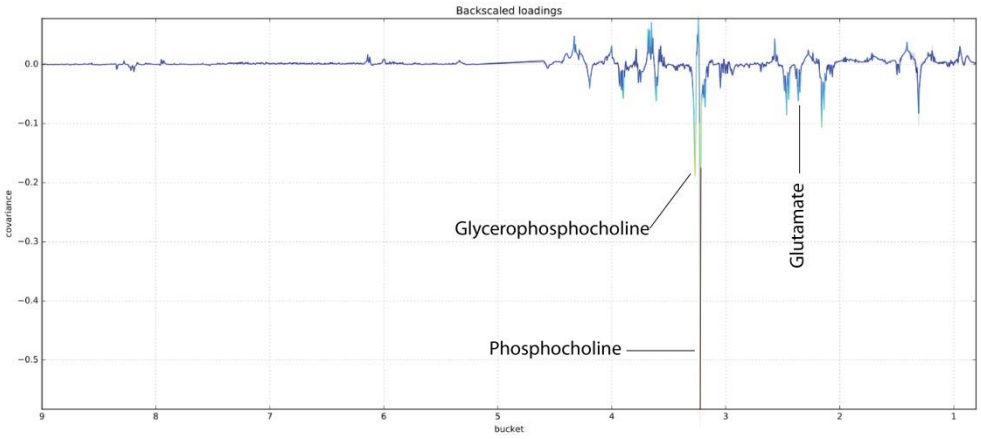

B

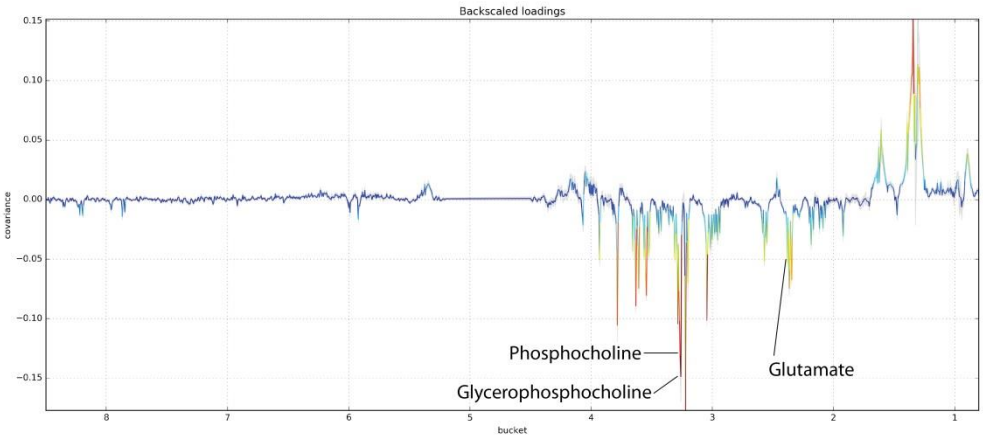

Figure 3.8 Metabolomic changes observed in 1542 and PC3 cell pellets in response to FASN knockdown: Back scale loadings plots highlighting differences in metabolites between shControl and shFASN A3 cell pellets for the 1542(**A**) and PC3 cell lines (**B**). For reference the back-scale loading plots are a pseudo-NMR spectrum showing which variables (chemicals shifts) in the data sets correlate with a class (peak height) and if that correlation is highly weighted (colour of the peak).

A

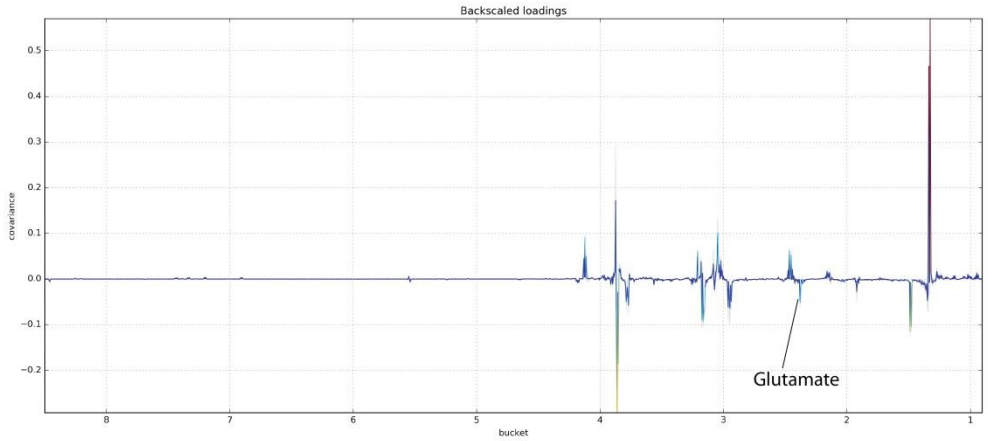

B

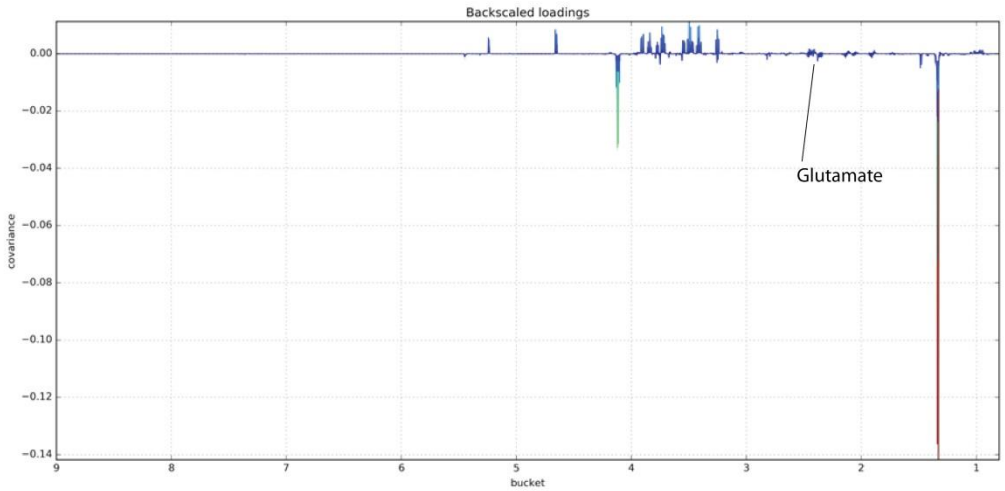

Figure 3.9 Metabolomic changes observed in 1542 and PC3 cell medium in response to FASN knockdown: Back scale loadings plots highlighting differences in metabolites between shControl and shFASN A3 cell medium for the 1542(**A**) and PC3 cell lines (**B**).

Metabolite Cell pellet	PPM	1542 Control v FASN A3 (%)	p-value (FDR adjusted)	PC3 Control v FASN A3 (%)	p-value (FDR adjusted)
Glutamate	2.36	-16.75	P < 0.001	-12.60	0.089
Phosphocholine	3.22	-29.55	P < 0.001	-8.98	0.204
Glycerophosphocholine	3.26	-42.12	P < 0.001	-18.66	0.032

Table 3.1 Changes in metabolites between shControl and shFASN A3 in 1542 and PC3 cell pellets: Assignment of metabolites based on their mass accuracy reading-PPM (parts per million). Negative (-) or positive (+) percentage (%) change in each metabolite was recorded in FASN knockdown cells compared to control. Statistical significance was determined by student's *t-test* false discovery rate (FDR) adjusted.

Metabolite Media	PPM	1542 Control v FASN A3 (%)	p-value (FDR adjusted)	PC3 Control v FASN A3 (%)	p-value (FDR adjusted)
Glutamate	2.36	-4.90	0.021	-11.79	P < 0.001

Table 3.2 Changes in metabolites between shControl and shFASN A3 in 1542 and PC3 cell media: Assignment of metabolites based on their mass accuracy reading-PPM (parts per million). Negative (-) or positive (+) percentage (%) change in each metabolite was recorded in FASN knockdown cells compared to control. Statistical significance was determined by student's *t-test* false discovery rate (FDR) adjusted.

3.2.6 Reduction in FASN levels are associated with morphological changes in prostate cancer cells

Having established that 1542 and PC3 shFASN cells have significantly decreased FASN levels, and are functionally different to shControl cells, it was decided to proceed and ascertain if the loss of FASN impacts on cellular behaviour. A common feature of cancer cells is their ability to change shape, this helps them adapt to new surroundings and is linked to an increased metastatic potential (Friedl and Wolf, 2003). Currently, FASN role in this facet of metastatic progression has been largely overlooked in multiple cancers. Evidence for its involvement has been shown in one study where FASN depletion induced marked morphological changes in LNCaP prostate cancer cells (De Schrijver et al., 2003). Here, microscopic analysis was conducted on control and FASN knockdown 1542 and PC3 cells in order to determine if FASN is involved in regulating the morphology of these cell lines. Overall, 90 cells (30 from three independent experiments) were analysed as this has been deemed an acceptable number to study morphological disparities (Al-Mahdi et al., 2015). Similar to the proliferation studies, morphological observations were carried out on matrix coated coverslips, including matrigel and type I collagen, in addition to non-coated glass coverslips.

Following quantification, differences in cell morphology were observed in both prostate cell lines in response to FASN knockdown (**Figure 3.10-3.13**). In 1542 and PC3 cells, a comparable decrease in cell area and perimeter was seen in both FASN depleted lines compared to their respective control cells when seeded on matrigel (**Figure 3.10-3.11A** and **Figure 3.12-3.13A**). Morphological changes of the same nature as a result of FASN knockdown were also observed in both cell lines when seeded onto glass and type I collagen. However, the overall decrease in cell area and perimeter was more modest when compared to cells that were seeded onto matrigel (**Figure 3.11B-C** and **Figure 3.13B-C**).

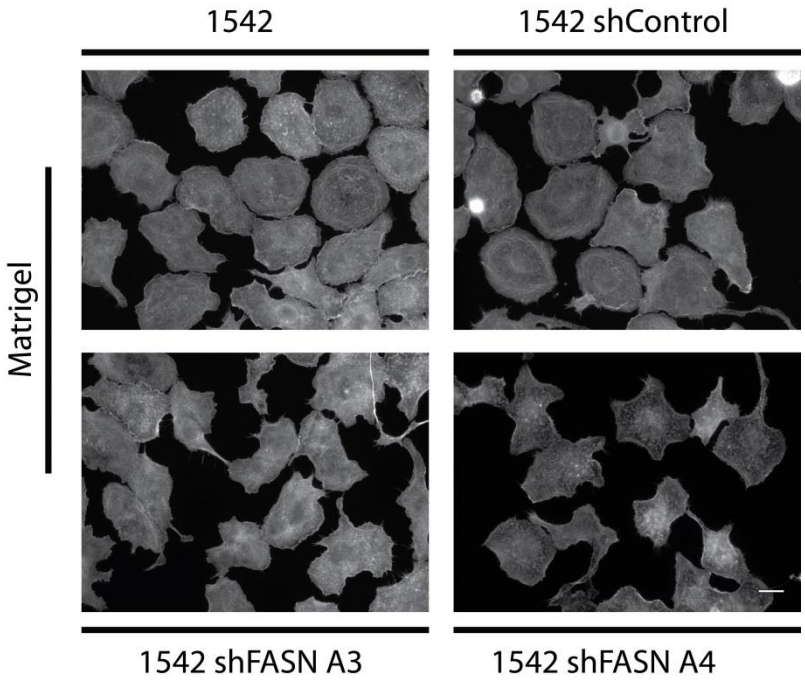

Figure 3.10 1542 cell morphology on Matrigel in response to FASN knockdown: 1542, 1542 shControl, 1542 shFASN A3 and 1542 shFASN A4 cells were seeded in the well of a six-well plate containing coverslips coated with 10 µg Matrigel. Cells were then fixed and stained for phalloidin. Images are representative of three independent experiments. Scale bar = 10 µm.

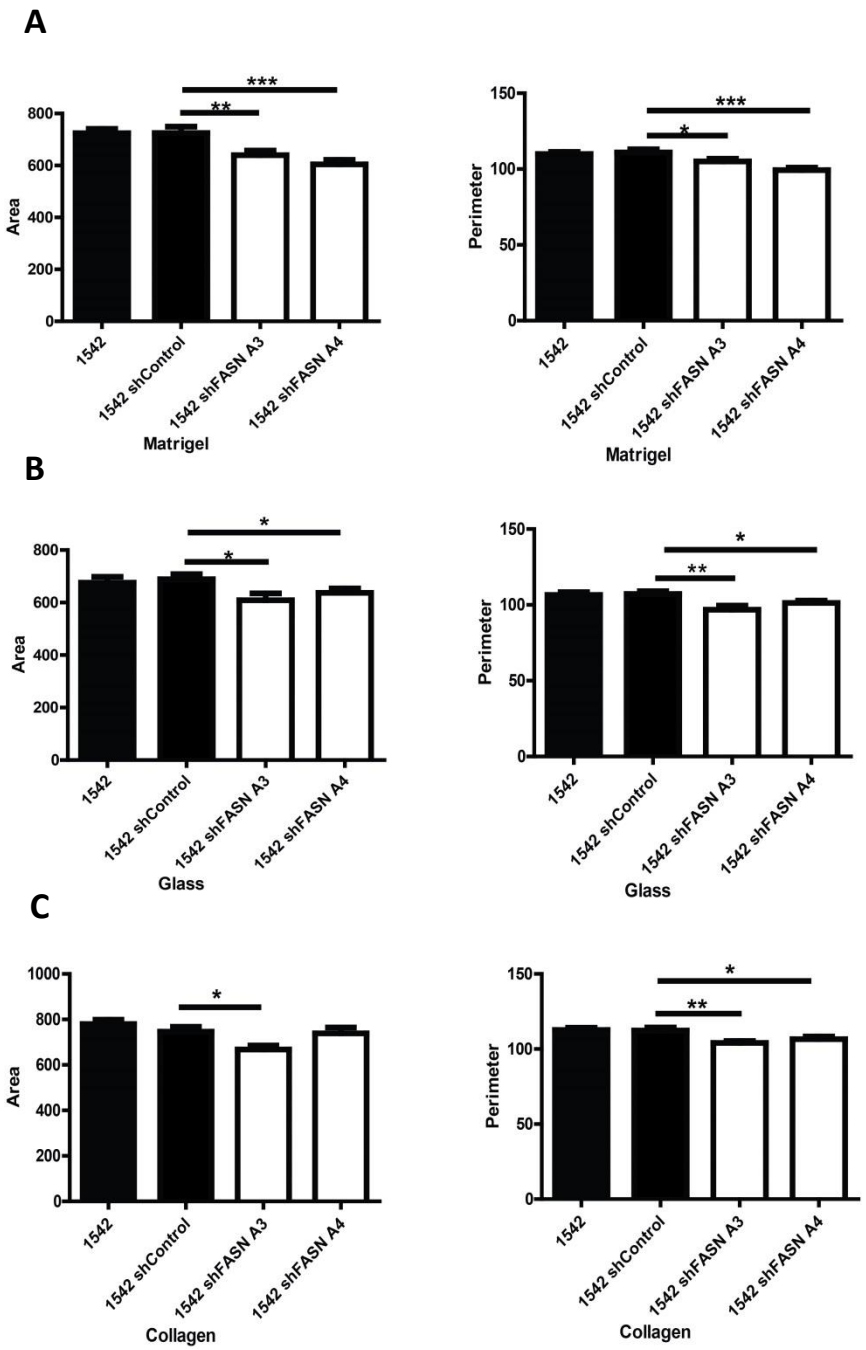

Figure 3.11 Silencing of FASN causes morphological changes in 1542 cells: ImageJ was used to calculate the cell area and perimeter of 90 cells per condition. From this data morphological differences between cell populations seeded onto matrigel (**A**), glass (**B**) and type I collagen (**C**) were quantified. Data represents the mean values ± SEM accumulated from three independent experiments. Statistical significance was determined by student's *t-test*. *p<0.05, **p<0.01, ***p<0.001.

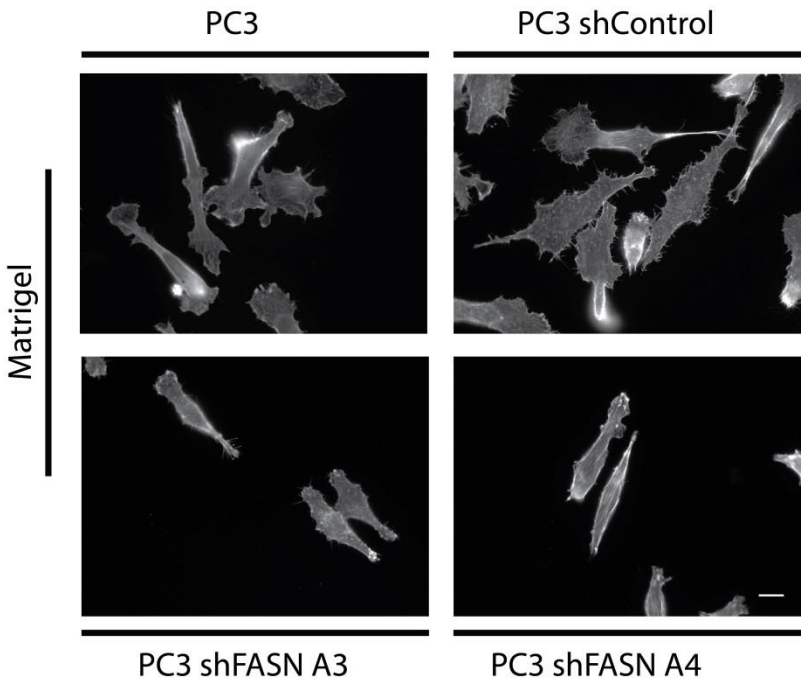

Figure 3.12 PC3 cell morphology on Matrigel in response to FASN knockdown: PC3, PC3 shControl, PC3 shFASN A3 and PC3 shFASN A4 cells were seeded in the well of a six-well plate containing coverslips coated with 10 μg Matrigel. Cells were then fixed and stained for phalloidin. Images are representative of three independent experiments. Scale bar = 10 μm.

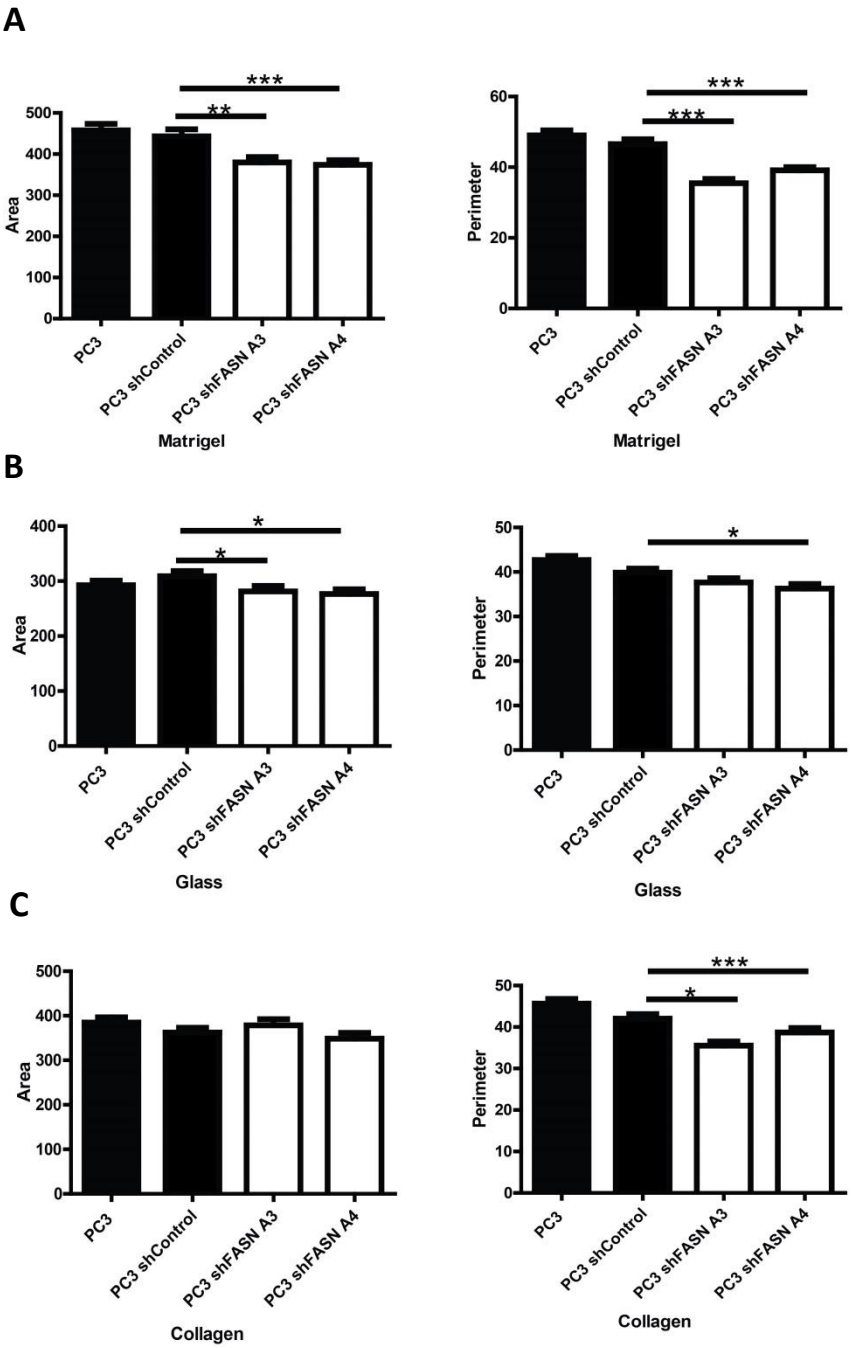

Figure 3.13 Silencing of FASN causes morphological changes in PC3 cells: ImageJ was used to calculate the cell area and perimeter of 90 cells per condition. From this data morphological differences between cell populations seeded onto matrigel (**A**), glass (**B**) and type I collagen (**C**) were quantified. Data represents the mean values ± SEM accumulated from three independent experiments. Statistical significance was determined by student's *t-test*. *p<0.05, **p<0.01, ***p<0.001.

3.3 Discussion

In this chapter, the FASN protein expression levels in cancer were determined and FASN depleted AR-independent prostate cancer cell lines were characterised for cell proliferative, metabolomic and morphological changes.

Within this study, FASN was found to be expressed in several different cancer cell lines including prostate, breast, pancreas and melanoma. This result agrees with the previous documentation of FASN as a commonly overexpressed protein in cancer (Corominas-Faja et al., 2017; Hamada et al., 2014; Innocenzi et al., 2003; Yang et al., 2011b). Additionally, FASN was also expressed in one non-cancerous breast cell line (MCF10A) and one non-cancerous transformed kidney cell line (HEK293). HEK293 cells have historically been selected to be a highly proliferative cell line and as such may have become dependent on *de novo* lipogenesis to accommodate this potentiated growth (Lin et al., 2014). In MCF10A cells, the expression level of FASN was comparable to MDA-MB-231 cells which are a highly metastatic breast cancer cell line. This contrasts what was observed in a study by Hopperton *et al* where they found MD-MB-231 cells to have increased FASN expression relative to MCF10A cells (Hopperton et al., 2014). Different results between our studies may have occurred due to the slightly different culture conditions of the MCF10A cells. Hopperton *et al* cultured MCF10A cells in standard growth media whilst the MCF10A cells used in this panel were cultured in media supplemented with insulin and EGF (Hopperton et al., 2014; Vazquez-Martin et al., 2008). Insulin and EGF are commonly added to the growth media of MCF10A cells and both have been shown to upregulate FASN expression (Radenne et al., 2008; Weng et al., 2007).

In a separate panel, FASN expression was found to be significantly higher in malignant prostate tissue than in benign prostate tissue. Moreover, the panel evidenced that FASN levels are associated with increased malignancy in prostate cancer. These results compliment findings in the literature and confirm FASN as a marker of tumorigenesis in prostate cancer (Hamada et al., 2014; Karantanos et al., 2016).

It has been well established now that FASN is upregulated in cancer to provide a selective proliferative advantage over normal cells (Chen et al., 2012). Inhibition of

FASN with RNAi or inhibitors has been shown to inhibit cellular proliferation in almost every type of cancer including prostate, lung, breast, ovarian, colorectal, pancreatic, melanoma, osteosarcoma, retinoblastoma, nasopharyngeal and liver (Daker et al., 2012; Deepa et al., 2013; Hu et al., 2016; Nishi et al., 2016; Singh et al., 2015; Veigel et al., 2015; Ventura et al., 2015; Yoshii et al., 2013; Zaytseva et al., 2012; Zecchin et al., 2011; Zhou et al., 2015). In agreement with the studies above it was found that knockdown of FASN in 1542, PC3 and DU145 cells significantly impaired the rate of cell proliferation. In addition, this proliferative defect occurred regardless of the surface the cells were seeded onto. Alternatively, growth curve analysis did not show a statistical difference in the rate of growth between control and FASN knockdown cells in any of the prostate cell lines (**Figure 3.4-3.6**). However, this is likely due to the fact that there was not a lot of difference in growth between control and FASN knockdown cells at Day 1 and Day 3. Typically, growth curve analysis is done on datasets with more time points giving a more accurate reading of the rate of change over time (Curran et al., 2010). Thus, in future it would be ideal to repeat the experiment measuring cell growth at each day.

The MTT assay results also showed that proliferative differences occurred earlier in the 1542 and PC3 cell line compared to the DU145 cell line upon FASN knockdown. One reason for this could be because DU145 cells have a slower doubling time compared to PC3 cells which means the separation rate between control and FASN knockdown cell populations occur earlier in PC3 (Cunningham and You, 2015). The same reason could also provide true for 1542 cells; however the doubling time for this cell line has not previously been documented. Alternatively, the timing of proliferative differences could be due to FASN affecting the metabolism of these cell lines differently (Ventura et al., 2015).

The role of FASN in cell proliferation has been extensively studied (Deepa et al., 2013; Knowles et al., 2004; Scaglia et al., 2014). During cell cycle progression there are lipogenic checkpoints at the G_2/M and G_1/S boundaries which require the partitioning of phospholipids and other fatty acids into the cell membrane in order for successful cell division to occur (Scaglia et al., 2014). Key lipids that are synthesised as a result of FASN activity which are involved in cell proliferation include phosphatidylcholine,

phosphatidylethanolamine, DAG and cholesterol esters (Veigel et al., 2015). All these lipids are important for membrane expansion and a reduction in their synthesis can cause a delay at either of the lipogenic checkpoints resulting in restricted cell division and growth (Scaglia et al., 2014).

FASN also regulates the F-box protein SKP2 which is a negative regulator of cyclin-dependent kinase inhibitors of the RB pathway such as p21 (Deepa et al., 2013). This explains why cell death has been observed upon FASN inhibition in some studies as proteins such as p21 accumulate and induce cell cycle arrest and apoptosis (Li et al., 2001). All FASN knockdown cell lines showed an increase in the readout signal over the course of the MTT assay which was in the same trend, but not as drastic as the control cells. These data suggest that the depletion of FASN most likely decreases overall lipid availability which in turn is responsible for hindering cell proliferation in 1542, PC3 and DU145 cells; however there is enough lipids and FASN protein not to induce arrest and apoptosis.

In addition to proliferative changes, FASN depletion in 1542 and PC3 cells also led to metabolic alterations. One metabolite that significantly decreased in the pellets of both cell lines was the choline derivative glycerophosphocholine. Choline metabolism is rapidly becoming regarded as a hallmark for tumour growth and progression. This has been evidenced by a study showing that an increase in the dietary intake of choline is associated with an increased risk of lethal prostate cancer (Richman et al., 2012). Glycerophosphocholine is formed as a result of the degradation of membrane phospholipid phosphatidylcholine (Glunde et al., 2011). Therefore a decrease in Glycerophosphocholine suggests that phosphatidylcholine synthesis has also declined (Kwon et al., 1995). Moreover, glycerophosphocholine can additionally be metabolized to choline and reused as a substrate for renewed synthesis of phosphatidylcholine (Fernandez-Murray and McMaster, 2005). Thus decreased Glycerophosphocholine levels leads to a reduction in the primer substrate needed to generate membrane lipids (Fernandez-Murray and McMaster, 2005). Furthermore, FASN inhibition has been shown to impair choline kinase activity which is required for the synthesis of phosphocholine, the precursor molecule of phosphatidylcholine (Ross et al., 2008). Phosphocholine levels were found to be decreased in the 1542 NMR spectra further

supporting the idea of reduced phosphatidylcholine production. Being essential in membrane synthesis, these changes in choline metabolism may partly aid in explaining the reduced proliferation phenotype seen in FASN knockdown cells.

Glutamate was another metabolite found to decrease in both prostate cancer cell lines upon FASN knockdown. Glutamate is a non-essential amino acid that is extensively involved in metabolic and oncogenic pathways in cancer (Koochekpour, 2013). A lowered intracellular level of glutamate in FASN depleted cells is most likely the result of reduced glutamine and α-ketoglutarate availability, key metabolites which can be processed to form glutamate (Hensley et al., 2013; Zhidenko et al., 1990). The consequence of this attenuated intracellular conversion is reduced glutamate secretion to trigger autocrine signalling. Evidence of this was verified in the NMR spectra which detailed depleted glutamate levels in the media of each cell line. High serum glutamate has been found to correlate with a higher Gleason score in prostate cancer (Koochekpour, 2013). Glutamatergic signalling is initiated upon the binding of glutamate to ionotropic (iGluR) and metabotropic glutamate receptors (mGluR), both of which have been found to be expressed in prostate cancer (Willard and Koochekpour, 2013). Glutamate blockage by receptor inhibition in PC3 and DU145 cells has been shown to decrease proliferation, migration and invasion (Koochekpour et al., 2012). It is possible that the synergistic loss of glutamate signalling in conjunction with choline depletion is contributing to the proliferative defect presented upon FASN knockdown in 1542 and PC3 cells.

Whilst proliferative defects are commonly associated with the loss of FASN, changes in cellular morphology are less well documented. In this chapter it was confirmed that FASN knockdown in all prostate cancer cell lines leads to morphological aberrations. Typically, FASN depleted cells exhibited a smaller shape relative to their control or wild-type counterparts. This phenotype was most markedly and consistently seen in 1542 and PC3 cells seeded onto matrigel. Changes in cell shape in all prostate cell lines was observed when seeded onto glass and collagen, however these differences were more modest and not always consistent between different shFASN clones.

The mechanism for how FASN may influence cell shape is unclear. It is possible that as a result of losing FASN, there is an unequivocal decrease in saturated fatty acids

available to completely form the cell membrane. This has been suggested in one previous study were the silencing of FASN led to a decrease in neutral lipids in the lipid bilayer of LNCaP cells (De Schrijver et al., 2003). Changes in cell shape are also frequently associated with reorganisation of the actin cytoskeleton. Rho GTPases modulate the actin cytoskeleton and silencing of their activity has been shown to profoundly affect cell spreading (Reymond et al., 2012; Sander et al., 1999). The link between FASN and Rho GTPases has not been extensively studied with only one study in colorectal cancer showing FASN knockdown correlates with the loss of RhoA expression (Zaytseva et al., 2012). This is something that will be explored in more detail in the later chapters of this thesis.

It currently is not clear why a difference in cell size was not consistently seen on all surfaces. One possibility is that changes in the lipid composition of the membrane as a result of FASN knockdown has disrupted the clustering of specific integrins (Pande, 2000). This has been previously reported in A375 melanoma cells which failed to spread due to the loss of integrin raft integrity (Wang et al., 2013a). Additionally, FASN may be regulating important proteins involved in adhesion. FASN has been shown to activate the tyrosine kinase Src which is essential for its ability to interact with specific integrin subunits (Di Vizio et al., 2008; Felsenfeld et al., 1999). Failure to interact has been shown to prevent fibroblast cells from being able to spread properly on fibronectin; however their spreading on vitronectin was unaffected (Felsenfeld et al., 1999).

In summary, the work presented here shows that FASN regulates cell proliferation and metabolic changes in prostate cancer. Moreover, FASN depletion was shown to induce morphological changes in prostate cancer cells suggesting that it may mediate cell cytoskeletal reorganization. Changes in the actin cytoskeleton are required for cell migration and invasion and so the role of FASN within this context will be explored in the next chapter.

3.4 Future work

In this chapter it was confirmed that FASN depletion induces phenotypic and metabolomic changes in prostate cancer. The metabolic profiling of each cell line was done in response to stable knockdown of FASN. In future experiments a comparison between stable shRNA knockdown, inducible ShRNA knockdown, siRNA knockdown and FASN inhibition could be conducted to identify which metabolites consistently change between treatments. This would help isolate key metabolites which are more sensitive to FASN activity and therefore more likely to be targetable. In addition to this, assessing the lipidomic profile of FASN depleted 1542 and PC3 cells via NMR or Mass spectrometry would be helpful in determining downstream targets. Staining of lipids using oil-red-o or BIODIPY could also be done as a quick experiment to assess changes in neutral lipids. Finally, it would also be worth investigating cell viability in response to FASN depletion in the prostate cell lines. This could be done by probing westerns for cell death proteins such as caspase-3 and performing FACS (Fluorescence-activated cell sorting) analysis which measures a specific dye that binds DNA allowing you to identify cell cycle disparities.

Chapter 4

Migratory characterisation of FASN depleted Prostate cancer cell lines

Chapter 4 – Migratory characterisation of FASN depleted prostate cancer cell lines

4.1 Introduction

One of the biggest challenges in modern medicine is the treatment of cancer at the later stages of progression (Chakraborty and Rahman, 2012). After the development of primary cancer within the prostate gland, a subset of cells will undergo further pathological changes (Banyard et al., 2014). These changes to the cells phenotypic properties are the beginning of a series of sequential and interrelated processes that are involved in cancer cell metastasis (Chambers et al., 2002). In prostate cancer widespread metastasis at the time of diagnosis occurs in approximately 20% of cases and is usually to the bone (Dasgupta et al., 2012). The first step of metastasis involves the dissemination of cells from the primary tumour mass into the surrounding stroma. This is followed by Intravasation of cells into local lymphatic or haematogenous vessels. Then eventually, a few cells will extravasate out of the vessel and into the surrounding tissue to form a secondary tumour site (Ye et al., 2007).

During the initial stages of metastasis the ability of cancer cells to segregate from the primary tumour and migrate into their surrounding environment is dependent on both intrinsic and extrinsic cues (Yamaguchi et al., 2005). Stromal cells situated in the ECM secrete cytokines such as HGF which is capable of increasing the motility of cancer cells through the activation of its cognate receptor c-Met (Jiang et al., 2005). In addition, dynamic reciprocity between the cell and its surrounding environment is also essential for cell migration (Schultz et al., 2011). The cell interacts with the ECM through adhesion contacts which mediate a link to the actin cytoskeleton and allow adhesions to be utilised as traction sites. (Huttenlocher and Horwitz, 2011). All facets of migration including cell polarity, cell shape, actomyosin contractility and cell adhesion turnover require reorganization of the actin cytoskeleton (Friedl and Wolf, 2003; Friedl and Wolf, 2009). Both ECM contact and stimulation by motogenic factors can induce changes in the cells actin cytoskeleton through the activation of Rho GTPase proteins (Huttenlocher and Horwitz, 2011; Royal et al., 2000).

FASN has been implicated in the migration and invasion of several different cancers including breast, colorectal, bladder and ovarian (Jiang et al., 2014; Li et al., 2012b; Zheng et al., 2016; Zhou et al., 2016). In addition, the silencing of FASN has been shown to impede the invasion of AR-dependent LNCaP prostate cancer cells *in vitro* and *in vivo* (Yoshii et al., 2013). However, targeting FASN specifically in AR-independent prostate cancer cell migration with RNAi has not been reported. Interestingly, Rae *et al* found that the migratory response in a wound healing assay was impaired when PC3 cells were treated with a FASN inhibitor, although proliferative differences were not completely controlled for with cell cycle inhibitors (Rae et al., 2015). In a separate study it was shown that the invasion of PC3 and DU145 cells *in vitro* was significantly reduced when the cells were incubated with ASC-J9, an androgen degradation enhancer which suppressed FASN expression (Wen et al., 2016). Whilst it is not yet completely clear how FASN drives cell migration, it is known that adding palmitate, the fatty acid product of FASN, to hepatocellular cancer cells induces morphological changes and cell invasion (Nath et al., 2015). This suggests that downstream fatty acid signalling may be involved in FASN-induced cell motility. In addition, FASN has been shown to modulate the expression of c-Met in prostate cancer cells which is associated with the increased invasiveness of this cancer (Coleman et al., 2009; Han et al., 2014).

In this chapter of the thesis, all aspects of motility including morphology and adhesion will be investigated in response to depleting FASN levels in AR-independent prostate cancer cells. 1542 will be used as the principle cell line in this study as it was derived from the prostate and so is most likely to accurately recapitulate the biological behaviour of prostate tumours (Schwab et al., 2000). Key assays will be then be confirmed in PC3 cells as a secondary prostate cell line.

4.2 Results

4.2.1 Overexpression of FASN is associated with an increase in the spread area of prostate cancer cells

In the last chapter it was observed that there was a decrease in the overall size of FASN knockdown prostate cancer cells relative to control cells. To further examine the influence FASN has on cell shape both 1542 and PC3 cells were transiently transfected with a FASN-overexpression construct to increase its baseline expression. This experiment was carried out on matrigel as the most notable and consistent effects with regard to changes in 1542 and PC3 cell shape in response to FASN knockdown were seen when seeded onto this matrix. Here It was observed that both 1542 and PC3 cells overexpressing FASN showed a significant increase in cell area and perimeter relative to control cells transfected with a GFP-alone vector (**Figure 4.1** and **Figure 4.2**).

4.2.2 Palmitate rescues FASN knockdown 1542 cell morphology

The morphological studies that have currently been presented in this thesis have identified a correlation between FASN expression and cell shape. The primary function of FASN is to synthesize the saturated fatty acid palmitate (Ventura et al., 2015). Thus, a rescue experiment was performed by adding exogenous palmitate to FASN depleted cells and assessing if they adopt a morphological phenotype similar to that of the control cells. As with previous experiments, 1542 shControl and 1542 shFASN A3 cells were seeded onto matrigel coated coverslips. BSA alone and BSA conjugated-palmitate 50 µM was added to two separate wells containing 1542 shFASN A3 cells. Cells were incubated with BSA and palmitate for 1 hour before fixing and staining. Imaging analysis of the staining shows that 1542 shFASN A3 cells treated with BSA alone exhibited a similar morphology to that of non-treated 1542 shFASN A3 cells (**Figure 4.3**). In contrast, the addition of palmitate significantly increased the area and perimeter of 1542 shFASN A3 cells relative to BSA treated cells making them similar in size to 1542 shControl cells and rescuing the control phenotype (**Figure 4.3**).

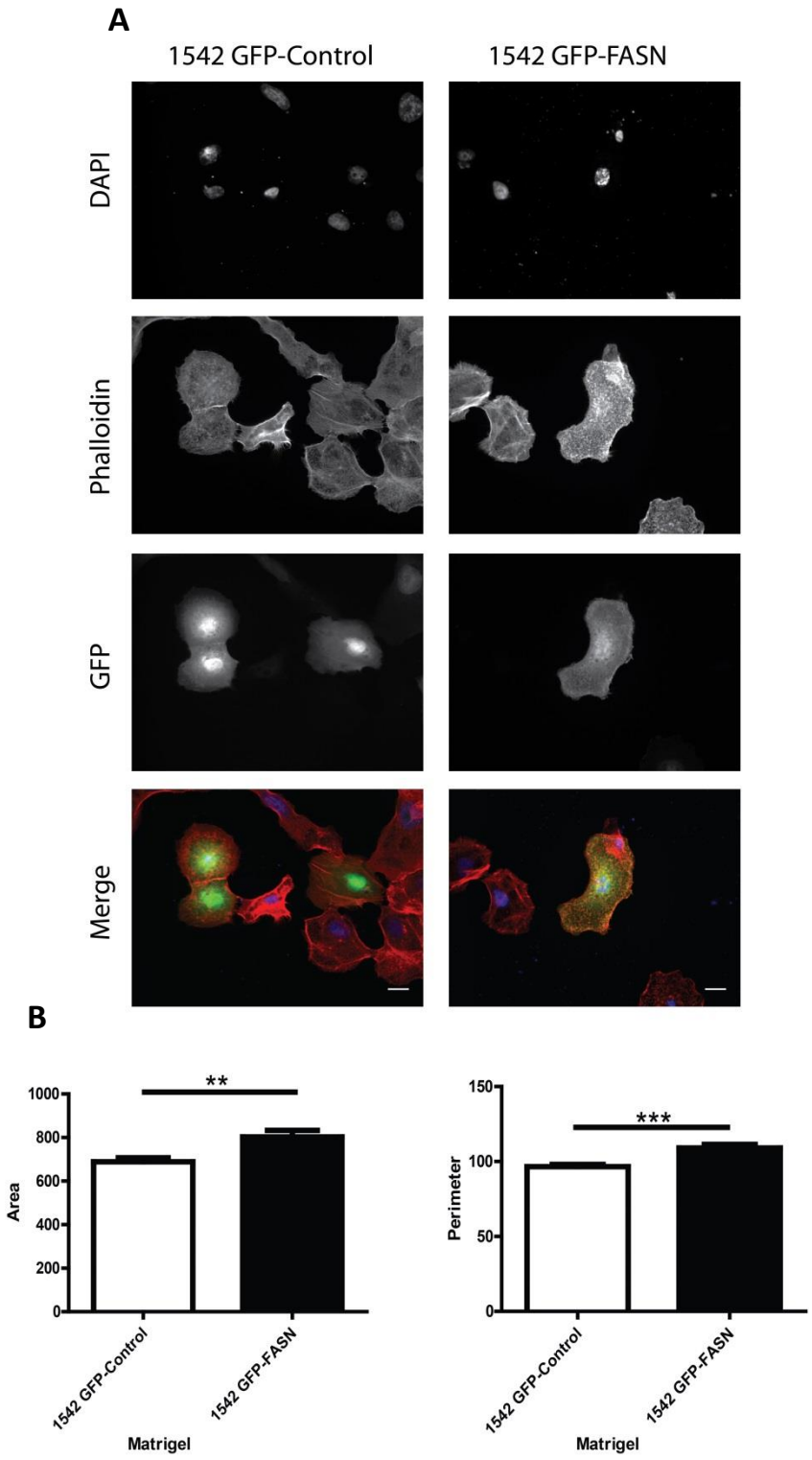

Figure 4.1 Overexpression of FASN causes morphological changes in 1542 cells: 1542 cells were seeded onto matrigel coated coverslips and then transiently transfected with either GFP- alone or GFP-FASN (**A**). Cells were stained with DAPI and Phalloidin. ImageJ was used to calculate the cell area and perimeter of 90 cells per condition and from this data morphological differences were quantified (**B**). Data represents the mean values ± SEM accumulated from three independent experiments. Scale bar = 10 µm. Statistical significance was determined by student's *t-test*. **p<0.01, ***p<0.001.

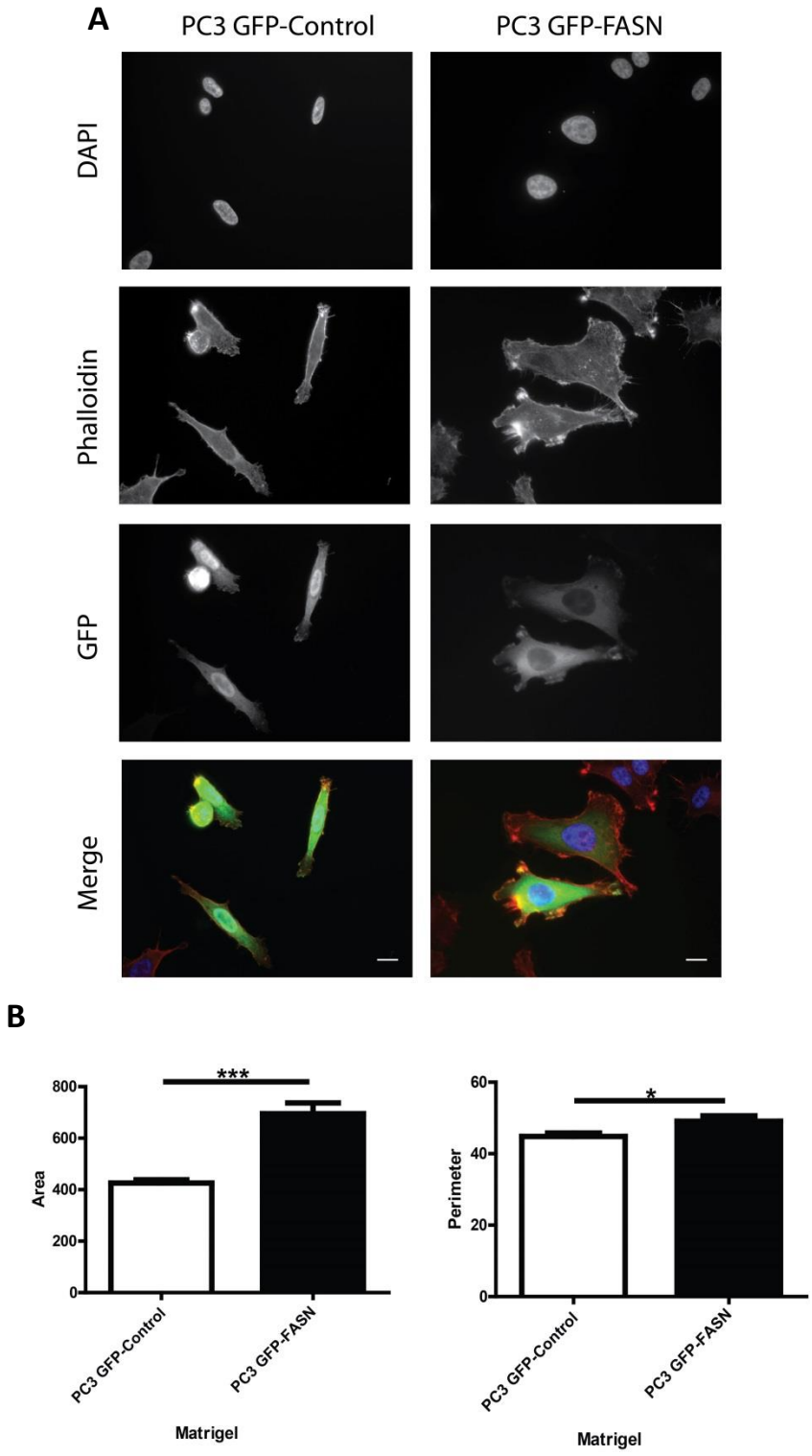

Figure 4.2 Overexpression of FASN causes morphological changes in PC3 cells: PC3 cells were seeded onto matrigel coated coverslips and then transiently transfected with either GFP- alone or GFP-FASN (**A**). Cells were stained with DAPI and Phalloidin. ImageJ was used to calculate the cell area and perimeter of 90 cells per condition and from this data morphological differences were quantified (**B**). Data represents the mean values ± SEM accumulated from three independent experiments. Scale bar = 10 µm. Statistical significance was determined by student's *t-test*. *p<0.05, ***p<0.001.

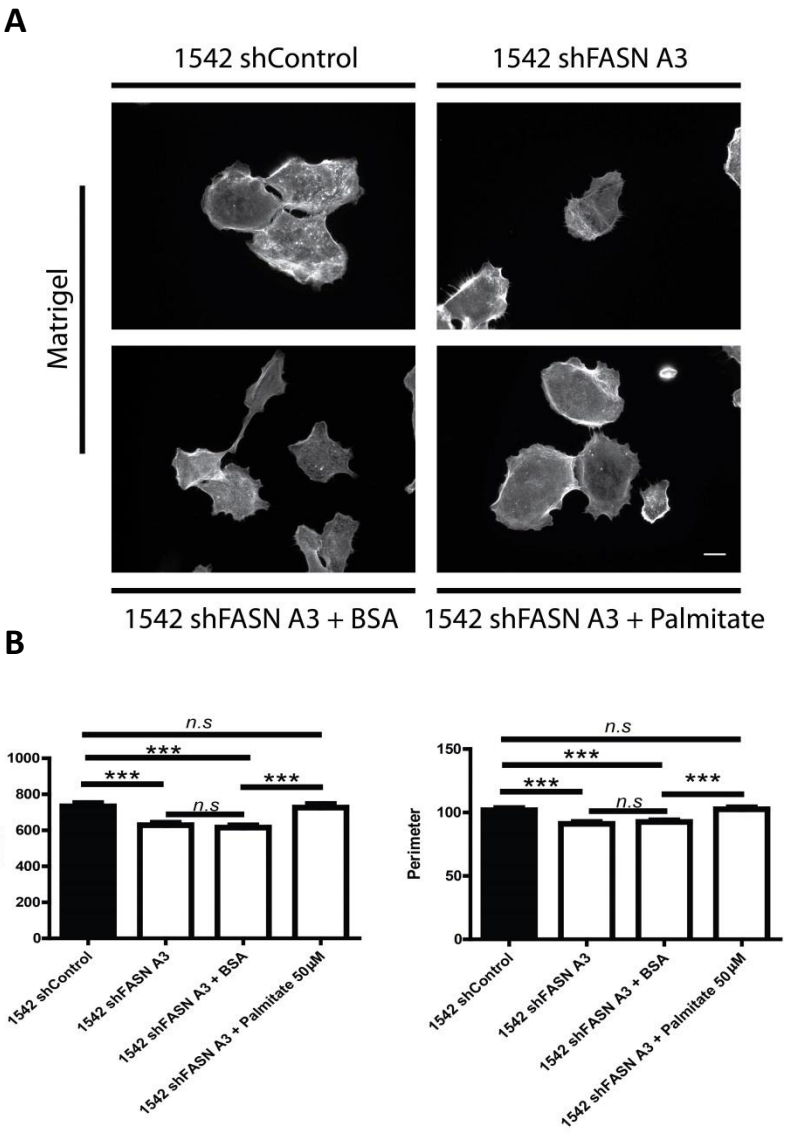

Figure 4.3 Palmitate rescues FASN knockdown morphological phenotype in 1542 cells: 1542 shControl and 1542 shFASN A3 cells were seeded onto matrigel coated coverslips. BSA and BSA conjugated-palmitate 50 µM was added to wells containing 1542 shFASN A3 cells. Cells were incubated for one hour before staining with phalloidin (**A**). ImageJ was used to calculate the cell area and perimeter of 90 cells per condition. This data was used to determine differences in cell perimeter and area between the different conditions (**B**).Data represents the mean values ± SEM accumulated from three independent experiments. Statistical significance was determined by student's *t-test*. **p<0.01 ***p<0.001. *n.s*= not significant. Bar= 10 µM

4.2.3 The effect of FASN knockdown on prostate cancer cell adhesion

For cells to migrate optimally they need to be able to interact with the surrounding ECM (Huttenlocher and Horwitz, 2011). The coordinated assembly and disassembly of adhesions during migration is important for several cellular processes including cell spreading, polarity and directional persistence (Choma et al., 2004; Huttenlocher and Horwitz, 2011).

Adhesion was measured by seeding prostate cancer cells into matrix-coated 96 well plates and then leaving them for one hour to attach. After this period, the wells were washed out with PBS to remove any non-adherent cells and then an MTT assay was carried out to measure the adherent cells. Adherence analysis showed that FASN knockdown in 1542 cells significantly increased cell-matrix adhesion when compared to their respective control cells (**Figure 4.4A-B**). A similar trend was seen in two independent experiments for PC3 cells also (**Figure 4.4C-D**) This effect on cell adhesion in response to silenced FASN expression was observed on both matrigel and type I collagen (**Figure 4.4A-D**).

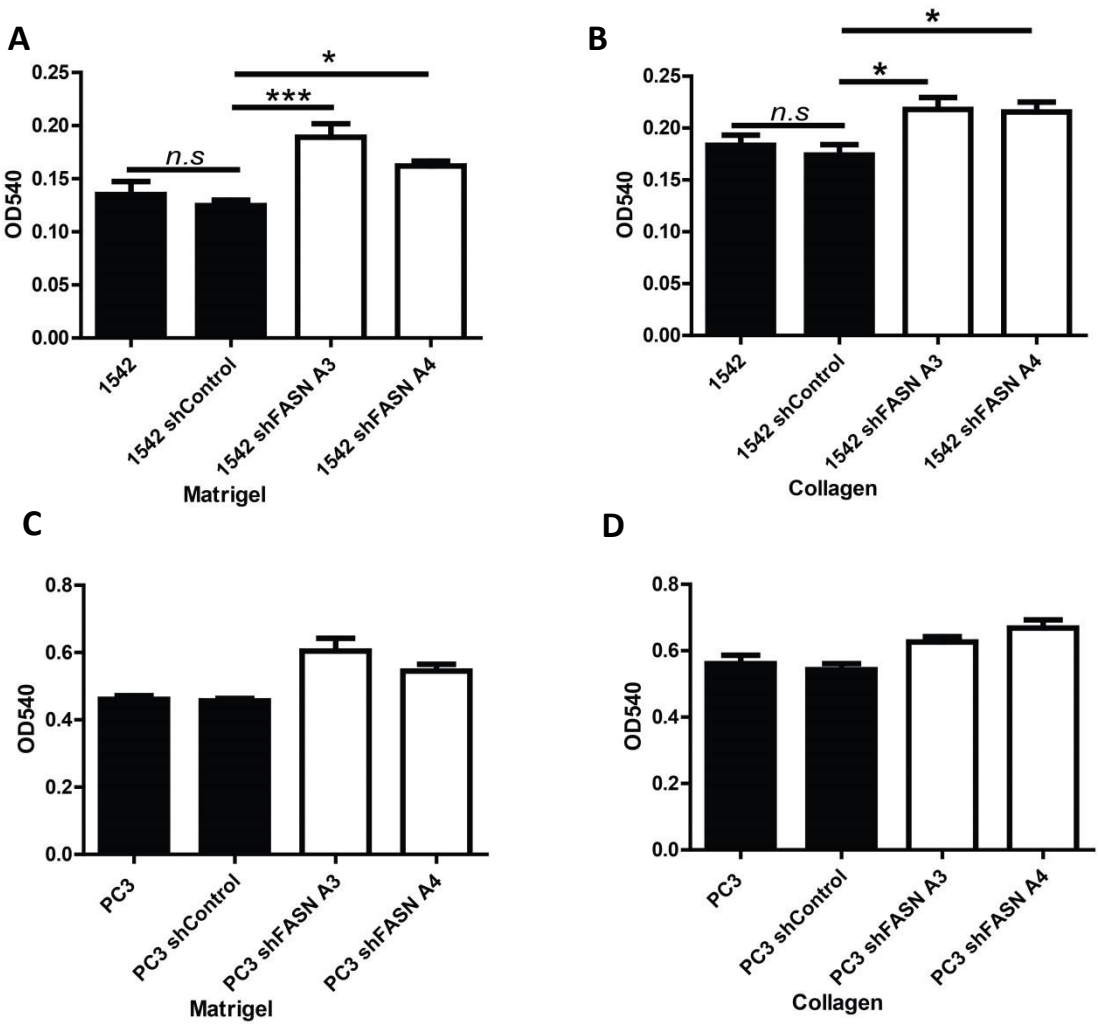

Figure 4.4 FASN depletion increases prostate cancer cell adhesion: 1542, 1542 shControl, 1542 shFASN A3 and 1542 shFASN A4 cells were seeded into the wells of a 96 well plate coated with matrigel (**A**) or type I collagen (**B**). Cells were left to adhere for one hour before being subjected to an MTT assay. The same experimental set up was conducted for the PC3 cell lines on matrigel (**C**) or type I collagen (**D**) also. Data represents the mean values ± SEM accumulated from three independent experiments in 1542 cells and two independent experiments in PC3 cells. Statistical significance was determined by an ANOVA Tukey test * $p<0.05$, ** $p<0.01$, ***$p<0.001$. . *n.s*= not significant.

4.2.4 Focal adhesion size is dependent on FASN expression

Previous work by Wells *et al* has confirmed a biphasic relationship between the size of paxillin-containing adhesions and the level of adherence in PAK4 silenced DU145 prostate cancer cells (Wells et al., 2010). Upon confirming that FASN knockdown increases prostate cancer cell adhesion it was decided to investigate if this phenotype correlates similarly with an increase in focal adhesion size. As a global adhesion defect was seen in both prostate cell lines, focal adhesions were only analysed in more detail in the 1542 cells as this is the main cell line of this study. 1542 shControl, 1542 shFASN A3 and 1542 shFASN A4 cells were seeded onto matrigel coated coverslips and then stained for paxillin (**Figure 4.5A**). Analysis of the staining revealed that FASN knockdown increases the number of 1542 cells with prominent paxillin (**Figure 4.5B**). In addition, an increase in the length of focal adhesions was observed in FASN depleted 1542 cells when compared to 1542 shControl cells (**Figure 4.5C**).

4.2.5 Paxillin associated focal adhesion length alters in response to palmitate addition in 1542 cells

Having shown that the morphology of FASN depleted 1542 cells could be rescued when incubated with palmitate a similar experiment was carried out to determine how paxillin staining alters in response to palmitate treatment (**Figure 4.6A**). Following quantification of staining, 1542 shFASN A3 cells incubated with palmitate exhibited a concomitant reduction in paxillin length and the number of cells with prominent paxillin (**Figure 4.6B** and **4.6C**). Palmitate treatment rescued paxillin staining to similar levels seen in 1542 shControl cells, although the rescue response is partial as paxillin length between BSA and palmitate treated cells is not significantly different (**Figure 4.6B** and **4.6C**). Alternatively 1542 shFASN A3 cells incubated with BSA alone were unaffected giving them identical paxillin numbers and length to untreated 1542 A3 cells (**Figure 4.6B** and **4.6C**).

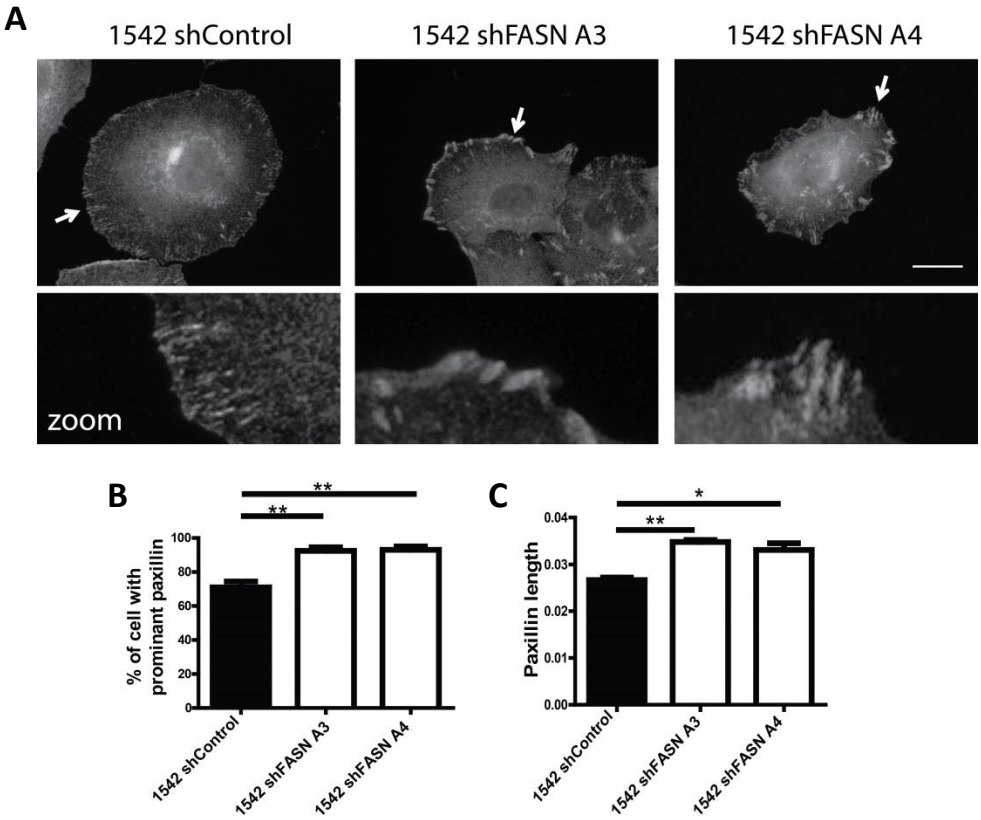

Figure 4.5 FASN Knockdown alters paxillin length in 1542 cells: 1542 shControl, 1542 shFASN A3 and 1542 shFASN A4 cells were seeded onto matrigel coated coverslips (10 µg/ml) and then stained for paxillin (**A**). The percentage of cells with visible paxillin was quantified in (**B**). The length of paxillin was measured in imageJ and quantified in (**C**). White arrows indicate the area that was magnified. The analysis is the sum of 60 cells per condition over three independent experiments. Data represents the mean values ± SEM. Statistical significance was determined by student's *t-test*. *p<0.05, **p<0.01. Bar= 10 µm.

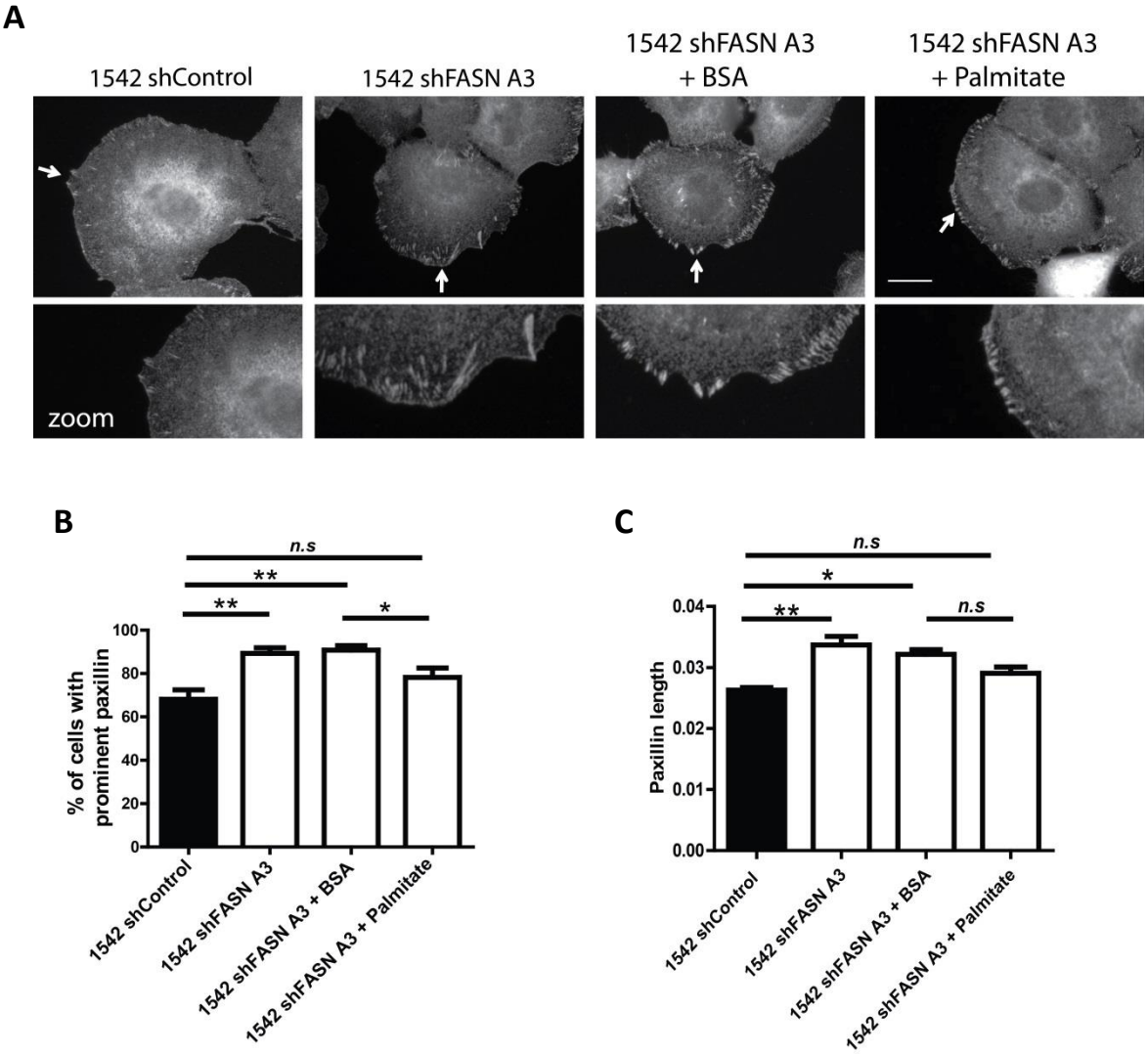

Figure 4.6 Exogenous palmitate rescues FASN knockdown 1542 cell paxillin length: 1542 shControl, 1542 shFASN A3, BSA-treated 1542 shFASN A3, BSA-Palmitate treated 1542 shFASN A3 were stained for paxillin (**A**). Quantification of the percentage of cells with visible paxillin is shown in (**B**). The length of paxillin was measured in imageJ and quantified in (**C**).Data represents the mean values ± SEM accumulated from three independent experiments. White arrows indicate the area that was magnified. Statistical significance was determined by student's *t-test*. *p<0.05, **p<0.01. *n/s*= not significant. Bar= 10 µM.

4.2.6 Reduced prostate cancer cell migration in response to FASN knockdown

This study has now identified observable changes in cell morphology and adhesion in response to FASN knockdown in prostate cancer cells. Defects in these phenotypes suggest a likely impact on cell migration (Hakkinen et al., 2011; Kim and Wirtz, 2013). HGF, a ligand that specifically complexes with c-Met, is abundantly expressed in the prostate microenvironment and is known to have mitogenic and motogenic activities on prostate cancer cells (Ye et al., 2007). FASN has been linked with c-Met in prostate cancer and so it was deemed pertinent to monitor the migratory ability of FASN knockdown cells in response to HGF (Coleman et al., 2009). Since a proliferation defect was observed in response to depleting FASN levels in both 1542 and PC3 cells (**Figure 3.4** and **Figure 3.5**), a random 2D migration assay was carried out on the basis that the measured variable is not significantly impacted by variations in proliferation rate.

In comparison to 1542 shControl cells, there was a significant reduction in the mean migratory speed of both 1542 shFASN A3 and 1542 shFASN A4 cells in the presence of HGF (**Figure 4.7** and see **Movies 1-4** on CD for representative movies on matrigel). Similarly, in the presence of HGF a reduction in cell speed was also seen in FASN knockdown PC3 cells when compared to PC3 shControl cells (**Figure 4.8** and see **Movies 5-8** on CD for representative movies on matrigel). Migratory ability in response to FASN knockdown in both cell lines was tested on matrigel and type I collagen coated wells which showed a consistent response across both substrata (**Figure 4.7A-C** and **Figure 4.8A-C**). Additionally, it should be noted that no cell death was observed in these movies over 16 hours supporting the notion that FASN knockdown cells are simply proliferating at a slower rate. These results reveal that FASN knockdown impairs HGF-induced migration in AR-independent prostate cancer cell lines 1542 and PC3.

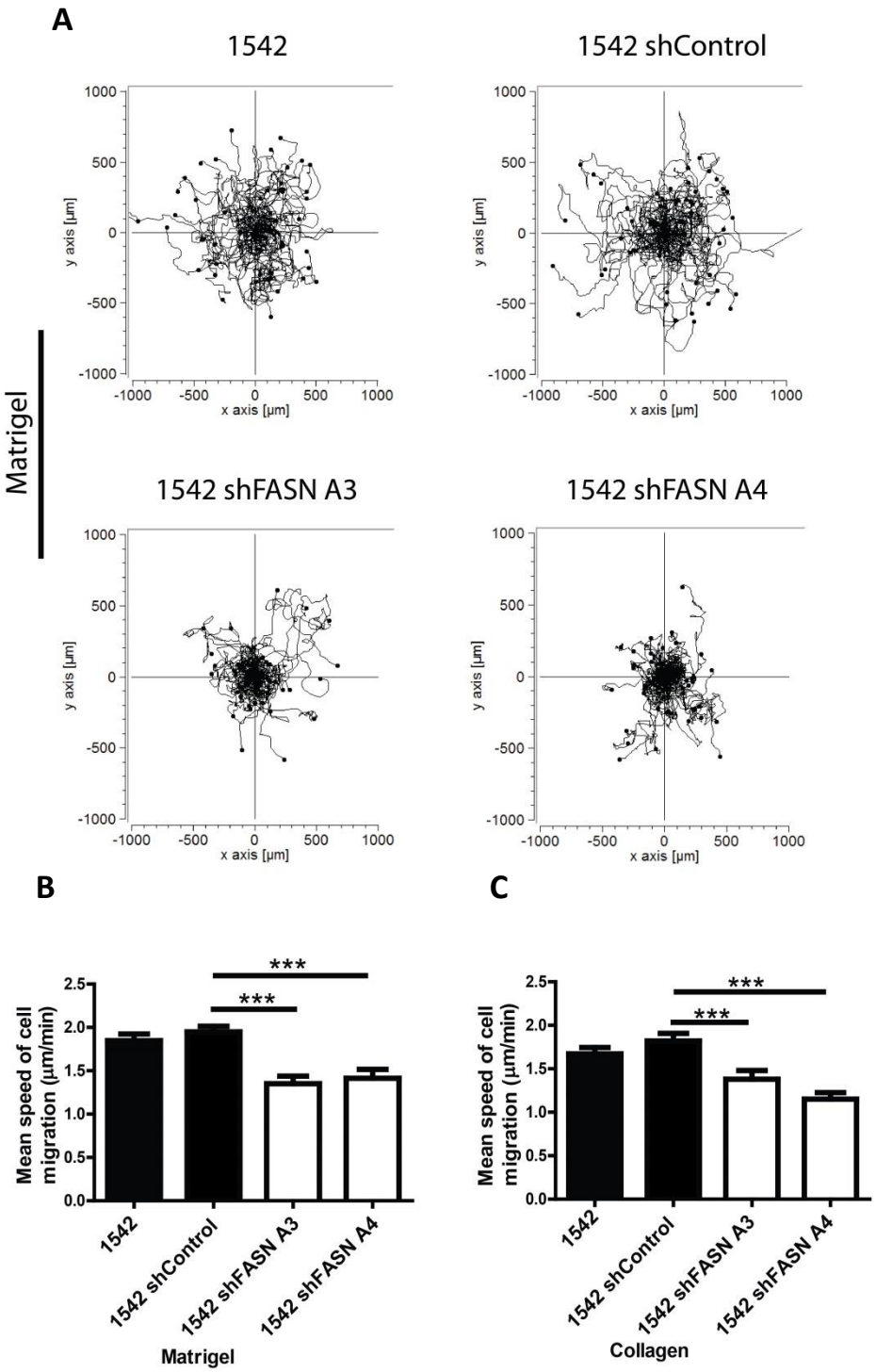

Figure 4.7 FASN knockdown impairs 1542 cell migration in the presence of HGF: 1542, 1542 shControl, 1542 shFASN A3 and 1542 shFASN A4 cells were seeded into matrigel or type I collagen coated wells , serum starved and then stimulated with 10 ng/ml HGF. Migration plots were created from the movies of cells migrating on matrigel (**A**) which were used as representations of each cell lines trajectory. Cells were filmed for 16 hours with images being taken at 5 minute intervals using the Olympus IX71 inverted time-lapse microscope at 10x magnification. The manual tracking plugin in imageJ was used to track up to 60 cells per condition. Migration trajectories were placed into Mathematica and then the speed of cell migration on matrigel (**B**) and type I collagen (**C**) was calculated. Data represents the mean values ± SEM accumulated from three independent experiments. Statistical significance was determined by student's *t-test*. *** p<0.001

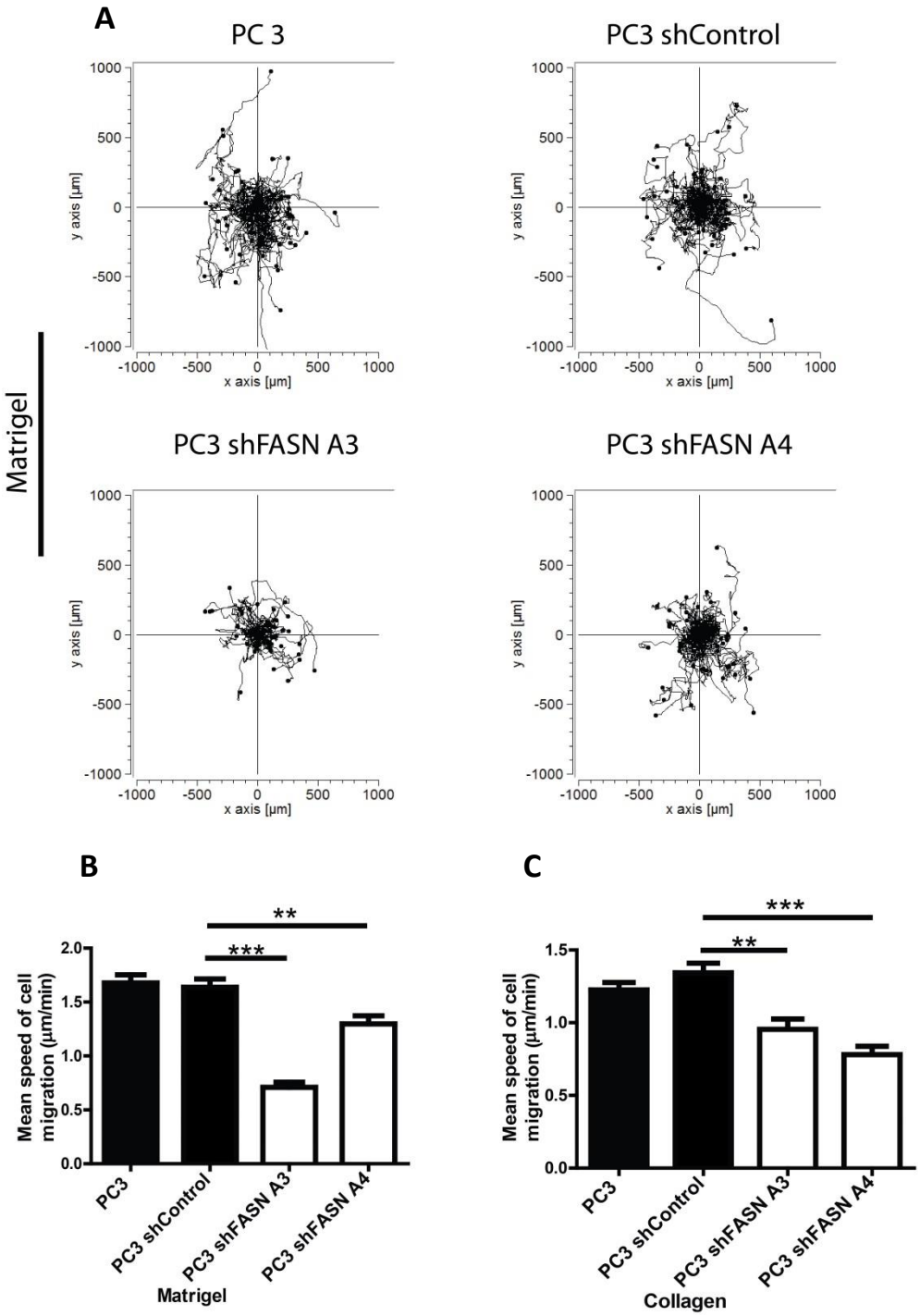

Figure 4.8 FASN knockdown impairs PC3 cell migration in the presence of HGF: PC3, PC3 shControl, PC3 shFASN A3 and PC3 shFASN A4 cells were seeded into matrigel or type I collagen coated wells , serum starved and then stimulated with 10 ng/ml HGF. Migration plots were created from the movies of cells migrating on matrigel (**A**) which were used as representations of each cell lines trajectory. Cells were filmed for 16 hours with images being taken at 5 minute intervals using the Olympus IX71 inverted time-lapse microscope at 10x magnification. The manual tracking plugin in imageJ was used to track up to 60 cells per condition. Migration trajectories were placed into Mathematica and then the speed of cell migration on matrigel (**B**) and type I collagen (**C**) was calculated. Data represents the mean values ± SEM accumulated from three independent experiments. Statistical significance was determined by student's *t-test*. ** p<0.01, *** p<0.001.

4.2.7 FASN inhibitors phenocopy FASN knockdown defect in HGF-induced prostate cancer cell migration

To further validate the role of FASN in prostate cancer cell migration a 2D migration assay was carried out testing the migratory response of 1542 and PC3 cells in the presence of HGF under the treatment of two well –known FASN inhibitors, C75 and orlistat. C75 is a cerulenin-derived semi-synthetic irreversible inhibitor which targets the β-ketoacyl synthase, enoyl reductase and the thioesterase domains of FASN (López and Diéguez, 2007). Orlistat is a semi-synthetic pancreatic lipase inhibitor which was originally developed as anti- type II diabetes drug. It was identified in a screen as an irreversible inhibitor of FASN targeting the thioesterase domain (Kridel et al., 2004).

Both 1542 and PC3 cells treated with either C75 or orlistat displayed a significant decrease in the mean migratory speed following HGF addition when compared to their respective DMSO controls (**Figure 4.9-4.10**). Both FASN inhibitors were equally effective in decreasing the migratory speed of PC3 cells (**Figure 4.10B** and see **Movies 12-14** on CD for representative movies), whilst C75 appeared to be a more potent inhibitor in 1542 cells (**Figure 4.9B** and see **Movies 9-11** on CD for representative movies). These results compliment the previous migration data and suggest FASN activity is directly linked to cell migration.

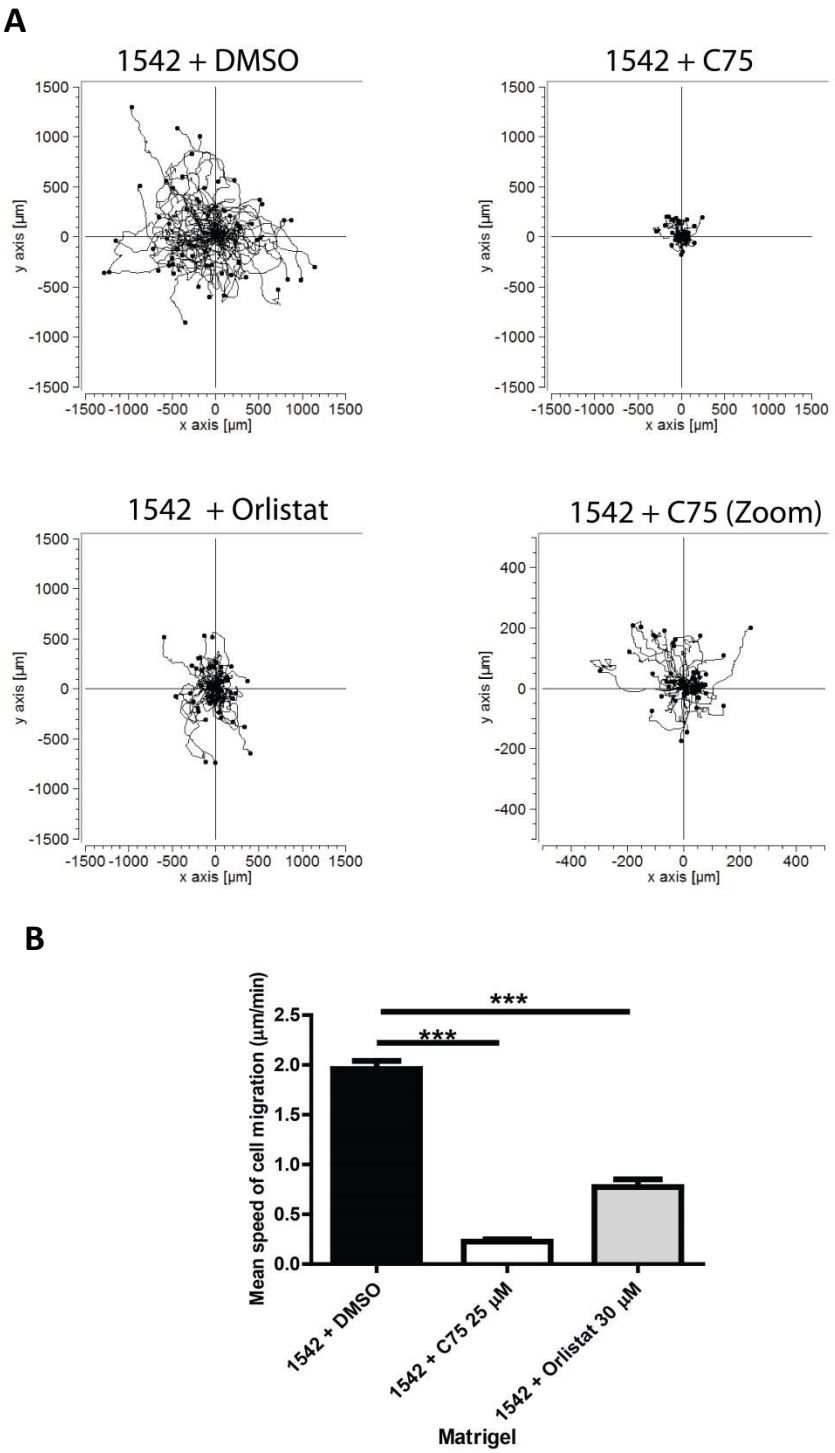

Figure 4.9 FASN inhibitors impair 1542 cell migration in the presence of HGF: 1542 cells were seeded into matrigel-coated wells, serum starved, incubated with DMSO, C75 or orlistat and then stimulated with 10 ng/ml HGF. Cells were filmed for 16 hours with images being taken at 5 minute intervals using the Olympus IX71 inverted time-lapse microscope at 10x magnification. The manual tracking plugin in imageJ was used to track up to 60 cells per condition. Migration trajectories were placed into Mathematica and then the speed of cell migration on matrigel (**B**) was calculated. Data represents the mean values ± SEM accumulated from three independent experiments. Migration plots for cells migrating on matrigel (**A**) were used as representations of each cell lines trajectory. An additional migratory trajectory for C75 that is 3 x zoomed in was included to clarify the cells have not died and are still migrating but just at a profoundly slower rate. Statistical significance was determined by student's *t-test*. *** $p<0.001$

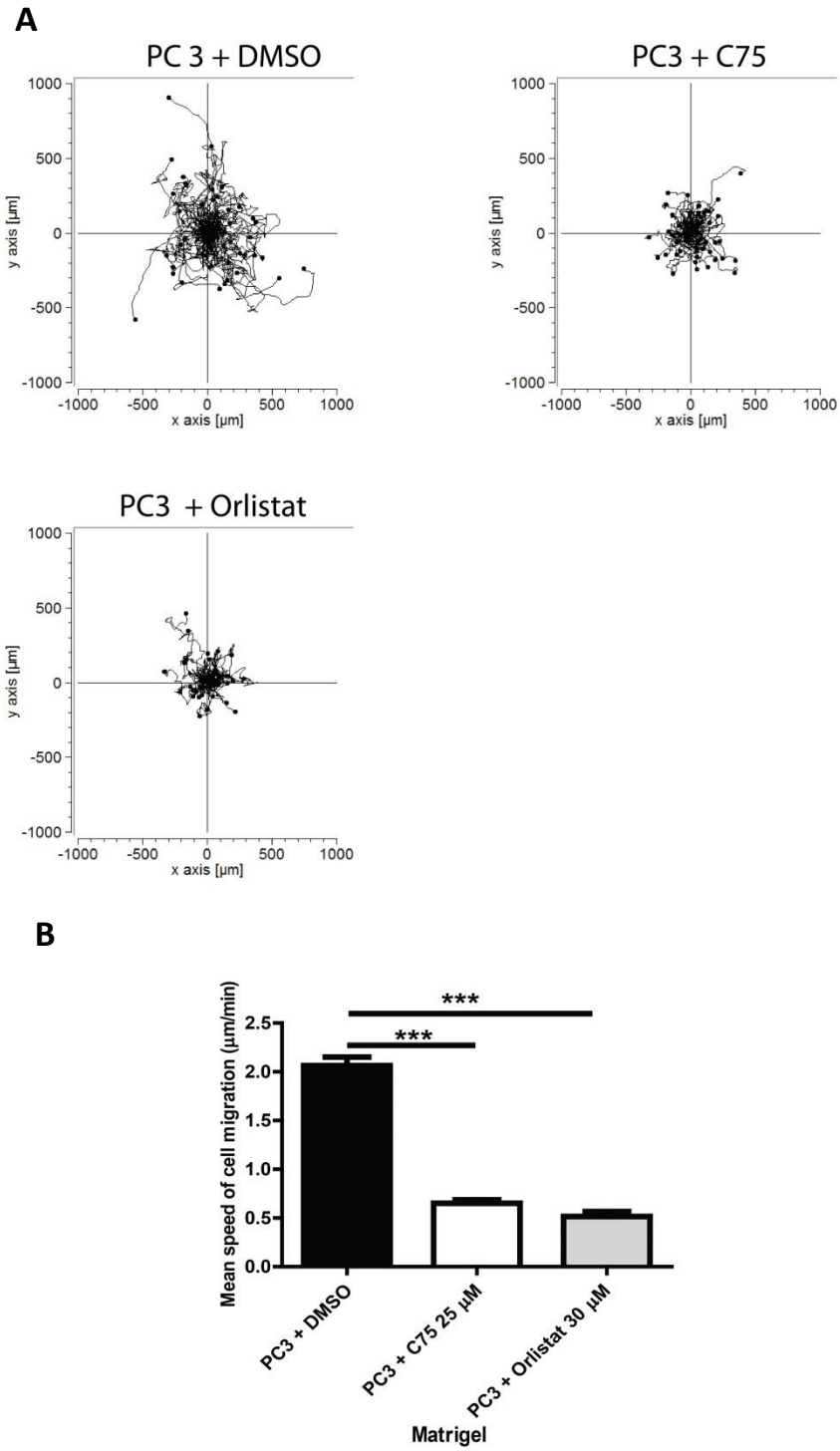

Figure 4.10 FASN inhibitors impair PC3 cell migration in the presence of HGF: PC3 cells were seeded into matrigel-coated wells, serum starved, incubated with DMSO, C75 or orlistat and then stimulated with 10 ng/ml HGF. Cells were filmed for 16 hours with images being taken at 5 minute intervals using the Olympus IX71 inverted time-lapse microscope at 10x magnification. The manual tracking plugin in imageJ was used to track up to 60 cells per condition. Migration trajectories were placed into Mathematica and then the speed of cell migration on matrigel (**B**) was calculated. Data represents the mean values ± SEM accumulated from three independent experiments. Migration plots for cells migrating on matrigel (**A**) were used as representations of each cell lines trajectory. Statistical significance was determined by student's *t-test*. *** $p<0.001$

4.2.8 FASN depletion reduces prostate cancer cell invasion

After confirming that FASN knockdown impairs prostate cancer cell migration in 2D it was decided to carry out a 3D invasion assay using these cell lines. Looking at cell motility in both models has become increasingly more important as studies are starting to identify differences between cell behaviour in 2D and 3D environments (Doyle et al., 2015). Previous work using an *in vitro* Boyden chamber invasion assay demonstrated that FASN knockdown in the prostate cells LNCaP reduced their invasive potential (Yoshii et al., 2013). The invasive ability of both 1524 and PC3 prostate cell lines was tested using the 3D inverted invasion assay. This assay was chosen over the Boyden chamber assay for two primary reasons. Firstly, it has been documented that cells are more easily displaced from the microenvironment in the Boyden chamber assay. Secondly, the inverted invasion assay requires cells to invade up into the matrix against gravity meaning they need to be more active in order to invade (McArdle et al., 2016).

In the inverted invasion assay, cells are seeded onto the bottom surface of a 96 well plate and then overlaid with type I collagen. Cells were left to invade into the collagen for 24 hours before being fixed, stained and then imaged on the confocal microscope. Longer time-points were not carried out on the basis that differences in proliferation rate between control and FASN knockdown cells occurred after 24 hours in the MTT assay. The invasion of cells was measured at 50 micrometres which was compared to the number of cells at the bottom of the well to get a relative invasion percentile.

From these results it has been found that a higher percentile of 1542 shControl cells invaded 50 µm into the collagen compared to 1542 shFASN A3 cells (**Figure 4.11A-B**). Likewise, when FASN was depleted in PC3 cells a reduction in the percentage of cells invading 50 µm was also seen compared to control shRNA cells (**Figure 4.12A-B**). The data from this assay show that decreasing FASN levels in AR-independent prostate cancer cells reduces cell invasiveness in a 3D collagen matrix.

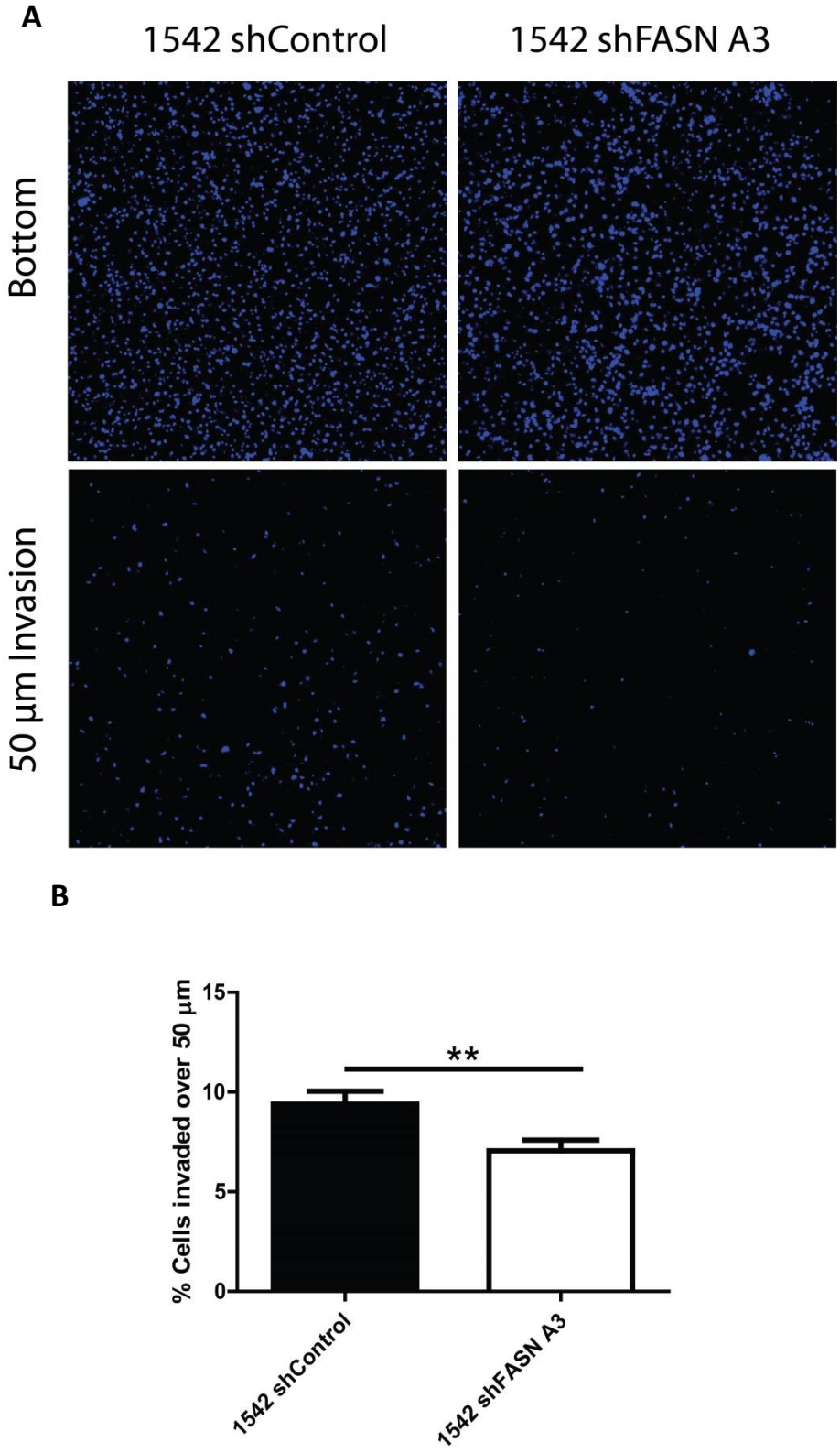

Figure 4.11 FASN knockdown impairs 1542 cell invasion: 1542 shControl and 1542 shFASN A3 were seeded into the bottom of a well and overlaid with a type I collagen plug. Media (10% FBS) was added on top and the cells were left to invade for 24 hours. Collagen plugs were fixed and the cells were stained with Hoechst. Confocal imaging was used to image cells at 0 µm and 50 µm (**A**) and then these images were used to calculate the percentage of cells invading over 50 µm. Data represents the mean values ± SEM accumulated from three independent experiments (**B**) Statistical significance was determined by student's *t-test*. ** p<0.01

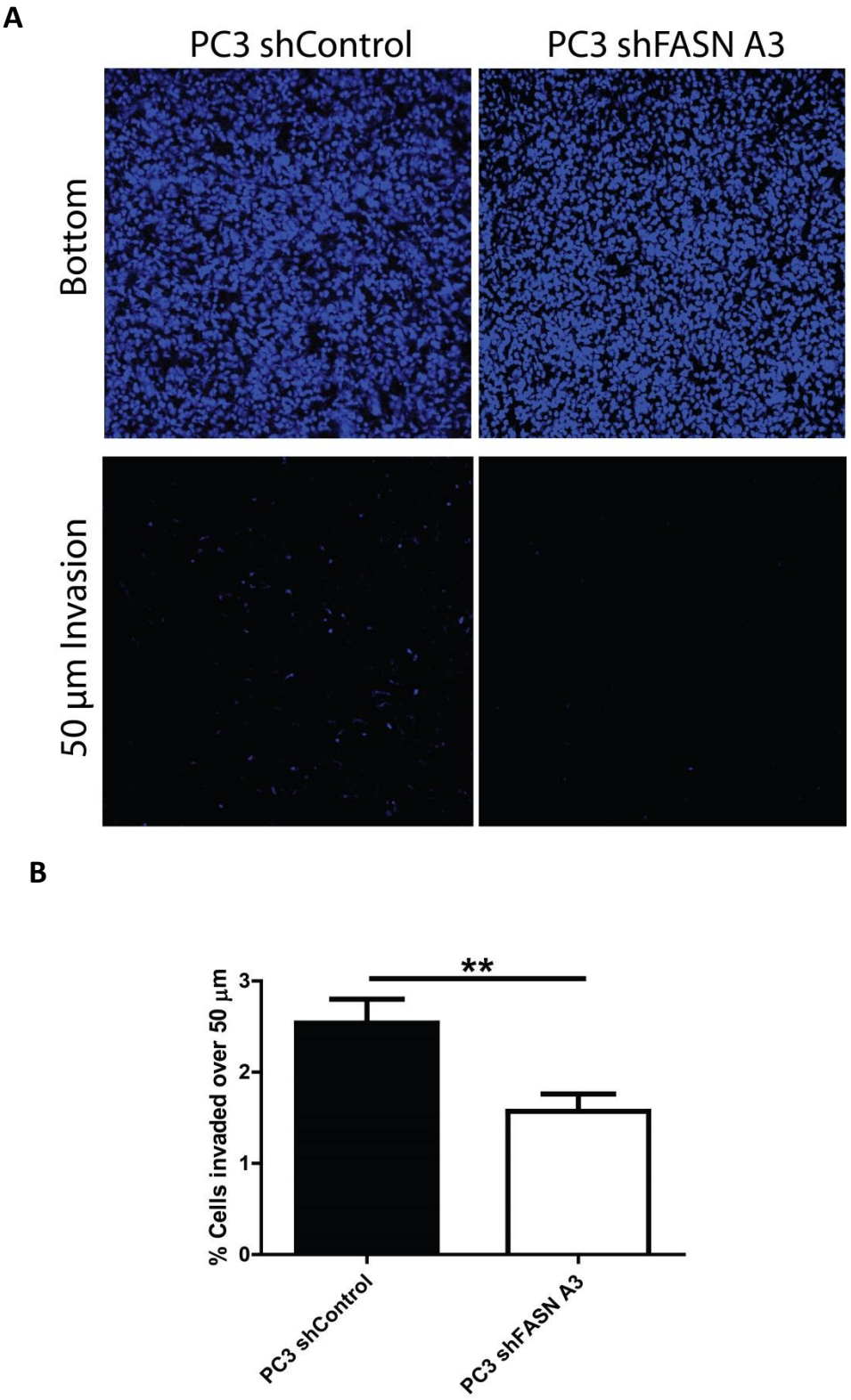

Figure 4.12 FASN knockdown impairs PC3 cell invasion: PC3 shControl and PC3 shFASN A3 were seeded into the bottom of a well and overlaid with a type I collagen plug. Media (10% FBS) was added on top and the cells were left to invade for 24 hours. Collagen plugs were fixed and the cells were stained with Hoechst. Confocal imaging was used to image cells at 0 µm and 50 µm (**A**) and then these images were used to calculate the percentage of cells invading over 50 µm. Data represents the mean values ± SEM accumulated from three independent experiments (**B**) Statistical significance was determined by student's *t-test*. ** p<0.01

4.3 Discussion

This chapter focussed on identifying if FASN plays a role as a regulator of AR-independent prostate cancer cell motility. To date there have been no studies in 1542 or PC3 cells regarding their migratory and invasive potential in response to direct silencing of FASN using stable shRNA. Results presented here have shown that 1542 and PC3 cell adhesion, migration and invasion are effected upon reducing intracellular FASN levels.

Changes in cell morphology are often regarded as an indicator of invasiveness in cancer (Friedl and Wolf, 2003). In chapter 3 it was shown that prostate cancer cells with depleted FASN levels exhibited a smaller cell shape when compared to their control counterparts. In this chapter FASN overexpression was found to induce the opposite effect and increase the overall size of both prostate cancer cell lines. Moreover, the addition of exogenous palmitate rescued control cell shape parameters in FASN knockdown prostate cancer cells. These results indicate that there is a synchronous relationship between FASN protein levels and cell morphology in AR-independent prostate cancer cells. In addition, they suggest that the morphological phenotype in prostate cancer is being regulated as a result of palmitate availability downstream of FASN.

Studies in the literature have found that supplementation of palmitate concomitantly increases overall cell size and induces an EMT phenotype in hepatocellular carcinoma cells (Leamy et al., 2014; Nath et al., 2015). Palmitate is involved in the synthesis of phospholipids which are one of the major lipid groups required for cell membrane expansion and maintenance of cell shape (Glenn et al., 1963; Leamy et al., 2014; Llado et al., 2014). Silencing of FASN reduces palmitate synthesis, and in LNCaP cells has been shown to decrease phospholipid availability (Knowles et al., 2008; Swinnen et al., 2003). In addition to membrane integrity, palmitate has also been found to be involved in the activation of Rho GTPases such as Cdc42 and Rac1 in hepatocytes (Sharma et al., 2012c). Both these proteins are involved in cytoskeletal reorganisation in cancer (Vega and Ridley, 2008). It could be speculated that the FASN knockdown morphological phenotype in 1542 and PC3 cells is the result of reduced palmitate

synthesis, and therefore attenuated Rho GTPase activity and membrane lipid synthesis.

Changes in signalling as a result of reduced expression of a particular protein can lead to several aberrations in normal cellular behaviour (Martin, 2003). Interestingly, it was observed that adhesion in FASN knockdown 1542 and PC3 cells increased relative to control cells. These findings contrast two other studies which have seen a decrease in cell adhesion in response to FASN knockdown (Yoshii et al., 2013; Zaytseva et al., 2012). Moreover, they conflict with one study which observed an increase in the adhesion of mouse embryonic fibroblasts in response to silencing AMP-activated protein kinase (AMPK), a negative regulator of FASN (Georgiadou et al., 2017). Perhaps it would be interesting in future studies to assess how AMPK levels alter in FASN knockdown prostate cells or if AMPK silencing in these cells produces a similar phenotype. It is not clear why the opposite phenotype has been observed in response to FASN depletion, however it has previously been shown that disruption of lipid raft activity increases melanoma cell adhesion (Wang et al., 2013a).

Adhesion and cell shape are highly interrelated, and together are both central features of cell migration (Schwartz and Horwitz, 2006). To further elaborate on the increased adhesion phenotype seen in response to FASN knockdown, paxillin was stained for in 1542 cells. Paxillin is a signal transduction adaptor protein which is targeted to focal adhesions through four LIM domains present at its c-terminal region (Bellis et al., 1995). Wells *et al* showed that silencing of PAK4 increased cell-substrate adhesion in DU145 prostate cancer cells which correlated with more elongated paxillin focal adhesions (Wells et al., 2010). Staining showed that this phenotype was essentially recapitulated in the FASN knockdown 1542 cells. When palmitate was added to the 1542 shFASN A3 cells, paxillin adhesion dynamics was almost fully rescued back to controls levels. Interestingly, there is a biphasic relationship between motility and adhesion size with either higher or lower concentrations of adhesive ligands being associated with slower migration speeds (Schwartz and Horwitz, 2006). These results suggest that FASN, along with its fatty acid product palmitate, are contributing to adhesion turnover and therefore cells devoid of their activity have an increased adhesion phenotype which could be impacting on cell migration.

There is currently mounting evidence to suggest that FASN is involved in both initiating and driving cell migration (Jiang et al., 2014; Li et al., 2014a). Results from the 2D migration assays that were carried out in 1542 and PC3 cells showed a clear decrease in the migration speed of FASN knockdown cells compared to control cells in response to HGF. These results agree with similar findings by Cao *et al* who found that FASN inhibition using quercetin impaired HGF-stimulated melanoma cell migration (Cao et al., 2015). In addition to confirming the effect of FASN knockdown in cell migration, this is also the first time that migratory speed has been recorded in the primary prostate cancer cell line 1542 in 2D. This data shows that on matrigel both 1542 and PC3 cells migrate at a similar speed, whilst on type I collagen 1542 cells migrate at a slightly increased speed relative to PC3 cells. One reason for this increased migratory speed in 1542 cells on type I collagen could be due to a more compatible ratio of integrin-adhesion receptors for this matrix (Witkowski et al., 1993).

The role of FASN in prostate cancer cell migration was further studied with the use of FASN inhibitors C75 and orlistat. Results showed that both FASN inhibitors significantly impeded 1542 and PC3 cell migration similar to what was observed in the shRNA studies. The effects of C75 and orlistat in 2D cancer cell migration have not been extensively studied. C75 is a more commonly used FASN inhibitor and has been cited to affect the wound healing response in prostate cancer and renal cancer cells (Horiguchi et al., 2008; Rae et al., 2015). Orlistat has not been tested in a 2D migratory assay, however it has been found to reduce melanoma and oral tongue squamous cell cancer invasion *in vivo* using mice models (Agostini et al., 2014; Seguin et al., 2012). C75 and orlistat reduced the migratory speed of PC3 cells to a similar effectiveness. In 1542 cells, C75 was found to be more potent than orlistat in reducing cell migration. This may have occurred as a result of 1542 cells being more sensitive to inhibition than PC3 cells at the chosen concentration of C75 used in the migration assay. The IC50 of inhibitors has been reported to vary in different cancer cell lines (Sadowski et al., 2014). Both FASN inhibitors produced much more dramatic decreases in cell migration when compared to stable shFASN cell lines. Several studies in the literature investigating the role of FASN in cancer have opted for the use of inhibitors over the use of RNA silencing technology (Agostini et al., 2014; Rae et al., 2015; Zhou et al., 2016). Inhibitors used at the optimal concertation are generally better tools for

completely diminishing a proteins activity in the cell. This is highlighted in one study where the authors treated LNCaP cells with either C75 or siRNA and found upon comparison that C75 was more effective in reducing cellular growth (Chen et al., 2012). In these studies it was decided to use FASN inhibitors in conjunction with shRNA as long term treatment with inhibitors can have cytotoxic effects (Rae et al., 2015).

All 2D migration assays carried out investigated the effect of FASN knockdown on prostate cancer cell migration in the presence of HGF. High levels of HGF circulate within the prostate tumour environment with its only known target being the tyrosine kinase receptor c-Met (Ye et al., 2007). HGF/c-Met signalling is known to active several downstream pathways including PI3K/AKT and MAPK, both of which have been implicated in cell survival, proliferation and migration (Organ and Tsao, 2011).

In addition to impairing prostate cancer cell migration in 2D, FASN knockdown reduced the invasive capabilities of 1542 and PC3 cells through a 3D matrix. These results agree with several studies in the literature which have found a reduction in the invasion of breast, colorectal, osteosarcoma, ovarian and melanoma cancer cells in response to FASN knockdown (Cao et al., 2015; Jiang et al., 2014; Singh et al., 2015; Wang et al., 2016; Wang et al., 2013b). Moreover, this data compliments the study by Wen *et al* that showed a reduction in PC3 cell invasion in response to suppressed FASN expression as result of ASC-J9 treatment (Wen et al., 2016). Cells navigating through a 3D matrix usually have to adopt slightly different mechanisms to that of cells moving across a flat surface. One example of this is the cells dependence on matrix metalloproteinases (MMP) to cleave and remodel the surrounding matrix allowing them to move past interstitial barriers. The use of MMPs in 2D is not as essential as the matrix does not form the same matrix barriers that are seen in 3D (Wu et al., 2014). Interestingly, a study by Zaytseva *et al* showed that when you inhibit FASN in colorectal cancer cells the expression of MMP9, a metalloproteinase that degrades collagen, is lost (Zaytseva et al., 2014). This could be linked to c-MET/PI3K signalling which has been shown to upregulate MMP9 (Chen et al., 2009).

Within this chapter it was demonstrated that the migration of both prostate cancer cell lines in response to HGF is dependent on the expression of FASN. Depletion of FASN also increased prostate cancer cell adhesion and the length of paxillin containing

adhesive contacts. The invasion of both 1542 and PC3 cells through a 3D collagen matrix was also impeded when FASN was depleted in these cell lines. Morphological studies carried out in the beginning of this chapter compliment the work done in chapter 3 and show that cell shape is dependent on FASN levels. These phenotypic changes in cell shape, adhesion, migration and invasion are indicative of changes in the actin cytoskeleton as a result of FASN knockdown. Thus in the next chapter the possible underlying mechanisms for the defects seen in both prostate cell lines as a result of reduced FASN levels will be investigated.

4.4 Future work

In future studies alternative migration assays could be performed, such as the chemotaxis assay, to identify if polarity as well as speed is being affected in response to FASN knockdown. Front-rear polarity is important in cell migration and confirming if this process is impacted upon the loss of FASN would help in identifying key downstream proteins that may be involved in FASN dependent cell migration (Huttenlocher, 2005). In addition, the use of conditioned media and other growth factors could be useful in determining if factors secreted by stromal cells could rescue the migration defect phenotype. Moreover, it would be interesting to assess if conditioned media from control prostate cells could rescue the migration of FASN knockdown cells. Prostate cancer cells have been shown to secrete exosomes that contain an abundance of FASN protein (Duijvesz et al., 2013). Perhaps FASN knockdown cells incubated with a high enough concentration of exosomes secreted by control cells could revert to a normal phenotype on the basis of taking up enough exogenous FASN protein. It would also be interesting to perform migration studies when overexpressing FASN. This was initially tried however a viable transfection efficiency only occurred when seeding the cells at a high density. This led to neighbouring cells being within a close proximity of each other which limited the space to migrate freely. Re-seeding the cells after transfection was attempted but generally cells would not recover. Perhaps it would be more practical to attempt overexpressing FASN in a normal epithelial cell line. This would be interesting in determining if solely overexpressing FASN is enough to drive the metastatic phenotype.

Chapter 5

Investigation of the underlying mechanisms in the FASN depleted prostate cancer phenotype.

Chapter 5 – Investigation of the underlying mechanisms in the FASN depleted prostate cancer phenotype

5.1 Introduction

Work within the previous two results chapters has confirmed that prostate cells with reduced FASN expression exhibit a different phenotype to prostate cells where endogenous FASN levels have not been altered. Changes in cell shape, adhesion, migration and invasion indicate that FASN may be directly involved in regulating signalling pathways and proteins that influence the actin cytoskeleton. Although several studies have delineated the oncogenic nature of FASN in lipogenesis (Menendez and Lupu, 2007), the precise underlying mechanism through which it induces reorganisation of the actin cytoskeleton and drives cell migration remains to be elucidated.

In chapter 4 motility in the presence of HGF was shown to be significantly impaired upon the silencing of FASN expression. HGF stimulation of c-Met leads to the activation of downstream receptor tyrosine kinase PI3K/AKT and MAPK signalling pathways which have been shown to induce actin cytoskeletal reorganisation (Organ and Tsao, 2011). FASN activity has been intimately linked with both these pathways whose aberrant activation is associated with a more aggressive tumour phenotype (Organ and Tsao, 2011). PI3K/AKT and MAPK signalling can regulate FASN expression, which in turn can activate EGFR leading to the constitutive activation of these oncogenic cascades through an auto-stimulatory loop (Huang et al., 2016; Liu et al., 2013b; Long et al., 2014; Menendez and Lupu, 2004). Recently, the PI3K/AKT signalling pathway has become increasingly associated with FASN-induced motility in cancer (Li et al., 2012a; Li et al., 2012b; Long et al., 2014). One study demonstrated that FASN inhibition in DU145 cells blocked the phosphorylation of c-Met and AKT which significantly impaired the cells ability to scatter in response to HGF (Coleman et al., 2009). Interestingly, another study has hypothesised a PI3K/AKT/FASN signalling axis whereby FASN is driving the migratory phenotype of osteosarcoma cells downstream of PI3K/AKT which can be abolished by PI3K inhibition (Zhou et al., 2015). The evidence from these studies suggests that the cross-talk between FASN and PI3K/AKT is likely to be synergistically enhancing each other's ability to drive cell migration, as

opposed to existing in a linear pathway. Comparatively, MAPK signalling has been shown to be important in cell growth; however its role within the context of FASN-induced migration remains to be addressed (Huang et al., 2016).

More recently, interest has been accumulating in the relatively unexplored palmitoylation-protein signalling network that lies directly downstream of FASN. Protein palmitoylation is a post-translational modification which involves the thioester linkage of palmitate moieties to cysteine residues (Bollu et al., 2015). The addition of palmitic acid allows for the specific localisation of proteins to subcellular compartments and ensures stable protein activity (Yang et al., 2010). In addition, stability through palmitoylation has been shown to be essential in some proteins with palmitoylation preventing their ubiquitination and protecting them from degradation (Linder and Deschenes, 2007). Proteins can also undergo other types of post-translational modifications including myristoylation and prenylation, however there are irreversible. In comparison, palmitoylation is a reversible modification which allows for more dynamic shuttling and signalling within the cell (Aicart-Ramos et al., 2011).

The Rho GTPases are amongst the most well studied proteins involved in regulating the actin cytoskeleton (Vega and Ridley, 2008). Several Rho GTPase proteins have now been confirmed to undergo palmitoylation which is important in mediating their intrinsic signalling (Aicart-Ramos et al., 2011). RhoU was one of the first Rho GTPases whose activity was shown to be dependent on palmitoylation. NIH 3T3 cells expressing a RhoU mutant devoid of its palmitoylation motif had severely stunted anchorage independent growth relative to cells expressing the wild-type variant (Berzat et al., 2005). In a different study, palmitoylation was shown to be important for the stability of Rac1 by targeting it to actin-cytoskeleton linked, detergent-resistant membranes, which led to unperturbed cell spreading and migration (Navarro-Lerida et al., 2012).

Additionally, there is also evidence suggesting that palmitate can regulate Rho GTPases that do not contain a palmitoylation motif. This has been shown in a study where the activity of Cdc42, another well characterised Rho GTPase in cell migration, increases upon palmitate treatment in hepatoma cells (Sharma et al., 2012c).

Despite FASN being the only known protein in the cell able to synthesize palmitic acid, there has never been a study investigating how abolishing its activity affects the palmitoylation of Rho GTPases. Furthermore, how FASN and palmitate may influence the expression, stability and activity of Rho GTPases in prostate cancer has also never been investigated. The current data in the literature does not evidence a strong link between FASN and the Rho GTPases. However, a study by Fiorentino *et al* showed that FASN overexpression increased Wnt-1 palmitoylation in prostate cancer cells (Fiorentino et al., 2008). This suggests that the activity of the Rho GTPases could be dependent on palmitate levels.

This chapter aims to identify and investigate a possible underlying mechanism that may explain the phenotypic changes observed in FASN knockdown prostate cancer cells. A two arm approach was adopted in this investigation which included screening proteins in the canonical c-Met transduction signalling pathway; and exploring changes in Rho GTPase palmitoylation in response to FASN knockdown in prostate cancer cells.

5.2 Results

5.2.1 FASN depletion leads to a reduction in c-Met but not PI3K/MAPK signalling

In the previous chapter it was observed that the knockdown or inhibition of FASN impaired motility in the presence of HGF. The c-Met receptor is a high affinity target of HGF and the binding of these two molecules leads to the concomitant activation of the PI3K/AKT and MAPK transduction pathways (Coleman et al., 2009; Sharma et al., 2003). Previously published studies have shown that the silencing or inhibition of FASN is associated with a decrease in AKT and ERK phosphorylation in prostate cancer (Coleman et al., 2009; Huang et al., 2016). Thus, it was decided to investigate if these pathways were being affected in the 1542 and PC3 prostate cancer cell lines in response to FASN depletion.

Western blot analysis revealed that total c-Met expression levels were significantly reduced but not depleted in FASN knockdown 1542 and PC3 cells (**Figure 5.1A-B** and **Figure 5.2A-B** respectively). Phosphorylation levels of c-Met at tyrosine 1234 and 1235 mirrored this slight reduction in both prostate cell lines, although this decrease may just be reflective of the overall lowered total c-Met levels (**Figure 5.1A-C** and **Figure 5.2A-C**). Downstream signalling from c-Met was completely unimpeded as shown by the indifferent AKT and ERK phosphorylation levels between control and FASN knockdown cells (**Figure 5.1D-G** and **Figure 5.2D-G**). Interestingly, in the PC3 shFASN A4 cells a notable increase in ERK phosphorylation was observed compared to all other lines (**Figure 5.2G**).

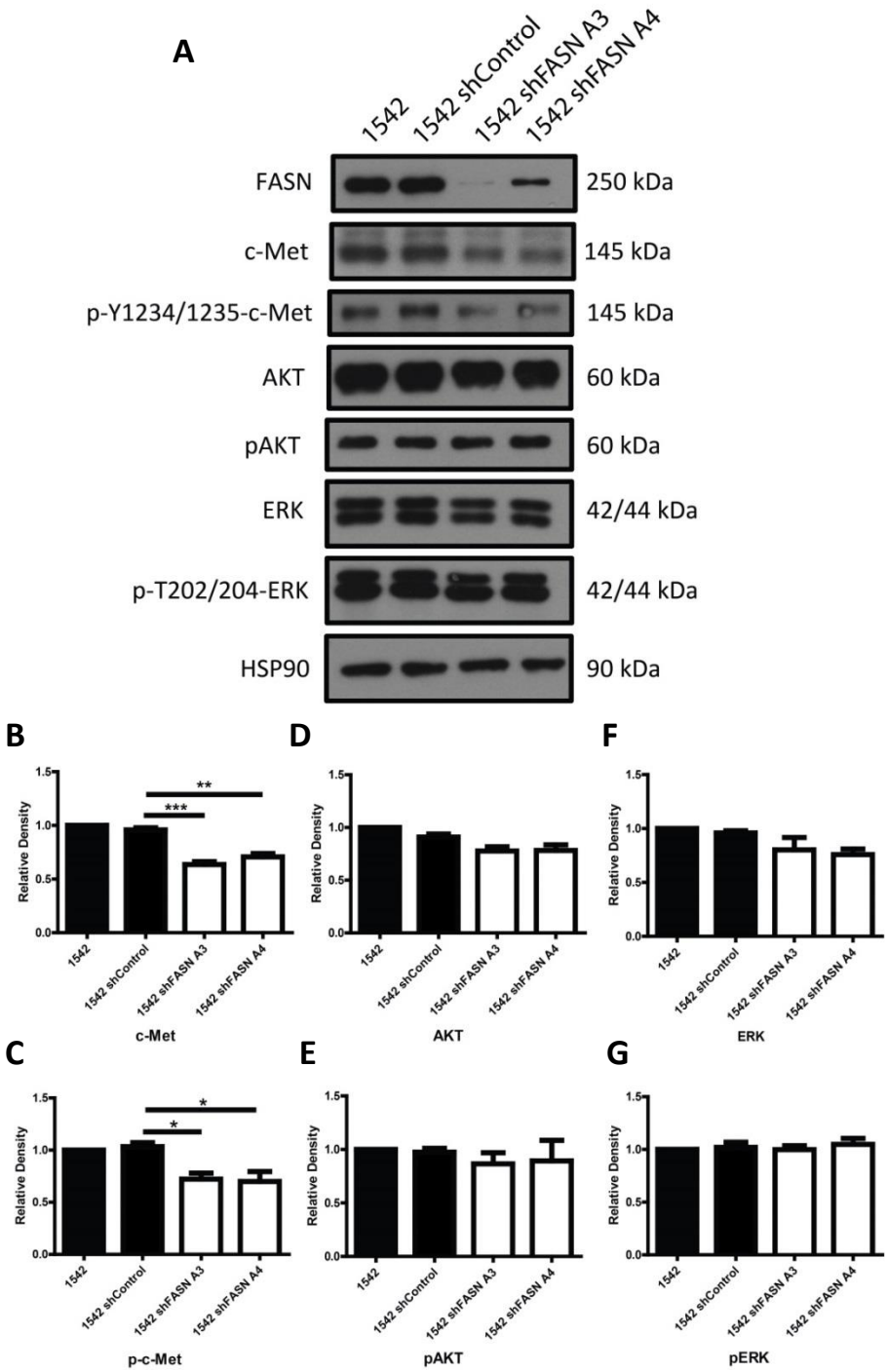

Figure 5.1 FASN depletion decreases total and phospho c-Met levels but does not affect downstream PI3K/MAPK signalling in 1542 cells: 1542, 1542 shControl, 1542 shFASN A3 and 1542 shFASN A4 cells were seeded into the wells of a 6-well plate. On the following day growth media was removed and replaced with serum starve media. Cells were starved for 24 hours before stimulating with 10 ng HGF for 15 minutes followed by lysing. Western blotting was then carried out (**A**) and then quantification of the antibodies c-Met (**B**), p-c-Met (**C**), AKT (**D**), pAKT (**E**), ERK (**F**), and pERK (**G**) was performed based on densitometry analysis. Data represents the mean values ± SEM accumulated from three independent experiments. Statistical significance was determined by student's *t-test*. * p<0.05, ** p<0.01, ***p<0.001.

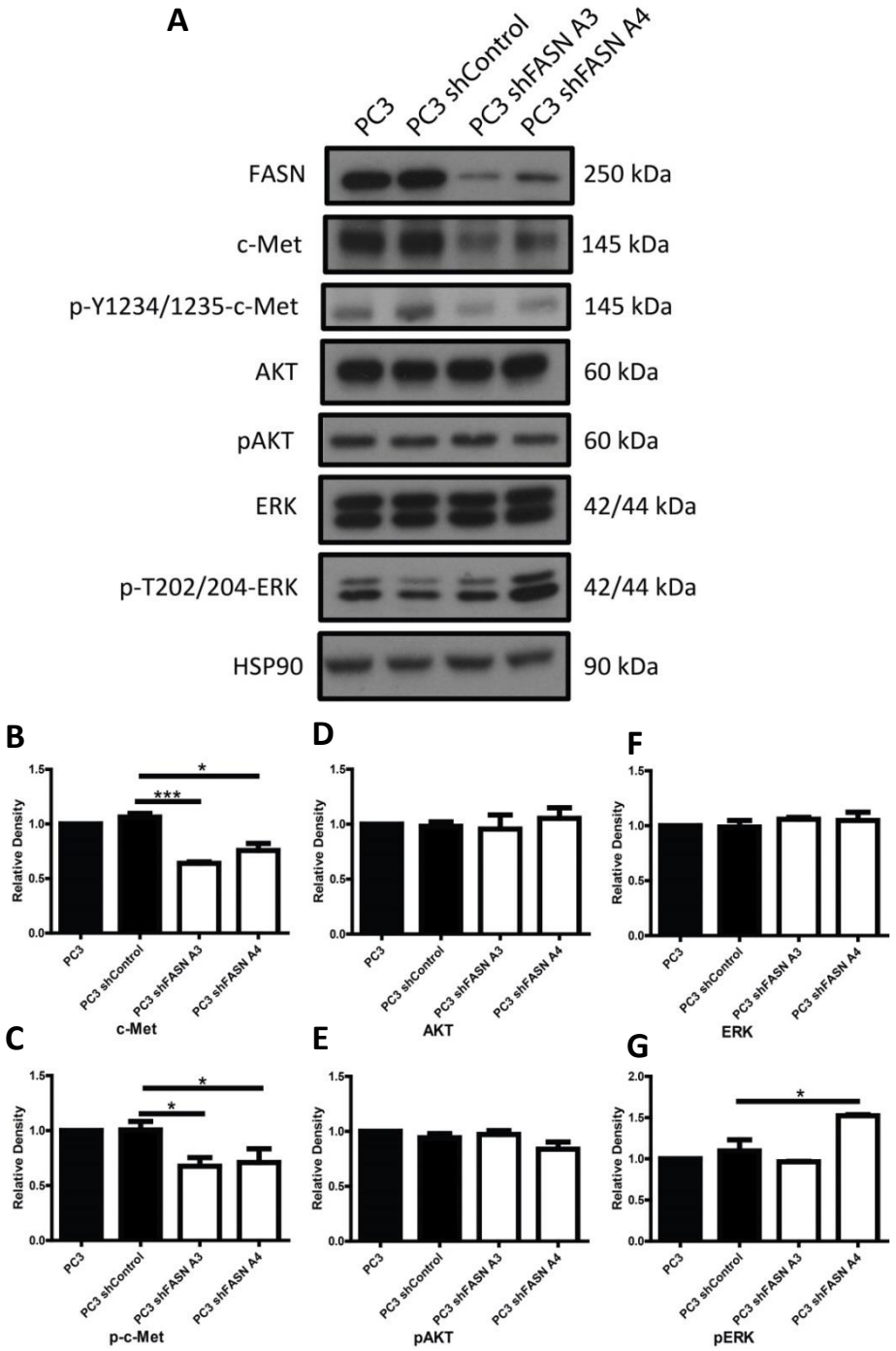

Figure 5.2 FASN depletion decreases total and phospho c-Met levels but does not affect downstream PI3K/MAPK signalling in PC3 cells: PC3, PC3 shControl, PC3 shFASN A3 and PC3 shFASN A4 cells were seeded into the wells of a 6-well plate. On the following day growth media was removed and replaced with serum starve media. Cells were starved for 24 hours before stimulating with 10 ng HGF for 15 minutes followed by lysing. Western blotting was then carried out (**A**) and then quantification of the antibodies c-Met (**B**),p-c-Met (**C**), AKT (**D**), pAKT (**E**), ERK (**F**), and pERK (**G**) was performed based on densitometry analysis. Data represents the mean values ± SEM accumulated from three independent experiments. Statistical significance was determined by student's *t-test*. * p<0.05, ***p<0.001.

5.2.2 Cdc42 isoform expression in prostate cancer and mRNA levels in response to FASN knockdown

Upon confirming that PI3K/AKT and MAPK signalling pathways were not significantly altered in response to FASN knockdown, the exploration of Rho GTPase palmitoylation in FASN depleted cells was carried out. RhoU , Rac1 and a Cdc42 variant have all been shown to be palmitoylated proteins, however the identification and role of palmitoylated Cdc42 in cancer has not been studied (Hodge and Ridley, 2016). In vertebrates two isoforms of Cdc42, labelled placental and brain, have arisen from alternative splicing (Nishimura and Linder, 2013). The localisation and activation of both Cdc42 isoforms relies on the attachment of lipid moieties which allows them to induce membrane protrusions and directed cell migration (Nishimura and Linder, 2013; O'Neill et al., 2016). The placental isoform is ubiquitously expressed and is the canonical Cdc42, whilst the brain isoform has only been found to be expressed in neuronal cells and platelet cells thus far (Dowal et al., 2011). There is high sequence homology between both Cdc42 isoforms with the main difference being that the placental isoform is prenylated only, whilst the brain isoform is prenylated and palmitoylated (Nishimura and Linder, 2013). To determine which Cdc42 isoforms are expressed in 1542 and PC3 cells, plasmids were purchased containing the cDNA for the prenylated and palmitoylated variant of Cdc42. Both plasmids were used as controls for primers specifically designed to bind each variant. Reverse transcription PCR analysis results showed that both 1542 and PC3 cells express the prenylated isoform, but not the palmitoylated isoform of Cdc42 (**Figure 5.3A** and **Figure 5.3B** respectively). There was an issue with the prenylated Cdc42 primers binding the cDNA of the palmitoylated variant of Cdc42. However, the primers targeting the palmitoylation region of the brain splice variant of Cdc42 did not amplify any DNA extracted from the cell lines or the prenylated Cdc42 construct. Therefore it is highly likely that both 1542 and PC3 cells do not express the palmitoylated Cdc42 variant which is in agreement with previous reports (Nishimura and Linder, 2013). With regards to the expression of prenylated Cdc42 in both prostate cell lines, there was no observable difference in mRNA levels between control and FASN knockdown cells (**Figure 5.3A** and **Figure 5.3B**).

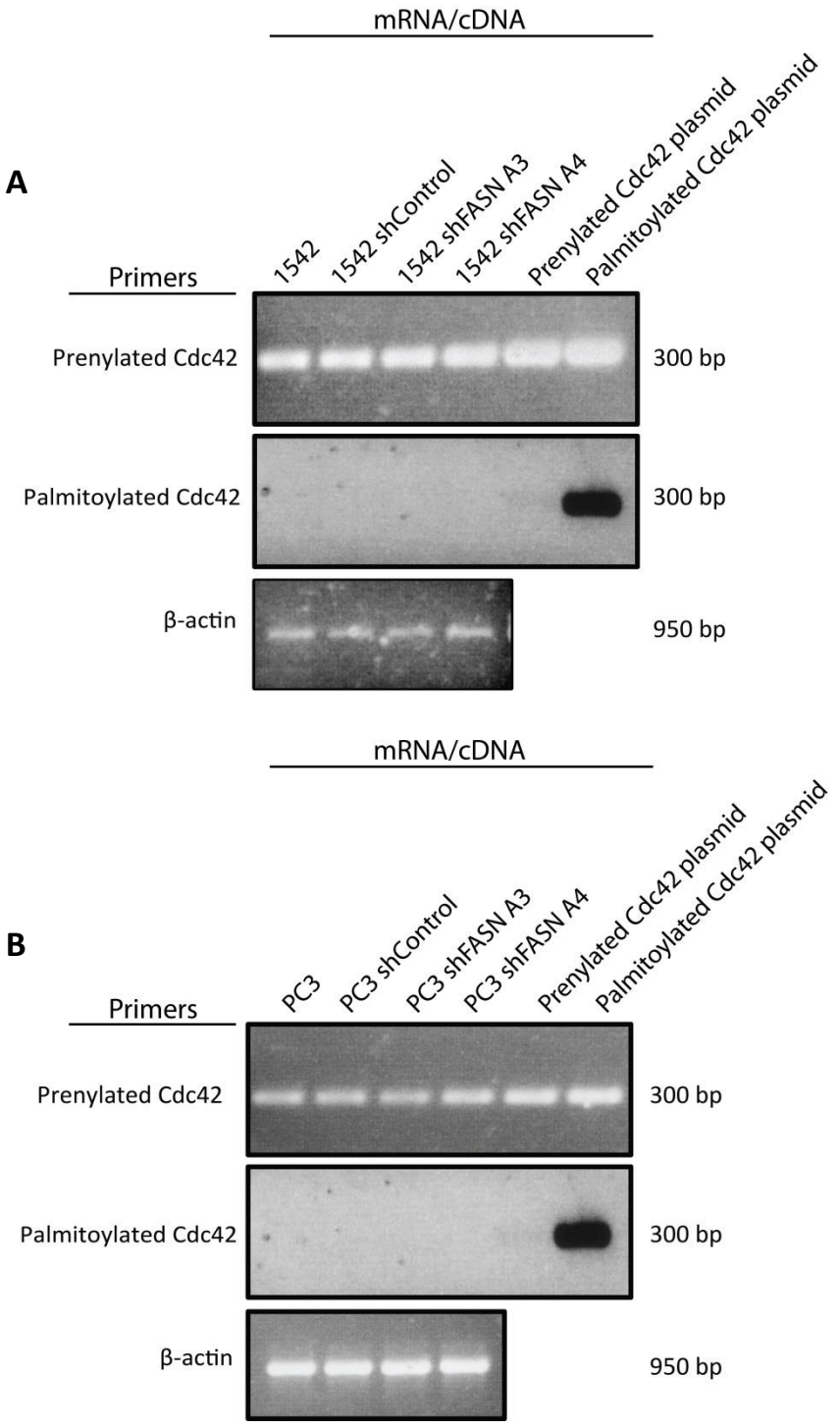

Figure 5.3 1542 and PC3 cells express the prenylated isoform of Cdc42 which is not affected transcriptionally by FASN knockdown: mRNA was extracted from 1542 and PC3 prostate cancer cells and then reverse transcribed into cDNA. PCR was then carried out with primers designed to amplify the prenylated isoform of Cdc42 (Placental variant) or the palmitoylated isoform of Cdc42 (brain variant). Purchased constructs containing either the prenylated or palmitoylated isoform of Cdc42 were used as controls for primer specificity. The amplified products for 1542 (**A**) and PC3 (**B**) were ran on a 2% agarose gel and then visualised under ultraviolet light. β-actin was used as a loading control.

5.2.3 Palmitoylation of Rho GTPases RhoU and Rac1

Since the palmitoylated isoform of Cdc42 was not found to be expressed in either 1542 or PC3 cells, it was decided to focus on the palmitoylation of RhoU and Rac1. RhoU is an atypical GTPase which is exclusively modified by palmitoylation (Berzat et al., 2005). The role of RhoU in prostate cancer has not been extensively studied, however in one study it was shown that the silencing of RhoU in PC3 cells impaired migration and invasion, although proliferative defects were not controlled for (Alinezhad et al., 2016). Moreover, in a different study the silencing of RhoU increased paxillin associated adhesion length in breast cancer cells mirroring the adhesion phenotype observed in FASN knockdown 1542 and PC3 cells (**Figure 4.4** and **Figure 4.5**),(Dart et al., 2015). Unlike RhoU, Rac1 is a well-studied Rho GTPase which has been shown to induce morphological changes and cell migration in PC3 cells (Kato et al., 2014). Interestingly, both these functions of Rac1 have now been confirmed to be largely dependent on palmitoylation (Navarro-Lerida et al., 2012).

A schematic depiction of the palmitoylation assay with a detailed description in the legend is shown in **Figure 5.4**. In brief, immunoprecipitation is carried out to capture the Rho proteins which are then incubated with NEM to block all cysteine residues. Following this, Rho proteins are then treated with hydroxylamine to remove palmitate from the cysteine residues. Biotin-BMCC is then added to bind the previously S-acylated protein residues and the resulting lysates can be processed by western blotting. The level of protein palmitoylation is detected with streptavidin-HRP probing (**Figure 5.4**). The control for the palmitoylation assay is essentially a duplicate of the lysate which has not been incubated with hydroxylamine. The absence of a signal in the control confirms that in the hydroxylamine positive lysate a biotin-BMCC palmitate switch has occurred. To confirm assay sensitivity GFP-RhoU and GFP-Rac1 were overexpressed in HEK293 cells and then subjected to the palmitoylation assay. Western blots in **Figure 5.5** show a positive exposure signal for both RhoU and Rac1 indicating that biotin-BMCC has successfully bound to previously palmitoylated cysteine residues. These results validate the assay and confirm that RhoU and Rac1 are palmitoylated.

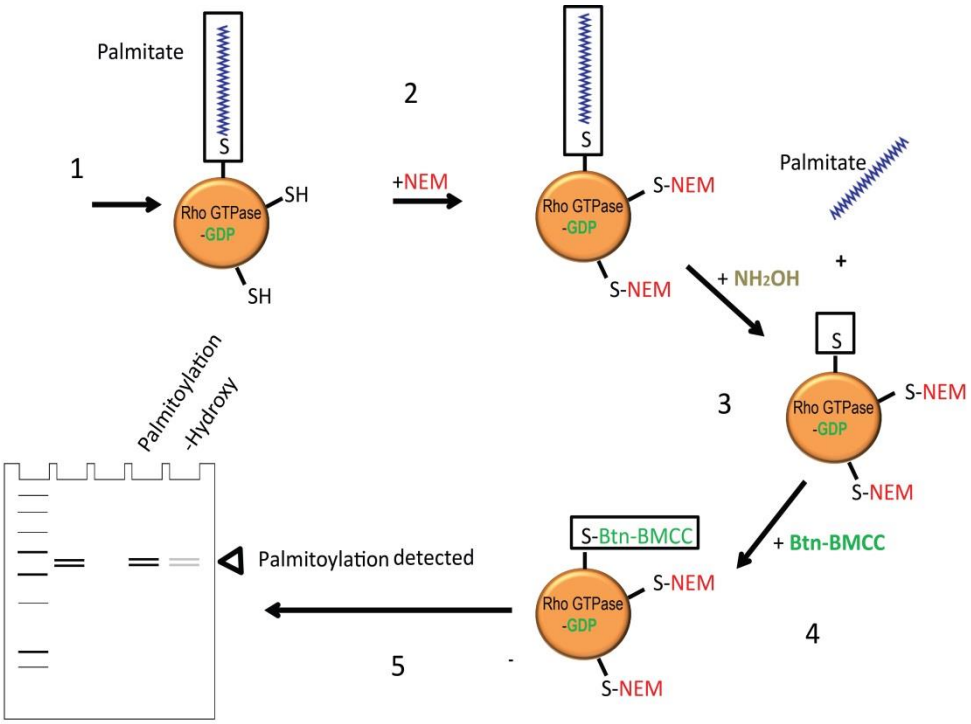

Figure 5.4 Schematic diagram of the palmitoylation assay: **1**) An immunoprecipitation is carried out to isolate the protein of interest. **2**) Lysates are then incubated with *N*-ethylmaleimide (NEM) which blocks all free sulfhydryl groups. **3**) Hydroxylamine (NH_2OH) is then added to the samples to cleave the thioester bond and remove palmitate from the cysteine residues. **4**) Cysteine residues with a now free sulfhydryl group can be bound by the thiol specific reagent biotin-BMCC (Btn-BMCC). **5**)Proteins are subjected to western blotting and probed with streptavidin-HRP which has an extremely high affinity for biotin (Drisdel et al., 2006).

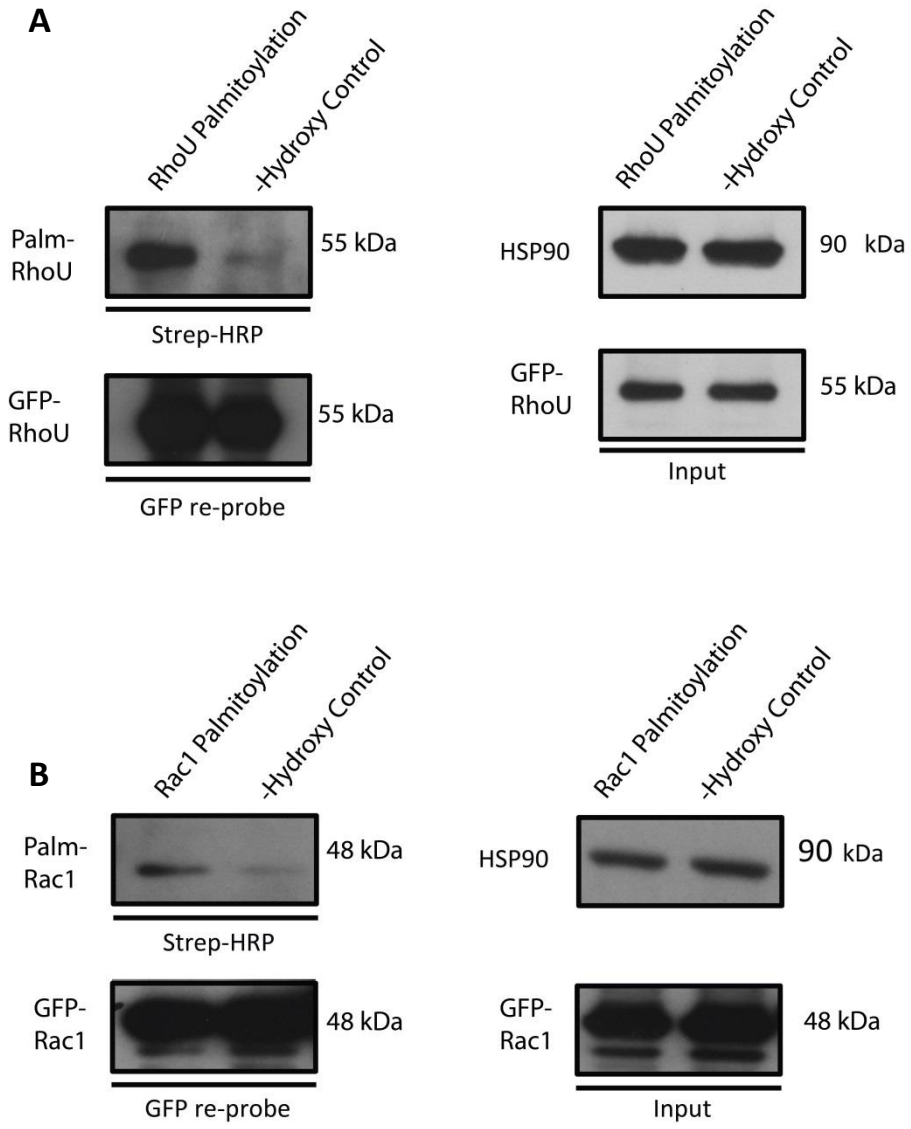

Figure 5.5 Palmitoylation of RhoU and Rac1: HEK293 cells were transfected with GFP-RhoU or GFP-Rac1 and then 48 hours the palmitoylation assay was carried out. The biotin-BMCC modified samples were detected using streptavidin-HRP. (**A**) Shows the palmitoylation of GFP-RhoU and (**B**) shows the palmitoylation of GFP-Rac1. The streptavidin-HRP probed blot was stripped to remove the palmitoylation signal and then probed for GFP confirming the total amount of GFP-RhoU or GFP-Rac1 that was immunoprecipitated. The whole cell lysate (WCL) was run in parallel acting as a control for the experiment and was probed for total GFP levels and the loading control HSP90. The blots are representative of three independent experiments.

5.2.4 RhoU and Rac1 palmitoylation increases when overexpressing FASN

Having established RhoU and Rac1 palmitoylation, the influence of FASN overexpression was tested given that it has been previosuly reported that Wnt1 palmitoylation alters concurently with increaseing levels of FASN (Fiorentino et al., 2008). FLAG-FASN was co-expressed with either GFP-RhoU or GFP-Rac1 in HEK293 cells and then the resulting level of palmitoylation was compared to HEK293 cells expressing the respective Rho GTPase only. The overexpression of FASN was found to significantly increase the level of palmitoylation in both Rho GTPases compared to cells expressing either GFP-RhoU and GFP-Rac1 alone (**Figure 5.6**).

5.2.5 Silencing of FASN reduces RhoU palmitoylation in prostate cancer cells

Upon confirming that RhoU and Rac1 palmitoylation increased in response to FASN overexpression, the palmitoylation levels of these two Rho GTPases in FASN depleted cells was tested. Before performing the palmitoylation assay endogenous levels of RhoU and Rac1 were probed for in order to identify whether the expression of these proteins changes in response to FASN knockdown. Western blot analysis showed that FASN knockdown in 1542 cells does not affect RhoU or Rac1 expression (**Figure 5.7A** and **5.7B** respectively).

For this experiment GFP-RhoU and GFP-Rac1 were overexpressed in 1542 shControl, 1542 shFASN A3 and 1542 shFASN A4 cells. The palmitoylation assay was carried out in the exact same manner as with the HEK293 cells. RhoU palmitoylation detected in extracts treated with hydroxylamine was significantly decreased in 1542 shFASN A3 (**Figure 5.8A**) and 1542 shFASN A4 cells (**Figure 5.8B**) compared to 1542 shControl cells. Alternatively Rac1 palmitoylation was not affected in 1542 shFASN A3 (**Figure 5.9A**) or 1542 shFASN A4 cells (**Figure 5.9B**).

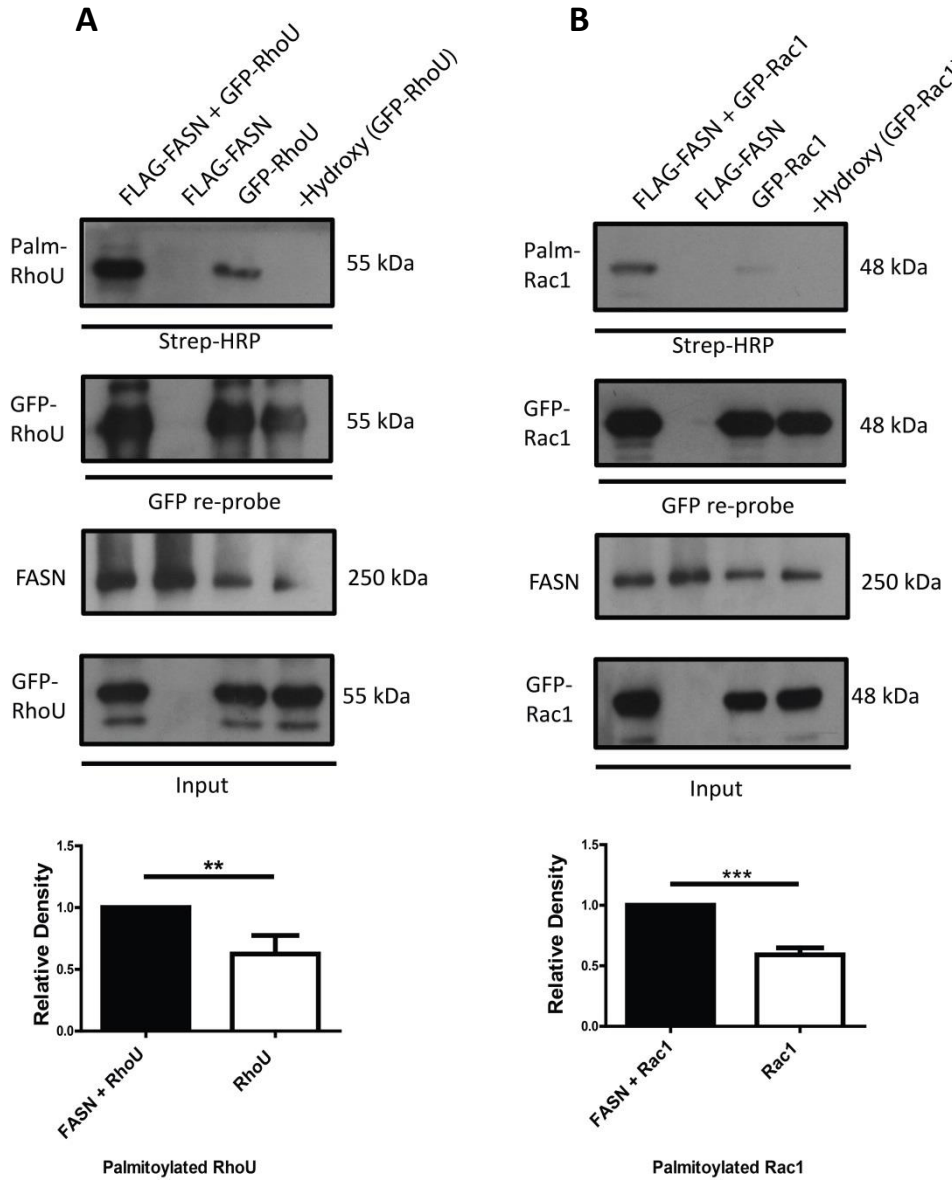

Figure 5.6 FASN overexpression increases RhoU and Rac1 palmitoylation: HEK293 cells were transfected with either GFP-RhoU or GFP-Rac1 alone, or with one of the Rho GTPases and FLAG-FASN. Cells were left for 48 hours and then the palmitoylation assay was carried out. The biotin-BMCC modified samples were detected using streptavidin-HRP. GFP-RhoU palmitoylation in response to FASN overexpression is shown in (**A**) along with the quantification of the palmitoylation signal which was determined by densitometry analysis. The same palmitoylation experiment was performed with GFP-Rac1 and is shown in (**B**) along with densitometry quantification. The streptavidin-HRP probed blots were stripped to remove the palmitoylation signal and then probed for GFP allowing for the quantification of total GFP-RhoU or GFP-Rac1. The WCL was run in parallel acting as a control for the experiment and probed for FASN and total GFP. Data represents the mean values ± SEM accumulated from three independent experiments. Statistical significance was determined by student's *t-test*. **p<0.01, ***p<0.001.

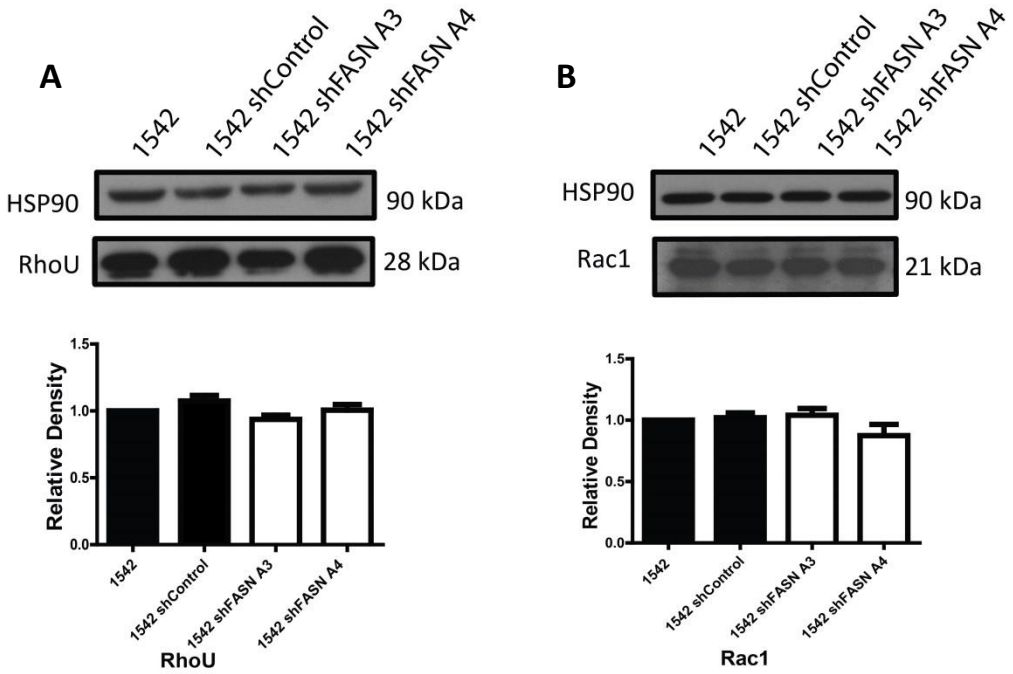

Figure 5.7 FASN knockdown does not affect RhoU or Rac1 expression in 1542 cells: Western blotting was carried out to determine the expression of RhoU (**A**) and Rac1 (**B**) in 1542, 1542 shControl, 1542 shFASN A3 and 1542 shFASN A4 cell lysates. Quantification of RhoU and Rac1 was determined by densitometry analysis. Data represents the mean values ± SEM accumulated from three independent experiments.

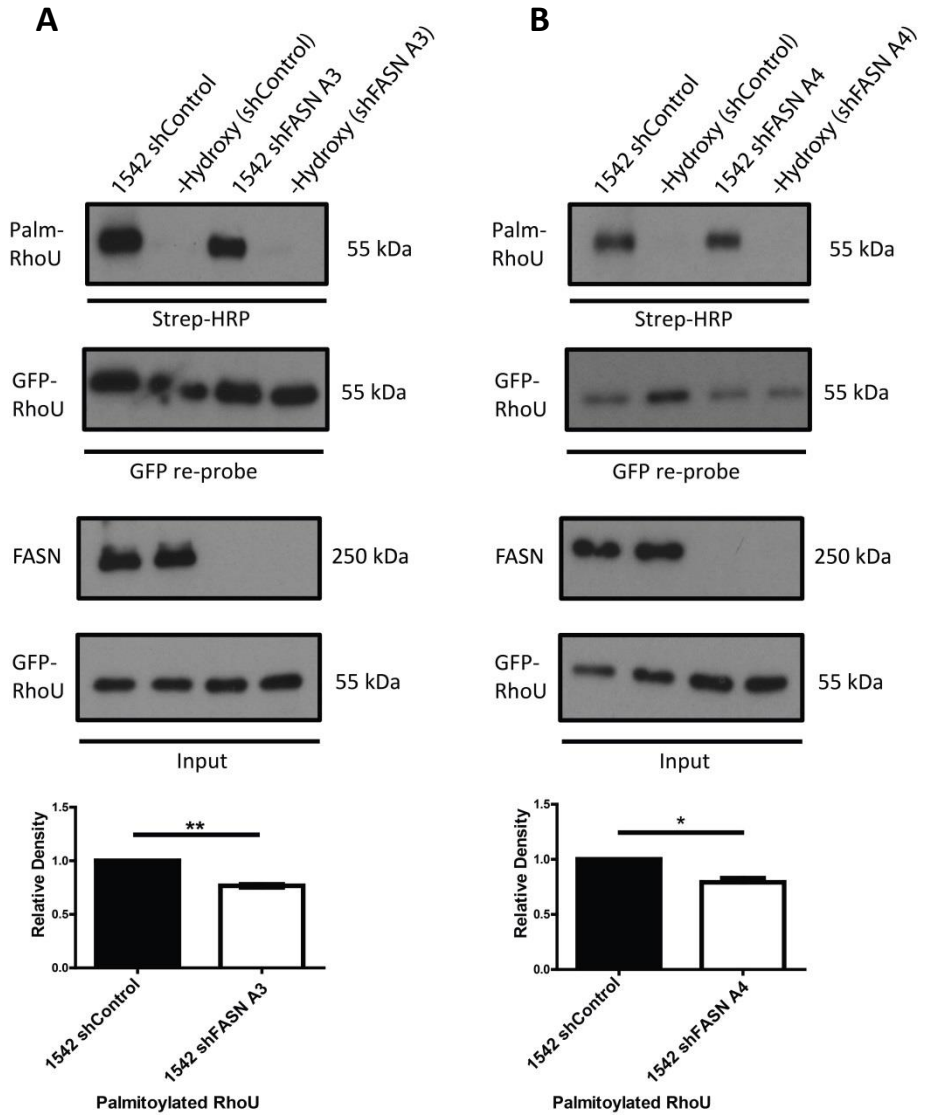

Figure 5.8 FASN knockdown decreases GFP-RhoU palmitoylation in 1542 cells: 1542 shControl, 1542 shFASN A3 and 1542 shFASN A4 cells were transfected with GFP-RhoU. Cells were left for 48 hours and then the palmitoylation assay was carried out. The biotin-BMCC modified samples were detected using streptavidin-HRP. Western blotting of RhoU palmitoylation in 1542 shControl and 1542 shFASN A3 along with quantification via densitometry analysis is seen in (**A**). The same experiment was performed in our second FASN knockdown cell line (shFASN A4) which can be seen in (**B**) along with quantification. The streptavidin-HRP probed blot was stripped to remove the palmitoylation signal and then probed for GFP allowing for quantification of total GFP-RhoU. The WCL was run in parallel acting as a control for the experiment and was probed for FASN and total GFP. Data represents the mean values ± SEM accumulated from three independent experiments. Statistical significance was determined by student's *t-test*. *p<0.05, **p<0.01.

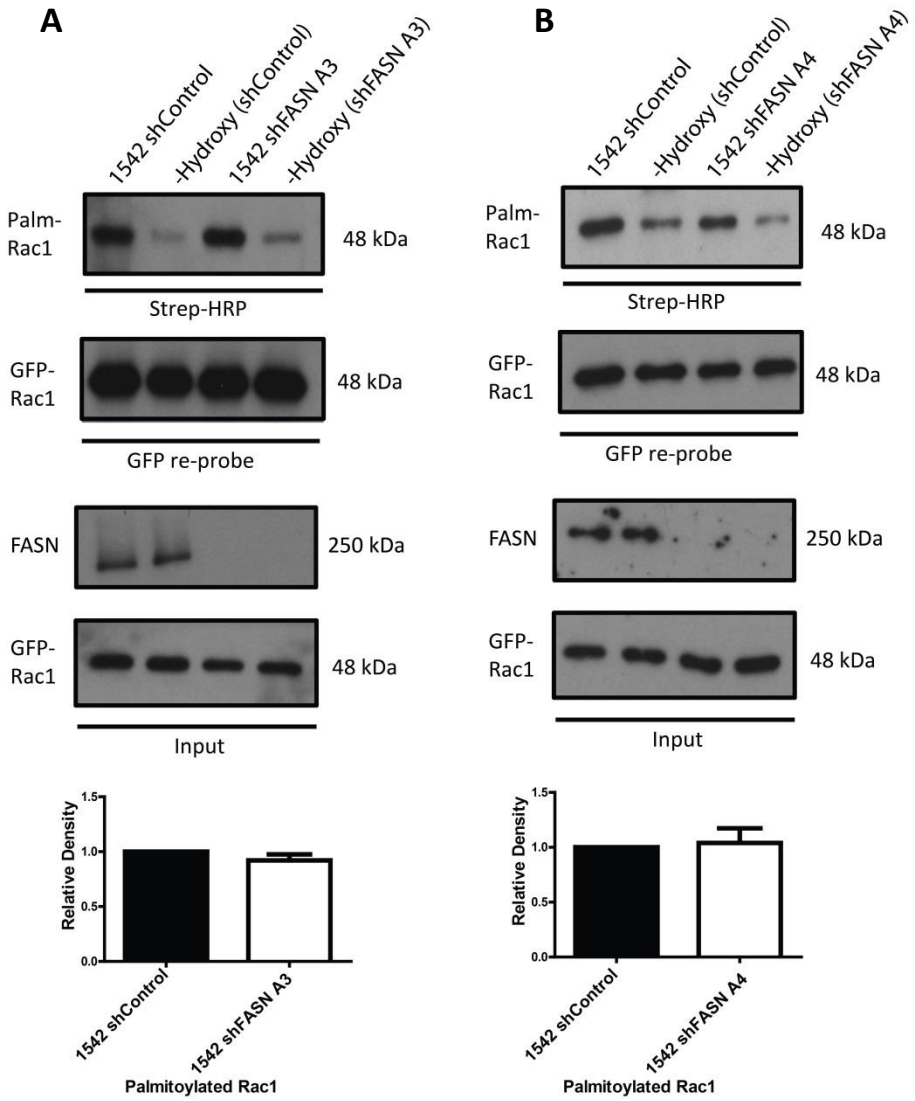

Figure 5.9 FASN knockdown does not affect GFP-Rac1 palmitoylation in 1542 cells: 1542 shControl, 1542 shFASN A3 and 1542 shFASN A4 cells were transfected with GFP-Rac1. Cells were left for 48 hours and then the palmitoylation assay was carried out. The biotin-bmcc modified samples were detected using streptavidin-HRP. Western blotting of Rac1 palmitoylation in 1542 shControl and 1542 shFASN A3 along with quantification via densitometry analysis can be seen in (**A**). The same experiment was performed in our second FASN knockdown cell line (FASN A4) which can be seen in (**B**) followed by quantification. The streptavidin-HRP probed blot was stripped to remove the palmitoylation signal and then probed for GFP allowing for the quantification of total GFP-Rac1. The WCL was run in parallel acting as a control for the experiment and was probed for FASN and total GFP. Data represents the mean values ± SEM accumulated from three independent experiments.

5.2.6 FASN knockdown reduces endogenous RhoU palmitoylation levels in prostate cancer cells

After confirming that GFP-RhoU palmitoylation is decreasing in response to FASN knockdown further studies were carried out to assess how the palmitoylation of endogenous RhoU is being modulated in the same system. The palmitoylation assay was carried out identically to previous experiments however the method of protein capture differed. Previous experiments used the GFP-Trap beads which required no addition of an IgG antibody. In this experiment the method of immunoprecipitation performed required the use of an in-house anti-PAK4 antibody to capture RhoU which has been shown to interact with a high affinity (Dart et al., 2015). In-house PAK4 antibody was used as there is no anti-RhoU antibody capable of efficiently immunoblotting endogenous RhoU protein. Western blot analysis showed that endogenous RhoU palmitoylation decreased in 1542 shFASN A3 (**Figure 5.10A**) and 1542 shFASN A4 cells (**Figure 5.10B**) compared to 1542 shControl cells. These results confirm that RhoU palmitoylation is FASN dependent.

5.2.7 Paxillin S272 adhesion decreases in response to FASN knockdown

In the previous chapter it was found that there was an increase in focal adhesion length and the adhesiveness of FASN knockdown prostate cancer cells. This observed phenotype suggests that focal adhesion turnover is being impeded in response to reduced FASN expression. Previous work in the lab by Dart *et al* showed that RhoU promotes paxillin phosphorylation and that silencing its activty led to larger and more numerous focal adhesions (Dart et al., 2015). In FASN knockdown cells, the palmitoylation levels of RhoU were found to be decreased. However, 1542 FASN knockdown cells treated with palmitate had a partial rescue in paxillin adhesion length (**Figure 4.6**). Thus, the palmitoyation of RhoU may be required for paxillin phosphorylation and so it was decided to immunoblot for the changes in either total paxillin or phosphorylated paxillin in 1542 and PC3 cells. Western blot analysis confirmed that there was a significant decrease in paxillin phosphorylation at serine 272 upon FASN knockdown in both 1542 and PC3 cells (**Figure 5.11A and 5.11B**).

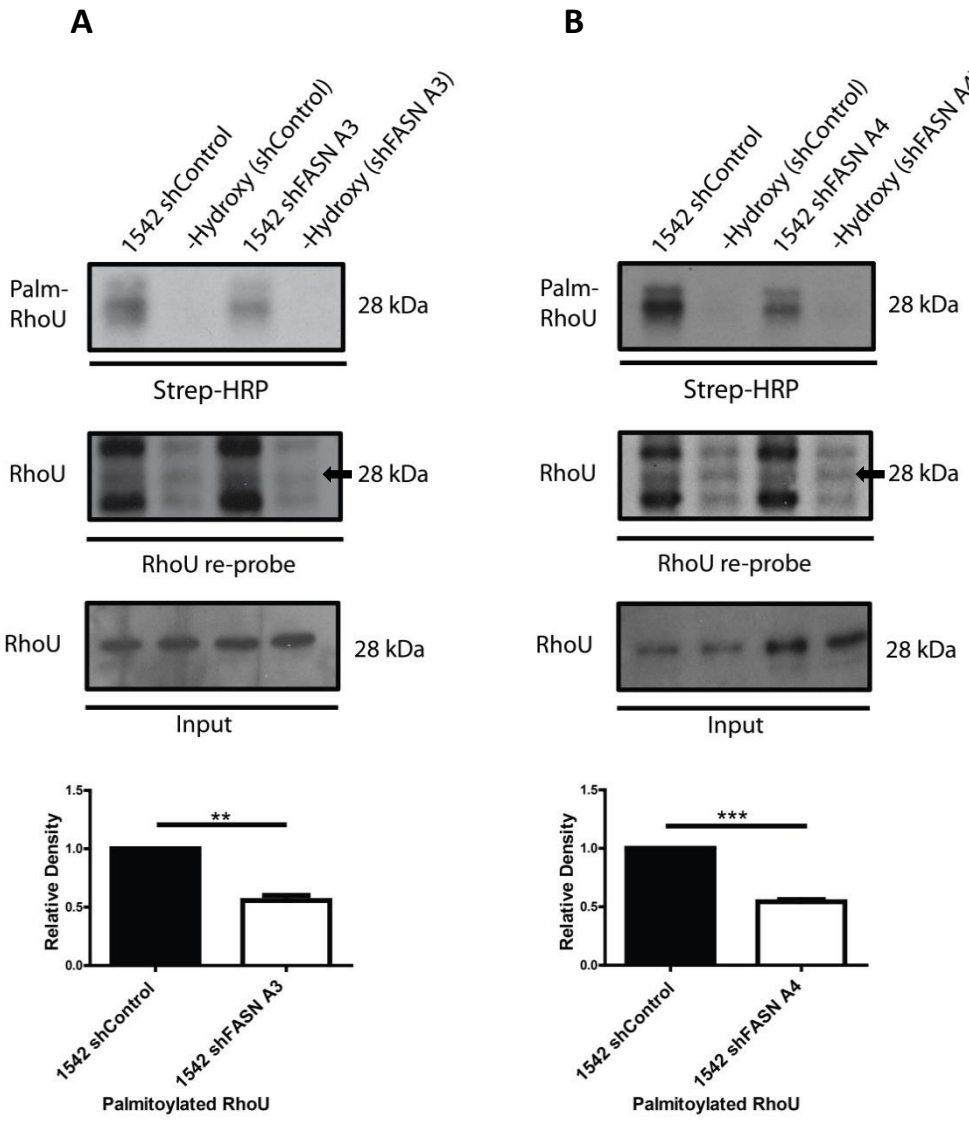

Figure 5.10 FASN knockdown decreases endogenous RhoU palmitoylation in 1542 cells: 1542 shControl, 1542 shFASN A3 and 1542 shFASN A4 cell lysates were incubated with in-house PAK4 IgG for 3 hours before agarose bead capture. After lysates were incubated with the beads for one hour the palmitoylation assay was carried out. The biotin-BMCC modified samples were detected using streptavidin-HRP. Western blotting of RhoU palmitoylation in 1542 shControl and 1542 shFASN A3 along with quantification via densitometry analysis can be seen in (**A**). The same experiment was performed with the second FASN knockdown cell line (shFASN A4) which can be seen in (**B**) along with the quantification. The streptavidin-HRP probed blot was stripped to remove the palmitoylation signal and immunoblotted for RhoU allowing for the quantification of total RhoU. The WCL was run in parallel acting as a control for the experiment and was probed for total RhoU. Data represents the mean values ± SEM accumulated from three independent experiments. Statistical significance was determined by student's *t-test*. **p<0.01, ***p<0.001.

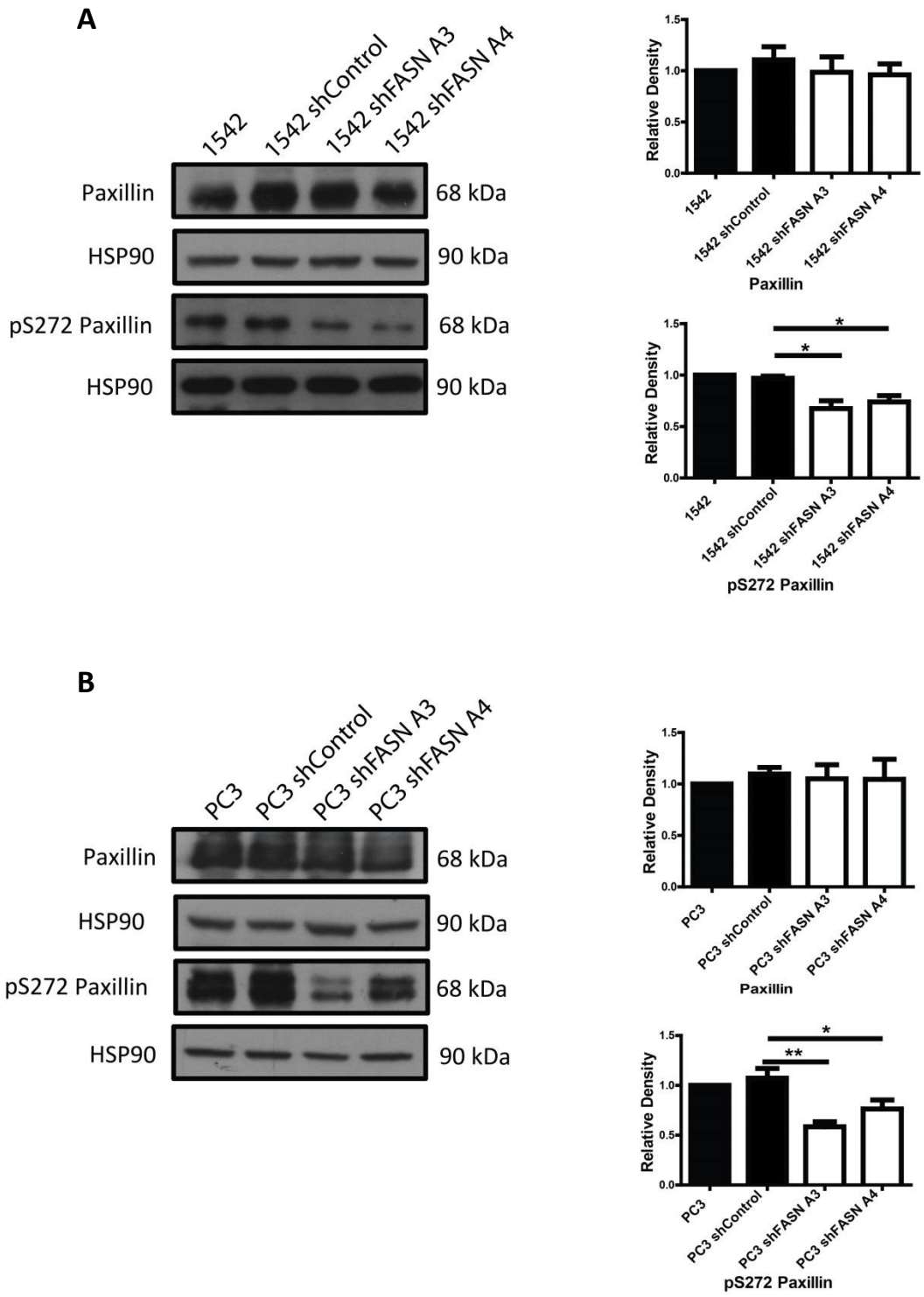

Figure 5.11 FASN knockdown decreases paxillin s272 phosphorylation in 1542 and PC3 cells: Western blotting was carried out to determine the expression of Paxillin and pS272 paxillin in 1542, 1542 shControl, 1542 shFASN A3 and 1542 shFASN A4 cell lysates. Quantification was then determined by densitometry analysis as seen in (**A**). The same was done for PC3 cells as shown by the western and quantification in (**B**). It should be noted that both pS272 paxillin bands were used for densitometry quantification in PC3 cells. Data represents the mean values ± SEM accumulated from three independent experiments. Statistical significance was determined by student's *t-test*. *p<0.05, **p<0.01.

5.2.8 FASN depletion and inhibition leads to loss of Cdc42

mRNA expression data showed that 1542 and PC3 cells express the prenylated, but not the palmitoylated variant of Cdc42. However, in both hepatocellular and cardiac muscle cells palmitate has been shown to modulate the expression and activity of Cdc42, which based on the other findings in the literature, is the prenylated isoform (Puthanveetil et al., 2011; Sharma et al., 2012c). Indeed FASN knockdown decreased cell size and migratory capacity producing a similar phenotype in PC3 cells to what has previously been reported in this cell line upon Cdc42 silencing (Reymond et al., 2012). Thus, total Cdc42 expression levels were probed for in both prostate cell lines. Western blotting analysis reveals that Cdc42 protein expression decreases in FASN knockdown 1542 cells compared to 1542 shControl cells (**Figure 5.12A**). Similarly, the same decrease in Cdc42 expression was validated in the best FASN knockdown PC3 cell line (**Figure 5.12B**). In addition to stable knockdown cell lines, the FASN inhibitor C75 was used to confirm if blocking FASN activity decreases Cdc42 expression. Both 1542 and PC3 cells treated with C75 showed a significant decrease in Cdc42 expression mirroring the same trend seen in the stable cell lines (**Figure 5.12C and 5.12D**).

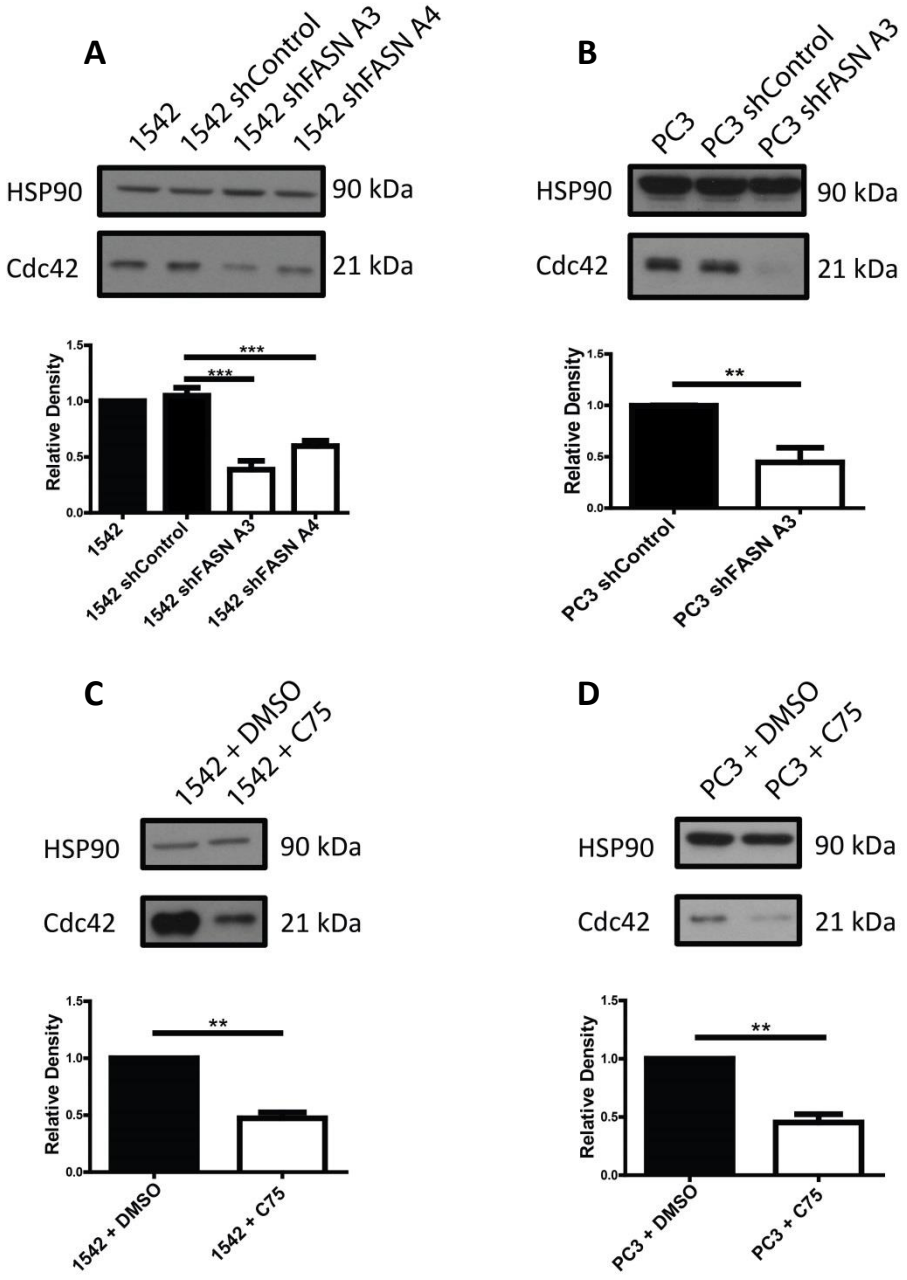

Figure 5.12 FASN knockdown and inhibition leads to decreased Cdc42 levels in 1542 and PC3 cells: Western blotting was carried out to determine the expression of Cdc42 (**A**) in 1542, 1542 shControl, 1542 shFASN A3 and 1542 shFASN A4 cell lysates. Quantification was then determined by densitometry analysis. The same was done for PC3 cells (comparing control against best FASN knockdown) as shown by the western in (**B**). 1542 and PC3 cells were treated with DMSO and C75 25 µM for 24 hours before lysing. Protein lysates were separated by SDS-PAGE and Cdc42 was probed for in 1542 (**C**) and PC3 (**D**) cells. Data represents the mean values ± SEM accumulated from three independent experiments. Statistical significance was determined by student's *t-test*. *p<0.05, **p<0.01, ***p<0.001.

5.2.9 Cdc42 overexpression rescues FASN knockdown 1542 cell morphology

In this chapter it has been found that Cdc42 protein levels are dependent on FASN expression and activity. It has been published that Cdc42 regulates PC3 cell morphology through its ability to affect the actin cytoskeleton (Reymond et al., 2012). Thus, it was decided to investigate if re-expressing Cdc42 could rescue the FASN knockdown morphology defect. To assess this 1542 shFASN A3 cells were seeded onto matrigel coated coverslips and then transfected with either GFP or GFP-Cdc42. Cell shape analysis was done on the phalloidin staining in keeping with all previous experiments (**Figure 5.13**). Results show a partial rescue in cell shape in GFP-Cdc42 expressing 1542 shFASN A3 cell compared to the same cells expressing GFP which still showed a reduction in cell size when compared to 1542 shControl cells (**Figure 5.13B**).

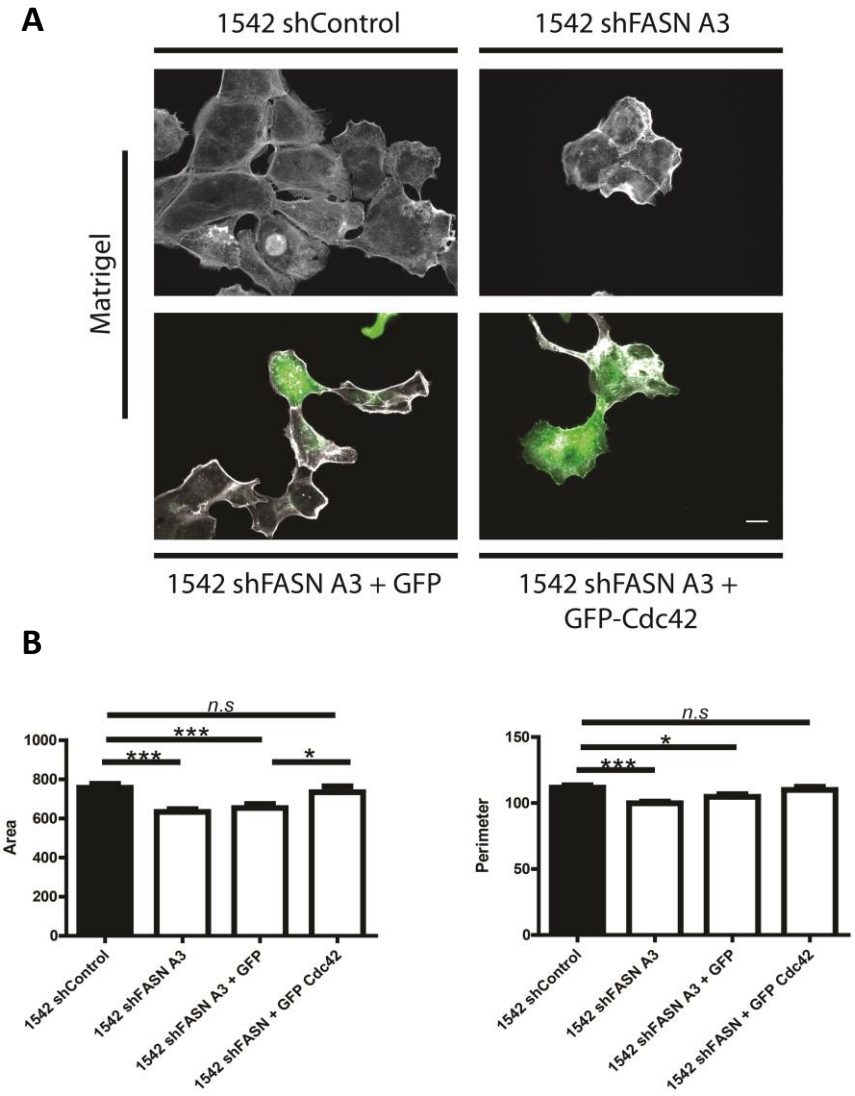

Figure 5.13 Cdc42 overexpression rescues the FASN knockdown morphological phenotype in 1542 cells: 1542 shControl and 1542 shFASN A3 cells were seeded onto matrigel coated coverslips. 1542 shFASN A3 cells were transiently transfected with either GFP or GFP-Cdc42. Cells were left for 24 hours before staining with phalloidin (**A**). For transfected cells the Images are a composite of phalloidin staining (Grey) and GFP fluorescence (Green). ImageJ was used to calculate the cell area and perimeter of 60 cells per condition. This data was used to determine differences in cell perimeter and area between our conditions (**B**). Data represents the mean values ± SEM accumulated from three independent experiments. Statistical significance was determined by student's *t-test*. *p<0.05 ***p<0.001 *n/s*= not significant. Bar= 10 µM.

5.2.10 Silencing of RhoU and inhibition of its palmitoylation leads to a loss in Cdc42 expression

The results so far reveal that RhoU palmitoylation and total Cdc42 expression decrease in a FASN knockdown background, however it is not known if these two proteins are linked. To investigate this, Cdc42 expression was probed for in 1542 cells with either depleted RhoU levels, or with normal, but non-palmitoylated RhoU levels. The silencing of RhoU in 1542 cells led to a significant decrease in Cdc42 expression compared to control cells (**Figure 5.14A**). Abrogating normal RhoU activity was accomplished by global blockage of palmitoylation with 2-bromopalmitate (2BP), a DHHC protein inhibitor, for 24 hours (Jennings et al., 2009). Prevention of palmitate incorporation did not affect total RhoU levels, however inhibition did significantly decrease Cdc42 levels in 2BP treated cells compared to DMSO control cells (**Figure 5.14B**).

5.2.11 Interaction studies show that RhoU associates with Cdc42

The results currently show that in FASN depleted cells there is a reduction in Cdc42 protein levels (**Figure 5.12**), but no change in mRNA levels (**Figure 5.3**). Furthermore, it has also been shown that a decrease in RhoU protein expression or palmitoylation also depletes Cdc42 protein levels (**Figure 5.14**). All this suggests that these two proteins may be binding. Cdc42 is known to homodimerize, and based on the extensive shared sequence homology it may also be able to heterodimerize with RhoU (Chuang et al., 2007; Zhang and Zheng, 1998). Mistargeting of RhoU, which has been reported in NIH 3T3 cells expressing palmitoylation mutants, may be failing to dimerize with Cdc42, which may be important in protecting it from degradation (Berzat et al., 2005). In order to help confirm this hypothesis it was first decided to identify if these two Rho GTPases interact with each other. Using the GFP-Trap system it was shown that Cdc42 and RhoU are interacting partners (**Figure 5.15**).

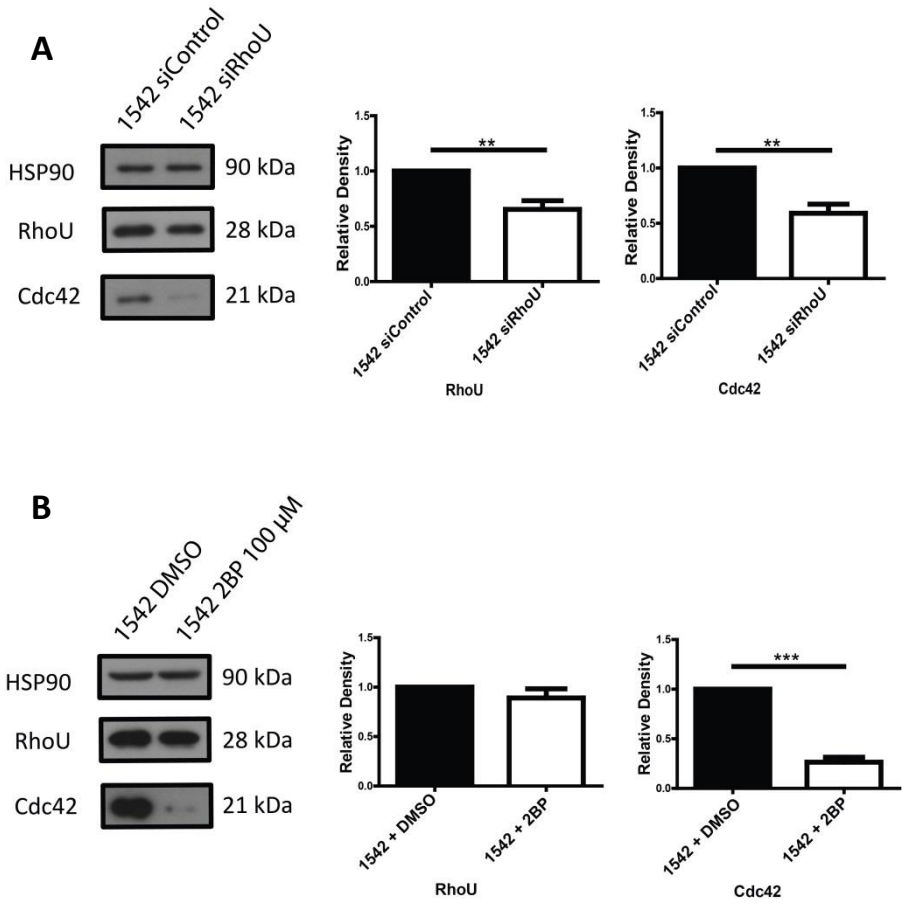

Figure 5.14 RhoU knockdown and palmitate inhibition leads to loss of Cdc42: For knockdown studies 1542 cells were transfected with siControl and siRhoU for 48 hours before harvesting. Palmitate incorporation inhibition was carried out by treating the cells with 2-Bromopalmitate (2BP) 100 µM for 24 hours. A DMSO control was prepared in parallel. Lysates were separated by SDS-PAGE and then immunoblotted for RhoU and Cdc42. Quantification of bands for RhoU siRNA knockdown (**A**) and RhoU palmitoylation inhibition (**B**) was carried out by densitometry analysis. Data represents the mean values ± SEM accumulated from three independent experiments. Statistical significance was determined by student's *t-test*. **p<0.01 ***p<0.001.

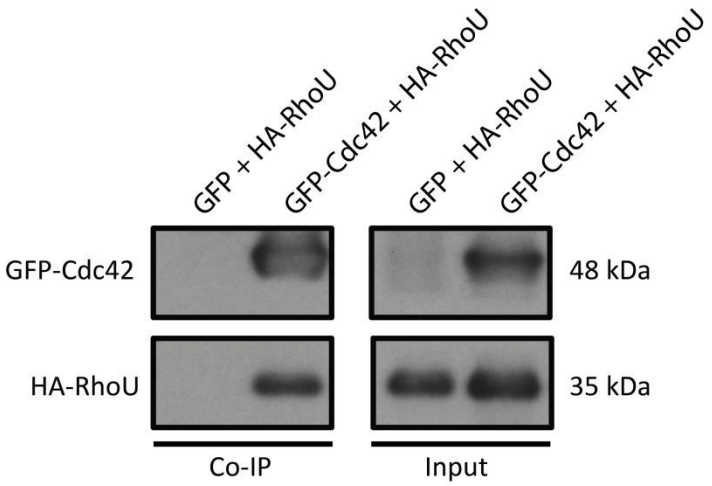

Figure 5.15 Co-immunoprecipitation of Cdc42 with RhoU: HEK293 cells were co-transfected with either GFP-Cdc42 and HA-RhoU or GFP alone and HA-RhoU. GFP was used as a negative control in this assay. After 48 hours the cells were lysed and a GFP-Trap was carried out. Lysates were subjected to SDS-PAGE gel electrophoresis and then the Co-IP western was immunoblotted using anti-GFP and anti-HA antibody. The WCL was run in parallel and probed for the same antibodies acting as a control for the total amount of protein expressed in the assay.

5.3 Discussion

The aim of this chapter was to elucidate molecular mechanisms that can account for the FASN depleted phenotype in prostate cancer. These mechanistic changes can then be correlated with the cell motility and invasive phenotypes characterised in chapter 4. In the current literature FASN has been identified to have a migratory role in several cancers including prostate, however the exact molecular mechanisms driving FASN-induced cell motility still remain to be fully elucidated (Coleman et al., 2009; Wen et al., 2016; Zaytseva et al., 2012).

In this chapter it was shown that FASN knockdown led to a small, but significant decrease in c-Met expression. This drop in c-Met levels however to not affect downstream PI3K/AKT and MAPK signalling. Additionally, for the first time a unique role for FASN in the regulation of RhoU palmitoylation and Cdc42 expression was identified in the chapter. It was further demonstrated that the re-expression of Cdc42 in FASN depleted cells could rescue the morphology defect. This chapter also showed that depletion of RhoU, or prevention of its palmitoylation, decreased Cdc42 expression. From this data a Co-IP was carried out and it was revealed for the first time that RhoU and Cdc42 are binding partners, or at least exist in a complex with each other.

The regulatory link between FASN and c-Met has been well documented across several studies (Coleman et al., 2009; Hu et al., 2016; Uddin et al., 2010). The results presented in this chapter showed a modest drop in c-Met levels in response to FASN knockdown complimenting these previously documented findings. A study by Hu *et al* has confirmed that FASN suppression affects c-Met on the post-translational level in hepatocellular carcinoma cells (Hu et al., 2016). This is further clarified in another recently published study by Coleman *et al* who found that c-Met receptor trafficking and stability in DU145 cells was dependent on palmitoylation, and that the prevention of this modification leads to a loss in total c-Met (Coleman et al., 2016). This reduction in palmitate, and therefore palmitoylation as a result of FASN knockdown may be the most likely explanation for the decrease in c-Met expression that was observed in 1542 and PC3 cells.

Downstream activation of AKT and ERK was unaffected in FASN depleted prostate cancer cells. ERK phosphorylation did increase in the PC3 shFASN A4 line; however it is unlikely this was a direct result of altered FASN expression since it was not observed in any of the other FASN knockdown clones. Previous studies have found that the inhibition of FASN usually correlates with the reduced phosphorylation of AKT and ERK (Chang et al., 2016; Coleman et al., 2009; Huang et al., 2016; Wang et al., 2013b). Reduced AKT phosphorylation has been shown to impair the FASN migratory phenotype in osteosarcoma cells (Zhou et al., 2015). ERK phosphorylation has not yet been shown to be important in FASN mediated cell migration with the majority of studies attributing its role mainly to growth (Coleman et al., 2009; Huang et al., 2016). Interestingly, in chapter 3 it was shown that FASN knockdown in 1542 and PC3 cells significantly decreased the rate of cellular proliferation. Since no decrease in ERK phosphorylation was seen in these same cells it would suggest that ERK activation is not essential in FASN-mediated cell growth.

One reason for AKT and ERK signalling being unperturbed in the FASN knockdown cell lines could be due to c-Met still being expressed at sufficient levels to elicit a response. Coleman *et al* found that c-Met expression was completely suppressed in response to FASN knockdown in DU145 cells (Coleman et al., 2009). Comparatively, in this study it was found that c-Met levels were still relatively high in the FASN knockdown prostate cancer cell lines. In addition, PC3 cells harbour a null variant of PTEN (PTEN status currently unknown for 1542 cells), the cells natural negative regulator of the PI3K/AKT signalling pathway (Majumder and Sellers, 2005). This means it may be more difficult to suppress AKT signalling without completely abolishing FASN activity as shown in a previous study with PTEN mutant cells treated with a FASN inhibitor (Ventura et al., 2015). Alternatively, cancer cells have been documented to re-wire their internal signalling to compensate with the loss or reduction of a certain protein (Zhang et al., 2014). This has been shown in a study by Ross *et al* were it was found that AKT phosphorylation recovered after 24 hours even though the PC3 cells were still under orlistat treatment (Ross et al., 2008). It could be possible that the stable long term reduction in FASN levels in both prostate cell lines have led to AKT and ERK signalling adapting to not be dependent on FASN expression. Whilst this cannot be confirmed at this moment in time, it would be interesting in future experiments to probe for

phospho-AKT and ERK in both prostate cell lines at a closer time-point to the initial knockdown of FASN. Regardless, this data confirms that AKT and ERK signalling is most likely not responsible for the migration defect seen in response to FASN knockdown in 1542 and PC3 cells.

In addition to looking at signal transduction pathways downstream of c-Met this chapter also focussed on exploring a potential role for FASN in the palmitoylation of Rho GTPases. The palmitoylated protein signalling network comprises over 300 proteins and is largely unexplored in cancer (Martin and Cravatt, 2009). It is only more recently that researchers are starting to acknowledge FASN as a crucial regulator of palmitoylation mediated protein signalling. The results presented in this chapter are the first to confirm a novel dependency on FASN for Rho GTPase palmitoylation. Overexpression of FASN in HEK293 cells led to an increase in RhoU and Rac1 palmitoylation. These findings are consistent with a previous report which demonstrated that Wnt-1 palmitoylation increases in FASN-overexpressing prostate epithelial cells (Fiorentino et al., 2008). Conversely, the silencing of FASN led to a decrease in RhoU palmitoylation. Unlike RhoU, Rac1 palmitoylation was not affected by FASN knockdown in 1542 cells. To date, only one other study has shown a differential S-acylation response between two proteins in a FASN depleted system. Wei *et al* found that FASN knockdown in Caco-2 colorectal cancer cells decreased mucin 2 palmitoylation but not affect claudin-1 palmitoylation (Wei et al., 2012). There is currently no explanation for this phenomenon however it could be speculated that the reduced pool of available palmitate may be prioritized to prevent catastrophic effects in the cell. Additionally, the different methods of palmitate attachment may also be influencing the increased likelihood of protein palmitoylation. The majority of cellular palmitoylation events are carried out by DHHC proteins; however substrate-specific PAT's and spontaneous acylation also mediate pamitoyl-CoA linkage (Corvi et al., 2001; Roth et al., 2006; Xue et al., 2004). Therefore it could be the case that Rac1 is posttranslationally modified via a different means to RhoU which may potentially give it more rapid or prioritized access to palmitate.

The role of RhoU in cancer is not as well studied as some of the other Rho GTPases. Furthermore, the consequences of impaired palmitoylation on its function have not

been fully elucidated. Tao *et al* first reported that RhoU could bind PAK1 to induce filopodium formation and stress fibre dissolution (Tao et al., 2001). Since then RhoU has been found to play an important role in the regulation of cell morphology, adhesion turnover, and cell migration (Alinezhad et al., 2016; Dart et al., 2015). Palmitoylation of RhoU has been found to be important in maintaining its functional integrity (Berzat et al., 2005). Blocking palmitoylation causes mislocalization and cytosolic accumulation of RhoU. Mislocalization of RhoU prevents PAK1 phosphorylation, causes changes in cellular morphology and impairs cell growth (Berzat et al., 2005; Tao et al., 2001). It is currently unclear how essential palmitoylation is for RhoU to induce cell migration. However, one study has found that the RhoU-EGFR interaction is dependent on RhoU palmitoylation and that the resulting complex enhances EGF-induced JNK activation and cell migration (Zhang et al., 2011).

It has been published that the silencing of RhoU in breast cancer cells results in increased cell-substrate adhesion and the formation of more elongated focal adhesions. This more adhesive phenotype is a consequence of reduced paxillin phosphorylation due to the loss of RhoU (Dart et al., 2015). This phenotype along with the resulting decrease in paxillin phosphorylation was essentially recapitulated here in the FASN knockdown prostate cancer cell lines. These results hint that the palmitoylation of RhoU is also important in paxillin adhesion dynamics. To further support this, in chapter 3 it was shown that the addition of palmitate to FASN knockdown 1542 cells almost fully restored the length of paxillin adhesions to the length observed in control cells. Thus, this data suggests that FASN dependent adhesion turnover is most likely being regulated by palmitoylated RhoU. It should be noted however that one study reported that palmitoylation of RhoU is not required for its targeting to focal adhesions (Ory et al., 2007).

In this chapter it was found that unlike RhoU and Rac1, Cdc42 protein expression levels decreased in response to FASN knockdown. This is the first time an association between FASN and the Rho GTPase Cdc42, or more specifically, the prenylated isoform of Cdc42, has been documented. Moreover, this result compliments a previously published study which showed an increase in Cdc42 expression in cardiomyocyte cells

treated with exogenous palmitate (Puthanveetil et al., 2011). Cdc42 is involved in the formation of filopodia and is a key protein in polarized cell motility (Keely et al., 1997). The silencing of Cdc42 has been shown to give PC3 cells more astrocyte-like morphology and impair their ability to migrate effectively through a monolayer of endothelial cells (Reymond et al., 2012). In this study FASN knockdown was shown to decrease the overall size of 1542 and PC3 cells. Re-expression of Cdc42 in FASN knockdown 1542 cells was able to partially rescue the wild-type morphological phenotype. This data strongly supports a role for Cdc42 in driving the morphological changes seen in FASN depleted prostate cancer cell, most likely through its ability to affect the actin cytoskeleton. It should be noted that overexpression of Cdc42 could have the same effect on the morphology of 1542 shControl cells, however this was not tested and thus something to be considered in future.

During cell migration there is a significant amount of cross-talk between Rho GTPase proteins. This has been shown by the activation of Rac1 by Cdc42 through the Rac GEF Tiam1 (Cau and Hall, 2005; Pegtel et al., 2007). Additionally, Rho GTPases exist in a signalling network where they can influence each other's levels. This has been observed in the degradation of RhoA which is mediated by smurf-1, a HECT E3 ligase recruited by active Cdc42 complexed with Par6 and PKCζ (Wang et al., 2003). In this study it was found that mRNA levels of prenylated Cdc42 did not change between control and FASN knockdown cell lines. These findings infer that in a FASN depleted background Cdc42 is being negatively regulated post-translationally. RhoU and Cdc42 share significant sequence homology and are both involved in filopodia formation (Tao et al., 2001). Interestingly, one study found that the FASN inhibitor orlistat significantly reduced the number of filopodial extensions in melanoma cells (Bastos et al., 2016). Even though there is functional overlap between these two proteins, how they might influence each other's activity has never been investigated. In this study it was shown that the silencing of RhoU in 1542 cells led to a decrease in Cdc42 expression. Moreover, RhoU and Cdc42 were identified as interacting partners. It is not clear how these two proteins interact, however Cdc42 is known to homodimerize and since it shares similar sequence homology with RhoU it could be binding via the same carboxyl-terminal polybasic domain (Zhang and Zheng, 1998). The complete inhibition of palmitoylation with 2BP also significantly ablated Cdc42 expression. PCR and DNA

gel electrophoresis results confirmed that both prostate cell lines only expressed the prenylated isoform of Cdc42 and not the palmitoylated isoform. This means that palmitoylation is not directly responsible for the changes in Cdc42 expression. Alternatively, the data presented here suggests that the palmitoylation of RhoU could be involved in regulating Cdc42 levels in the cell.

In rat bladder carcinoma cells Cdc42 has been shown to be susceptible to poly-ubiquitination and proteasomal degradation (Doye et al., 2002). Interestingly, it has been found that DHHC dependent palmitoylation of proteins increases stability and protection from proteasome degradation (Percherancier et al., 2001; Wang et al., 2010). Thus, it could be the case that if Cdc42 is in a heterodimeric complex with RhoU, it may be less prone to targeting by E3 ubiquitin ligases. In addition to possibly preventing protein degradation, the binding of RhoU to Cdc42 could potentially enhance cell migration in a way that is yet to be determined. Prenylation and palmitoylation differ in that the latter is reversible (Aicart-Ramos et al., 2011). It may be that the activity of Cdc42 within the cell is increased upon binding to RhoU due to its ability to dynamically shuttle between intracellular compartments. Moreover, it has been shown that the biological activity of H-Ras, a protein that can be both prenylated and palmitoylated, is greatly compromised upon the prevention of one of these modifications (Cadwallader et al., 1994). RhoU cannot be prenylated and Cdc42 cannot be palmitoylated, thus the binding of these two proteins may stabilise and synergistically enhance each other's signalling at the plasma membrane.

In summary, the work presented in this chapter demonstrated that FASN regulates RhoU and Cdc42 post-translationally through direct and indirect means respectively. Additionally, an interaction between RhoU and Cdc42 was found and may be important in FASN-driven cell migration. Evidence for this theory is shown by FASN knockdown cells phenocopying the increased focal adhesion phenotype seen in RhoU depleted cells (Dart et al., 2015).

5.4 Future work

HGF/c-Met signalling is known to drive the activation of several downstream molecules (Organ and Tsao, 2011). Whilst PI3K/AKT and MAPK signalling appeared to be unaffected in FASN knockdown cells it would be interesting to confirm what changes, if any, have occurred in other downstream effector pathways of c-Met.

It may also be worth trying to further confirm that palmitoylated Cdc42 is not expressed in the PC3 and 1542 cells lines. An alternative approach could be to use the palmitoylation assay protocol on a large concentration of protein lysate to isolate palmitoylated proteins specifically via streptavidin purification. Then these purified protein lysates can be run and separated on a western blot and probed for palmitoyl-Cdc42 which is confirmed by a positive signal in the hydroxylamine positive lysate (Dowal et al., 2011).

Exploring the effects of reduced RhoU palmitoylation in cell migration is also something to be investigated. This could be done by re-expressing siRNA resistant wild-type- and palmitoylation mutant RhoU in RhoU knockdown cells. In addition elucidating how RhoU or palmitate is preventing Cdc42 degradation would be beneficial. Moreover, it needs to be confirmed if Cdc42 can be blotted from immunoprecipitated RhoU. Finally, creating domain mutants would also be useful in validating which domain mediates RhoU and Cdc42 binding.

Chapter 6

Patho-Epidemiological study: Is the expression of FASN, RhoU, Cdc42, c-Met and HER2 associated with prostate cancer severity?

Chapter 6 – Patho-Epidemiological study: Is the expression of FASN, RhoU, Cdc42, c-Met and HER2 associated with prostate cancer severity?

6.1 Introduction

In the previous chapter of this thesis it was shown that FASN expression is linked to the expression of Cdc42 and the activity of RhoU in prostate cancer cell lines. In addition, c-Met levels were also found to be modestly reduced in a FASN knockdown background. To compliment these findings it was decided to perform a pilot patho-epidemiological study which would assess the expression of FASN, along with these biologically linked proteins, in human prostate cancer tissue. The epidermal growth factor receptor HER2 was not studied in the previous chapters, however it was decided to include it in the panel of proteins as there is now evidence in the literature which suggests that HER2 may influence prostate cancer metastasis to the bone (Day et al., 2017). In addition, to more specific interest to this project, several papers have now shown that HER2 and FASN exist in a signalling axis which drives cell migration in osteocarcinoma and colorectal cancer cells (Li et al., 2013; Long et al., 2014). This raises the question of whether anti-HER2 drugs alone, or in combination with FASN inhibitors could be used to treat prostate cancer patients (Blancafort et al., 2015). Another protein included in the panel was Ki67 which is a marker that is strictly associated with cellular proliferation (expressed at every stage of the cell cycle except G_0) and commonly used in TMAs (Scholzen and Gerdes, 2000). More specifically, given that uncontrolled cell growth is a common feature in tumours, Ki67 acts as a control to help confirm how 'benign' or 'cancerous' the tissue is aiding histopathological assessment (Scholzen and Gerdes, 2000).

Thus, this study was set out to investigate whether the expression of FASN, RhoU, Cdc42, c-Met and HER2 were associated with prostate cancer severity, which is based on tissue type (dominant Gleason, abbreviated as DG, highest Gleason, abbreviated as HG, and benign tissue) and Ki67 expression levels. It should be noted that FASN expression has previously been reported to increase in prostate cancer relative to normal prostate tissue (Rossi et al., 2003). Thus in this study FASN staining acts somewhat as a control which is expected to differ between the benign and cancerous tissue types.

6.2 Results

6.2.1 High expression of FASN, RhoU, Cdc42, c-Met and HER2 in biopsy cores is predictive of prostate tissue type

The cohort for this pilot study consisted of 85 men (mean age 67.18) who had undergone a radical prostatectomy. The majority of these men had a Gleason score of 7 (60.00% 51/85), whilst the minority had a Gleason score of 5 (2.35% 2/85) (**Table 6.1**). Univariate logistic regression was carried out to predict if any of the biomarkers were abnormally expressed in either benign or cancerous tissue (Dominant Gleason-DG and Highest Gleason-HG). In the univariate analysis, relative to benign tissue, both DG and HG cancerous tissue types were shown to be significantly associated with an increase in the protein expression of FASN, RhoU, Cdc42 and c-Met (**Table 6.2** and **Figure 6.1**). Additionally, the HG tissue type was found to be predictive of increased HER2 expression, OR 1.82 (95% CI: 1.19-2.78), when compared to benign prostate tissue (**Table 6.2**). For the DG tissue type there was also a positive association with HER2 expression, however the findings were not statistically significant, OR 2.10 (95% CI: 0.90-4.89), (**Table 6.2**). This association can also be seen in **Table 6.3** which shows almost twice as many DG cases with high HER2 staining (21.95% 18/82) compared to benign tissue (11.76% 10/85).

Table 6.1 Baseline characteristics of radical prostatectomy patients included in the UCAN database. SD= Standard deviation, IQR= Interquartile range.

Factor	Study Population (N=85)
Mean age (SD), years	67.18 (5.81)
Gleason score at time of diagnosis	
5	2 (2.35)
6	19 (22.35)
7	**51 (60.00)**
3+4	37 (43.43)
4+3	14 (16.67)
8	9 (10.59)
9	4 (4.71)
Median PSA (IQR Q1-Q3)	6.4 (4.6-8.1)

Table 6.2 Univariate odds ratios (OR) with 95% confidence intervals (CI) to predict abnormal expression levels of FASN, RhoU, c-Met, HER2, and Ki67 based on prostate tissue type (i.e. dominant and highest Gleason score tissue versus benign tissue).

	Univariate
Biomarker	**OR (95% CI)**
FASN	
Benign tissue	1.00 (Ref)
Dominant Gleason	12.40 (5.96-25.79)
Highest Gleason	4.24 (2.81-6.39)
RhoU	
Benign tissue	1.00 (Ref)
Dominant Gleason	3.13 (1.68-6.50)
Highest Gleason	3.37 (2.03-5.57)
Cdc42	
Benign tissue	1.00 (Ref)
Dominant Gleason	3.30 (1.62-6.72)
Highest Gleason	2.57 (1.73-3.64)
c-Met	
Benign tissue	1.00 (Ref)
Dominant Gleason	37.63 (8.67-163.35)
Highest Gleason	6.25 (2.97-13.12)
HER2	
Benign tissue	1.00 (Ref)
Dominant Gleason	2.10 (0.90-4.89)
Highest Gleason	1.82 (1.19-2.78)

Table 6.3 Distribution expression levels of FASN, RhoU, c-Met, HER2, and Ki67 by prostate tissue type: Benign tissue N=85, Dominant Gleason N=82, Highest Gleason N=66. 0=low/negative staining intensity, 1= High staining intensity.

Biomarker	FASN Total (%)	RhoU Total (%)	Cdc42 Total (%)	c-Met Total (%)	HER2 Total (%)	Ki67 Total (%)
Benign tissue						
0	68 (80.00)	41 (48.24)	70 (82.35)	83 (97.65)	75 (88.24)	85 (100.00)
1	17 (20.00)	44 (51.76)	15 (17.65)	2 (2.74)	10 (11.76)	0 (0.00)
Dominant Gleason						
0	20 (24.39)	18 (21.95)	48 (58.54)	43 (53.44)	64 (78.05)	44 (53.66)
1	62 (75.61)	64 (78.05)	34 (41.46)	39 (47.56)	18 (21.95)	38 (46.34)
Highest Gleason						
0	12 (18.18)	5 (7.58)	28 (42.42)	34 (51.52)	45 (69.23)	29 (43.94)
1	54 (81.82)	61 (92.42)	38 (57.58)	32 (48.48)	20 (30.77)	37 (56.06)

6.2.2 Ki67 expression in prostate cancer is associated with the expression of all biological markers

As mentioned in the introduction to this chapter, Ki67 has been regarded as one of the most promising immunohistochemical biomarkers for identifying proliferating cell fractions and is often correlated with the clinical course of cancer (Scholzen and Gerdes, 2000). Univariate analysis in **Table 6.4** reveals that the expression of FASN, RhoU, Cdc42, c-Met and HER2 is positively associated with Ki67 expression. Subsequently, when performing multivariable analyses it was found that FASN, Cdc42 and c-Met expression remain statistically significant and positively associated with Ki67 expression. RhoU was also still positively associated, but the finding became not statistically significant, OR 2.61 (95% CI: 0.94-7.20). The association between HER2 expression and Ki67 expression disappeared, OR 1.07 (95% CI: 0.47-2.44) (**Table 6.4**).

Table 6.4 Odds ratios (OR) and 95% confidence intervals (CI) for the association between the biomarkers FASN, RhoU, Cdc42, c-Met and HER2 and high expression levels of ki67: The univariate model assessed the association of each biomarker against Ki67 expression, whilst the multivariable assessed how all the biomarkers associated with Ki67 expression in one model.

Biomarker	Ki67	
	Univariate OR (95% CI)	**Multivariable OR (95% CI)**
FASN	7.50 (3.67-15.30)	3.70 (1.67-8.16)
RhoU	6.67 (2.72-16.31)	2.61 (0.94-7.20)
Cdc42	4.95 (2.74-8.92)	2.58 (1.30-5.12)
c-Met	5.21 (2.85-9.51)	2.79 (1.38-5.65)
HER2	3.25 (1.69-6.26)	1.07 (0.47-2.44)

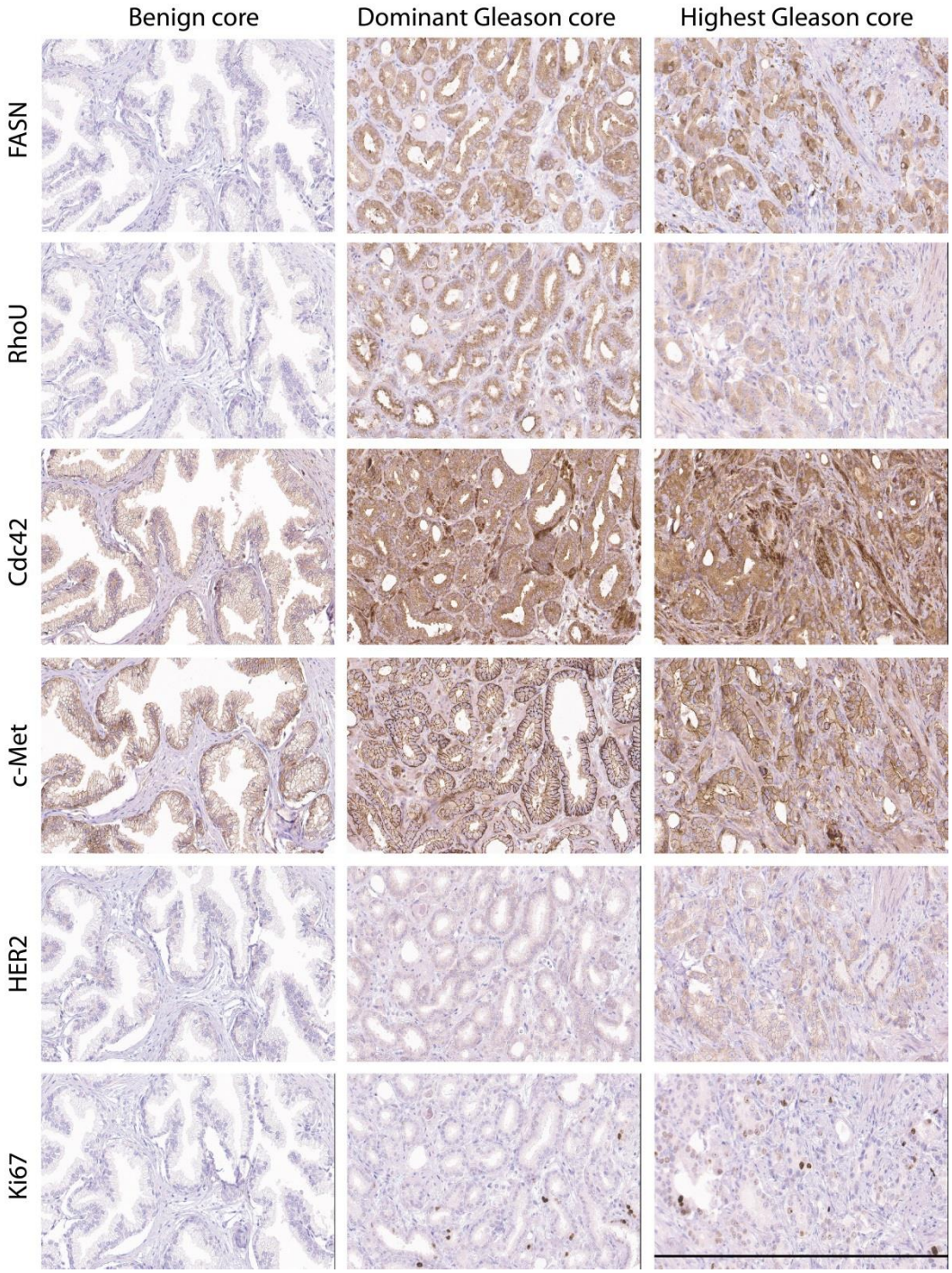

Figure 6.1 Representative immunohistochemistry for FASN, RhoU, Cdc42, c-Met, HER2 and Ki67 in benign tissue and prostatic adenocarcinoma (dominant and highest Gleason): Images for each protein were taken from the same core on the same TMA. Magnification x200 as shown by the scale bar.

6.3 Discussion

The aim of this part of my thesis was to identify if the proteins FASN, RhoU, Cdc42, HER2 and Ki67 were differentially expressed in prostate cancer tissue when compared to benign prostate tissue. Indeed an increase in the expression of all proteins was observed in cancerous tissue. In this study, DG prostate cancer tissue was 12.4 times, 3.13 times, 3.30 times and 37.63 times more likely to be associated with higher expression levels of FASN, RhoU, Cdc42 and c-Met, respectively, than benign prostate tissue. Additionally, HG prostate cancer tissue was 4.24 times, 3.17 times, 2.57 times, 6.25 and 1.82 times more likely to be associated with higher expression levels of FASN, RhoU, Cdc42, c-Met and HER2, respectively, than benign prostate tissue.

The results for FASN immunohistochemical staining agree with several published findings in the literature which have shown it to be more highly expressed in cancerous prostate tissue than non-cancerous prostate tissue (Cheng et al., 2015; Hamada et al., 2014; Rossi et al., 2003; Swinnen et al., 2002; Van de Sande et al., 2005). To date this is the first study to show a differential expression profile for RhoU at the protein level between normal prostate tissue and cancerous prostate tissue. This result compliments the findings from another study by Alinezhad *et al* where the authors found RhoU mRNA levels to be increased in cancerous prostate tissue when comparing to benign prostate tissue (Alinezhad et al., 2016). Similar to RhoU, this is also the first study to show that increased Cdc42 expression is associated with prostatic carcinoma status. Two other studies in the literature have shown similar results but in ovarian and cervical cancer (Guo et al., 2015; Ye et al., 2015). Higher c-Met expression in prostate cancer relative to non-malignant prostate tissue has also been well documented in the literature (Jacobsen et al., 2013; Knudsen et al., 2002). As discussed in the previous chapter, c-Met and FASN are intimately linked in prostate cancer (Coleman et al., 2009). c-Met receptor stability is dependent on palmitoylation and FASN expression is dependent on the PI3K/AKT and MAPK signalling downstream of c-Met (Coleman et al., 2016; Huang et al., 2016). Further evidence of this has been observed in a study by Uddin *et al* who found that FASN overexpression in diffuse Large B-cell Lymphoma is significantly associated with the overexpression of c-Met (Uddin et al., 2010). In this study, the HG prostate cancer tissue type was associated

with HER2 overexpression. This finding agrees with a previously published study by Day *et al* who found that HER2 expression to be low in the primary prostate tumour, but high in prostate cancer tissue (Day et al., 2017).

Ki67 has been shown to be a promising biomarker for predicting prostate cancer disease stage (Berney et al., 2009). Univariate analysis showed that the expression of all the biomarkers positively associated with Ki67 expression. When performing a multivariable analysis, which included all the biomarkers, the association for RhoU became weaker and HER2 expression was no longer associated with ki67 expression. This suggests that FASN, Cdc42 and c-Met expression levels are better predictors for Ki67 expression than RhoU and HER2.

This is not the first study to show a link between FASN and Ki67. FASN expression has been shown to be significantly associated with Ki67 expression in osteosarcomas, soft tissue sarcomas, endometrial cancer and pancreatic cancer (Alo et al., 2007; Liu et al., 2012; Pizer et al., 1998; Takahiro et al., 2003). In addition, one study by Swinnen *et al* showed there was a close association between the expression of FASN and Ki67 in the early stages of prostate cancer progression (Swinnen et al., 2002). Similarly, the expression levels of c-Met and Ki67 have also previously been shown to be significantly associated but in non-small-cell lung cancer and gastric cancer (Masuya et al., 2004; Wu et al., 2009).

This is also the first study to show that the expression of the Rho GTPases Cdc42 and RhoU is positively associated with the expression of Ki67 in prostate cancer. Both Cdc42 and RhoU have been shown to drive cell proliferation and a more aggressive cancer phenotype in *vitro*, however to date their relationship with the proliferating marker Ki67 has not previously been evaluated in tissue (Gao et al., 2015; Zhang et al., 2011).

6.4 Future work

The results generated from this pilot study have provided a good basis for looking at some of these proteins in a more robust study. In the future it would be useful to look at the expression of these proteins in a larger sized cohort. This may help with one of the limitations of this study which was a weak distribution of patients between Gleason score categories. Since 60% of the men in this study had a Gleason score of 7, it was not possible to link biomarker staining based on high or low Gleason. In addition to obtaining more patient tissue with different Gleason scores it would also be worth assessing the expression of these proteins in metastatic tissue (lymphatic, microvascular, perineuronal, and bone). The expression of FASN has been shown to increase in castrate-resistant prostate cancer which is correlated with metastatic disease (Pizer et al., 2001). Thus, it would be interesting to see if the expression of the Rho GTPase proteins also changes during metastatic progression.

In a future study it would also be good to associate the expression of these biomarkers with patient characteristics such as metabolic syndrome, androgen therapy, tumour size, family history and ethnicity. It is currently still not clear if FASN and *de novo* lipogenesis are strong contributors towards metabolic syndrome in prostate cancer patients, however there is supporting evidence (Tian et al., 2011; Wakil and Abu-Elheiga, 2009). Ethnicity is also a strong driving factor for prostate cancer development and severity. Typically, the highest incidence of prostate cancer has been reported in black men followed by Caucasian men and then Asian men. At the moment it is still unclear why black African Caribbean men are at higher risk of developing prostate cancer. However it could be speculated that differences in the expression of some of the biomarkers at different stages of progression may be a driving factor for differences between ethnicities.

Additionally, a future study would also benefit from patient survival data. It could more specifically look at associating some of the biomarkers with disease-free progression, biochemical recurrence/PSA failure rate and metastasis free survival. This would give a more detailed evaluation for the use of the biomarkers as potential prognostic factors.

Lastly, it may also be worth linking disease progression with FASN levels in the blood. This is a relatively new avenue; however several studies have already shown that FASN is detectable in the serum of pancreatic, colorectal, breast, and gastric cancer patients and its levels seem to correlate with stage of progression (Ito et al., 2014; Notarnicola et al., 2012; Walter et al., 2009; Wang et al., 2001).

Chapter 7

Concluding Remarks

Chapter 7 – Concluding remarks

Currently, there is mounting evidence which suggests that FASN is involved in prostate cancer progression, however little is known about the pathways or proteins that act downstream of FASN to drive a more aggressive phenotype in prostate cancer (Menendez and Lupu, 2007). This study focussed on investigating if FASN was involved in regulating proteins that induced actin cytoskeletal changes and cell migration in AR-independent prostate cancer. Firstly, it was demonstrated that the depletion of FASN impaired cell proliferation which confirmed a well-known response to targeting this protein. In addition, FASN is a central protein in metabolism, and silencing its expression led to the generation of metabolically different prostate cancer cell lines. Cell shape has been linked to cell invasiveness and in this study a novel correlation between FASN expression levels and changes in prostate cancer cell shape was observed. Adhesion is also an essential process in cell migration; it was found that FASN knockdown concurrently increased cellular adhesion and the length of paxillin containing adhesions. Additionally, FASN depletion reduced the migratory capability of prostate cancer cells in both 2D migration and 3D invasion assays. The migration defect was also shown to be phenocopied through pharmacological inhibition of FASN. The mechanistic studies of this thesis revealed that RhoU palmitoylation levels were dependent on FASN expression levels. Moreover, the expression of Cdc42 (prenylated isoform) decreased in response to FASN knockdown or inhibition. Further investigation showed that Cdc42 expression levels were dependent on RhoU expression and palmitoylation levels. Following this, it was hypothesized that RhoU and Cdc42 could be interacting partners which was indeed confirmed by Co-IP. To compliment these Lab based findings a pilot patho-epidemiological study was carried out and it was revealed that prostate cancer severity is associated with increased expression levels of FASN, RhoU and Cdc42.

FASN has previously been reported to be important in the migration of several different cancers (Menendez and Lupu, 2007). However, this is the first study to show that the direct silencing of FASN in AR- independent prostate cancer significantly impairs cell migration and invasion. Moreover, the data from this study has revealed

an entirely novel mechanism by which FASN might be driving the migratory phenotype in prostate cancer.

As previously discussed in chapter 5, FASN and palmitate are rarely linked despite the fact palmitate is solely synthesised by FASN (Kuhajda et al., 1994). Palmitate has several important functions in cancer including regulating the attachment of proteins to intracellular membranes through palmitoylation (Aicart-Ramos et al., 2011). In this study it was revealed that the depletion of FASN in prostate cancer leads to a decrease in the palmitoylation of the atypical Rho GTPase RhoU. The silencing of RhoU has been shown to reduce the migratory capacity of PC3 cells, MDA-MB-231 breast cancer cells and NIH 3T3 fibroblast cells (Alinezhad et al., 2016; Dart et al., 2015; Ory et al., 2007). Alternatively, nothing is currently known about how reduced palmitoylation affects RhoU induced cell migration. However, it is known that prevention of this modification does lead to growth and morphology changes in NIH 3T3 fibroblast cells (Berzat et al., 2005). Previously published studies have shown that the blockage of Rac1 and MMP14 palmitoylation significantly reduces migration speed (Anilkumar et al., 2005; Navarro-Lerida et al., 2012). Thus, since RhoU activity at the membrane is entirely dependent on palmitoylation, it would be reasonable to assume that a reduction in its palmitoylation could be having an effect on the migration of FASN depleted prostate cancer cells.

One way prostate cancer cell migration could be affected upon a reduction in RhoU palmitoylation is through paxillin-mediated adhesion turnover. The phosphorylation of paxillin at serine 272 is required for adhesion disassembly (Nayal et al., 2006). Activated paxillin recruits and is sequestered away from adhesions by GIT1, an ARF GTPase-activating protein. Failure of S272 paxillin phosphorylation prevents binding with GIT1 and leads to decreased adhesion turnover and cell migration (Nayal et al., 2006). Here, prostate cancer substrate adhesion and the length of paxillin containing adhesions increased in response to FASN depletion. This mirrors the adhesion defect that has been reported in RhoU silenced breast cancer and fibroblast cells (Dart et al., 2015; Ory et al., 2007). In addition, the length of paxillin containing adhesions was rescued in FASN knockdown prostate cancer cells incubated with palmitate. Thus, it could be speculated that the exogenous palmitate taken up by the cells has been used

to restore RhoU palmitoylation and subsequent paxillin phosphorylation. It is currently unclear how RhoU mediates paxillin phosphorylation, however it has been speculated it could be through PKC, PKA (protein kinase A), PKG (protein kinase G) or myosin light chain kinase (Dart et al., 2015).

In addition to RhoU, this study also identified a second Rho GTPase, Cdc42, as a novel downstream target of FASN. FASN knockdown cells were smaller in size and migrated at a reduced speed when compared to their control counterparts. These same phenotypes have previously been reported in PC3 cells silenced for Cdc42 (Reymond et al., 2012). Upon finding that FASN knockdown and Cdc42 knockdown PC3 cells shared similar phenotypes, Cdc42 levels were probed for in both prostate cell lines used in this study and indeed a decrease was observed. Moreover, Cdc42 re-expression partially rescued the morphological defect seen in FASN knockdown cells confirming it as a target protein partly responsible for this phenotype.

Due to pharmacological inhibition of FASN also decreasing Cdc42 expression, it was speculated that perhaps the palmitoylated splice variant of Cdc42 was being affected as a result of reduced palmitate biosynthesis. However, palmitoylated Cdc42 mRNA was un-detectable in both the 1542 and PC3 cell lines. Therefore this data suggests that in these prostate cell lines the prenylated, and not the palmitoylated, isoform of Cdc42 is being affected in response to the loss of FASN expression or activity.

In chapter 5 it was shown that FASN knockdown led to a decrease in the protein levels of Cdc42, but not the mRNA levels. This indicated that Cdc42 protein levels were decreasing as a result of post-translational targeting. Interestingly, further investigation found that Cdc42 protein levels decreased in RhoU silenced prostate cancer cells. Moreover, global blockage of palmitoylation also decreased Cdc42 expression levels. Thus, from these findings it was hypothesised that perhaps palmitoylated RhoU interacts with Cdc42 to prevent its subsequent degradation. It is not currently known if Rho GTPases can heterodimerize with other Rho GTPases. However, it has been shown that several Rho GTPases including Cdc42, RhoA and Rac1 are able to homodimerize (Zhang and Zheng, 1998). Due to the extensive sequence homology between RhoU and Cdc42 it was speculated that these two proteins could be interacting partners and indeed a Co-IP in chapter 5 confirmed that this was the

case. Further studies will need to be carried out to determine exactly what domains of RhoU are interacting with Cdc42. One possibility is via the carboxyl-terminal polybasic domain that is responsible for Cdc42 homodimerization. RhoU has an extended carboxyl-terminal domain relative to Cdc42. However there is a consensus sequence of amino acids in this region that may mediate the binding of these two proteins due to their highly positively charged surface (Zhang and Zheng, 1998). In addition, unlike Cdc42 homodimerization which negatively regulates the proteins activity, the binding of a different sequence within this domain by RhoU may positively regulate both proteins (Zhang and Zheng, 1998).

The binding of RhoU to prenylated Cdc42 could be mutually increasing the stability of both proteins. Protein palmitoylation promotes a more stable association with the membrane than prenylation, although proteins with dual acylation such as H-Ras demonstrate very strong membrane kinetics (Cadwallader et al., 1994; Peitzsch and McLaughlin, 1993; Shahinian and Silvius, 1995). Moreover, palmitoylated RhoU could also be regulating Cdc42 activation and localisation to different intracellular locations. The addition of palmitate to hepatocellular carcinoma cells has been shown to increase Cdc42 activation (Sharma et al., 2012c). Interestingly, lipid rafts are enriched by GEFs, and have been shown to increase the activation of palmitoylated Rho GTPases such as Rac1 (Moissoglu and Schwartz, 2014). Prenylated proteins have a low affinity for lipid rafts due to the branching of the prenyl groups. However, it has been suggested that perhaps one of the ways that prenylated proteins are capable of targeting to lipid rafts is through their ability to bind palmitoylated proteins (Brown, 2006).

Currently, nothing is known about how particular RhoGTPase may protect other Rho GTPases from protein degradation. However, palmitoylation has been shown to be important in modulating protein stability and degradation (Linder and Deschenes, 2007). Previous studies have observed that blocking palmitoylation in PC3 cells decreases the expression of the proteins EGFR and integrin α6β1 (Bollu et al., 2015; Sharma et al., 2012b). Similarly in DU145 cells, inhibition of palmitoylation has been shown to lead to a loss in the total levels of c-Met, EGFR and the integrin subunit β4 (Coleman et al., 2009; Coleman et al., 2016). The role of palmitoylation in regulating

Rho GTPase stability has not been extensively researched. Interestingly, the current studies suggest that palmitoylation may affect certain Rho GTPases differently. Blocking palmitoylation does not lead to Rac1 or RhoU degradation, but severely affects their stability (Berzat et al., 2005; Navarro-Lerida et al., 2012). Conversely, palmitoylation has been shown to be required for rapid lysosomal degradation of RhoB (Perez-Sala et al., 2009). Further studies will need to be carried out to determine how palmitoylated RhoU protects Cdc42 from proteasome degradation. One of the current difficulties with this at the moment is that the exact mechanism of Cdc42 degradation has not been well studied. One study has shown that cullin-1 (CUL1), a core component of multiple cullin-RING-SCF (S phase kinase associated protein 1 (SKP1)-CUL1-F-box protein) ubiquitin ligase complexes, binds Cdc42 (Senadheera et al., 2001; Skaar et al., 2013). This interaction is believed to depend on subcellular localisation as it has been shown that Rac3 association and proteasomal degradation via CUL1 seems to specifically occur at the perinuclear region (Senadheera et al., 2001). Thus, it could be speculated that the binding of palmitoylated RhoU sequesters Cdc42 to different intracellular compartments away from ubiquitin ligases such as CUL1 that target it for degradation.

Upon finding that FASN, RhoU and Cdc42 were linked in prostate cancer cell migration *in vitro*, it was decided to further investigate these proteins in a clinical setting. In chapter 6, a pilot patho-epidemiology study was carried out using tissue from a cohort of 85 men who underwent a radical prostatectomy. Immunohistochemical staining revealed that the increased expression of FASN, RhoU and Cdc42 associated with prostate cancer severity. This is the first study to show that the Rho GTPases RhoU and Cdc42 are potential biomarkers at the protein level for prostate cancer status. Moreover, the findings of this patho-epi study concur with the lab based findings and together suggest a role for FASN, RhoU and Cdc42 in prostate cancer. They also add to the current evidence in the literature which suggests FASN is worth targeting in patients with more aggressive disease in addition to the early stages of cancer (Flavin et al., 2011). Currently, one FASN inhibitor, named TVB-2640, has become the first oral, selective, and reversible FASN inhibitor to be tested clinically. Two separate phase I studies in breast cancer and non-small cell lung cancer have shown favourable results with a median increase in patient disease-free survival and overall survival

whilst taking TVB-2640 alone, and in combination with other chemotherapeutic drugs (Brenner et al., 2017; O'Farrell et al., 2016).

Currently a clinical trial is being undertaken in the UK assessing TVB-2640 effectiveness in several solid tumour types including breast, ovarian, prostate, colon, pancreatic and non-Hodgkins Lymphoma (ClincalTrials.gov: NCT02223247). Promising results from these trails could make the FASN inhibitor TVB-2640 a common combination therapy drug and encourage its use during the early stages of cancer development.

In conclusion the findings from this thesis propose a novel model whereby FASN is responsible for the palmitoylation of RhoU which is then capable of binding Cdc42, preventing its degradation. This allows for un-perturbed downstream signalling from both of the Rho GTPases initiating proper cell spreading, adhesion turnover, and cell migration (**Figure 7.1**).

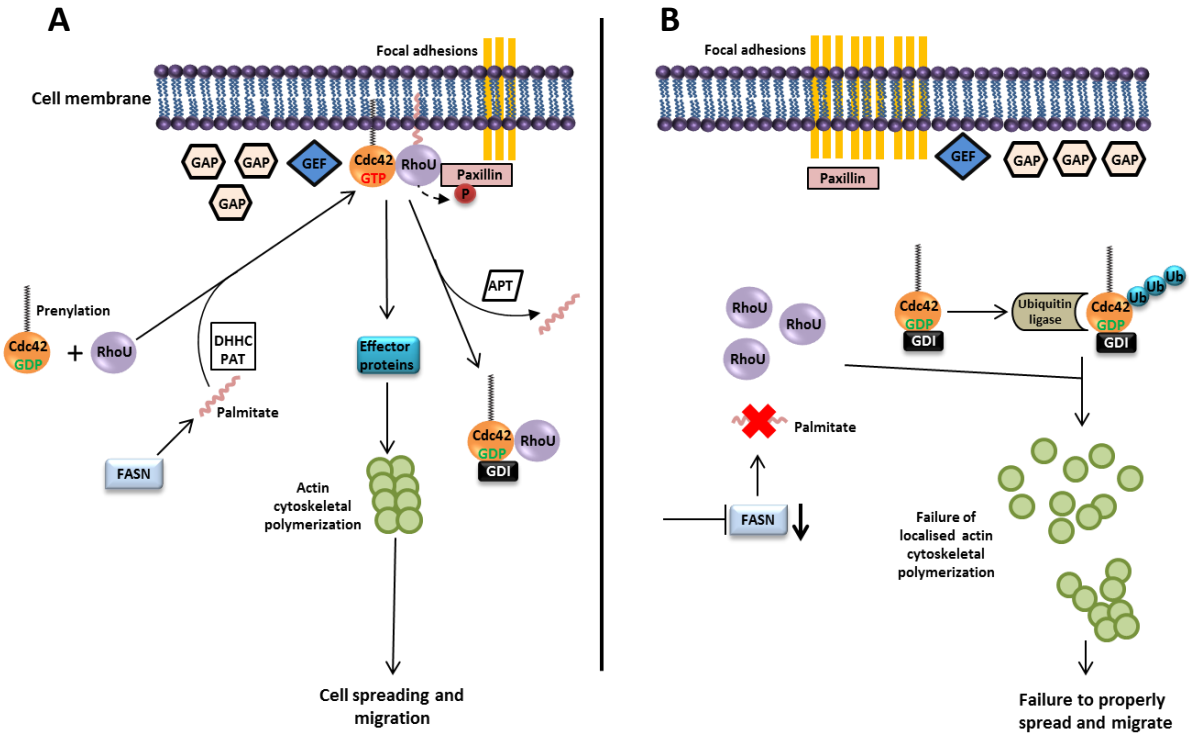

Figure 7.1 A proposed model for the role of FASN and its downstream targets RhoU and Cdc42 in prostate cancer cell migration: **A**) FASN synthesises palmitate which is used in the palmitoylation of RhoU via DHHC PATs. Palmitoylated RhoU binds prenylated Cdc42 and both proteins tether to the cell membrane where Cdc42 can be activated by GEFs. Here, Cdc42 and RhoU signal and activate downstream effector proteins which induce changes in the actin cytoskeleton. RhoU is also involved in mediating the turnover of focal adhesions through paxillin phosphorylation. These signalling events allow for unperturbed cell spreading and migration in prostate cancer. The palmitate moiety can also be removed from RhoU via APTs which would allow it and Cdc42 to dynamically localise to different subcellular locations. **B**) In a FASN knockdown or inhibited cell, palmitate synthesis is severely diminished abolishing RhoU palmitoylation which leads to its cytosolic accumulation. Palmitoylated RhoU is no longer able to sequester Cdc42 away from the ubiquitin ligases which lead to it being targeted for degradation. Moreover, the prevention of RhoU palmitoylation leads to a decrease in paxillin phosphorylation which impedes focal adhesion turnover. Perturbed RhoU and Cdc42 signalling as a result of targeting FASN activity abolishes proper cell spreading and migration. Proteins that don't directly act on a target are represented by dashed arrows.

References

ACS. 2016. American Cancer Society.*Survival Rates for Prostate Cancer* [Online]. America: American Cancer Society, 2016 [Viewed 30 January 2017] Available from:https://www.cancer.org/cancer/prostate-cancer/detection-diagnosis-staging/survival-rates.html#references.

Afshar, M., F. Evison, N.D. James, and P. Patel. 2015. Shifting paradigms in the estimation of survival for castration-resistant prostate cancer: A tertiary academic center experience. *Urol Oncol*. 33:338.e331-337.

Agostini, M., L.Y. Almeida, D.C. Bastos, R.M. Ortega, F.S. Moreira, F. Seguin, K.G. Zecchin, H.F. Raposo, H.C. Oliveira, N.D. Amoedo, T. Salo, R.D. Coletta, and E. Graner. 2014. The fatty acid synthase inhibitor orlistat reduces the growth and metastasis of orthotopic tongue oral squamous cell carcinomas. *Molecular cancer therapeutics*. 13:585-595.

Aicart-Ramos, C., R.A. Valero, and I. Rodriguez-Crespo. 2011. Protein palmitoylation and subcellular trafficking. *Biochimica et biophysica acta*. 1808:2981-2994.

Akin, O., E. Sala, C.S. Moskowitz, K. Kuroiwa, N.M. Ishill, D. Pucar, P.T. Scardino, and H. Hricak. 2006. Transition zone prostate cancers: features, detection, localization, and staging at endorectal MR imaging. *Radiology*. 239:784-792.

Al-Mahdi, R., N. Babteen, K. Thillai, M. Holt, B. Johansen, H.L. Wetting, O.M. Seternes, and C.M. Wells. 2015. A novel role for atypical MAPK kinase ERK3 in regulating breast cancer cell morphology and migration. *Cell Adh Migr*. 9:483-494.

Alan, J.K., A.C. Berzat, B.J. Dewar, L.M. Graves, and A.D. Cox. 2010. Regulation of the Rho Family Small GTPase Wrch-1/RhoU by C-Terminal Tyrosine Phosphorylation Requires Src. *Molecular and cellular biology*. 30:4324-4338.

Alfarouk, K.O., D. Verduzco, C. Rauch, A.K. Muddathir, H.H.B. Adil, G.O. Elhassan, M.E. Ibrahim, J. David Polo Orozco, R.A. Cardone, S.J. Reshkin, and S. Harguindey. 2014. Glycolysis, tumor metabolism, cancer growth and dissemination. A new pH-based etiopathogenic perspective and therapeutic approach to an old cancer question. *Oncoscience*. 1:777-802.

Alinezhad, S., R.M. Vaananen, J. Mattsson, Y. Li, T. Tallgren, N. Tong Ochoa, A. Bjartell, M. Akerfelt, P. Taimen, P.J. Bostrom, K. Pettersson, and M. Nees. 2016. Validation of Novel Biomarkers for Prostate Cancer Progression by the Combination of Bioinformatics, Clinical and Functional Studies. *PloS one*. 11:e0155901.

Alizadeh, A.M., S. Shiri, and S. Farsinejad. 2014. Metastasis review: from bench to bedside. *Tumour biology : the journal of the International Society for Oncodevelopmental Biology and Medicine*. 35:8483-8523.

Alo, P.L., M. Amini, F. Piro, L. Pizzuti, V. Sebastiani, C. Botti, R. Murari, G. Zotti, and U. Di Tondo. 2007. Immunohistochemical expression and prognostic significance of fatty acid synthase in pancreatic carcinoma. *Anticancer research*. 27:2523-2527.

Anderson, A.M., and M.A. Ragan. 2016. Palmitoylation: a protein S-acylation with implications for breast cancer. *Npj Breast Cancer*. 2:16028-16038.

Anderson, S.M., M.C. Rudolph, J.L. McManaman, and M.C. Neville. 2007. Key stages in mammary gland development. Secretory activation in the mammary gland: it's not just about milk protein synthesis! *Breast Cancer Research*. 9:204-218.

Anilkumar, N., T. Uekita, J.R. Couchman, H. Nagase, M. Seiki, and Y. Itoh. 2005. Palmitoylation at Cys574 is essential for MT1-MMP to promote cell migration. *FASEB journal : official publication of the Federation of American Societies for Experimental Biology*. 19:1326-1328.

Armstrong, A.J., M.S. Marengo, S. Oltean, G. Kemeny, R.L. Bitting, J.D. Turnbull, C.I. Herold, P.K. Marcom, D.J. George, and M.A. Garcia-Blanco. 2011. Circulating tumor cells from patients with advanced prostate and breast cancer display both epithelial and mesenchymal markers. *Molecular cancer research*. 9:997-1007.

Aspenstrom, P., A. Ruusala, and D. Pacholsky. 2007. Taking Rho GTPases to the next level: the cellular functions of atypical Rho GTPases. *Experimental cell research*. 313:3673-3679.

Ayala, A.G., and J.Y. Ro. 2007. Prostatic intraepithelial neoplasia: recent advances. *Archives of pathology & laboratory medicine*. 131:1257-1266.

Azrad, M., C. Turgeon, and W. Demark-Wahnefried. 2013. Current evidence linking polyunsaturated Fatty acids with cancer risk and progression. *Front Oncol*. 3:224-236.

Baenke, F., B. Peck, H. Miess, and A. Schulze. 2013. Hooked on fat: the role of lipid synthesis in cancer metabolism and tumour development. *Disease models & mechanisms*. 6:1353-1363.

Baldwin, T., A. Sakthianandeswaren, J.M. Curtis, B. Kumar, G.K. Smyth, S.J. Foote, and E. Handman. 2007. Wound healing response is a major contributor to the severity of cutaneous leishmaniasis in the ear model of infection. *Parasite immunology*. 29:501-513.

Bandyopadhyay, S., R. Zhan, Y. Wang, S.K. Pai, S. Hirota, S. Hosobe, Y. Takano, K. Saito, E. Furuta, M. Iiizumi, S. Mohinta, M. Watabe, C. Chalfant, and K. Watabe. 2006. Mechanism of apoptosis induced by the inhibition of fatty acid synthase in breast cancer cells. *Cancer research*. 66:5934-5940.

Banyard, J., I. Chung, M. Migliozzi, D.T. Phan, A.M. Wilson, B.R. Zetter, and D.R. Bielenberg. 2014. Identification of genes regulating migration and invasion using a new model of metastatic prostate cancer. *BMC cancer*. 14:387-402.

Barron, D.A., and D.R. Rowley. 2012. The reactive stroma microenvironment and prostate cancer progression. *Endocrine-related cancer*. 19:R187-204.

Bastos, D.C., J. Paupert, C. Maillard, F. Seguin, M.A. Carvalho, M. Agostini, R.D. Coletta, A. Noel, and E. Graner. 2016. Effects of fatty acid synthase inhibitors on lymphatic vessels: an in vitro and in vivo study in a melanoma model. *Laboratory investigation; a journal of technical methods and pathology*. 97:194-206.

Bellis, S.L., J.T. Miller, and C.E. Turner. 1995. Characterization of tyrosine phosphorylation of paxillin in vitro by focal adhesion kinase. *The Journal of biological chemistry*. 270:17437-17441.

Benjamin, D.I., D.S. Li, W. Lowe, T. Heuer, G. Kemble, and D.K. Nomura. 2015. Diacylglycerol Metabolism and Signaling Is a Driving Force Underlying FASN Inhibitor Sensitivity in Cancer Cells. *ACS chemical biology*. 10:1616-1623.

Berney, D.M., A. Gopalan, S. Kudahetti, G. Fisher, L. Ambroisine, C.S. Foster, V. Reuter, J. Eastham, H. Moller, M.W. Kattan, W. Gerald, C. Cooper, P. Scardino, and J. Cuzick. 2009. Ki-67 and outcome in clinically localised prostate cancer: analysis of conservatively treated prostate cancer patients from the Trans-Atlantic Prostate Group study. *British journal of cancer*. 100:888-893.

Berthold, J., K. Schenková, S. Ramos, Y. Miura, M. Furukawa, P. Aspenström, and F. Rivero. 2008. Characterization of RhoBTB-dependent Cul3 ubiquitin ligase complexes – Evidence for an autoregulatory mechanism. *Experimental cell research*. 314:3453-3465.

Berzat, A.C., J.E. Buss, E.J. Chenette, C.A. Weinbaum, A. Shutes, C.J. Der, A. Minden, and A.D. Cox. 2005. Transforming activity of the Rho family GTPase, Wrch-1, a Wnt-regulated Cdc42 homolog, is dependent on a novel carboxyl-terminal palmitoylation motif. *The Journal of biological chemistry*. 280:33055-33065.

Bhavsar, A., and S. Verma. 2014. Anatomic Imaging of the Prostate. *BioMed Research International*. 2014:1-9.

Bhavsar, P.J., E. Infante, A. Khwaja, and A.J. Ridley. 2013. Analysis of Rho GTPase expression in T-ALL identifies RhoU as a target for Notch involved in T-ALL cell migration. *Oncogene*. 32:198-208.

Black, A.R., and J.D. Black. 2012. Protein kinase C signaling and cell cycle regulation. *Frontiers in Immunology*. 3:423.

Blancafort, A., A. Giro-Perafita, G. Oliveras, S. Palomeras, C. Turrado, O. Campuzano, D. Carrion-Salip, A. Massaguer, R. Brugada, M. Palafox, J. Gomez-Miragaya, E. Gonzalez-Suarez, and T. Puig. 2015. Dual fatty acid synthase and HER2 signaling blockade shows marked antitumor activity against breast cancer models resistant to anti-HER2 drugs. *PloS one*. 10:e0131241.

Blaskovic, S., M. Blanc, and F.G. van der Goot. 2013. What does S-palmitoylation do to membrane proteins? *The FEBS journal*. 280:2766-2774.

Blom, M., K. Reis, J. Heldin, J. Kreuger, and P. Aspenstrom. 2017. The atypical Rho GTPase RhoD is a regulator of actin cytoskeleton dynamics and directed cell migration. *Experimental cell research*. 352:255-264.

Bollu, L.R., R.R. Katreddy, A.M. Blessing, N. Pham, B. Zheng, X. Wu, and Z. Weihua. 2015. Intracellular activation of EGFR by fatty acid synthase dependent palmitoylation. *Oncotarget*. 6:34992-35003.

Bonkhoff, H., U. Stein, and K. Remberger. 1994. The proliferative function of basal cells in the normal and hyperplastic human prostate. *Prostate*. 24:114-118.

Brandt, B., R. Junker, C. Griwatz, S. Heidl, O. Brinkmann, A. Semjonow, G. Assmann, and K.S. Zanker. 1996. Isolation of prostate-derived single cells and cell clusters from human peripheral blood. *Cancer research*. 56:4556-4561.

Brazier, H., G. Pawlak, V. Vives, and A. Blangy. 2009. The Rho GTPase Wrch1 regulates osteoclast precursor adhesion and migration. *The international journal of biochemistry & cell biology*. 41:1391-1401.

Brenner, A.J., G. Falchook, M. Patel, J.R. Infante, H.T. Arkenau, E.M. Dean, E. Borazanci, J.S. Lopez, K. Moore, P. Schmid, A.E. Frankel, S. Jones, W. McCulloch, G. Kemble, K. Grimmer, and H. Burris. 2017. Abstract P6-11-09: Heavily pre-treated breast cancer patients show promising responses in the first in human study of the first-In-class fatty acid synthase (FASN) inhibitor, TVB-2640 in combination with paclitaxel. *Cancer research*. 77:P6-11-09.

Bright, R.K., C.D. Vocke, M.R. Emmert-Buck, P.H. Duray, D. Solomon, P. Fetsch, J.S. Rhim, W.M. Linehan, and S.L. Topalian. 1997. Generation and genetic characterization of immortal human prostate epithelial cell lines derived from primary cancer specimens. *Cancer research*. 57:995-1002.

Brown, D.A. 2006. Lipid rafts, detergent-resistant membranes, and raft targeting signals. *Physiology (Bethesda, Md.)*. 21:430-439.

Byrne, K.M., N. Monsefi, J.C. Dawson, A. Degasperi, J.C. Bukowski-Wills, N. Volinsky, M. Dobrzynski, M.R. Birtwistle, M.A. Tsyganov, A. Kiyatkin, K. Kida, A.J. Finch, N.O. Carragher, W. Kolch, L.K. Nguyen, A. von Kriegsheim, and B.N. Kholodenko. 2016. Bistability in the Rac1, PAK, and RhoA Signaling Network Drives Actin Cytoskeleton Dynamics and Cell Motility Switches. *Cell systems*. 2:38-48.

Cadwallader, K.A., H. Paterson, S.G. Macdonald, and J.F. Hancock. 1994. N-terminally myristoylated Ras proteins require palmitoylation or a polybasic domain for plasma membrane localization. *Molecular and cellular biology*. 14:4722-4730.

Cairns, R.A., I.S. Harris, and T.W. Mak. 2011. Regulation of cancer cell metabolism. *Nature reviews. Cancer*. 11:85-95.

Camassei, F.D., R. Cozza, A. Acquaviva, A. Jenkner, L. Rava, R. Gareri, A. Donfrancesco, C. Bosman, P. Vadala, T. Hadjistilianou, and R. Boldrini. 2003a. Expression of the lipogenic enzyme fatty acid synthase (FAS) in retinoblastoma and its correlation with tumor aggressiveness. *Investigative ophthalmology & visual science*. 44:2399-2403.

Camassei, F.D., A. Jenkner, L. Rava, C. Bosman, P. Francalanci, A. Donfrancesco, P.L. Alo, and R. Boldrini. 2003b. Expression of the lipogenic enzyme fatty acid synthase (FAS) as a predictor of poor outcome in nephroblastoma: an interinstitutional study. *Medical and pediatric oncology*. 40:302-308.

Cao, H.H., C.Y. Cheng, T. Su, X.Q. Fu, H. Guo, T. Li, A.K. Tse, H.Y. Kwan, H. Yu, and Z.L. Yu. 2015. Quercetin inhibits HGF/c-Met signaling and HGF-stimulated melanoma cell migration and invasion. *Molecular cancer*. 14:103.

Caraglia, M., D. Santini, M. Marra, B. Vincenzi, G. Tonini, and A. Budillon. 2006. Emerging anti-cancer molecular mechanisms of aminobisphosphonates. *Endocrine-related cancer*. 13:7-26.

Cau, J., and A. Hall. 2005. Cdc42 controls the polarity of the actin and microtubule cytoskeletons through two distinct signal transduction pathways. *Journal of cell science*. 118:2579-2587.

Cerne, D., I.P. Zitnik, and M. Sok. 2010. Increased fatty acid synthase activity in non-small cell lung cancer tissue is a weaker predictor of shorter patient survival than increased lipoprotein lipase activity. *Archives of medical research*. 41:405-409.

Chakraborty, S., and T. Rahman. 2012. The difficulties in cancer treatment. *Ecancermedicalscience*. 6:ed16.

Chambers, A.F., A.C. Groom, and I.C. MacDonald. 2002. Dissemination and growth of cancer cells in metastatic sites. *Nature reviews. Cancer*. 2:563-572.

Chang, L., P. Wu, R. Senthilkumar, X. Tian, H. Liu, X. Shen, Z. Tao, and P. Huang. 2016. Loss of fatty acid synthase suppresses the malignant phenotype of colorectal cancer cells by down-regulating energy metabolism and mTOR signaling pathway. *Journal of cancer research and clinical oncology*. 142:59-72.

Chang, R.T., R. Kirby, and B.J. Challacombe. 2012. Is there a link between BPH and prostate cancer? *The Practitioner*. 256:13-62.

Chao, Y., Q. Wu, M. Acquafondata, R. Dhir, and A. Wells. 2012. Partial Mesenchymal to Epithelial Reverting Transition in Breast and Prostate Cancer Metastases. *Cancer Microenvironment*. 5:19-28.

Chen, H.W., Y.F. Chang, H.Y. Chuang, W.T. Tai, and J.J. Hwang. 2012. Targeted therapy with fatty acid synthase inhibitors in a human prostate carcinoma LNCaP/tk-luc-bearing animal model. *Prostate cancer and prostatic diseases*. 15:260-264.

Chen, J.S., Q. Wang, X.H. Fu, X.H. Huang, X.L. Chen, L.Q. Cao, L.Z. Chen, H.X. Tan, W. Li, J. Bi, and L.J. Zhang. 2009. Involvement of PI3K/PTEN/AKT/mTOR pathway in invasion and metastasis in hepatocellular carcinoma: Association with MMP-9. *Hepatology research : the official journal of the Japan Society of Hepatology*. 39:177-186.

Chen, N., and Q. Zhou. 2016. The evolving Gleason grading system. *Chinese journal of cancer research = Chung-kuo yen cheng yen chiu*. 28:58-64.

Cheng, J., R.P. Ondracek, D.C. Mehedint, K.A. Kasza, B. Xu, S. Gill, G. Azabdaftari, S. Yao, C.D. Morrison, J.L. Mohler, and J.R. Marshall. 2015. Association of Fatty Acid Synthase Polymorphisms and Expression with Outcomes after Radical Prostatectomy. *Prostate cancer and prostatic diseases*. 18:182-189.

Chirala, S.S., H. Chang, M. Matzuk, L. Abu-Elheiga, J. Mao, K. Mahon, M. Finegold, and S.J. Wakil. 2003. Fatty acid synthesis is essential in embryonic development: Fatty acid synthase null mutants and most of the heterozygotes die in utero. *Proceedings of the National Academy of Sciences of the United States of America*. 100:6358-6363.

Chirala, S.S., A. Jayakumar, Z.W. Gu, and S.J. Wakil. 2001. Human fatty acid synthase: role of interdomain in the formation of catalytically active synthase dimer. *Proceedings of the National Academy of Sciences of the United States of America*. 98:3104-3108.

Chirala, S.S., and S.J. Wakil. 2004. Structure and function of animal fatty acid synthase. *Lipids*. 39:1045-1053.

Choi, W.I., B.N. Jeon, H. Park, J.Y. Yoo, Y.S. Kim, D.I. Koh, M.H. Kim, Y.R. Kim, C.E. Lee, K.S. Kim, T.F. Osborne, and M.W. Hur. 2008. Proto-oncogene FBI-1 (Pokemon) and SREBP-1 synergistically activate transcription of fatty-acid synthase gene (FASN). *The Journal of biological chemistry*. 283:29341-29354.

Choma, D.P., K. Pumiglia, and C.M. DiPersio. 2004. Integrin alpha3beta1 directs the stabilization of a polarized lamellipodium in epithelial cells through activation of Rac1. *Journal of cell science*. 117:3947-3959.

Chrisofos, M., A.G. Papatsoris, A. Lazaris, and C. Deliveliotis. 2007. Precursor lesions of prostate cancer. *Critical reviews in clinical laboratory sciences*. 44:243-270.

Chuang, Y.Y., A. Valster, S.J. Coniglio, J.M. Backer, and M. Symons. 2007. The atypical Rho family GTPase Wrch-1 regulates focal adhesion formation and cell migration. *Journal of cell science*. 120:1927-1934.

Clark, A.G., and D.M. Vignjevic. 2015. Modes of cancer cell invasion and the role of the microenvironment. *Current opinion in cell biology*. 36:13-22.

Coleman, D.T., R. Bigelow, and J.A. Cardelli. 2009. Inhibition of fatty acid synthase by luteolin post-transcriptionally down-regulates c-Met expression independent of proteosomal/lysosomal degradation. *Molecular cancer therapeutics*. 8:214-224.

Coleman, D.T., A.L. Gray, S.J. Kridel, and J.A. Cardelli. 2016. Palmitoylation regulates the intracellular trafficking and stability of c-Met. *Oncotarget*. 7:32664-32677.

Cooper, J.A., and D. Sept. 2008. New insights into mechanism and regulation of actin capping protein. *International review of cell and molecular biology*. 267:183-206.

Corominas-Faja, B., L. Vellon, E. Cuyas, M. Buxo, B. Martin-Castillo, D. Serra, J. Garcia, R. Lupu, and J.A. Menendez. 2017. Clinical and therapeutic relevance of the metabolic oncogene fatty acid synthase in HER2+ breast cancer. *Histology and histopathology*. 32:687-698.

Corvi, M.M., C.L. Soltys, and L.G. Berthiaume. 2001. Regulation of mitochondrial carbamoyl-phosphate synthetase 1 activity by active site fatty acylation. *The Journal of biological chemistry*. 276:45704-45712.

Cui, Y., and S. Yamada. 2013. N-cadherin dependent collective cell invasion of prostate cancer cells is regulated by the N-terminus of alpha-catenin. *PloS one*. 8:e55069.

Cunningham, D., and Z. You. 2015. In vitro and in vivo model systems used in prostate cancer research. *Journal of biological methods*. 2:1-14.

Curran, P.J., K. Obeidat, and D. Losardo. 2010. Twelve Frequently Asked Questions About Growth Curve Modeling. *Journal of cognition and development : official journal of the Cognitive Development Society*. 11:121-136.

Currie, E., A. Schulze, R. Zechner, T.C. Walther, and R.V. Farese, Jr. 2013. Cellular fatty acid metabolism and cancer. *Cell metabolism*. 18:153-161.

Daker, M., M. Ahmad, and A.S. Khoo. 2012. Quercetin-induced inhibition and synergistic activity with cisplatin - a chemotherapeutic strategy for nasopharyngeal carcinoma cells. *Cancer cell international*. 12:34.

Danilova, O.V., L.J. Dumont, N.B. Levy, F. Lansigan, W.B. Kinlaw, A.V. Danilov, and P. Kaur. 2013. FASN and CD36 predict survival in rituximab-treated diffuse large B-cell lymphoma. *Journal of hematopathology*. 6:11-18.

Dart, A.E., G.M. Box, W. Court, M.E. Gale, J.P. Brown, S.E. Pinder, S.A. Eccles, and C.M. Wells. 2015. PAK4 promotes kinase-independent stabilization of RhoU to modulate cell adhesion. *The Journal of cell biology*. 211:863-879.

Dasgupta, S., S. Srinidhi, and J.K. Vishwanatha. 2012. Oncogenic activation in prostate cancer progression and metastasis: Molecular insights and future challenges. *Journal of carcinogenesis*. 11:4.

Day, K.C., G.L. Hiles, M. Kozminsky, S.J. Dawsey, A. Paul, L.J. Broses, R. Shah, L.P. Kunja, C. Hall, N. Palanisamy, S. Daignault-Newton, L. El-Sawy, S.J. Wilson, A. Chou, K.W. Ignatoski, E. Keller, D. Thomas, S. Nagrath, T. Morgan, and M.L. Day. 2017. HER2 and EGFR Overexpression Support Metastatic Progression of Prostate Cancer to Bone. *Cancer research*. 77:74-85.

De Marzo, A.M., E.A. Platz, S. Sutcliffe, J. Xu, H. Gronberg, C.G. Drake, Y. Nakai, W.B. Isaacs, and W.G. Nelson. 2007. Inflammation in prostate carcinogenesis. *Nature reviews. Cancer*. 7:256-269.

De Schrijver, E., K. Brusselmans, W. Heyns, G. Verhoeven, and J.V. Swinnen. 2003. RNA interference-mediated silencing of the fatty acid synthase gene attenuates growth and induces morphological changes and apoptosis of LNCaP prostate cancer cells. *Cancer research*. 63:3799-3804.

Deepa, P.R., S. Vandhana, U. Jayanthi, and S. Krishnakumar. 2012. Therapeutic and toxicologic evaluation of anti-lipogenic agents in cancer cells compared with non-neoplastic cells. *Basic & clinical pharmacology & toxicology*. 110:494-503.

Deepa, P.R., S. Vandhana, and S. Krishnakumar. 2013. Fatty acid synthase inhibition induces differential expression of genes involved in apoptosis and cell proliferation in ocular cancer cells. *Nutrition and cancer*. 65:311-316.

DerMardirossian, C., and G.M. Bokoch. 2005. GDIs: central regulatory molecules in Rho GTPase activation. *Trends in cell biology*. 15:356-363.

Dhanasekaran, A., S.K. Gruenloh, J.N. Buonaccorsi, R. Zhang, G.J. Gross, J.R. Falck, P.K. Patel, E.R. Jacobs, and M. Medhora. 2008. Multiple antiapoptotic targets of the PI3K/Akt survival pathway are activated by epoxyeicosatrienoic acids to protect cardiomyocytes from hypoxia/anoxia. *American journal of physiology. Heart and circulatory physiology*. 294:H724-735.

Di, J., H. Huang, D. Qu, J. Tang, W. Cao, Z. Lu, Q. Cheng, J. Yang, J. Bai, Y. Zhang, and J. Zheng. 2015a. Rap2B promotes proliferation, migration, and invasion of human breast cancer through calcium-related ERK1/2 signaling pathway. *Scientific reports*. 5:12363.

Di, J., H. Huang, Y. Wang, D. Qu, J. Tang, Q. Cheng, Z. Lu, Y. Zhang, and J. Zheng. 2015b. p53 target gene Rap2B regulates the cytoskeleton and inhibits cell spreading. *Journal of cancer research and clinical oncology*. 141:1791-1798.

Di Vizio, D., R.M. Adam, J. Kim, R. Kim, F. Sotgia, T. Williams, F. Demichelis, K.R. Solomon, M. Loda, M.A. Rubin, M.P. Lisanti, and M.R. Freeman. 2008. Caveolin-1 interacts with a lipid raft-associated population of fatty acid synthase. *Cell Cycle*. 7:2257-2267.

Dowal, L., W. Yang, M.R. Freeman, H. Steen, and R. Flaumenhaft. 2011. Proteomic analysis of palmitoylated platelet proteins. *Blood*. 118:e62-e73.

Doye, A., A. Mettouchi, G. Bossis, R. Clement, C. Buisson-Touati, G. Flatau, L. Gagnoux, M. Piechaczyk, P. Boquet, and E. Lemichez. 2002. CNF1 exploits the ubiquitin-proteasome machinery to restrict Rho GTPase activation for bacterial host cell invasion. *Cell*. 111:553-564.

Doyle, A.D., N. Carvajal, and A. Jin. 2015. Local 3D matrix microenvironment regulates cell migration through spatiotemporal dynamics of contractility-dependent adhesions. 6:8720.

Drisdel, R.C., J.K. Alexander, A. Sayeed, and W.N. Green. 2006. Assays of protein palmitoylation. *Methods (San Diego, Calif.)*. 40:127-134.

Duijvesz, D., K.E. Burnum-Johnson, M.A. Gritsenko, A.M. Hoogland, M.S. Vredenbregt-van den Berg, R. Willemsen, T. Luider, L. Pasa-Tolic, and G. Jenster. 2013. Proteomic profiling of exosomes leads to the identification of novel biomarkers for prostate cancer. *PloS one*. 8:e82589.

Ellerbroek, S.M., and M.S. Stack. 1999. Membrane associated matrix metalloproteinases in metastasis. *BioEssays : news and reviews in molecular, cellular and developmental biology*. 21:940-949.

Epstein, J.I., M. Carmichael, and A.W. Partin. 1995. OA-519 (fatty acid synthase) as an independent predictor of pathologic state in adenocarcinoma of the prostate. *Urology*. 45:81-86.

Faure, S., and P. Fort. 2011. Atypical RhoV and RhoU GTPases control development of the neural crest. *Small GTPases*. 2:310-313.

Feldman, B.J., and D. Feldman. 2001. The development of androgen-independent prostate cancer. *Nature reviews. Cancer*. 1:34-45.

Felgueiras, J., J.V. Silva, and M. Fardilha. 2014. Prostate cancer: the need for biomarkers and new therapeutic targets. *Journal of Zhejiang University. Science. B*. 15:16-42.

Felsenfeld, D.P., P.L. Schwartzberg, A. Venegas, R. Tse, and M.P. Sheetz. 1999. Selective regulation of integrin--cytoskeleton interactions by the tyrosine kinase Src. *Nat Cell Biol*. 1:200-206.

Fernandez-Murray, J.P., and C.R. McMaster. 2005. Glycerophosphocholine catabolism as a new route for choline formation for phosphatidylcholine synthesis by the Kennedy pathway. *The Journal of biological chemistry*. 280:38290-38296.

Fiorentino, M., G. Zadra, E. Palescandolo, G. Fedele, D. Bailey, C. Fiore, P.L. Nguyen, T. Migita, R. Zamponi, D. Di Vizio, C. Priolo, C. Sharma, W. Xie, M.E. Hemler, L. Mucci, E. Giovannucci, S. Finn, and M. Loda. 2008. Overexpression of fatty acid synthase is associated with palmitoylation of Wnt1 and cytoplasmic stabilization of beta-catenin in prostate cancer. *Laboratory investigation; a journal of technical methods and pathology*. 88:1340-1348.

Fischer, K.R., A. Durrans, S. Lee, J. Sheng, F. Li, S.T. Wong, H. Choi, T. El Rayes, S. Ryu, J. Troeger, R.F. Schwabe, L.T. Vahdat, N.K. Altorki, V. Mittal, and D. Gao. 2015. Epithelial-to-mesenchymal transition is not required for lung metastasis but contributes to chemoresistance. *Nature*. 527:472-476.

Fisher, G., Z.H. Yang, S. Kudahetti, H. Møller, P. Scardino, J. Cuzick, and D.M. Berney. 2013. Prognostic value of Ki-67 for prostate cancer death in a conservatively managed cohort. *British journal of cancer*. 108:271-277.

Flavin, R., S. Peluso, P.L. Nguyen, and M. Loda. 2010. Fatty acid synthase as a potential therapeutic target in cancer. *Future oncology (London, England)*. 6:551-562.

Flavin, R., G. Zadra, and M. Loda. 2011. Metabolic alterations and targeted therapies in prostate cancer. *The Journal of pathology*. 223:283-294.

Fort, P., L. Guemar, E. Vignal, N. Morin, C. Notarnicola, P. de Santa Barbara, and S. Faure. 2011. Activity of the RhoU/Wrch1 GTPase is critical for cranial neural crest cell migration. *Developmental biology*. 350:451-463.

Fransson, A., A. Ruusala, and P. Aspenstrom. 2003. Atypical Rho GTPases have roles in mitochondrial homeostasis and apoptosis. *The Journal of biological chemistry*. 278:6495-6502.

Friedl, P., and S. Alexander. 2011. Cancer invasion and the microenvironment: plasticity and reciprocity. *Cell*. 147:992-1009.

Friedl, P., and K. Wolf. 2003. Tumour-cell invasion and migration: diversity and escape mechanisms. *Nature reviews. Cancer*. 3:362-374.

Friedl, P., and K. Wolf. 2009. Proteolytic interstitial cell migration: a five-step process. *Cancer metastasis reviews*. 28:129-135.

Fukuda, H., N. Iritani, T. Sugimoto, and H. Ikeda. 1999. Transcriptional regulation of fatty acid synthase gene by insulin/glucose, polyunsaturated fatty acid and leptin in hepatocytes and adipocytes in normal and genetically obese rats. *Eur J Biochem*. 260:505-511.

Gabrielson, E.W., M.L. Pinn, J.R. Testa, and F.P. Kuhajda. 2001. Increased fatty acid synthase is a therapeutic target in mesothelioma. *Clinical cancer research : an official journal of the American Association for Cancer Research*. 7:153-157.

Gad, A.K., V. Nehru, A. Ruusala, and P. Aspenstrom. 2012. RhoD regulates cytoskeletal dynamics via the actin nucleation-promoting factor WASp homologue associated with actin Golgi membranes and microtubules. *Molecular biology of the cell*. 23:4807-4819.

Gansler, T.S., W. Hardman, 3rd, D.A. Hunt, S. Schaffel, and R.A. Hennigar. 1997. Increased expression of fatty acid synthase (OA-519) in ovarian neoplasms predicts shorter survival. *Human pathology*. 28:686-692.

Gao, M., L. Liu, S. Li, X. Zhang, Z. Chang, and M. Zhang. 2015. Inhibition of cell proliferation and metastasis of human hepatocellular carcinoma by miR-137 is regulated by CDC42. *Oncology reports*. 34:2523-2532.

Georgiadou, M., J. Lilja, and G. Jacquemet. 2017. AMPK negatively regulates tensin-dependent integrin activity. *The Journal of cell biology*. 216:1107-1121.

Glenn, J.L., E. Opalka, and K. Tischer. 1963. The incorporation of labeled palmitic acid into the phospholipids of normal and fatty livers. *The Journal of biological chemistry*. 238:1249-1254.

Glunde, K., Z.M. Bhujwalla, and S.M. Ronen. 2011. Choline metabolism in malignant transformation. *Nature reviews. Cancer*. 11:835-848.

Gong, Y., U.D. Chippada-Venkata, and W.K. Oh. 2014. Roles of Matrix Metalloproteinases and Their Natural Inhibitors in Prostate Cancer Progression. *Cancers*. 6:1298-1327.

Gonzalez-Guerrico, A.M., I. Espinoza, B. Schroeder, C.H. Park, C.M. Kvp, A. Khurana, B. Corominas-Faja, E. Cuyas, T. Alarcon, C. Kleer, J.A. Menendez, and R. Lupu. 2016. Suppression of endogenous lipogenesis induces reversion of the malignant phenotype and normalized differentiation in breast cancer. *Oncotarget*. 7:71151-71168.

Gordetsky, J., and J. Epstein. 2016. Grading of prostatic adenocarcinoma: current state and prognostic implications. *Diagnostic Pathology*. 11:25.

Graner, E., D. Tang, S. Rossi, A. Baron, T. Migita, L.J. Weinstein, M. Lechpammer, D. Huesken, J. Zimmermann, S. Signoretti, and M. Loda. 2004. The isopeptidase USP2a regulates the stability of fatty acid synthase in prostate cancer. *Cancer cell*. 5:253-261.

Greaves, J., G.R. Prescott, Y. Fukata, M. Fukata, C. Salaun, and L.H. Chamberlain. 2009. The Hydrophobic Cysteine-rich Domain of SNAP25 Couples with Downstream Residues to Mediate Membrane Interactions and Recognition by DHHC Palmitoyl Transferases. *Molecular biology of the cell*. 20:1845-1854.

Guan, X. 2015. Cancer metastases: challenges and opportunities. *Acta Pharmaceutica Sinica. B*. 5:402-418.

Guan, X., and C.A. Fierke. 2011. Understanding Protein Palmitoylation: Biological Significance and Enzymology. *Science China. Chemistry*. 54:1888-1897.

Guo, Y., S.R. Kenney, L. Cook, S.F. Adams, T. Rutledge, E. Romero, T.I. Oprea, L.A. Sklar, E. Bedrick, C.L. Wiggins, H. Kang, L. Lomo, C.Y. Muller, A. Wandinger-Ness, and L.G. Hudson. 2015. A Novel Pharmacologic Activity of Ketorolac for Therapeutic Benefit in Ovarian Cancer Patients. *Clinical cancer research : an official journal of the American Association for Cancer Research*. 21:5064-5072.

Hakkinen, K.M., J.S. Harunaga, A.D. Doyle, and K.M. Yamada. 2011. Direct comparisons of the morphology, migration, cell adhesions, and actin cytoskeleton of fibroblasts in four different three-dimensional extracellular matrices. *Tissue engineering. Part A*. 17:713-724.

Hamada, S., A. Horiguchi, K. Kuroda, K. Ito, T. Asano, K. Miyai, and K. Iwaya. 2014. Increased fatty acid synthase expression in prostate biopsy cores predicts higher Gleason score in radical prostatectomy specimen. *BMC clinical pathology*. 14:3.

Hamidi, H., M. Lu, K. Chau, L. Anderson, M. Fejzo, C. Ginther, R. Linnartz, A. Zubel, D.J. Slamon, and R.S. Finn. 2014. KRAS mutational subtype and copy number predict in vitro response of human pancreatic cancer cell lines to MEK inhibition. *British journal of cancer*. 111:1788-1801.

Hammerich, K.H., G.E. Ayala, and T.M. Wheeler. 2009. Anatomy of the prostate gland and surgical pathology of prostate cancer. *Cambridge University, Cambridge*:1-10.

Han, Y., Y. Luo, J. Zhao, M. Li, and Y. Jiang. 2014. Overexpression of c-Met increases the tumor invasion of human prostate LNCaP cancer cells in vitro and in vivo. *Oncology letters*. 8:1618-1624.

Hao, Q., T. Li, X. Zhang, P. Gao, P. Qiao, S. Li, and Z. Geng. 2014. Expression and roles of fatty acid synthase in hepatocellular carcinoma. *Oncology reports*. 32:2471-2476.

Head, B.P., H.H. Patel, and P.A. Insel. 2014. Interaction of membrane/lipid rafts with the cytoskeleton: impact on signaling and function: membrane/lipid rafts, mediators of cytoskeletal arrangement and cell signaling. *Biochimica et biophysica acta*. 1838:532-545.

Heasman, S.J., and A.J. Ridley. 2008. Mammalian Rho GTPases: new insights into their functions from in vivo studies. *Nature reviews. Molecular cell biology*. 9:690-701.

Heerboth, S., G. Housman, M. Leary, M. Longacre, S. Byler, K. Lapinska, A. Willbanks, and S. Sarkar. 2015. EMT and tumor metastasis. *Clinical and Translational Medicine*. 4:6.

Henderson, V., B. Smith, L.J. Burton, D. Randle, M. Morris, and V.A. Odero-Marah. 2015. Snail promotes cell migration through PI3K/AKT-dependent Rac1 activation as well as PI3K/AKT-independent pathways during prostate cancer progression. *Cell Adhesion & Migration*. 9:255-264.

Hensley, C.T., A.T. Wasti, and R.J. DeBerardinis. 2013. Glutamine and cancer: cell biology, physiology, and clinical opportunities. *J Clin Invest*. 123:3678-3684.

Hodge, R.G., and A.J. Ridley. 2016. Regulating Rho GTPases and their regulators. *Nature reviews. Molecular cell biology*. 17:496-510.

Hopperton, K.E., R.E. Duncan, R.P. Bazinet, and M.C. Archer. 2014. Fatty acid synthase plays a role in cancer metabolism beyond providing fatty acids for phospholipid synthesis or sustaining elevations in glycolytic activity. *Experimental cell research*. 320:302-310.

Horiguchi, A., T. Asano, T. Asano, K. Ito, M. Sumitomo, and M. Hayakawa. 2008. Pharmacological inhibitor of fatty acid synthase suppresses growth and invasiveness of renal cancer cells. *The Journal of urology*. 180:729-736.

Hou, W., M. Fei, X.I.A. Qin, X. Zhu, J. Greshock, P. Liu, Y. Zhou, H.U.I. Wang, B.-C. Ye, and C.Y. Qin. 2012. High overexpression of fatty acid synthase is associated with poor survival in Chinese patients with gastric carcinoma. *Experimental and Therapeutic Medicine*. 4:999-1004.

Hu, J., L. Che, L. Li, M.G. Pilo, A. Cigliano, S. Ribback, X. Li, G. Latte, M. Mela, M. Evert, F. Dombrowski, G. Zheng, X. Chen, and D.F. Calvisi. 2016. Co-activation of AKT and c-Met triggers rapid hepatocellular carcinoma development via the mTORC1/FASN pathway in mice. *Scientific reports*. 6:20484.

Huang, M., A. Koizumi, S. Narita, T. Inoue, N. Tsuchiya, H. Nakanishi, K. Numakura, H. Tsuruta, M. Saito, S. Satoh, H. Nanjo, T. Sasaki, and T. Habuchi. 2016. Diet-induced alteration of fatty acid synthase in prostate cancer progression. *Oncogenesis*. 5:e195.

Humphrey, P.A. 2004. Gleason grading and prognostic factors in carcinoma of the prostate. *Modern pathology : an official journal of the United States and Canadian Academy of Pathology, Inc*. 17:292-306.

Humphrey, P.A. 2012. Histological variants of prostatic carcinoma and their significance. *Histopathology*. 60:59-74.

Huttenlocher, A. 2005. Cell polarization mechanisms during directed cell migration. *Nat Cell Biol*. 7:336-337.

Huttenlocher, A., and A.R. Horwitz. 2011. Integrins in cell migration. *Cold Spring Harbor perspectives in biology*. 3:a005074.

Innocenzi, D., P.L. Alo, A. Balzani, V. Sebastiani, V. Silipo, G. La Torre, G. Ricciardi, C. Bosman, and S. Calvieri. 2003. Fatty acid synthase expression in melanoma. *Journal of cutaneous pathology*. 30:23-28.

Ito, T., K. Sato, H. Maekawa, M. Sakurada, H. Orita, K. Shimada, H. Daida, R.Y.O. Wada, M. Abe, O. Hino, and Y. Kajiyama. 2014. Elevated levels of serum fatty acid synthase in patients with gastric carcinoma. *Oncology letters*. 7:616-620.

Iwai, S., A. Yonekawa, C. Harada, M. Hamada, W. Katagiri, M. Nakazawa, and Y. Yura. 2010. Involvement of the Wnt-beta-catenin pathway in invasion and migration of oral squamous carcinoma cells. *International journal of oncology*. 37:1095-1103.

Jacobsen, F., S.N. Ashtiani, P. Tennstedt, H. Heinzer, R. Simon, G. Sauter, H. Sirma, M.C. Tsourlakis, S. Minner, T. Schlomm, and U. Michl. 2013. High c-MET expression is frequent but not associated with early PSA recurrence in prostate cancer. *Exp Ther Med*. 5:102-106.

Jennings, B.C., M.J. Nadolski, Y. Ling, M.B. Baker, M.L. Harrison, R.J. Deschenes, and M.E. Linder. 2009. 2-Bromopalmitate and 2-(2-hydroxy-5-nitro-benzylidene)-benzo[b]thiophen-3-one inhibit DHHC-mediated palmitoylation in vitro. *Journal of lipid research*. 50:233-242.

Jeong, J.H., A. Bhatia, Z. Toth, S. Oh, K.S. Inn, C.P. Liao, P. Roy-Burman, J. Melamed, G.A. Coetzee, and J.U. Jung. 2011. TPL2/COT/MAP3K8 (TPL2) activation promotes androgen depletion-independent (ADI) prostate cancer growth. *PloS one*. 6:e16205.

Jiang, L., H. Wang, J. Li, X. Fang, H. Pan, X. Yuan, and P. Zhang. 2014. Up-regulated FASN expression promotes transcoelomic metastasis of ovarian cancer cell through epithelial-mesenchymal transition. *International journal of molecular sciences*. 15:11539-11554.

Jiang, P., A. Enomoto, and M. Takahashi. 2009. Cell biology of the movement of breast cancer cells: intracellular signalling and the actin cytoskeleton. *Cancer letters*. 284:122-130.

Jiang, W.G., T.A. Martin, C. Parr, G. Davies, K. Matsumoto, and T. Nakamura. 2005. Hepatocyte growth factor, its receptor, and their potential value in cancer therapies. *Critical reviews in oncology/hematology*. 53:35-69.

Kaighn, M.E., K.S. Narayan, Y. Ohnuki, J.F. Lechner, and L.W. Jones. 1979. Establishment and characterization of a human prostatic carcinoma cell line (PC-3). *Investigative urology*. 17:16-23.

Karantanos, T., P.G. Corn, and T.C. Thompson. 2013. Prostate cancer progression after androgen deprivation therapy: mechanisms of castrate resistance and novel therapeutic approaches. *Oncogene*. 32:5501-5511.

Karantanos, T., S. Karanika, J. Wang, G. Yang, M. Dobashi, S. Park, C. Ren, L. Li, S.P. Basourakos, A. Hoang, E. Efstathiou, X. Wang, P. Troncoso, M. Titus, B. Broom, J. Kim, P.G. Corn, C.J. Logothetis, and T.C. Thompson. 2016. Caveolin-1 regulates hormone resistance through lipid synthesis, creating novel therapeutic opportunities for castration-resistant prostate cancer. *Oncotarget*. 7:46321-46334.

Kato, T., K. Kawai, Y. Egami, Y. Kakehi, and N. Araki. 2014. Rac1-dependent lamellipodial motility in prostate cancer PC-3 cells revealed by optogenetic control of Rac1 activity. *PloS one*. 9:e97749.

Katsurada, A., N. Iritani, H. Fukuda, Y. Matsumura, N. Nishimoto, T. Noguchi, and T. Tanaka. 1990. Effects of nutrients and hormones on transcriptional and post-transcriptional regulation of fatty acid synthase in rat liver. *European Journal of Biochemistry*. 190:427-433.

Keely, P.J., J.K. Westwick, I.P. Whitehead, C.J. Der, and L.V. Parise. 1997. Cdc42 and Rac1 induce integrin-mediated cell motility and invasiveness through PI(3)K. *Nature*. 390:632-636.

Khan, M.I., A. Hamid, V.M. Adhami, R.K. Lall, and H. Mukhtar. 2015. Role of Epithelial Mesenchymal Transition in Prostate Tumorigenesis. *Current pharmaceutical design*. 21:1240-1248.

Kim, D.-H., and D. Wirtz. 2013. Focal adhesion size uniquely predicts cell migration. *The FASEB Journal*. 27:1351-1361.

Knowles, L.M., F. Axelrod, C.D. Browne, and J.W. Smith. 2004. A fatty acid synthase blockade induces tumor cell-cycle arrest by down-regulating Skp2. *The Journal of biological chemistry*. 279:30540-30545.

Knowles, L.M., C. Yang, A. Osterman, and J.W. Smith. 2008. Inhibition of fatty-acid synthase induces caspase-8-mediated tumor cell apoptosis by up-regulating DDIT4. *The Journal of biological chemistry*. 283:31378-31384.

Knudsen, B.S., G.A. Gmyrek, J. Inra, D.S. Scherr, E.D. Vaughan, D.M. Nanus, M.W. Kattan, W.L. Gerald, and G.F. Vande Woude. 2002. High expression of the Met receptor in prostate cancer metastasis to bone. *Urology*. 60:1113-1117.

Konstantinopoulos, P.A., M.V. Karamouzis, and A.G. Papavassiliou. 2007. Post-translational modifications and regulation of the RAS superfamily of GTPases as anticancer targets. *Nature reviews. Drug discovery*. 6:541-555.

Koochekpour, S. 2013. Glutamate, a metabolic biomarker of aggressiveness and a potential therapeutic target for prostate cancer. *Asian journal of andrology*. 15:212-213.

Koochekpour, S., S. Majumdar, G. Azabdaftari, K. Attwood, R. Scioneaux, D. Subramani, C. Manhardt, G.D. Lorusso, S.S. Willard, H. Thompson, M. Shourideh, K. Rezaei, O. Sartor, J.L. Mohler, and R.L. Vessella. 2012. Serum Glutamate Levels Correlate with Gleason Score and Glutamate Blockade Decreases Proliferation, Migration, and Invasion and Induces Apoptosis in Prostate Cancer Cells. *Clinical cancer research : an official journal of the American Association for Cancer Research*. 18:5888-5901.

Krakhmal, N.V., M.V. Zavyalova, E.V. Denisov, S.V. Vtorushin, and V.M. Perelmuter. 2015. Cancer Invasion: Patterns and Mechanisms. *Acta Naturae*. 7:17-28.

Kridel, S.J., F. Axelrod, N. Rozenkrantz, and J.W. Smith. 2004. Orlistat is a novel inhibitor of fatty acid synthase with antitumor activity. *Cancer research*. 64:2070-2075.

Krušlin, B., M. Ulamec, and D. Tomas. 2015. Prostate cancer stroma: an important factor in cancer growth and progression. *Bosnian journal of basic medical sciences*. 15:1-8.

Kryvenko, O.N., M. Jankowski, D.A. Chitale, D. Tang, A. Rundle, S. Trudeau, and B.A. Rybicki. 2012. Inflammation and preneoplastic lesions in benign prostate as risk factors for prostate cancer. *Modern pathology : an official journal of the United States and Canadian Academy of Pathology, Inc*. 25:1023-1032.

Kuhajda, F.P. 2000. Fatty-acid synthase and human cancer: new perspectives on its role in tumor biology. *Nutrition (Burbank, Los Angeles County, Calif.)*. 16:202-208.

Kuhajda, F.P. 2006. Fatty acid synthase and cancer: new application of an old pathway. *Cancer research*. 66:5977-5980.

Kuhajda, F.P., K. Jenner, F.D. Wood, R.A. Hennigar, L.B. Jacobs, J.D. Dick, and G.R. Pasternack. 1994. Fatty acid synthesis: a potential selective target for antineoplastic therapy. *Proceedings of the National Academy of Sciences of the United States of America*. 91:6379-6383.

Kuhajda, F.P., S. Piantadosi, and G.R. Pasternack. 1989. Haptoglobin-related protein (Hpr) epitopes in breast cancer as a predictor of recurrence of the disease. *N Engl J Med*. 321:636-641.

Kumar, V.L., and P.K. Majumder. 1995. Prostate gland: structure, functions and regulation. *International urology and nephrology*. 27:231-243.

Kutys, M.L., and K.M. Yamada. 2014. An extracellular matrix-specific GEF-GAP interaction regulates Rho GTPase crosstalk for 3D collagen migration. *Nature cell biology*. 16:909-917.

Kwon, E.D., K.Y. Jung, L.C. Edsall, H.Y. Kim, A. Garcia-Perez, and M.B. Burg. 1995. Osmotic regulation of synthesis of glycerophosphocholine from phosphatidylcholine in MDCK cells. *The American journal of physiology*. 268:C402-412.

Lacasa, D., X. Le Liepvre, P. Ferre, and I. Dugail. 2001. Progesterone stimulates adipocyte determination and differentiation 1/sterol regulatory element-binding protein 1c gene expression. potential mechanism for the lipogenic effect of progesterone in adipose tissue. *The Journal of biological chemistry*. 276:11512-11516.

Leamy, A.K., R.A. Egnatchik, M. Shiota, P.T. Ivanova, D.S. Myers, H.A. Brown, and J.D. Young. 2014. Enhanced synthesis of saturated phospholipids is associated with ER stress and lipotoxicity in palmitate treated hepatic cells. *Journal of lipid research*. 55:1478-1488.

Levental, I., D. Lingwood, M. Grzybek, U. Coskun, and K. Simons. 2010. Palmitoylation regulates raft affinity for the majority of integral raft proteins. *Proceedings of the National Academy of Sciences of the United States of America*. 107:22050-22054.

Li, J., L. Dong, D. Wei, X. Wang, S. Zhang, and H. Li. 2014a. Fatty acid synthase mediates the epithelial-mesenchymal transition of breast cancer cells. *International journal of biological sciences*. 10:171-180.

Li, J., Q. Wen, L. Xu, W. Wang, J. Luo, S. Chu, G. Xie, L. Shi, D. Huang, J. Li, and S. Fan. 2014b. Fatty acid synthase–associated protein with death domain: a prognostic factor for survival in patients with nasopharyngeal carcinoma. *Human pathology*. 45:2447-2452.

Li, J.N., M. Gorospe, F.J. Chrest, T.S. Kumaravel, M.K. Evans, W.F. Han, and E.S. Pizer. 2001. Pharmacological inhibition of fatty acid synthase activity produces both cytostatic and cytotoxic effects modulated by p53. *Cancer research*. 61:1493-1499.

Li, L., L. Che, K.M. Tharp, H.M. Park, M.G. Pilo, D. Cao, A. Cigliano, G. Latte, Z. Xu, S. Ribback, F. Dombrowski, M. Evert, G.J. Gores, A. Stahl, D.F. Calvisi, and X. Chen. 2016. Differential requirement for de novo lipogenesis in cholangiocarcinoma and hepatocellular carcinoma of mice and humans. *Hepatology (Baltimore, Md.)*. 63:1900-1913.

Li, N., X. Bu, X. Tian, P. Wu, L. Yang, and P. Huang. 2012a. Fatty acid synthase regulates proliferation and migration of colorectal cancer cells via HER2-PI3K/Akt signaling pathway. *Nutrition and cancer*. 64:864-870.

Li, N., X. Bu, P. Wu, P. Wu, and P. Huang. 2012b. The "HER2-PI3K/Akt-FASN Axis" regulated malignant phenotype of colorectal cancer cells. *Lipids*. 47:403-411.

Li, N., H. Lu, C. Chen, X. Bu, and P. Huang. 2013. Loss of fatty acid synthase inhibits the "HER2-PI3K/Akt axis" activity and malignant phenotype of Caco-2 cells. *Lipids in health and disease*. 12:83.

Li, W., and Y. Kang. 2016. Probing the Fifty Shades of EMT in Metastasis. *Trends in cancer*. 2:65-67.

Li, Y., J. Webster-Cyriaque, C.C. Tomlinson, M. Yohe, and S. Kenney. 2004. Fatty acid synthase expression is induced by the Epstein-Barr virus immediate-early protein BRLF1 and is required for lytic viral gene expression. *Journal of virology*. 78:4197-4206.

Lin, Y.C., M. Boone, L. Meuris, I. Lemmens, N. Van Roy, A. Soete, J. Reumers, M. Moisse, S. Plaisance, R. Drmanac, J. Chen, F. Speleman, D. Lambrechts, Y. Van de Peer, J. Tavernier, and N. Callewaert. 2014. Genome dynamics of the human embryonic kidney 293 lineage in response to cell biology manipulations. *Nature communications*. 5:4767.

Linder, M.E., and R.J. Deschenes. 2007. Palmitoylation: policing protein stability and traffic. *Nature reviews. Molecular cell biology*. 8:74-84.

Litvinov, I.V., L. Antony, S.L. Dalrymple, R. Becker, L. Cheng, and J.T. Isaacs. 2006. PC3, but not DU145, human prostate cancer cells retain the coregulators required for tumor suppressor ability of androgen receptor. *Prostate*. 66:1329-1338.

Liu, H., Y. Liu, and J.T. Zhang. 2008. A new mechanism of drug resistance in breast cancer cells: fatty acid synthase overexpression-mediated palmitate overproduction. *Molecular cancer therapeutics*. 7:263-270.

Liu, T., D.E. Mendes, and C.E. Berkman. 2013a. From AR to c-Met: androgen deprivation leads to a signaling pathway switch in prostate cancer cells. *International journal of oncology*. 43:1125-1130.

Liu, Z.L., J.H. Mao, A.F. Peng, Q.S. Yin, Y. Zhou, X.H. Long, and S.H. Huang. 2013b. Inhibition of fatty acid synthase suppresses osteosarcoma cell invasion and migration via downregulation of the PI3K/Akt signaling pathway in vitro. *Molecular medicine reports*. 7:608-612.

Liu, Z.L., G.A.O. Wang, A.F. Peng, Q.F. Luo, Y. Zhou, and S.H. Huang. 2012. Fatty acid synthase expression in osteosarcoma and its correlation with pulmonary metastasis. *Oncology letters*. 4:878-882.

Llado, V., D.J. Lopez, M. Ibarguren, M. Alonso, J.B. Soriano, P.V. Escriba, and X. Busquets. 2014. Regulation of the cancer cell membrane lipid composition by NaCHOleate: effects on cell signaling and therapeutical relevance in glioma. *Biochimica et biophysica acta*. 1838:1619-1627.

Lonergan, P.E., and D.J. Tindall. 2011. Androgen receptor signaling in prostate cancer development and progression. *Journal of carcinogenesis*. 10:20.

Long, X.H., G.M. Zhang, A.F. Peng, Q.F. Luo, L. Zhang, H.C. Wen, R.P. Zhou, S. Gao, Y. Zhou, and Z.L. Liu. 2014. Lapatinib alters the malignant phenotype of osteosarcoma cells via downregulation of the activity of the HER2-PI3K/AKT-FASN axis in vitro. *Oncology reports*. 31:328-334.

Lupu, R., and J.A. Menendez. 2006. Targeting fatty acid synthase in breast and endometrial cancer: An alternative to selective estrogen receptor modulators? *Endocrinology*. 147:4056-4066.

Lynen, F., and S. Ochoa. 1953. Enzymes of fatty acid metabolism. *Biochimica et biophysica acta*. 12:299-314.

Lyons, S.M., E. Alizadeh, J. Mannheimer, K. Schuamberg, J. Castle, B. Schroder, P. Turk, D. Thamm, and A. Prasad. 2016. Changes in cell shape are correlated with metastatic potential in murine and human osteosarcomas. *Biology Open*. 5:289-299.

López, M., and C. Diéguez. 2007. C75, a Fatty Acid Synthase (FAS) Inhibitor *Metabolic & Immune Drug Discovery*. 1:53-62.

Machesky, L.M. 2008. Lamellipodia and filopodia in metastasis and invasion. *FEBS letters*. 582:2102-2111.

Maier, T., M. Leibundgut, D. Boehringer, and N. Ban. 2010. Structure and function of eukaryotic fatty acid synthases. *Quarterly reviews of biophysics*. 43:373-422.

Majumder, P.K., and W.R. Sellers. 2005. Akt-regulated pathways in prostate cancer. *Oncogene*. 24:7465-7474.

Mammoto, T., S.M. Parikh, A. Mammoto, D. Gallagher, B. Chan, G. Mostoslavsky, D.E. Ingber, and V.P. Sukhatme. 2007. Angiopoietin-1 requires p190 RhoGAP to protect against vascular leakage in vivo. *The Journal of biological chemistry*. 282:23910-23918.

Martin, B.R., and B.F. Cravatt. 2009. Large-scale profiling of protein palmitoylation in mammalian cells. *Nature methods*. 6:135-138.

Martin, G.S. 2003. Cell signaling and cancer. *Cancer cell*. 4:167-174.

Masuya, D., C. Huang, D. Liu, T. Nakashima, K. Kameyama, R. Haba, M. Ueno, and H. Yokomise. 2004. The tumour–stromal interaction between intratumoral c-Met and stromal hepatocyte growth factor associated with tumour growth and prognosis in non-small-cell lung cancer patients. *British journal of cancer*. 90:1555-1562.

McArdle, T.J., B.M. Ogle, and F.K. Noubissi. 2016. An In Vitro Inverted Vertical Invasion Assay to Avoid Manipulation of Rare or Sensitive Cell Types. *Journal of Cancer*. 7:2333-2340.

McColl, B., R. Garg, P. Riou, K. Riento, and A.J. Ridley. 2016. Rnd3-induced cell rounding requires interaction with Plexin-B2. *Journal of cell science*. 129:4046-4056.

McNeal, J.E., A. Villers, E.A. Redwine, F.S. Freiha, and T.A. Stamey. 1991. Microcarcinoma in the prostate: its association with duct-acinar dysplasia. *Human pathology*. 22:644-652.

Menendez, J.A., and R. Lupu. 2004. Fatty acid synthase-catalyzed de novo fatty acid biosynthesis: from anabolic-energy-storage pathway in normal tissues to jack-of-all-trades in cancer cells. *Archivum immunologiae et therapiae experimentalis*. 52:414-426.

Menendez, J.A., and R. Lupu. 2007. Fatty acid synthase and the lipogenic phenotype in cancer pathogenesis. *Nature reviews. Cancer*. 7:763-777.

Menendez, J.A., I. Mehmi, E. Atlas, R. Colomer, and R. Lupu. 2004a. Novel signaling molecules implicated in tumor-associated fatty acid synthase-dependent breast cancer cell proliferation and survival: Role of exogenous dietary fatty acids, p53-p21WAF1/CIP1, ERK1/2 MAPK, p27KIP1, BRCA1, and NF-kappaB. *International journal of oncology*. 24:591-608.

Menendez, J.A., S. Ropero, I. Mehmi, E. Atlas, R. Colomer, and R. Lupu. 2004b. Overexpression and hyperactivity of breast cancer-associated fatty acid synthase (oncogenic antigen-519) is insensitive to normal arachidonic fatty acid-induced suppression in lipogenic tissues but it is selectively inhibited by tumoricidal alpha-linolenic and gamma-linolenic fatty acids: a novel mechanism by which dietary fat can alter mammary tumorigenesis. *International journal of oncology*. 24:1369-1383.

Mian, B.M., P. Troncoso, K. Okihara, V. Bhadkamkar, D. Johnston, A.O. Reyes, and R.J. Babaian. 2002. Outcome of patients with Gleason score 8 or higher prostate cancer following radical prostatectomy alone. *The Journal of urology*. 167:1675-1680.

Minner, S., B. Jessen, L. Stiedenroth, E. Burandt, J. Kollermann, M. Mirlacher, A. Erbersdobler, C. Eichelberg, M. Fisch, T.H. Brummendorf, C. Bokemeyer, R. Simon, T. Steuber, M. Graefen, H. Huland, G. Sauter, and T. Schlomm. 2010. Low level HER2 overexpression is associated with rapid tumor cell proliferation and poor prognosis in prostate cancer. *Clinical cancer research : an official journal of the American Association for Cancer Research*. 16:1553-1560.

Moissoglu, K., and M.A. Schwartz. 2014. Spatial and temporal control of Rho GTPase functions. *Cellular Logistics*. 4:e943618.

Moon, Y.S., M.J. Latasa, M.J. Griffin, and H.S. Sul. 2002. Suppression of fatty acid synthase promoter by polyunsaturated fatty acids. *Journal of lipid research*. 43:691-698.

Morley, S., M.H. Hager, S.G. Pollan, B. Knudsen, D. Di Vizio, and M.R. Freeman. 2014. Trading in your spindles for blebs: the amoeboid tumor cell phenotype in prostate cancer. *Asian journal of andrology*. 16:530-535.

Mosmann, T. 1983. Rapid colorimetric assay for cellular growth and survival: application to proliferation and cytotoxicity assays. *Journal of immunological methods*. 65:55-63.

Mullins, R.D., J.A. Heuser, and T.D. Pollard. 1998. The interaction of Arp2/3 complex with actin: nucleation, high affinity pointed end capping, and formation of branching networks of filaments. *Proceedings of the National Academy of Sciences of the United States of America*. 95:6181-6186.

Murphy, D.A., and S.A. Courtneidge. 2011. The 'ins' and 'outs' of podosomes and invadopodia: characteristics, formation and function. *Nature reviews. Molecular cell biology*. 12:413-426.

Nagaraja, G.M., M. Othman, B.P. Fox, R. Alsaber, C.M. Pellegrino, Y. Zeng, R. Khanna, P. Tamburini, A. Swaroop, and R.P. Kandpal. 2006. Gene expression signatures and biomarkers of noninvasive and invasive breast cancer cells: comprehensive profiles by representational difference analysis, microarrays and proteomics. *Oncogene*. 25:2328-2338.

Naik, P. 2011. Essentials of Biochemistry. Jaypee Brothers, Medical Publishers.

Narumiya, S., M. Tanji, and T. Ishizaki. 2009. Rho signaling, ROCK and mDia1, in transformation, metastasis and invasion. *Cancer metastasis reviews*. 28:65-76.

Nath, A., I. Li, L.R. Roberts, and C. Chan. 2015. Elevated free fatty acid uptake via CD36 promotes epithelial-mesenchymal transition in hepatocellular carcinoma. *Scientific reports*. 5:14752.

Navarro-Lerida, I., S. Sanchez-Perales, M. Calvo, C. Rentero, Y. Zheng, C. Enrich, and M.A. Del Pozo. 2012. A palmitoylation switch mechanism regulates Rac1 function and membrane organization. *The EMBO journal*. 31:534-551.

Nayal, A., D.J. Webb, C.M. Brown, E.M. Schaefer, M. Vicente-Manzanares, and A.R. Horwitz. 2006. Paxillin phosphorylation at Ser273 localizes a GIT1–PIX–PAK complex and regulates adhesion and protrusion dynamics. *The Journal of cell biology*. 173:587-589.

Nishi, K., K. Suzuki, J. Sawamoto, Y. Tokizawa, Y. Iwase, N. Yumita, and T. Ikeda. 2016. Inhibition of Fatty Acid Synthesis Induces Apoptosis of Human Pancreatic Cancer Cells. *Anticancer research*. 36:4655-4660.

Nishimura, A., and M.E. Linder. 2013. Identification of a novel prenyl and palmitoyl modification at the CaaX motif of Cdc42 that regulates RhoGDI binding. *Molecular and cellular biology*. 33:1417-1429.

Nobes, C.D., and A. Hall. 1995. Rho, rac, and cdc42 GTPases regulate the assembly of multimolecular focal complexes associated with actin stress fibers, lamellipodia, and filopodia. *Cell*. 81:53-62.

Notarnicola, M., V. Tutino, M. Calvani, D. Lorusso, V. Guerra, and M.G. Caruso. 2012. Serum levels of fatty acid synthase in colorectal cancer patients are associated with tumor stage. *Journal of gastrointestinal cancer*. 43:508-511.

Nwosu, V., J. Carpten, J.M. Trent, and R. Sheridan. 2001. Heterogeneity of genetic alterations in prostate cancer: evidence of the complex nature of the disease. *Human molecular genetics*. 10:2313-2318.

O'Connor, K., and M. Chen. 2013. Dynamic functions of RhoA in tumor cell migration and invasion. *Small GTPases*. 4:141-147.

O'Neill, P.R., V. Kalyanaraman, and N. Gautam. 2016. Subcellular optogenetic activation of Cdc42 controls local and distal signaling to drive immune cell migration. *Molecular biology of the cell*. 27:1442-1450.

O'Farrell, M., T. Heuer, K. Grimmer, R. Crowley, J. Waszczuk, M. Fridlib, R. Ventura, C. Rubio, J. Lai, D. Buckley, W. McCulloch, and G. Kemble. 2016. Abstract LB-214: FASN inhibitor TVB-2640 shows pharmacodynamic effect and evidence of clinical activity in KRAS-mutant NSCLC patients in a phase I study. *Cancer research*. 76:LB-214.

Ogino, S., K. Nosho, J.A. Meyerhardt, G.J. Kirkner, A.T. Chan, T. Kawasaki, E.L. Giovannucci, M. Loda, and C.S. Fuchs. 2008. Cohort study of fatty acid synthase expression and patient survival in colon cancer. *Journal of clinical oncology : official journal of the American Society of Clinical Oncology*. 26:5713-5720.

Ohtaka, K., S. Watanabe, R. Iwazaki, M. Hirose, and N. Sato. 1996. Role of extracellular matrix on colonic cancer cell migration and proliferation. *Biochemical and biophysical research communications*. 220:346-352.

Organ, S.L., and M.S. Tsao. 2011. An overview of the c-MET signaling pathway. *Therapeutic advances in medical oncology*. 3:S7-s19.

Orgaz, J.L., P. Pandya, R. Dalmeida, P. Karagiannis, B. Sanchez-Laorden, A. Viros, J. Albrengues, F.O. Nestle, A.J. Ridley, C. Gaggioli, R. Marais, S.N. Karagiannis, and V. Sanz-Moreno. 2014. Diverse matrix metalloproteinase functions regulate cancer amoeboid migration. *Nature communications*. 5:4255.

Ory, S., H. Brazier, and A. Blangy. 2007. Identification of a bipartite focal adhesion localization signal in RhoU/Wrch-1, a Rho family GTPase that regulates cell adhesion and migration. *Biology of the cell*. 99:701-716.

Oyasu, R., X. Yang, and O. Yoshida. 2008. Questions in Daily Urologic Practice. 287 pp.

Pande, G. 2000. The role of membrane lipids in regulation of integrin functions. *Current opinion in cell biology*. 12:569-574.

Parri, M., and P. Chiarugi. 2010. Rac and Rho GTPases in cancer cell motility control. *Cell communication and signaling : CCS*. 8:23.

Parsons, J.T., A.R. Horwitz, and M.A. Schwartz. 2010a. Cell adhesion: integrating cytoskeletal dynamics and cellular tension. *Nature reviews. Molecular cell biology*. 11:633-643.

Parsons, J.T., A.R. Horwitz, and M.A. Schwartz. 2010b. Cell adhesion: integrating cytoskeletal dynamics and cellular tension. *Nature reviews. Molecular cell biology*. 11:633-643.

Pegtel, D.M., S.I. Ellenbroek, A.E. Mertens, R.A. van der Kammen, J. de Rooij, and J.G. Collard. 2007. The Par-Tiam1 complex controls persistent migration by stabilizing microtubule-dependent front-rear polarity. *Current biology : CB*. 17:1623-1634.

Peitzsch, R.M., and S. McLaughlin. 1993. Binding of acylated peptides and fatty acids to phospholipid vesicles: pertinence to myristoylated proteins. *Biochemistry*. 32:10436-10443.

Pellegrin, S., and H. Mellor. 2005. The Rho family GTPase Rif induces filopodia through mDia2. *Current biology : CB*. 15:129-133.

Percherancier, Y., T. Planchenault, A. Valenzuela-Fernandez, J.L. Virelizier, F. Arenzana-Seisdedos, and F. Bachelerie. 2001. Palmitoylation-dependent control of degradation, life span, and membrane expression of the CCR5 receptor. *The Journal of biological chemistry*. 276:31936-31944.

Perez-Sala, D., P. Boya, I. Ramos, M. Herrera, and K. Stamatakis. 2009. The C-terminal sequence of RhoB directs protein degradation through an endo-lysosomal pathway. *PloS one*. 4:e8117.

Peskin, C.S., G.M. Odell, and G.F. Oster. 1993. Cellular motions and thermal fluctuations: the Brownian ratchet. *Biophysical journal*. 65:316-324.

Pienta, K.J., and D. Bradley. 2006. Mechanisms underlying the development of androgen-independent prostate cancer. *Clinical cancer research : an official journal of the American Association for Cancer Research*. 12:1665-1671.

Pizer, E.S., S.F. Lax, F.P. Kuhajda, G.R. Pasternack, and R.J. Kurman. 1998. Fatty acid synthase expression in endometrial carcinoma: correlation with cell proliferation and hormone receptors. *Cancer*. 83:528-537.

Pizer, E.S., B.R. Pflug, G.S. Bova, W.F. Han, M.S. Udan, and J.B. Nelson. 2001. Increased fatty acid synthase as a therapeutic target in androgen-independent prostate cancer progression. *Prostate*. 47:102-110.

Puthanveetil, P., Y. Wang, D. Zhang, F. Wang, M.S. Kim, S. Innis, T. Pulinilkunnil, A. Abrahani, and B. Rodrigues. 2011. Cardiac triglyceride accumulation following acute lipid excess occurs through activation of a FoxO1-iNOS-CD36 pathway. *Free radical biology & medicine*. 51:352-363.

Putzi, M.J., and A.M. De Marzo. 2000. Morphologic transitions between proliferative inflammatory atrophy and high-grade prostatic intraepithelial neoplasia. *Urology*. 56:828-832.

Radenne, A., M. Akpa, C. Martel, S. Sawadogo, D. Mauvoisin, and C. Mounier. 2008. Hepatic regulation of fatty acid synthase by insulin and T3: evidence for T3 genomic and nongenomic actions. *American journal of physiology. Endocrinology and metabolism*. 295:E884-894.

Rae, C., U. Haberkorn, J.W. Babich, and R.J. Mairs. 2015. Inhibition of Fatty Acid Synthase Sensitizes Prostate Cancer Cells to Radiotherapy. *Radiation research*. 184:482-493.

Raftopoulou, M., and A. Hall. 2004. Cell migration: Rho GTPases lead the way. *Developmental biology*. 265:23-32.

Rangan, V.S., and S. Smith. 2002. Chapter 6 Fatty acid synthesis in eukaryotes. *In* New Comprehensive Biochemistry. Vol. Volume 36. Elsevier. 151-179.

Resh, M.D. 2016. Fatty acylation of proteins: The long and the short of it. *Prog Lipid Res*. 63:120-131.

Reymond, N., B.B. d'Agua, and A.J. Ridley. 2013. Crossing the endothelial barrier during metastasis. *Nature reviews. Cancer*. 13:858-870.

Reymond, N., J.H. Im, R. Garg, F.M. Vega, B. Borda d'Agua, P. Riou, S. Cox, F. Valderrama, R.J. Muschel, and A.J. Ridley. 2012. Cdc42 promotes transendothelial migration of cancer cells through beta1 integrin. *The Journal of cell biology*. 199:653-668.

Richman, E.L., S.A. Kenfield, M.J. Stampfer, E.L. Giovannucci, S.H. Zeisel, W.C. Willett, and J.M. Chan. 2012. Choline intake and risk of lethal prostate cancer: incidence and survival. *The American journal of clinical nutrition*. 96:855-863.

Ridley, A.J., M.A. Schwartz, K. Burridge, R.A. Firtel, M.H. Ginsberg, G. Borisy, J.T. Parsons, and A.R. Horwitz. 2003. Cell migration: integrating signals from front to back. *Science (New York, N.Y.)*. 302:1704-1709.

Risse, S.L., B. Vaz, M.F. Burton, P. Aspenstrom, R.P. Piekorz, L. Brunsveld, and M.R. Ahmadian. 2013. SH3-mediated targeting of Wrch1/RhoU by multiple adaptor proteins. *Biological chemistry*. 394:421-432.

Roberts, P.J., N. Mitin, P.J. Keller, E.J. Chenette, J.P. Madigan, R.O. Currin, A.D. Cox, O. Wilson, P. Kirschmeier, and C.J. Der. 2008. Rho Family GTPase modification and dependence on CAAX motif-signaled posttranslational modification. *The Journal of biological chemistry*. 283:25150-25163.

Rohrig, F., and A. Schulze. 2016. The multifaceted roles of fatty acid synthesis in cancer. *Nature reviews. Cancer*. 16:732-749.

Ross, J., A.M. Najjar, M. Sankaranarayanapillai, W.P. Tong, K. Kaluarachchi, and S.M. Ronen. 2008. Fatty acid synthase inhibition results in a magnetic resonance-detectable drop in phosphocholine. *Molecular cancer therapeutics*. 7:2556-2565.

Rossi, S., E. Graner, P. Febbo, L. Weinstein, N. Bhattacharya, T. Onody, G. Bubley, S. Balk, and M. Loda. 2003. Fatty acid synthase expression defines distinct molecular signatures in prostate cancer. *Molecular cancer research* 1:707-715.

Roth, A.F., J. Wan, A.O. Bailey, B. Sun, J.A. Kuchar, W.N. Green, B.S. Phinney, J.R. Yates, 3rd, and N.G. Davis. 2006. Global analysis of protein palmitoylation in yeast. *Cell*. 125:1003-1013.

Royal, I., N. Lamarche-Vane, L. Lamorte, K. Kaibuchi, and M. Park. 2000. Activation of Cdc42, Rac, PAK, and Rho-Kinase in Response to Hepatocyte Growth Factor Differentially Regulates Epithelial Cell Colony Spreading and Dissociation. *Molecular biology of the cell*. 11:1709-1725.

Ruusala, A., and P. Aspenström. 2008. The Atypical Rho GTPase Wrch1 Collaborates with the Nonreceptor Tyrosine Kinases Pyk2 and Src in Regulating Cytoskeletal Dynamics. *Molecular and cellular biology*. 28:1802-1814.

Rysman, E., K. Brusselmans, K. Scheys, L. Timmermans, R. Derua, S. Munck, P.P. Van Veldhoven, D. Waltregny, V.W. Daniels, J. Machiels, F. Vanderhoydonc, K. Smans, E. Waelkens, G. Verhoeven, and J.V. Swinnen. 2010. De novo lipogenesis protects cancer cells from free radicals and chemotherapeutics by promoting membrane lipid saturation. *Cancer research*. 70:8117-8126.

Sadowski, M.C., R.H. Pouwer, J.H. Gunter, A.A. Lubik, R.J. Quinn, and C.C. Nelson. 2014. The fatty acid synthase inhibitor triclosan: repurposing an anti-microbial agent for targeting prostate cancer. *Oncotarget*. 5:9362-9381.

Sahai, E., and C.J. Marshall. 2002. RHO-GTPases and cancer. *Nature reviews. Cancer*. 2:133-142.

Saini, K.S., S. Loi, E. de Azambuja, O. Metzger-Filho, M.L. Saini, M. Ignatiadis, J.E. Dancey, and M.J. Piccart-Gebhart. 2013. Targeting the PI3K/AKT/mTOR and Raf/MEK/ERK pathways in the treatment of breast cancer. *Cancer treatment reviews*. 39:935-946.

Sakamoto, S., and N. Kyprianou. 2010. Targeting anoikis resistance in prostate cancer metastasis. *Molecular aspects of medicine*. 31:205-214.

Sander, E.E., J.P. ten Klooster, S. van Delft, R.A. van der Kammen, and J.G. Collard. 1999. Rac downregulates Rho activity: reciprocal balance between both GTPases determines cellular morphology and migratory behavior. *The Journal of cell biology*. 147:1009-1022.

Saras, J., P. Wollberg, and P. Aspenstrom. 2004. Wrch1 is a GTPase-deficient Cdc42-like protein with unusual binding characteristics and cellular effects. *Experimental cell research*. 299:356-369.

Scaglia, N., S. Tyekucheva, G. Zadra, C. Photopoulos, and M. Loda. 2014. De novo fatty acid synthesis at the mitotic exit is required to complete cellular division. *Cell Cycle*. 13:859-868.

Schiller, J., and K. Arnold. 2002. Application of high resolution 31P NMR spectroscopy to the characterization of the phospholipid composition of tissues and body fluids - a methodological review. *Medical science monitor : international medical journal of experimental and clinical research*. 8:Mt205-222.

Scholzen, T., and J. Gerdes. 2000. The Ki-67 protein: from the known and the unknown. *J Cell Physiol*. 182:311-322.

Schultz, G.S., J.M. Davidson, R.S. Kirsner, P. Bornstein, and I.M. Herman. 2011. Dynamic reciprocity in the wound microenvironment. *Wound repair and regeneration : official publication of the Wound Healing Society [and] the European Tissue Repair Society*. 19:134-148.

Schwab, T.S., T. Stewart, J. Lehr, K.J. Pienta, J.S. Rhim, and J.A. Macoska. 2000. Phenotypic characterization of immortalized normal and primary tumor-derived human prostate epithelial cell cultures. *Prostate*. 44:164-171.

Schwartz, M.A., and A.R. Horwitz. 2006. Integrating adhesion, protrusion, and contraction during cell migration. *Cell*. 125:1223-1225.

Sebti, S.M., and C.J. Der. 2003. Opinion: Searching for the elusive targets of farnesyltransferase inhibitors. *Nature reviews. Cancer*. 3:945-951.

Seguin, F., M.A. Carvalho, D.C. Bastos, M. Agostini, K.G. Zecchin, M.P. Alvarez-Flores, A.M. Chudzinski-Tavassi, R.D. Coletta, and E. Graner. 2012. The fatty acid synthase inhibitor orlistat reduces experimental metastases and angiogenesis in B16-F10 melanomas. *British journal of cancer*. 107:977-987.

Senadheera, D., L. Haataja, J. Groffen, and N. Heisterkamp. 2001. The small GTPase Rac interacts with ubiquitination complex proteins Cullin-1 and CDC23. *International journal of molecular medicine*. 8:127-133.

Shafi, A.A., A.E. Yen, and N.L. Weigel. 2013. Androgen receptors in hormone-dependent and castration-resistant prostate cancer. *Pharmacology & therapeutics*. 140:223-238.

Shahinian, S., and J.R. Silvius. 1995. Doubly-lipid-modified protein sequence motifs exhibit long-lived anchorage to lipid bilayer membranes. *Biochemistry*. 34:3813-3822.

Sharma, C., I. Rabinovitz, and M.E. Hemler. 2012a. Palmitoylation by DHHC3 is critical for the function, expression, and stability of integrin alpha6beta4. *Cellular and molecular life sciences* 69:2233-2244.

Sharma, C., I. Rabinovitz, and M.E. Hemler. 2012b. Palmitoylation by DHHC3 is critical for the function, expression, and stability of integrin α6β4. *Cellular and molecular life sciences : CMLS*. 69:2233-2244.

Sharma, G.D., J. He, and H.E. Bazan. 2003. p38 and ERK1/2 coordinate cellular migration and proliferation in epithelial wound healing: evidence of cross-talk activation between MAP kinase cascades. *The Journal of biological chemistry*. 278:21989-21997.

Sharma, M., F. Urano, and A. Jaeschke. 2012c. Cdc42 and Rac1 are major contributors to the saturated fatty acid-stimulated JNK pathway in hepatocytes. *Journal of hepatology*. 56:192-198.

Shurbaji, M.S., G.R. Pasternack, and F.P. Kuhajda. 1991. Expression of haptoglobin-related protein in primary and metastatic breast cancers. A longitudinal study of 48 fatal tumors. *American journal of clinical pathology*. 96:238-242.

Shutes, A., A.C. Berzat, A.D. Cox, and C.J. Der. 2004. Atypical mechanism of regulation of the Wrch-1 Rho family small GTPase. *Current biology : CB*. 14:2052-2056.

Singh, R., V. Yadav, S. Kumar, and N. Saini. 2015. MicroRNA-195 inhibits proliferation, invasion and metastasis in breast cancer cells by targeting FASN, HMGCR, ACACA and CYP27B1. *Scientific reports*. 5:17454.

Siraj, A., M. Al-Rasheed, M. Ahmed, M. Ibrahim, A. Al-Nuaim, F. Al-Dayel, P. Bavi, A. Hussain, S. Uddin, and K. Al-Kuraya. 2014. Fatty acid synthase is a potential target for a subset of papillary thyroid cancers. *Cancer research*. 68:3025.

Sit, S.T., and E. Manser. 2011. Rho GTPases and their role in organizing the actin cytoskeleton. *Journal of cell science*. 124:679-683.

Skaar, J.R., J.K. Pagan, and M. Pagano. 2013. Mechanisms and function of substrate recruitment by F-box proteins. *Nature reviews. Molecular cell biology*. 14:369-381.

Small, J.V., G. Isenberg, and J.E. Celis. 1978. Polarity of actin at the leading edge of cultured cells. *Nature*. 272:638-639.

Smith, M.A., E. Blankman, N.O. Deakin, L.M. Hoffman, C.C. Jensen, C.E. Turner, and M.C. Beckerle. 2013. LIM domains target actin regulators paxillin and zyxin to sites of stress fiber strain. *PloS one*. 8:e69378.

Smith, S. 2006. Structural biology. Architectural options for a fatty acid synthase. *Science (New York, N.Y.)*. 311:1251-1252.

Smith, S., A. Witkowski, and A.K. Joshi. 2003. Structural and functional organization of the animal fatty acid synthase. *Progress in Lipid Research*. 42:289-317.

Sossey-Alaoui, K., T.A. Ranalli, X. Li, A.V. Bakin, and J.K. Cowell. 2005. WAVE3 promotes cell motility and invasion through the regulation of MMP-1, MMP-3, and MMP-9 expression. *Experimental cell research*. 308:135-145.

Stone, K.R., D.D. Mickey, H. Wunderli, G.H. Mickey, and D.F. Paulson. 1978. Isolation of a human prostate carcinoma cell line (DU 145). *International journal of cancer. Journal international du cancer*. 21:274-281.

Suburu, J., and Y.Q. Chen. 2012. Lipids and Prostate Cancer. *Prostaglandins & other lipid mediators*. 98:1-10.

Sugino, T., K. Baba, N. Hoshi, K. Aikawa, O. Yamaguchi, and T. Suzuki. 2011. Overexpression of fatty acid synthase in human urinary bladder cancer and combined expression of the synthase and Ki-67 as a predictor of prognosis of cancer patients. *Medical molecular morphology*. 44:146-150.

Sul, H.S., and D. Wang. 1998. Nutritional and hormonal regulation of enzymes in fat synthesis: studies of fatty acid synthase and mitochondrial glycerol-3-phosphate acyltransferase gene transcription. *Annual review of nutrition*. 18:331-351.

Swinnen, J.V., T. Roskams, S. Joniau, H. Van Poppel, R. Oyen, L. Baert, W. Heyns, and G. Verhoeven. 2002. Overexpression of fatty acid synthase is an early and common event in the development of prostate cancer. *International journal of cancer. Journal international du cancer*. 98:19-22.

Swinnen, J.V., P.P. Van Veldhoven, L. Timmermans, E. De Schrijver, K. Brusselmans, F. Vanderhoydonc, T. Van de Sande, H. Heemers, W. Heyns, and G. Verhoeven. 2003. Fatty acid synthase drives the synthesis of phospholipids partitioning into detergent-resistant membrane microdomains. *Biochemical and biophysical research communications*. 302:898-903.

Szolkiewicz, M., T. Nieweglowski, J. Korczynska, E. Sucajtys, E. Stelmanska, E. Goyke, J. Swierczynski, and B. Rutkowski. 2002. Upregulation of fatty acid synthase gene expression in experimental chronic renal failure. *Metabolism: clinical and experimental*. 51:1605-1610.

Taddei, M.L., M. Parri, A. Angelucci, F. Bianchini, C. Marconi, E. Giannoni, G. Raugei, M. Bologna, L. Calorini, and P. Chiarugi. 2011. EphA2 induces metastatic growth regulating amoeboid motility and clonogenic potential in prostate carcinoma cells. *Molecular cancer research*. 9:149-160.

Tai, S., Y. Sun, J.M. Squires, H. Zhang, W.K. Oh, C.Z. Liang, and J. Huang. 2011. PC3 is a cell line characteristic of prostatic small cell carcinoma. *Prostate*. 71:1668-1679.

Takahiro, T., K. Shinichi, and S. Toshimitsu. 2003. Expression of fatty acid synthase as a prognostic indicator in soft tissue sarcomas. *Clinical cancer research : an official journal of the American Association for Cancer Research*. 9:2204-2212.

Tao, W., D. Pennica, L. Xu, R.F. Kalejta, and A.J. Levine. 2001. Wrch-1, a novel member of the Rho gene family that is regulated by Wnt-1. *Genes Dev*. 15:1796-1807.

Thalmann, G.N., P.E. Anezinis, S.M. Chang, H.E. Zhau, E.E. Kim, V.L. Hopwood, S. Pathak, A.C. von Eschenbach, and L.W. Chung. 1994. Androgen-independent cancer progression and bone metastasis in the LNCaP model of human prostate cancer. *Cancer research*. 54:2577-2581.

Thupari, J.N., E.K. Kim, T.H. Moran, G.V. Ronnett, and F.P. Kuhajda. 2004. Chronic C75 treatment of diet-induced obese mice increases fat oxidation and reduces food intake to reduce adipose mass. *American journal of physiology. Endocrinology and metabolism*. 287:E97-e104.

Tian, W.-x., X.-f. Ma, S.-y. Zhang, Y.-h. Sun, and B.-h. Li. 2011. Fatty acid synthase inhibitors from plants and their potential application in the prevention of metabolic syndrome. *Clinical Oncology and Cancer Research*. 8:1-9.

Tischler, V., F.R. Fritzsche, J. Gerhardt, C. Jager, C. Stephan, K. Jung, M. Dietel, H. Moch, and G. Kristiansen. 2010. Comparison of the diagnostic value of fatty acid synthase (FASN) with alpha-methylacyl-CoA racemase (AMACR) as prostatic cancer tissue marker. *Histopathology*. 56:811-815.

Tomlins, S.A., M.A. Rubin, and A.M. Chinnaiyan. 2006. Integrative biology of prostate cancer progression. *Annual review of pathology*. 1:243-271.

Topalian, S.L., W.M. Linehan, R.K. Bright, and C.D. Vocke. 2006. Immortal human prostate epithelial cell lines and clones and their applications in the research and therapy of prostate cancer. Google Patents.

Tsuji, T., M. Yoshinaga, S. Togami, T. Douchi, and Y. Nagata. 2004. Fatty acid synthase expression and clinicopathological findings in endometrial cancer. *Acta obstetricia et gynecologica Scandinavica*. 83:586-590.

Tuxhorn, J.A., G.E. Ayala, M.J. Smith, V.C. Smith, T.D. Dang, and D.R. Rowley. 2002. Reactive stroma in human prostate cancer: induction of myofibroblast phenotype and extracellular matrix remodeling. *Clinical cancer research : an official journal of the American Association for Cancer Research*. 8:2912-2923.

Uddin, S., A.R. Hussain, M. Ahmed, R. Bu, S.O. Ahmed, D. Ajarim, F. Al-Dayel, P. Bavi, and K.S. Al-Kuraya. 2010. Inhibition of fatty acid synthase suppresses c-Met receptor kinase and induces apoptosis in diffuse large B-cell lymphoma. *Molecular cancer therapeutics*. 9:1244-1255.

Valastyan, S., and R.A. Weinberg. 2011. Tumor Metastasis: Molecular Insights and Evolving Paradigms. *Cell*. 147:275-292.

Van de Sande, T., E. De Schrijver, W. Heyns, G. Verhoeven, and J.V. Swinnen. 2002. Role of the phosphatidylinositol 3'-kinase/PTEN/Akt kinase pathway in the overexpression of fatty acid synthase in LNCaP prostate cancer cells. *Cancer research*. 62:642-646.

Van de Sande, T., T. Roskams, E. Lerut, S. Joniau, H. Van Poppel, G. Verhoeven, and J.V. Swinnen. 2005. High-level expression of fatty acid synthase in human prostate cancer tissues is linked to activation and nuclear localization of Akt/PKB. *The Journal of pathology*. 206:214-219.

van Zijl, F., G. Krupitza, and W. Mikulits. 2011a. Initial steps of metastasis: cell invasion and endothelial transmigration. *Mutation research*. 728:23-34.

van Zijl, F., G. Krupitza, and W. Mikulits. 2011b. Initial steps of metastasis: Cell invasion and endothelial transmigration. *Mutation Research/Reviews in Mutation Research*. 728:23-34.

Vance, D.E., and J.E. Vance. 2008. CHAPTER 8 - Phospholipid biosynthesis in eukaryotes. *In* Biochemistry of Lipids, Lipoproteins and Membranes (Fifth Edition). Elsevier, San Diego. 213-244.

Varkaris, A., P.G. Corn, S. Gaur, F. Dayyani, C.J. Logothetis, and G.E. Gallick. 2011. The role of HGF/c-Met signaling in prostate cancer progression and c-Met inhibitors in clinical trials. *Expert opinion on investigational drugs*. 20:1677-1684.

Vazquez-Martin, A., R. Colomer, J. Brunet, R. Lupu, and J.A. Menendez. 2008. Overexpression of fatty acid synthase gene activates HER1/HER2 tyrosine kinase receptors in human breast epithelial cells. *Cell proliferation*. 41:59-85.

Vega, F.M., and A.J. Ridley. 2008. Rho GTPases in cancer cell biology. *FEBS letters*. 582:2093-2101.

Veigel, D., R. Wagner, G. Stubiger, M. Wuczkowski, M. Filipits, R. Horvat, B. Benhamu, M.L. Lopez-Rodriguez, A. Leisser, P. Valent, M. Grusch, F.G. Hegardt, J. Garcia, D. Serra, N. Auersperg, R. Colomer, and T.W. Grunt. 2015. Fatty acid synthase is a metabolic marker of cell proliferation rather than malignancy in ovarian cancer and its precursor cells. *International journal of cancer. Journal international du cancer*. 136:2078-2090.

Veldscholte, J., C.A. Berrevoets, C. Ris-Stalpers, G.G. Kuiper, G. Jenster, J. Trapman, A.O. Brinkmann, and E. Mulder. 1992. The androgen receptor in LNCaP cells contains a mutation in the ligand binding domain which affects steroid binding characteristics and response to antiandrogens. *The Journal of steroid biochemistry and molecular biology*. 41:665-669.

Ventura, R., K. Mordec, J. Waszczuk, Z. Wang, J. Lai, M. Fridlib, D. Buckley, G. Kemble, and T.S. Heuer. 2015. Inhibition of de novo Palmitate Synthesis by Fatty Acid Synthase Induces Apoptosis in Tumor Cells by Remodeling Cell Membranes, Inhibiting Signaling Pathways, and Reprogramming Gene Expression. *EBioMedicine*. 2:808-824.

Wagner, R., G. Stubiger, D. Veigel, M. Wuczkowski, P. Lanzerstorfer, J. Weghuber, E. Karteris, K. Nowikovsky, N. Wilfinger-Lutz, C.F. Singer, R. Colomer, B. Benhamu, M.L. Lopez-Rodriguez, P. Valent, and T.W. Grunt. 2017. Multi-level suppression of receptor-PI3K-mTORC1 by fatty acid synthase inhibitors is crucial for their efficacy against ovarian cancer cells. *Oncotarget*. 8:11600-11613.

Wakil, S.J., and L.A. Abu-Elheiga. 2009. Fatty acid metabolism: target for metabolic syndrome. *Journal of lipid research*. 50:S138-S143.

Wallace, D.M., G.D. Chisholm, and W.F. Hendry. 1975. T.N.M. classification for urological tumours (U.I.C.C.) - 1974. *British journal of urology*. 47:1-12.

Walter, K., S.M. Hong, S. Nyhan, M. Canto, N. Fedarko, A. Klein, M. Griffith, N. Omura, S. Medghalchi, F. Kuhajda, and M. Goggins. 2009. Serum fatty acid synthase as a marker of pancreatic neoplasia. *Cancer epidemiology, biomarkers & prevention : a publication of the American Association for Cancer Research, cosponsored by the American Society of Preventive Oncology*. 18:2380-2385.

Wang, H., Q.F. Luo, A.F. Peng, X.H. Long, T.F. Wang, Z.L. Liu, G.M. Zhang, R.P. Zhou, S. Gao, Y. Zhou, and W.Z. Chen. 2014. Positive feedback regulation between Akt phosphorylation and fatty acid synthase expression in osteosarcoma. *International journal of molecular medicine*. 33:633-639.

Wang, H., Q. Xi, and G. Wu. 2016. Fatty acid synthase regulates invasion and metastasis of colorectal cancer via Wnt signaling pathway. *Cancer medicine*. 5:1599-1606.

Wang, H.R., Y. Zhang, B. Ozdamar, A.A. Ogunjimi, E. Alexandrova, G.H. Thomsen, and J.L. Wrana. 2003. Regulation of cell polarity and protrusion formation by targeting RhoA for degradation. *Science (New York, N.Y.)*. 302:1775-1779.

Wang, J., Y. Xie, D.W. Wolff, P.W. Abel, and Y. Tu. 2010. DHHC protein-dependent palmitoylation protects regulator of G-protein signaling 4 from proteasome degradation. *FEBS letters*. 584:4570-4574.

Wang, R., J. Bi, K.K. Ampah, X. Ba, W. Liu, and X. Zeng. 2013a. Lipid rafts control human melanoma cell migration by regulating focal adhesion disassembly. *Biochimica et biophysica acta*. 1833:3195-3205.

Wang, S., T. Watanabe, K. Matsuzawa, A. Katsumi, M. Kakeno, T. Matsui, F. Ye, K. Sato, K. Murase, I. Sugiyama, K. Kimura, A. Mizoguchi, M.H. Ginsberg, J.G. Collard, and K. Kaibuchi. 2012. Tiam1 interaction with the PAR complex promotes talin-mediated Rac1 activation during polarized cell migration. *The Journal of cell biology*. 199:331-345.

Wang, T.F., H. Wang, A.F. Peng, Q.F. Luo, Z.L. Liu, R.P. Zhou, S. Gao, Y. Zhou, and W.Z. Chen. 2013b. Inhibition of fatty acid synthase suppresses U-2 OS cell invasion and migration via downregulating the activity of HER2/PI3K/AKT signaling pathway in vitro. *Biochemical and biophysical research communications*. 440:229-234.

Wang, Y., F.P. Kuhajda, J.N. Li, E.S. Pizer, W.F. Han, L.J. Sokoll, and D.W. Chan. 2001. Fatty acid synthase (FAS) expression in human breast cancer cell culture supernatants and in breast cancer patients. *Cancer letters*. 167:99-104.

Wei, J., G. Xu, M. Wu, Y. Zhang, Q. Li, P. Liu, T. Zhu, A. Song, L. Zhao, Z. Han, G. Chen, S. Wang, L. Meng, J. Zhou, Y. Lu, S. Wang, and D. Ma. 2008. Overexpression of vimentin contributes to prostate cancer invasion and metastasis via src regulation. *Anticancer research*. 28:327-334.

Wei, X., Z. Yang, F.E. Rey, V.K. Ridaura, N.O. Davidson, J.I. Gordon, and C.F. Semenkovich. 2012. Fatty acid synthase modulates intestinal barrier function through palmitoylation of mucin 2. *Cell host & microbe*. 11:140-152.

Welch, M.D., A.H. DePace, S. Verma, A. Iwamatsu, and T.J. Mitchison. 1997. The human Arp2/3 complex is composed of evolutionarily conserved subunits and is localized to cellular regions of dynamic actin filament assembly. *The Journal of cell biology*. 138:375-384.

Wells, C.M., A.D. Whale, M. Parsons, J.R.W. Masters, and G.E. Jones. 2010. PAK4: a pluripotent kinase that regulates prostate cancer cell adhesion. *Journal of cell science*. 123:1663-1673.

Welsh, J.B., L.M. Sapinoso, A.I. Su, S.G. Kern, J. Wang-Rodriguez, C.A. Moskaluk, H.F. Frierson, Jr., and G.M. Hampton. 2001. Analysis of gene expression identifies candidate markers and pharmacological targets in prostate cancer. *Cancer research*. 61:5974-5978.

Wen, S., Y. Niu, S.O. Lee, S. Yeh, Z. Shang, H. Gao, Y. Li, F. Chou, and C. Chang. 2016. Targeting fatty acid synthase with ASC-J9 suppresses proliferation and invasion of prostate cancer cells. *Molecular carcinogenesis*. 55:2278-2290.

Weng, M.S., C.T. Ho, Y.S. Ho, and J.K. Lin. 2007. Theanaphthoquinone inhibits fatty acid synthase expression in EGF-stimulated human breast cancer cells via the regulation of EGFR/ErbB-2 signaling. *Toxicology and applied pharmacology*. 218:107-118.

Willard, S.S., and S. Koochekpour. 2013. Glutamate signaling in benign and malignant disorders: current status, future perspectives, and therapeutic implications. *International journal of biological sciences*. 9:728-742.

Wilt, T.J., and H.U. Ahmed. 2013. Prostate cancer screening and the management of clinically localized disease. *BMJ (Clinical research ed.)*. 346:f325.

Witkowski, C.M., I. Rabinovitz, R.B. Nagle, K.S. Affinito, and A.E. Cress. 1993. Characterization of integrin subunits, cellular adhesion and tumorgenicity of four human prostate cell lines. *Journal of cancer research and clinical oncology*. 119:637-644.

Wright, J.L., C.A. Salinas, D.W. Lin, S. Kolb, J. Koopmeiners, Z. Feng, and J.L. Stanford. 2009. Prostate cancer specific mortality and Gleason 7 disease differences in prostate cancer outcomes between cases with Gleason 4 + 3 and Gleason 3 + 4 tumors in a population based cohort. *The Journal of urology*. 182:2702-2707.

Wu, H.-b., P. Zhang, X.-q. Li, J. Wu, J. Yu, and B. Jiang. 2009. Expression of c-met, e2f-1 and Ki-67 in tissues of gastric cancer. *Journal of Shanghai Jiaotong University (Medical Science)*. 29:1482-1486.

Wu, P.H., A. Giri, S.X. Sun, and D. Wirtz. 2014. Three-dimensional cell migration does not follow a random walk. *Proceedings of the National Academy of Sciences of the United States of America*. 111:3949-3954.

Xue, L., D.R. Gollapalli, P. Maiti, W.J. Jahng, and R.R. Rando. 2004. A palmitoylation switch mechanism in the regulation of the visual cycle. *Cell*. 117:761-771.

Yamaguchi, H., and J. Condeelis. 2007. Regulation of the actin cytoskeleton in cancer cell migration and invasion. *Biochimica et biophysica acta*. 1773:642-652.

Yamaguchi, H., J. Wyckoff, and J. Condeelis. 2005. Cell migration in tumors. *Current opinion in cell biology*. 17:559-564.

Yang, L., F. Zhang, X. Wang, Y. Tsai, K.H. Chuang, P.C. Keng, S.O. Lee, and Y. Chen. 2016. A FASN-TGF-beta1-FASN regulatory loop contributes to high EMT/metastatic potential of cisplatin-resistant non-small cell lung cancer. *Oncotarget*. 7:55543-55554.

Yang, P.Y., K. Liu, M.H. Ngai, M.J. Lear, M.R. Wenk, and S.Q. Yao. 2010. Activity-based proteome profiling of potential cellular targets of Orlistat--an FDA-approved drug with anti-tumor activities. *Journal of the American Chemical Society*. 132:656-666.

Yang, Y., H. Li, Z. Li, Z. Zhao, M. Yip-Schneider, Q. Fan, C.M. Schmidt, E.G. Chiorean, J. Xie, L. Cheng, J.-H. Chen, and J.-T. Zhang. 2011a. Role of fatty acid synthase in gemcitabine and radiation resistance of pancreatic cancers. *International journal of biochemistry and molecular biology*. 2:89-98.

Yang, Y., H. Liu, Z. Li, Z. Zhao, M. Yip-Schneider, Q. Fan, C.M. Schmidt, E.G. Chiorean, J. Xie, L. Cheng, J.H. Chen, and J.T. Zhang. 2011b. Role of fatty acid synthase in gemcitabine and radiation resistance of pancreatic cancers. *International journal of biochemistry and molecular biology*. 2:89-98.

Yang, Y.A., W.F. Han, P.J. Morin, F.J. Chrest, and E.S. Pizer. 2002. Activation of fatty acid synthesis during neoplastic transformation: role of mitogen-activated protein kinase and phosphatidylinositol 3-kinase. *Experimental cell research*. 279:80-90.

Ye, H., Y. Zhang, L. Geng, and Z. Li. 2015. Cdc42 expression in cervical cancer and its effects on cervical tumor invasion and migration. *International journal of oncology*. 46:757-763.

Ye, L., H.G. Kynaston, and W.G. Jiang. 2007. Bone metastasis in prostate cancer: molecular and cellular mechanisms (Review). *International journal of molecular medicine*. 20:103-111.

Yeh, S., H.K. Lin, H.Y. Kang, T.H. Thin, M.F. Lin, and C. Chang. 1999. From HER2/Neu signal cascade to androgen receptor and its coactivators: a novel pathway by induction of androgen target genes through MAP kinase in prostate cancer cells. *Proceedings of the National Academy of Sciences of the United States of America*. 96:5458-5463.

Yilmaz, M., and G. Christofori. 2009. EMT, the cytoskeleton, and cancer cell invasion. *Cancer metastasis reviews*. 28:15-33.

Yoon, S., M.Y. Lee, S.W. Park, J.S. Moon, Y.K. Koh, Y.H. Ahn, B.W. Park, and K.S. Kim. 2007. Up-regulation of acetyl-CoA carboxylase alpha and fatty acid synthase by human epidermal growth factor receptor 2 at the translational level in breast cancer cells. *The Journal of biological chemistry*. 282:26122-26131.

Yoshii, Y., T. Furukawa, N. Oyama, Y. Hasegawa, Y. Kiyono, R. Nishii, A. Waki, A.B. Tsuji, C. Sogawa, H. Wakizaka, T. Fukumura, H. Yoshii, Y. Fujibayashi, J.S. Lewis, and T. Saga. 2013. Fatty acid synthase is a key target in multiple essential tumor functions of prostate cancer: uptake of radiolabeled acetate as a predictor of the targeted therapy outcome. *PloS one*. 8:e64570.

Zadra, G., C. Photopoulos, and M. Loda. 2013. The fat side of prostate cancer. *Biochimica et biophysica acta*. 1831:1518-1532.

Zaidi, N., L. Lupien, N.B. Kuemmerle, W.B. Kinlaw, J.V. Swinnen, and K. Smans. 2013. Lipogenesis and lipolysis: the pathways exploited by the cancer cells to acquire fatty acids. *Progress in lipid research*. 52:585-589.

Zaytseva, Y.Y., V.A. Elliott, P. Rychahou, W.C. Mustain, J.T. Kim, J. Valentino, T. Gao, K.L. O'Connor, J.M. Neltner, E.Y. Lee, H.L. Weiss, and B.M. Evers. 2014. Cancer cell-associated fatty acid synthase activates endothelial cells and promotes angiogenesis in colorectal cancer. *Carcinogenesis*. 35:1341-1351.

Zaytseva, Y.Y., J.W. Harris, M.I. Mitov, J.T. Kim, D.A. Butterfield, E.Y. Lee, H.L. Weiss, T. Gao, and B.M. Evers. 2015. Increased expression of fatty acid synthase provides a survival advantage to colorectal cancer cells via upregulation of cellular respiration. *Oncotarget*. 6:18891-18904.

Zaytseva, Y.Y., P.G. Rychahou, P. Gulhati, V.A. Elliott, W.C. Mustain, K. O'Connor, A.J. Morris, M. Sunkara, H.L. Weiss, E.Y. Lee, and B.M. Evers. 2012. Inhibition of fatty acid synthase attenuates CD44-associated signaling and reduces metastasis in colorectal cancer. *Cancer research*. 72:1504-1517.

Zecchin, K.G., F.A. Rossato, H.F. Raposo, D.R. Melo, L.C. Alberici, H.C. Oliveira, R.F. Castilho, R.D. Coletta, A.E. Vercesi, and E. Graner. 2011. Inhibition of fatty acid synthase in melanoma cells activates the intrinsic pathway of apoptosis. *Laboratory investigation; a journal of technical methods and pathology*. 91:232-240.

Zhang, B., and Y. Zheng. 1998. Negative regulation of Rho family GTPases Cdc42 and Rac2 by homodimer formation. *The Journal of biological chemistry*. 273:25728-25733.

Zhang, J.S., A. Koenig, C. Young, and D.D. Billadeau. 2011. GRB2 couples RhoU to epidermal growth factor receptor signaling and cell migration. *Molecular biology of the cell*. 22:2119-2130.

Zhang, M., Y.D. Chai, J. Brumbaugh, X. Liu, R. Rabii, S. Feng, K. Misuno, D. Messadi, and S. Hu. 2014. Oral cancer cells may rewire alternative metabolic pathways to survive from siRNA silencing of metabolic enzymes. *BMC cancer*. 14:223.

Zheng, R., A. Iwase, R. Shen, O.B. Goodman, Jr., N. Sugimoto, Y. Takuwa, D.J. Lerner, and D.M. Nanus. 2006. Neuropeptide-stimulated cell migration in prostate cancer cells is mediated by RhoA kinase signaling and inhibited by neutral endopeptidase. *Oncogene*. 25:5942-5952.

Zheng, S.S., J.G. Gao, Z.J. Liu, X.H. Zhang, S. Wu, B.W. Weng, Y.L. Wang, S.C. Hou, and B. Jiang. 2016. Downregulation of fatty acid synthase complex suppresses cell migration by targeting phosphor-AKT in bladder cancer. *Molecular medicine reports*. 13:1845-1850.

Zheng, X., J.L. Carstens, J. Kim, M. Scheible, J. Kaye, H. Sugimoto, C.C. Wu, V.S. LeBleu, and R. Kalluri. 2015. Epithelial-to-mesenchymal transition is dispensable for metastasis but induces chemoresistance in pancreatic cancer. *Nature*. 527:525-530.

Zhidenko, A.A., V.V. Grubinko, and A.F. Iavonenko. 1990. [Features of the interconversion of alpha-ketoglutarate--glutamate in brain mitochondria of exothermic animals during hibernation]. *Ukrainskii biokhimicheskii zhurnal (1978)*. 62:79-83.

Zhou, L., S. Jiang, Q. Fu, K. Smith, K. Tu, H. Li, and Y. Zhao. 2016. FASN, ErbB2-mediated glycolysis is required for breast cancer cell migration. *Oncology reports*. 35:2715-2722.

Zhou, Y., L.B. Zhu, A.F. Peng, T.F. Wang, X.H. Long, S. Gao, R.P. Zhou, and Z.L. Liu. 2015. LY294002 inhibits the malignant phenotype of osteosarcoma cells by modulating the phosphatidylinositol 3kinase/Akt/fatty acid synthase signaling pathway in vitro. *Molecular medicine reports*. 11:1352-1357.